Charles University

Faculty of Arts

Institute of Classical Archaeology

Classical Archaeology

Dissertation

Paola Pizzo, MA.

STAROVĚKÉ VÁPENNÉ TECHNOLOGIE KYPRU: MEZIOBOROVÁ STUDIE VÁPENNÝCH A SÁDROVÝCH OMÍTEK Z OBLASTI PAFOSU

Discovering the Ancient plaster industry of Cyprus – multidisciplinary study of lime and gypsum plasters from the Paphian region.

Dissertation supervisors: Ing. Jan Válek, Ph.D.; Mgr. Jana Maříková-Kubková, Ph.D.

Dissertation consultant: prof. PhDr. Peter Pavúk, Ph.D.

2024

Univerzita Karlova

Filozofická fakulta

Ústav pro Klasickou Archeologii

Klasická Archeologie

Disertační práce

Paola Pizzo, MA.

STAROVĚKÉ VÁPENNÉ TECHNOLOGIE KYPRU: MEZIOBOROVÁ STUDIE VÁPENNÝCH A SÁDROVÝCH OMÍTEK Z OBLASTI PAFOSU

Discovering the Ancient plaster industry of Cyprus – multidisciplinary study of lime and gypsum plasters from the Paphian region.

Vedoucí práce: Ing. Jan Válek, Ph.D.; Mgr. Jana Mařiková-Kubková, Ph.D.

Konzultant: prof. PhDr. Peter Pavúk, Ph.D.

2024

I hereby declare that I have written this dissertation independently, using only the mentioned and duly cited sources and literature, and that the work has not been used in another university study programme or to obtain the same or another academic title.

Prague, 23rd October 2024 Paola Pizzo, MA.

To my brother and my grandfather

ACKNOWLEDGMENTS

This project is part of the PlaCe Innovative Training Network, a high-profile partnership dedicated to the interdisciplinary study of pre-modern ceramics and plasters, fully funded by Europe's Horizon2020, the EU Research and Innovation funding programme, as a Marie Skłodowska-Curie Action running from 2021 to 2025, under the Grant Agreement no. 956410. I would like to personally thank all the Institutes involved in the network for the training and assistance provided during these three and a half years of research. In particular, my gratitude goes to Dr. Maria Dikomitou-Eliadou and the STARC centre of the Cyprus Institute, to the Department of Archaeology of UCL, and to the Archaeological Research Unit of the University of Cyprus.

This project would not have been possible without the cooperation of the archaeologists who kindly provided their permission to take samples and assisted me throughout the whole analytical process by providing fundamental background information about the archaeological context. In no particular order, I would like to extend my gratitude to Dr. Lindy Crewe, Professor Maria Iacovou, Dr. Craig Barker, Dr. Artemis Georgiou, Dr. Ewdoksia Papuci-Władyka, Professor Joan Connelly. Acknowledgments are due to the Cypriot American Archaeological Research Institute (CAARI), the Department of Antiquities of Cyprus, the Cyprus Museum and the Archaeological Museum of the Paphos District.

The supervision and assistance of all the colleagues at the Institute of Theoretical and Applied Mechanics and at Centrum Telč was fundamental for my personal growth and for the completion of this thesis. Specifically, I would like to thank Dr. Petr Kozlovcev, Dr. Dita Frankeová, Dr. Alberto Viani, Sylwia Svorová-Pawelkowicz, Petra Macová and Irena Adámková. Special thanks go to the Institute of Archaeology in Prague (ARUP) and to all the team at the Institute of Classical Archaeology of Charles University (UKAR).

Lastly, this thesis would not have been even possible without the utmost support of my family and friends, who stayed by my side through the difficulties of the PhD path. I would like to personally thank my parents and my brother, who supported my dream of being an archaeologist since I was but a small kid; my aunt Anna, and my grandparents. My dear friends Enrico and Kim also had a pivotal role in the last three years (and more) of my life, so my gratitude extends to them, as well as to my fellow PhD students of the PlaCe project and of UKAR, and to my dear study-mates Elena, Dorka, Lukáš and Soňa.

This PhD project was possible thanks to a collective effort of people who effectively came together to participate and contribute to what you can read here. I have carried out the analysis and the research, but without the training, supervision, support, encouragement and knowledge of my colleagues and teachers, I would not have concluded such a valuable study.

LIST OF ABBREVIATIONS

Chronological abbreviations

MBA – Middle Bronze Age

LBA – Late Bronze Age

IA – Iron Age

(L-)H – (Late-) Hellenistic

(E/L-)R – (Early/Late-) Roman

Contextual abbreviations

KISS – Indicates the samples collected from the site of Kissonerga-*Skalia.*

KPH – Indicates the samples collected from Kouklia-*Palaepaphos* (loc. *Hadjiabdoulla*).

LCY – Indicates geological limestone samples.

GCY – Indicates geological gypsum samples.

MCY – Indicates marble samples.

NPA – Indicates the samples collected from the Agora in Nea Paphos.

NPER – Indicates the samples collected from the so-called Early Roman House in Nea Paphos.

NPHH – Indicates the samples collected from the so-called Hellenistic House in Nea Paphos.

NPT – Indicates the samples collected from the Theatre area in Nea Paphos.

NPVT – Indicates the samples collected from the Villa of Theseus in Nea Paphos.

YE – Indicates the sample collected from the East Building on Yeronisos Island.

YM – Indicates the samples collected in Yeronisos Island whose context is unclear.

YSC – Indicates the samples collected from the South-Central Complex in Yeronisos Island.

YSW – Indicates the samples collected from the so-called South-Western Building in Yeronisos.

YW – Indicates the samples collected from the western sector of Yeronisos Island.

Analytical abbreviations

AF – Amorphous phase(s)

BF – Bright Field, analytical mode in the polarized microscope.

BRP – Binder-Related Particles

CI – Cementation Index

CL – Cathodoluminescence

H_2O A – Water absorption test

FTIR – Fourier-Transform InfraRed spectroscopy

NHL – Natural Hydraulic Lime

O – Organic residue analysis

OM – Optical Microscopy

P – Open Porosity

PLM – Polarized Light Microscopy

PPL – Plain Polarized Light

R/RS – Raman Spectroscopy

SEM-EDS – Scanning Electron Microscopy coupled with Energy Dispersive X-Ray Spectroscopy

TA-DSC – Thermal Analysis-Differential Scanning Calorimetry

(TA-)EGA – (Thermal Analysis-) Evolved Gas Analysis

TS – Thin Section

XPL – Cross Polarized Light

XRD-QPA – X-Ray (powdered) Diffraction-Quantitative Phase Analysis

UBL – Under burnt lime

UV – Ultraviolet light

Other common abbreviations

a.s.l – Above Sea Level

DoA – Department of Antiquities

INDEX

INTRODUCTION

The present thesis analyses the production of plasters in the Southwestern part of Cyprus over a broad chronological range, spanning from the end of the Late Bronze Age and the Early Roman period. While plasters are a widely studied material across archaeological contexts worldwide (Lijith *et al.* 2024; Quilici *et al.* 2024; Piovesan *et al.* 2023; Schrøder Daugbjerg *et al.* 2022; Secco *et al.* 2022; Fisher *et al.* 2019; Moreno-Alcaide, Compaña-Prieto 2018; Tenconi *et al.* 2018), research concerning this category of findings is still scarce in the frame of Cypriot archaeology.
A new wave of interest towards understanding plaster production in Cyprus rose in the early 2000s with a series of papers concerning this topic from a variety of perspectives (Amadio 2018; Balandier *et al.* 2017; Turco *et al.* 2016; Theodoridou *et al*. 2013a; Philokyprou 2012a, 2012b). Before these publications, knowledge related to the plaster industry on the island was limited to short paragraphs and comments on the margins of the excavations monographs (for instance Karageorgis, Demas 1988) without a wider perspective, neither synchronically, nor diachronically. Furthermore, the majority of the recently published works deals with plasters from a conservation perspective. The significant studies of Theodoridou, Philokyprou, and Ioannou – for instance – constitute an essential information guidebook on how to approach these materials in a strategic and systematized way; however, most of their publications focus on the production of suitable repairing materials or on the proposition of new conservation techniques (Fournari *et al.* 2023; Theodoridou *et al.* 2013b; Ioannou *et al.* 2010). While the analytical method may be the same, the approach and interpretation of data strongly vary depending on the adopted perspectives; thus, conservators, material scientists, and engineers will draw different conclusions than archaeologists. In this sense, the works of Amadio, Balandier, and Turco represent perfect examples of analytical studies conducted with archaeological questions in mind. Nonetheless, these studies are geographically limited to the sites of reference and expand little in terms of diachronic developments or intra-site comparisons.
The topic of plaster production can be approached from a variety of different perspectives, with thousands of publications produced every year about this material. The existence of such a wide array of points of view complicates the outline of a clear state-of-the-art and study review. In the present thesis, significant papers are brought up and discussed throughout the main text, with the first chapter focusing particularly on plasters from both archaeological and material engineering perspectives.

The scarce availability of knowledge and data on this topic in Cyprus prompted the initiation of the present project as part of the Marie Curie Innovative Training Network PlaCe: "Interdisciplinary studies of pre-modern Plasters and Ceramics from the eastern Mediterranean". In order to maintain a certain degree of feasibility over the limited time window for this research, a restricted geographical area was selected spreading in a radius around the site of Nea Paphos, in

order to begin the plasters' characterization process in a specific region and later, possibly, expand it island-wide with future research.

The present thesis has developed around three major axes, focusing on different aspects of the production of plasters. The first objective is the characterization of a hundred selected samples in order to create a systematized database and grouping method, which allows to expand the research from a broader island and extra-island perspective, while simultaneously having a common terminology and set of characteristics. In principle, the major objective is to create a structure similar to the one adopted for the study of ceramics, which is based on fabrics that can be compared across time and spaces, while maintaining constant pivotal characteristics.
Secondly, this research aims at answering questions related to the technological aspects of the production process. The investigation is especially focused on inquiries concerning raw material selection and provisioning, which prompted a circumscribed geological survey of the area and the adoption of experimental archaeology techniques. Other than raw materials' sourcing, the focus is on the identification of specific production, curing and hardening conditions. The chronological period selected (LBA-ER) suffers from the lack of archaeological evidence of kilns – or any other structure – employed for the production of lime-based plasters. The characterization of the archaeological plasters could significantly improve our knowledge of the industry even from the perspective of the used equipment and tools. A further point connected with technology is proving if there are specific links between recipes, production tools/processes, and the functionality of the plasters, allowing to identify trends in fashion or in the industry.
Lastly, the present thesis focuses on the individuation of synchronic and diachronic trends, aiming at pinpointing the eventual existence of developments and changes ascribable to the occurrence of external factors, such as the phenomenon of Romanization of the island, or the occupation of it by Ptolemaic rulers. In addition to the questions listed above, there are site-specific issues relating to each specific archaeological, geological and historical context.

It is fundamental to stress the importance of interdisciplinarity for the successful completion of the present PhD project. Multiscale analyses allow for a comprehensive understanding of the archaeological materials, enabling researchers to interpret aspects of production and use that would not be visible at a macroscopic level. Experimental archaeology further enhances the interpretative process, allowing for first-hand experience with the studied material. Although scientific analyses from the world of the so-called hard sciences have been introduced and combined with archaeology for more than 50 years now, it is still quite common that the archaeologists do not perform the analyses themselves, neither they work directly with the data. While this approach still allows for a full interpretation, it can often cause incomprehension and issues stemming from different terminology and interpretative methods or tools. This thesis aims to stand in the middle of archaeology and hard sciences, effectively adopting both points of views and crafting new terminology and analytical processes tailored for archaeology.

References

Amadio, M.

2018. From deposits to social practices: Integrated micromorphological analysis of floor sequences at Middle Bronze Age Erimi-Laonin tou Porakou, Cyprus. *Journal of Archaeological Science: Reports* 21, pp. 433–449. https://doi.org/10.1016/j.jasrep.2018.07.023

Balandier, C., C. Joliot, M. Ménager, F. Vouve, C. Vieillescazes

2017. Chemical analyses of Roman wall paintings recently found in Paphos, Cyprus: The complementarity of archaeological and chemical studies. *Journal of Archaeological Science: Reports* 14, pp. 332–339. https://doi.org/10.1016/j.jasrep.2017.06.016

Fisher, K. D., S. W. Manning, T. M. Urban

2019, New approaches to Late Bronze Age urban landscapes on Cyprus: investigation at Kalavasos–Ayios Dhimitrios, 2012-2016. *American Journal of Archaeology* 123(3), pp. 473–507. http://dx.doi.org/10.3764/aja.123.3.0473

Fournari, R., L. Kyriakou, I. Ioannou

2023. On the Effect of Poor-Quality Aggregates on the Physico-Mechanical Performance of Repair Lime-Based Mortars, in V. Bokan Bosiljkov, A. Padovnik, T. Turk (eds.), *Conservation and Restoration of Historic Mortars and Masonry Structures*. HMC 2022. RILEM Bookseries, vol. 42. Springer, pp. 416–425. https://doi.org/10.1007/978-3-031-31472-8_33

Ioannou, I., M.F. Petrou, R. Fournari, A. Andreou, C. Hadjigeorgiou, B. Tsikouras, K. Hatzipanagiotou

2010. Crushed limestone as an aggregate in concrete production: the Cyprus case. *Geological Society, London, Special Publications,* v. 331, pp. 127–135. https://doi.org/10.1144/sp331.11

Karageorgis, V., M. Demas

1988. *Excavations at Maa-Palaeokastro, 1979-1986.* Nicosia: Dept. of Antiquities.

Lijith, K.P., V.S.N.S. Goli, R. Yadav, M.R. Singh

2024. Provenance studies on ancient mud mortars, plasters, and floor soils of India's Raigad hill fort. *Microchemical Journal* 199, 110223. https://doi.org/10.1016/j.microc.2024.110223

Moreno-Alcaide, M., J.M. Compaña-Prieto

2018. Roman plasters and mortars from ancient *Cosa* (Tuscany-Italy). Mineralogical characterisation and construction from *domus* 10.1 (House with Cryptoporticus).

Journal of Archaeological Science: Reports 19, pp. 127–137. https://doi.org/10.1016/j.jasrep.2018.02.025

PHILOKYPROU, M.

2012a. The Earliest Use of Lime and Gypsum Mortars in Cyprus, in J. Válek, J.J. Hughes, C.J.W.P. Groot (eds.), *Historic Mortars. Characterisation, Assessment and Repair, RILEM Bookseries* 7, pp. 25–36, Springer. https://doi.org/10.1007/978-94-007-4635-0_3

2012b. The Beginnings of Pyrotechnology in Cyprus. *International Journal of Architectural Heritage* 6, pp. 172–199. https://doi.org/10.1080/15583058.2010.528145

PIOVESAN, R., C. MAZZOLI, L. MARITAN

2023. Production recipes of mortar-based materials from ancient Pompeii by quantitative image analysis approach: The microstratigraphy of plasters in the Temple of Venus. *Journal of Cultural Heritage* 59, pp. 57–68. https://doi.org/10.1016/j.culher.2022.11.002

QUILICI, M., J. ELSEN, I. UYTTERHOEVEN, B. BEAUJEAN, P. DEGRYSE

2024. Mortar recipes from the Roman Imperial Bath-Gymnasium and Urban Mansion of Sagalassos – A technological perspective. *Journal of Archaeological Science: Reports* 57, 104674. https://doi.org/10.1016/j.jasrep.2024.104674

SCHRØDER DAUGBJERG, T., A. LICHTENBERGER, A. LINDROOS, R. RAJA, J. OLSEN

2022. Revisiting radiocarbon dating of lime mortar and lime plaster from Jerash in Jordan: Sample preparation by stepwise injection of diluted phosphoric acid. *Journal of Archaeological Science: Reports* 41, 103244. https://doi.org/10.1016/j.jasrep.2021.103244

SECCO, M., Y. ASSCHER, G. RICCI, S. TAMBURINI, N. PRETO, J. SHARVIT, G. ARTIOLI

2022. Cementation processes of Roman pozzolanic binders from Caesarea Maritima (Israel). *Construction and Building Materials* 355, 129128. https://doi.org/10.1016/j.conbuildmat.2022.129128

THEODORIDOU, M., I. IOANNOU, M. PHILOKYPROU

2013a. New evidence of early use of artificial pozzolanic material in mortars. *Journal of Archaeological Science* 40, pp. 3263–3269. https://doi.org/10.1016/j.jas.2013.03.027

THEODORIDOU, M., M. LOFA, I. IOANNOU
2013b. *Historic gypsum mortars from Cyprus: characterization and reinvention for conservation purposes*. HMC2013 3rd Historic Mortars Conference, 11–14 Sep 2013 Glasgow, Scotland

TENCONI, M. I. KARATASIOS, F. BALA'AWI, V. KILIKOGLOU
2018. Technological and microstructural characterization of mortars and plasters from the Roman site of Qasr Azraq, in Jordan. *Journal of Cultural Heritage* 33, pp. 100–116. https://doi.org/10.1016/j.culher.2018.03.005

TURCO, F., P. DAVIT, F. CHELAZZI, A. BORGHI, L. BOMBARDIERI, L. OPERTI
2016. Characterization of Late Prehistoric Plasters and Mortars from Erimi – Laonin tou Porakou (Limassol, Cyprus). *Archaeometry* 58, pp. 284–296. https://doi.org/10.1111/arcm.12168

PART 1. MATERIALS AND CONTEXT

Chapter 1.1: Plasters and mortars

Plasters and mortars are construction materials composed of a binder and one or more aggregates, the nature of which strongly varies according to the function of the mixture (Arizzi, Cultrone 2021; Ergenç *et al.* 2021; Quinn 2013) (terminology in accordance with EN 16572 (2015)). Although the choice of the binder strongly depends on the local geological availability (Marinowitz *et al.* 2012; Philokyprou 2012a), lime is historically the most common binder type (Ergenç *et al.* 2021; Theodoridou *et al*. 2013), with gypsum and mud being still relevantly present in archaeological records around the world (Arizzi, Cultrone 2021; Pedergnana, Elias-Ozkan 2021; Artioli *et al.* 2019; Elsen *et al.* 2012; Weiner 2010). Cyprus is no exception in this regard, even more so considering the presence of readily available limestone and gypsiferous deposits on the island (Philokyprou 2012a, 2012b). Through the characterization of the binder(s) it is possible to reconstruct the processes of production, from the selection of the raw materials to the creation of specific mortar mixtures.

A great deal of troubles for archaeologists and material scientists working with this type of samples is caused by the lack of a univocal terminology for referring to plasters and mortars. While typically material scientists define plasters according to their functions, in the archaeological records the terms "plaster", "mortar", "cement", and even "stucco" are used interchangeably. Even the samples under study in this specific project had been previously mislabelled as something entirely different. Thus, it is of uttermost importance that the terminology in use in the present research is clearly defined, providing an explanation for each term employed.

Plasters

According to the Concise Oxford Dictionary of Archaeology a plaster is "a mixture of sand and lime, or crushed gypsum […], which is spread onto walls and ceilings in order to produce a hard smooth surface when dry". According to EN 16572 (2015, 9), from an engineering perspective, a plaster is a "coating composed of one or more mortar layers applied in one accomplishment sequence, used on internal masonry surface such as ceiling, walls, and partition". In this thesis, the term "plaster" has been extended also to describe the coating of external walls – defined as "renders" according to EN 16572 (2015, 9) – and floors.

Mortars

This term is possibly even more problematic for archaeologists and scientists. As a matter of fact, the noun "mortar" describes a wide category of grinding tools commonly documented in the archaeological records all over the world, while it is used to describe a specific mixture of binders and aggregates in the world of material sciences. According to the above-mentioned European Standard, a mortar is a "material traditionally composed of one or more (usually inorganic) binders, aggregates, water, possible additives and admixtures combined to form a paste used in masonry for bedding, jointing and bonding, and for surface finishing (plastering and rendering) of masonry

units, which subsequently sets to form a stiff material" (EN 16572 2015, 5; Arizzi, Cultrone 2021, 2; Ergenç *et al.* 2021, 197). Mortars can be variously grouped according to their function, or their physical and chemical properties. The term "mortar" is often used by material scientists to describe the general category.

Binders

Both mortars and plasters are always composed of a binding material and one or multiple types of aggregates. The binding material, known as "binder", has adhesive and cohesive properties which hold the aggregates' particles together. There are different types of binders, both organic and inorganic, the most common of which are lime (Weiner 2010), gypsum, mud and clay (Arizzi, Cultrone 2021, 2).

For the purposes of this thesis, it is necessary to make further distinctions between the different types of lime binders in relation to their setting conditions. There are two major categories of lime binders: aerial lime, which sets and hardens as a result of the reaction between calcium hydroxide ($Ca(OH)_2$) and the carbon dioxide (CO_2) naturally present in the atmosphere; and hydraulic lime binders, which are able to set in wet conditions. Within these two groups, it is possible to further differentiate the binders according to their chemical properties, as shown in the following table (**tab. 1**; see **fig. 1** for a visual representation of the binders' groups).

Another controversial issue in this regard concerns the distinction between hydraulic and watertight plasters. By definition, a hydraulic binder can set in wet conditions – or even underwater in the case of the highly hydraulic ones – and is not water-soluble (Arizzi, Cultrone 2021; Deloye 1993; Elsen *et al.* 2012; Turco *et al.* 2016), thus it is suitable for the construction or coating of water-resistant architecture. In terms of chemical composition, a binder is considered hydraulic when hydrated calcium-(alumina)-silicate phases are detected (C-(A)-S-H) (Arizzi, Cultrone 2021; Diekamp *et al.* 2012; Weiner 2010); the silica (alumina) minerals responsible for these phases can be naturally present in the original rock – natural hydraulic limes – or can be admixed to a fresh mortar in the form of pozzolanic volcanic rocks/ashes or clay-based aggregates (i.e. ceramic or brick fragments) (Elsen *et al.* 2012); volcanic ashes are not available in Cyprus, thus ceramic fragments were used as pozzolans since as early as the Late Bronze Age (Turco *et al.* 2016). When an air lime binder is mixed with pozzolanic aggregates, a chemical reaction in the form of a visible reaction rim is expected (Arizzi, Cultrone 2021; Diekamp *et al.* 2012); however, the absence of this feature does not necessarily imply the lack of a reaction, as in some cases the reaction is too weak to be visible or measurable (Calzolari *et al.* 2023). A mortar based on non-hydraulic or feebly hydraulic limes can still possess certain waterproofing properties, if, for instance, the surface is polished with a tool reducing superficial porosity, or organic additives such as oils or waxes are added or applied on it, *de facto* making it water repellent (Centauro *et al.* 2017; Jayasingh, Baby 2022).

Type of binder	Sub-type of lime	Characteristics
Aerial lime	—	Lime sets and hardens due to the reaction between calcium hydroxide and carbon dioxide (Arizzi, Cultrone 2021, 2).
Lime + pozzolans	Air lime + pozzolans	Natural (= volcanic ash) or artificial (= clay and bricks) pozzolanic material is added to air or hydraulic lime creating a stronger compound with watertightness properties.
	Hydraulic lime + pozzolans	
Hydraulic lime	Natural hydraulic lime (NHL)	Lime produced from stones that naturally contain silica and alumina in a variable proportion between 5–25% (Arizzi, Cultrone 2021, 3); usually fired at high temperatures (800–1200°C) in order to produce unstable silica-alumina phases. The reaction produces lime with enough CaO to allow for slaking with water.
	Natural cement	Modern construction material obtained by burning limestones naturally rich in silica and alumina content (up to 45%) at controlled temperatures never excessing 1250°C (Arizzi, Cultrone 2021, 3). The major difference between natural cement and NHL is the amount of free CaO for the slaking. The production of natural cements leaves a low content of CaO; thus, slaking is possible only if the burnt product is crushed and grinded.

Table 1) List of the most common typologies of lime binders with their respective sub-groups.

Aggregates

The term "aggregate" is used to describe all the particles that are added to the binder to enhance the properties of the final mixture. Aggregates can be inorganic or organic, and usually possess different characteristics according to the purpose(s) they answer to. For inorganic aggregates, the most important properties to keep in consideration are the shape of grains and granulometry. Sharp, angular aggregates generally reduce shrinkage phenomena, while improving cohesive properties (Doleželová *et al.* 2018, 5) and increasing compressive strength. Rounded, smooth aggregates – on the other hand – have the tendency to decrease the mechanical properties and the strength of the mortar mixtures, although they enhance properties such as workability of fresh mortars. Dimensions of the aggregates' grains and particles equally influence the performance of the final product: coarse aggregates prevent cracking and can consistently influence the pores' structure, while simultaneously creating a comparatively stronger plaster (Stefanidou *et al.* 2005, 917).

Larger particles allow for a reduced sensibility to volume changes (Stefanidou *et al.* 2005, 919) and are beneficial for mixtures applied in thick layers (Doleželová *et al.* 2018); on the contrary, fine aggregates create a close structure, generally less porous. The ratio in which aggregates and binders are mixed can also influence the overall performance of plasters, with lower A:B ratios usually resulting in higher strength.
Organic aggregates, and specifically fibres, are used to improve the tensile strength of the plasters, creating a more durable material (Di Bella *et al.* 2014). Di Bella's study has proven how the admixture of natural fibres to mortars can minimize the effects of impact and abrasion.

Chapter 1.1.1: Classification of plasters and mortars
It is possible to classify plasters and mortars according to different factors: most commonly, they are grouped in relation to their binder type, and sub-grouped in relation to either physical or chemical properties. In this thesis, the samples are subdivided and classified according to three different systems:

1. Classification according to binder type
As seen in the previous paragraphs, there are multiple types of binders. Samples are grouped according to the main component in the following categories: aerial lime-based; natural hydraulic lime-based (NHL); gypsum-based; there are – although quite rare – occurrences of plasters composed of mixtures of different binders, namely lime and gypsum or lime and clays.

2. Classification according to functional category
According to this classification, plasters and mortars can be distributed in groups that reflect their primary function. Although in the archaeological context it can be complicated to clearly identify this functionality, context interpretation and micromorphological analyses can help in attributing purposes with a certain extent of confidence. From an engineering perspective, mortars are the mixtures employed in the masonry, while plasters are used to coat surfaces (and more specifically, inner ones). The primary functional categories in consideration in this study are masonry mortars; wall plasters, without distinction between inner and outer walls; floor plasters; and waterproofing plasters.

3. Classification into systems
To ease the comparison between samples of the same binder type, but different functional categories, a sub-division of samples according to "systems" was created. The definition of "system" is equivalent to the one of "fabric" in ceramic studies (on the topic see Quinn 2022): a system consists of a mixture of a certain type of binder (lime, gypsum or NHL) with specific aggregates, in varying proportions; these mixtures present similarities, such as a typical macrostructure or a distinctive finishing. Six different systems were identified (see **fig. 1**): system 1 including lime-based double-layered wall plasters; System 2 for the single-layered, lime-based

plasters with ceramic aggregates; System 3 for the multi-layered lime-based plasters; system 4 for the miscellaneous lime-based plasters; system 5 for the NHL plasters; system 6 for the gypsum plasters.

Most of these groups are also associated with specific functional uses of the different plasters. System 1, which contains a substantial amount of the samples collected, groups together mortars used as wall plastering, or as decorative coating surfaces (as in the case of the seat covers of the theatre in Nea Paphos). System 2 – the second most numerous category – includes samples generally associated with structures ascribed to water/liquid containment or disposal, and hence generally referred to as "waterproofing mortars". System 3 includes a relatively small amount of samples usually associated with paving structures; while system 4 includes specimens whose function is still uncertain or without any available parallel for comparison. System 5 includes less than a dozen of samples associated with hydraulic properties, and thus quite similar – on a functional level – to System 2. System 6 is constituted by the gypsum-based samples, whose function – at least in the region under study – seems to be associated almost exclusively with masonry binding.

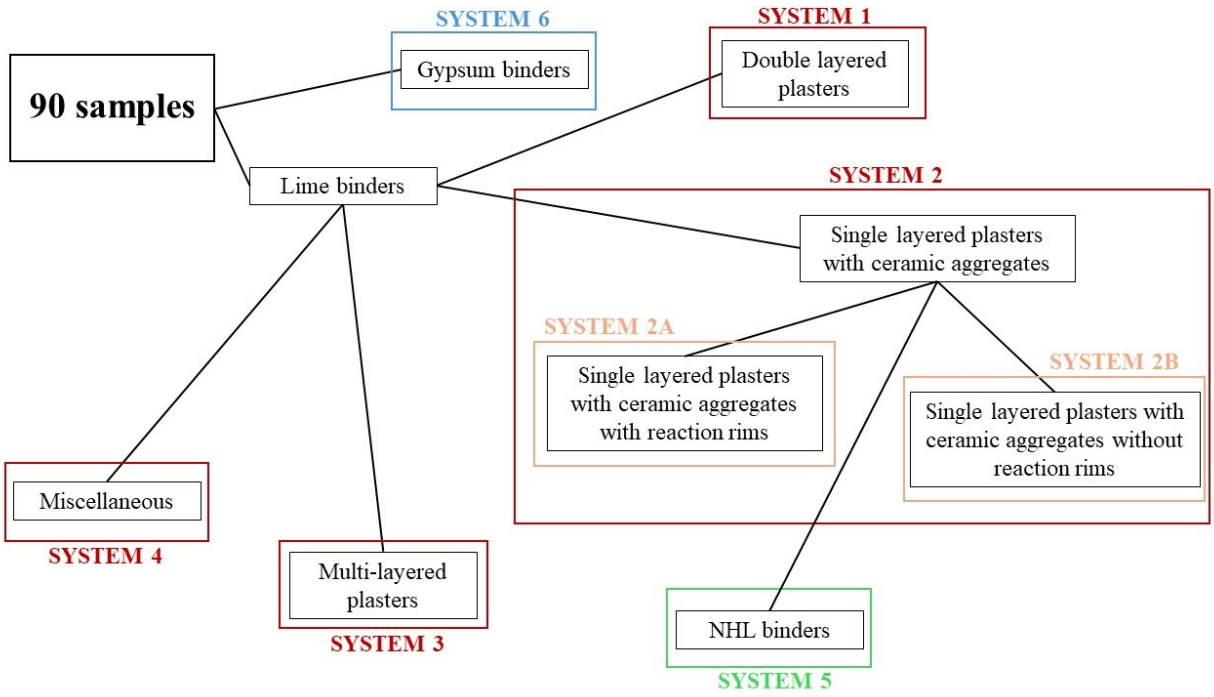

Figure 1) *Schematic illustration of the process of subdivision of the samples in the different groups (called "system"). The first division was based on macroscopic observations related to the binders and the structure of each plaster. According to this preliminary sorting method, we sub-divided the samples in 2 macro-categories: lime-based and gypsum-based plasters. Among the lime-based specimens we distinguished four categories: double-layered plasters, multi-layered plasters, single-layered plasters with ceramic aggregates, and finally some miscellaneous samples. Within the plasters with ceramic aggregates, we distinguished, based on the chemical composition and microstructure, two sub-categories and one completely separated group of samples: the sub-categories consist of plasters with chemical reaction rims in the microstructure (2A) and plasters without reaction rims (2B); while the completely separated group is constituted by samples containing natural hydraulic lime binder. The systems were later renumbered to have ordinal sequence.*

Chapter 1.2: Study case – the main archaeological sites in the Paphian region between the Late Bronze Age and the Roman period

The present research considered the main archaeological sites in the area of Paphos (**fig. 2**) during the period comprised between the end of the Bronze Age (approximately 1200 BCE) and the Roman times (until approximately the 3rd century CE, with sporadic samples dating to the 4th and 6th). The modern-day district of Paphos is constellated by numerous archaeological sites, with up to 119 settlements identified solely for the Hellenistic period (Lund 2015, 20). The longevity of the homonymous town of Nea Paphos allows for a diachronic study of the plaster production, enabling the understanding of the technological developments over a broad range of time. These reasons prompted the present research in the area around this specific archaeological site.

The following chapters will offer a brief overview of the sites, providing the geographical context, a brief history of the site and the account of studies and research related to them. The list of archaeological sites presented here is by no means exhaustive or representative of the entirety of the settlements in the Paphian region. The selected sites are among the most significant settlements for the time period considered, and – thanks to a comprehensive and thorough documentation – the most relevant for the study of plasters and mortars. For instance, Maa-*Palaiokastro* has a prominent role in the history of the region of Paphos, but due to the excavations being dated to the 70s, the documentation relating to plasters and mortars is scarce and does not allow for a significant study, as important contextual information are missing.

Chapter 1.2.1: Kissonerga-Skalia

Introduction

Kissonerga-*Skalia* is the oldest archaeological site considered in the present study. Interconnected in a complex urban pattern involving several archaeological areas located in close proximity, *Skalia* lies just 300 m from the coast, about 7 km from modern-day Paphos, on a low hill supplied by two water streams now dried (Crewe 2017, 144-145; Crewe 2013, 49; Crewe, Hill 2012, 206). Although the settlement is located on the coastline, the shores offer harbour only to small boats and could not have functioned as a large-scale commercial port (Crewe 2017, 144). Regardless, inhabitants of *Skalia* were importing materials from other contemporary Cypriot sites and remained up to date with trends and fashion of production from across the Mediterranean (Crewe 2017, 146).

The foundation of the site can be dated to ca. 2400 BCE, but the settlement lays adjacent to the Neolithic site of Kissonerga-*Mosphilia* and might constitute its direct prosecution (**fig. 3**). The whole area, richly inhabited since the Pre-Pottery Neolithic, sees a horizon of settlement abandonment during the early-Late Bronze Age, which only terminated with the foundation of Maa-*Palaeokastro* in ca. 1225 BCE (Crewe 2017, 146-147; Crewe 2013, 49; Crewe, Hill 2012). *Skalia* was equally abandoned during the transitional period from the MBA to the LBA (ca. 1600 BCE); the process that led to the abandonment of the site does not seem to be connected with sudden or violent events, but rather resembles a pattern of slow fall in disuse (Crewe 2017, 146).

Dr. L. Crewe (2017; 2013) has formulated the hypothesis of settlers' migration to the contemporary founded settlements of *Toumba tou Skourou* or Palaepaphos.

Excavation history

The archaeological area around the modern-day village of Kissonerga is well renowned since three different major sites have been already unearthed. Proceeding in chronological order, the earliest settlement to appear in the area is Kissonerga-*Mylouthkia*, excavated between 1976 and 1996 by E. Peltenburg and the Lemba Archaeological Project team of the University of Edinburgh (Peltenburg, Bolger 1998). This site was founded during the Pre-Pottery Neolithic period, ca. 8300 BCE, and seem to have been intensively in use until the Middle Chalcolithic, approximately 3500–3400 BCE (Peltenburg 2003). Few years after the start of the excavations at the site of *Mylouthkia*, the Lemba Archaeological Project discovered a second site, located approximately 1 km far from the coast. This second locality, known as Kissonerga-*Moshphilia* was extensively excavated by the same team between 1979 and 1992 and revealed four main occupation phases spanning between the Late Neolithic and the Late Chalcolithic. Located only a couple of hundred metres from *Mosphilia*, the site of *Skalia* was identified. Excavations at Kissonerga-*Skalia*, under the direction of Dr. L. Crewe from the University of Manchester and the Cyprus American Archaeological Research Institute, begun in the early 2000s and have been focused on the latest phases of inhabitation, dated to ca. MC III – LC IA period (Crewe 2013, 49). The site lies under a terrain interested by intense agricultural activities, a factor that created relevant disturbance in the stratigraphic sequence (Crewe 2017, 146; Crewe, Hill 2012, 214), and consequently in the proper interpretation of the settlement history.

Excavated structures and areas

Focusing mainly on the latest phases of occupation of the settlement, it is possible to observe how a coherent architectural plan of levelling and filling of previous strata was carried out before the abandonment of the site (Crewe, Souter 2023, 180; Crewe 2017, 145). Extensive levelling and surface equalizing are visible especially in a large courtyard space, known as Area B (**fig. 4**), limited by walls on at least two sides. The construction technique for these walls is the first striking peculiarity of the area: in all previously known sites in the proximity of Kissonerga, wall masonry consisted of rubble walls made of unworked stones and reused ground stones; Area B walls, on the other hand, are built with limestone slabs filled with a rubble core (Crewe 2013, 49; Crewe, Hill 2012, 213). Unearthing of a complex dedicated to water drainage further enhanced the idea of the community effort in planning, constructing and managing this impressive – although short-lived – area (Crewe, Souter 2023, 179), which is unparalleled for dimensions in MBA Cyprus (Crewe, Hill 2012, 234). This courtyard hosts, in an open or semi-roofed area delimited by curtain walls, a mud-plastered, domed, oval feature (Ft. 33) correlated with heating or firing activities (Crewe, Hill 2012, 213-224 including analysis of material culture associated). The complex structure of this domed feature, its positioning and large dimensions, all suggest a carefully planned architecture employed

for a communal or industrial activity that envisaged the use of heat for drying or preserving food (Crewe, Hill 2012, 216-217). Although the interpretation of this structure is largely problematic due to the lack of characteristic elements, parallel studies with similar and coeval Near Eastern findings led to interpret the oval mud-dome as a drying chamber for malt in the process of beer production (Crewe 2017, 144; Crewe, Hill 2012). This interpretation is further supported by other elements of the material assemblage of Skalia, including scattered seeds in the paleobotanical record, and pottery decorations depicting everyday life scenes. The presence of the large drying oven Ft. 33 suggests that the entirety of Area B was part of a large-scale built complex, possibly visible from the sea; these structures appear all over Cyprus during the transitional period from the MC to the LC.

The courtyard was not only an area for the production of beers; during the excavation campaigns finds associated with activities varying from metal production to cooking and weaving have been unearthed (Crewe, Souter 2023). Furthermore, on the western end of the courtyard, a room with peculiar architecture and material artefacts has surfaced. This space – known as Room 954 – is characterized by the presence of benches on three of the four walls, as well as a consistent presence of fine ware and exceptionally well-preserved faunal remains (Crewe, Souter 2023). The nature of the findings, along with the position on the possible very end of the terrace, suggest the use of room 954 must have been connected with a convivial space, not related to the rest of the working complex.

In addition to Area B, another large open space is featured in Area G2, where traces of a large rectangular construction, unroofed, were excavated. This feature was used in relation to pyrotechnological activities; however, the full extent of the built structure was never exploited, with activities been limited to circumscribed smaller areas within it (Crewe 2015, 355). Area G2 has parallels only in the site of Alambra, where two similar constructions were interpreted as ovens or hearths.

Dating to earlier phases of the Bronze Age, few linear units, most likely domestic, have been identified to the South of the courtyard (Crewe, Hill 2012, 206), in the so-called area D. The interpretation of their function is largely based on the associated material culture, which includes objects of everyday use, along with food waste and scraps. Area K, to the north of Area B, revealed the presence of a designated burial area, although the modest grave goods accompanying the tombs suggest a dating period in the Chalcolithic horizon.

Sampling in the site of Kissonerga was focused on the open spaces, given the dating to the transitional period between the Middle and the Late Bronze Age. The preservation status of the site (discussed above) has complicated the sampling procedure, as some of the plastered features were in a preservation status which would not have allowed for a proper characterisation. This is especially true for the floor structures, featuring a white, thin layer of plaster – possibly lime-based. Samples were instead collected from the lining of the emplacements and kilns in areas P and B2.

Chapter 1.2.2: Yeronisos Island

Introduction

Possibly connected to the mainland until the Early Holocene (Connelly, McCartney 2004), Yeronisos (or Geronisos) is a small offshore island located 280 m from the coast, in front of the modern town of Agios Georgios tis Pegeias, about 18 km from modern-day Paphos (Connelly 2002; 2005). It has been defined as an "isle beyond an isle" (Connelly 2002, 245; 2010b, 18; both previous quotes refer to poet E. Flecker in *A Ship, An Isle, A Sickle Moon*). The name "Yeronisos" derives from Greek and can be roughly translated to "sacred island", suggesting the religious character of the site. The island retains a name connected to sacredness since Antiquity (see Pliny, *Nat. Hist.* 5.129-131, where an island named *Hiera* is mentioned between Paphos and the Akamas Peninsula; and Strabo, *Geo.* 14.6.4), although, in ancient sources, it is occasionally confused with the coastal site of Geroskipou. Yeronisos was never interested by permanent settling, but rather by occasional visitations, possibly related to the ritual character of the site.

Until 1980s no excavations where conducted on the island, although knowledge of the possible presence of archaeological material was in possess of archaeologists since much earlier. In fact, both the American consul L. Palma di Cesnola and British archaeologist D. G. Hogarth, who excavated sites on the opposite-facing Cape Drepano, were informed of the presence of archaeological material on Yeronisos (then called Saint George's Island) as early as the late 1880s (Connelly 2002). In 1936, a publication by R. Gunnis listed a series of Neolithic and Roman findings on the island, constituting the first ever published material related to Yeronisos; this list was referring to a report he received from A. Westholm, while Gunnis himself did not witness the material (Connelly, McCartney 2004). Nonetheless, it was not until 1982 that systematic excavations took place on Yeronisos, when the Department of Antiquity requested a trial excavation before the construction of a casino (Connelly 2010b; Hadjisavvas 1983). S. Hadjisavvas' excavations consisted of a trench running along the axis of the island; it was evident since this preliminary expedition that the small island was an important archaeological testimony. A peculiar aspect of Yeronisos' findings was the consistency in terms of historical period: the material culture was predominantly attributable to a narrow time frame, namely the 1st century BCE, leading to suspect the presence of a very rare, undisturbed Hellenistic site (Connelly 2010b). The New York University was awarded, in 1990, the license to excavate the site; since then, several excavation campaigns took place, mainly published in reports of the RDAC series (Connelly 2002, 2005, 2010a; Connelly, McCartney 2004).

Archaeological excavations and consequent study seasons established a reliable chronology, distinguishing three main phases of occupation on Yeronisos (**fig. 5-6**): Early Chalcolithic, Late Hellenistic and Early Byzantine (Connelly 2002). The first visit, during the Early Chalcolithic (3900–3500 BCE), is represented in the archaeological record predominantly by stone tools and pottery assemblage, and it was initially erroneously dated to the Neolithic period. After a nearly 35 centuries gap (Connelly 2005, 169), the following material evidence points to a flourishing phase during the Late Hellenistic, possibly contemporary to the restoration of Ptolemaic rule under

Cleopatra VII (1st century BCE, specifically between 44–30 BCE as testified by 14 coins unearthed on the site); this phase, by far the most thriving, saw the island as seat of a Sanctuary associated with the cult of Apollo (Connelly 2002). The earthquake of 17 BCE greatly damaged the buildings on the island, causing a long abandonment period that terminated only during the 6th century CE. Visitors in this period, as well as during the following episode of the 13th century, seem to have been visiting and inhabiting the island in a non-continuous manner, rather than establishing a permanent settlement. The steep elevation of Yeronisos, the hardship of finding a secure harbour, and the scarcity of resources available locally greatly disfavoured the site from being subject of permanent settling. Careful planning of the relatively restricted space (the island measures up to 100 m in width and 270 m in max. length) responded to the difficult building environment: the central part of the island was exploited as quarrying and water collection site, while the outlines were designed as building areas.

A notable challenge for the archaeologists working on Yeronisos is the presence of a prosperous ecosystem for sea birds' nesting, which has led to the necessity of developing specific methodologies to preserve the important natural habitat (see more in Connelly 2002).

Material Evidence from the Early Chalcolithic

Of this earliest phase of occupation little evidence is remaining. Findings are mostly consisting of stone tools and chipping stones, while no buildings have been identified. Furthermore, the Chalcolithic material was deliberately reused in several Hellenistic constructions (Connelly, McCartney 2004), making the understanding of this earlier chronological phase increasingly complicated.

Overall, the material distribution of Early Chalcolithic (EC) findings highlights a concentration over the southern and eastern ends of the island, with little to no material in the northern and western sides (Connelly, McCartney 2004); however, the deposits located under the Hellenistic Central South Complex have only been partially unearthed, to preserve the overlaying Hellenistic *strata*. A conspicuous amount of EC material was also detected in the filling of the circular dancing platform, yet it was clearly in secondary use and no longer *in situ*. Higher concentrations could possibly mirror the occupation areas; however, erosion and later disturbances are factors that must be kept in mind when adopting this assumption.

The assemblage of EC findings includes ceramic, ground stone tools, and chipped stones (Connelly, McCartney 2004). The analysis of the pottery samples did not reveal any specific or suggestive distribution pattern, if not the presence of isolated Coarse Ware (CW) trays comparable to the ones of contemporary Lemba-*Lakkous*. Similarly, the ground stones are also compatible with the standard Cypriot Chalcolithic sets; however, it is noteworthy that the raw materials included volcanic rocks, imported from the mainland, and Akamas red sandstone, native to the Akamas peninsula. Import of these goods highlights two different aspects: on one hand, it demonstrates the extended geological knowledge of Cypriots already in the EC; moreover, it strengthens the idea that visits on the island were on a seasonal basis. The reduced size of the chipped stone assemblage

can be easily explained by the lack of raw material available, this issue further explain the heavy exhaustion of the retrieved tools, which all display well-worn out edges.
The only architectural feature belonging to the Chalcolithic age is a trampled earthen soil located at the eastern end of the island, directly under Byzantine levels identified as storage associated with the East Building. Remarkably, this area lacked the presence of any Hellenistic find. Under this floor, covered by large boulder stones, archaeologists found a ritual deposit containing ground stone tools, ash, a cracked heat stone, and a broken stone figurine (Connelly 2005, 169; Connelly, McCartney 2004, 22–23). The religious function of the pit has been deduced from the presence of the figurine, the neatly construction of the deposit, and finally from the role played by the ash and heat stone. Despite two fire-related markers are found inside the pit, no traces of fire are visible on the other objects. Both ash and the heat stone were intentionally transported from a different area (Connelly, McCartney 2004, 23), highlighting the special significance of this deposit, which was not functioning as a mere discard area.
As mentioned before, EC material was often found in association to Hellenistic one, in position of re-use. Particularly, chipped stones have been retrieved from the South-Central Complex in contexts related to food processing and consumption (Connelly, McCartney 2004), or – at any rate – in spaces dedicated to working activities. Chalcolithic finds were also employed in the wall construction, with ground stones and tools being incorporated in the masonry.

Yeronisos during the Ptolemaic Restoration

Yeronisos went through a proper golden age under the Late Hellenistic phase, and more specifically during the 1st century BCE, under the rule of Queen Cleopatra VII and Ptolemy XVI Caesar. Archaeologists were able to unearth three huge buildings dating to this period, constructed with high quality materials and rich in terms of material culture associated. Also dating to the Ptolemaic Restoration is one of the two cisterns (Connelly *et al.* 2002) and the North ascension rampart (Connelly 2010a). This latter feature was still preserved for a 10 m length when excavations begun back in 1990, however, it is almost completely lost nowadays, with the large ashlar blocks lying in the sea. Scanty findings of reused masonry point out to the presence of a pre-existing Hellenistic phase, whose date and documentation are still under discussion. This cistern was not the sole device for water collection: large *pithoi* were unearthed continuously during the excavation seasons of 2009-2015 on the Southern edge of Yeronisos, suggesting they were instalments related to water storage.
The first excavated Late Hellenistic building is the so-called Southwest Complex, already partially unearthed during the trench excavations of Dr. S. Hadjisavvas in 1982. To date, the sequences are difficult to outline, and the individual features are largely dated based on the material associated (including a bronze coin of Cleopatra VII and Ptolemy XVI Caesar). A circular rubble wall on the western end clearly belongs to a secondary phase as it bears a cross engraving on one of the stones. The function of this building still remains partially obscure. The findings, which include cooking ware, animal bones and abundant drinking cups, suggest that the Southwest Complex hosted

activities related to cooking and food processing, be it connected to household or religious consumption. The location of the building, right next to the entrance to the plateau, and the fine masonry would make the scale pend over a ritual interpretation.

As previously mentioned, the site was almost grazed to the ground by the devastating earthquake of 17 BCE. Evidence of this violent event are represented in the material distribution across the Hellenistic strata, with broken tiles plunged into the plaster floors and ceramic fragments of the same vessels spread across several meters. The heterogeneity of material, accompanied by the remarkable lack of complete vessels suggest that the site might have even been later re-employed as a ditch area.

Contemporary to the Southwest Complex is the so-called West Building, which is believed to be the richest building on Yeronisos (Connelly 2002, 264). This structure is currently scarcely preserved, as most of it fell into the sea as a result of the several earthquakes of the 6th century CE. Preliminary hypotheses on the purpose of the building were formulated by S. Hadjisavvas during the course of his excavations in 1982. The material evidence led the archaeologist to label the building as a kitchen, possibly result of Byzantine reuse, as attested by the presence of a parapet rubble wall to protect the building in its collapsed side. The excavations of 1992-1994 led by New York University unearthed precious material, including other Ptolemaic coins dating to the reign of Cleopatra VII and Ptolemy XVI Caesar. The analysis of the new assemblage and the whole remaining planimetry allowed the excavator to identify the building as a temple (Connelly 2002, 264–266). During the excavations of 2016, an extensive study focusing on Hellenistic architecture was conducted by Prof. P. Broucke, concluding that the temple was a small Ionic structure built on top of a podium with fine limestone blocks plastered to resemble marble (Department of Antiquities, Press Release 2016). An interesting finding during the excavations campaigns of 2016-2017 concerns the foundations of this temple building, which were set around the governing unit of Egyptian ell, suggesting direct involvement of Egyptian workforces.

The last, only in order of excavation, building belonging to the Late Hellenistic period is the Central South Complex. In this case, as well as in the other two above-mentioned buildings, part of the construction was lost due to earthquakes; the presence of the already identified typology of rubble wall on the edge of the cliff allows to hypothesise that in Byzantine times the island had lost part of its southern borders (Connelly 2005). Part of the building was even robbed of the ashlar blocks, which were re-employed to build the neighbouring Basilica possibly in the 6th century CE (Connelly 2005), and the three great Christian Basilicas on the coastal site of Agios Georgios. Despite the destruction caused by natural phenomena and the subsequent spoliation of the highest quality materials, several findings – including pigmented wall plaster, roof tiles and structural elements – are testimony to the prestige of the building.

The walls, set directly upon the bedrock, present traces of reused precedent Hellenistic material, hinting to an earlier phase of construction still largely unknown. The rooms uncovered inside the complex presented a mirroring structure with low benches on the corner; around these platform, abundant archaeological findings were brought to light, including cooking ware, drinking and

eating vessels, lamps, and objects made of precious materials (Connelly 2005, 157 for the full catalogue of findings). An interesting finding, a pile of unused roof tiles to the North of the Complex, suggests that the building might have still been partially under construction or repair at the time of destruction.

The building retained a clear function associated with food processing; individual cooking positions and even a hearth were discovered during the archaeological campaigns prior to 2005. A quick look at the ceramic assemblage highlights a diet rich in liquids and consumed in small portions. The reduced dimensions of the tableware has led to the formulation of two different hypotheses: either the food was made to be consumed by children, or it was prepared as part of a ritual (which would justify the refined quality of the ceramic fabrics). The presence of children in the island is also attested by the presence of *ostraka* used for writing exercises, and of a limestone tablet inscribed with ordinal numbers. Other immediate associations for the interpretation of the material assemblage of the Hellenistic phase, and of the Central Southwest Complex in particular, include the ceremonial pyres documented from several areas of Athens, although in that context those are associated with private/domestic environment, rather than religion.

This brief list of architectural remains alone suffices to deduce the character of Yeronisos as a single-use, religious site. Despite the type of rituals involved are not fully clear to date, the presence of high-end materials, ritual drinking vessels, and Ptolemaic *ostraka* points to the clear sacredness aspect of the island, with the suggestive landscape likely playing a role. Key elements to strengthen this hypothesis are the so-called amulets of Yeronisos, loom weight-like seals with decorations drawn from either the every-day life or Greek and Ptolemaic iconography, with parallels found in the Ptolemaic temple of Horus in Edfu (Egypt). However, for the correct interpretation of the religious character of the island the central circular platform, also dated to this period, must be carefully analysed.

The circular structure, located in front of the northernmost entrance of the island, consists of two superimposing platforms of different diameters. The outer wall measures 21 m, while the inner just 13 m. The two concentric walls both contained the same type of fill, consisting of a silty yellowish clay allochthonous to Yeronisos geology. Given the remarkable hardness of this material, which has been even defined as “cement-like” (Connelly 2010a, 297), it is possible that archaeologists were dealing with sea sand brought uphill from the shores of the island. The platform is believed to have functioned as a dance floor, whereas dances were part of the rituals and especially connected to Apollo (for a broader discussion on the interpretation, see Connelly 2010a).

Later phases of settlement

Apart from the previously mentioned circuit wall unearthed on the southern and western ends of Yeronisos, other Byzantine findings include three houses and, likely, a Church, located on the eastern cliff (Connelly 2010a). To date, most of this eastern building is lost to the sea, as result of erosion and earthquakes. It is utterly remarkable to notice how the island retained a sacred character throughout a chronological span of a millennium, and the shift between different religions.

Contemporary to the latest visits at the site, currently dated to the 6th and 13th centuries, was the rise of a prosperous religious community on the coastal town of Agios Georgios. It has been theorised (Connelly 2010a, 297) that the same worshippers of Agios Georgios turned to the island as an isolated pilgrimage site.

Another interesting finding that post-dates the Hellenistic phases is a tomb, cut between the walls of the circular dancing platform. The modest burial contained the body of a female individual between 43-58 years of age; the woman was not accompanied by any form of jewellery or grave goods. The skeleton was dated with ^{14}C method, with results that puzzle archaeologists up to date. The broad period of death is comprised between the 1st and the 3rd century CE with a 95% accuracy (Connelly 2010a, 303). There are no other findings that date to this period, and the island was long considered abandoned until the pilgrimages of the 6th century CE. Palaeopathological analysis detected the presence of no relevant diseases, apart from diffuse idiopathic skeletal hyperostosis (DISH), relatable to a protein-rich diet. This information, accompanied by the presence of all teeth and the advanced age of death all point to a wealthy Roman woman, likely Christian, given the orientation of the grave. This individual sepulchre is not evidence of another visiting phase previously not encountered, but rather the results of personal choices, possibly related to religion, of the wealthy subject to be buried in a remote and modest tomb.

More clearly readable data concern the visitations of the 6th century CE, to which three square houses and a church are associated (Connelly 2010a).

In association to the houses and the so-called East Building is a squared cistern with polygonal platform (Cistern 2 in Connelly *et al.* 2002; also mentioned in Connelly, McCartney 2004 in regard to the Chalcolithic materials). It is unclear whether the previous Hellenistic cistern was no longer functional, or if it was not sufficient to supply for the water needs of the newly established Byzantine community. After this phase of occupation, no further archaeological record has been identified.

<u>Yeronisos from a geological perspective</u>

Geologically speaking, Yeronisos is largely made of calcareous materials, with two different formations having been recognised by geologists: namely, a harder and thicker layer of shells and maritime bioclasts, compacted together by calcite, constitutes the *substratum* for a thinner stratum of a geological formation known locally as *kafkalla* (Connelly 2002). Wave erosion has been identified as one of the highest risk factors for the archaeological remains on Yeronisos. Effectively, over the centuries, the small island has lost a relatively significant amount of surface area, as highlighted by the loss of parts of the buildings and the presence of circuit Byzantine parapet walls on the edges of the cliffs (Connelly 2002, 250). In particular, the southern and western ends crumbled prior to the 6th century CE, possibly during the earthquakes of the 4th century CE, when also the North access rampart collapsed to the sea (Connelly 2010a); the eastern end survived until at least the 6th century CE, when Christian pilgrims built a religious edifice, now almost completely caved in the sea.

Chapter 1.2.3: Kouklia-Palaepaphos

Introduction

A great deal of confusion has been generated by the name of this site. Known and founded as the city-kingdom of Paphos, this site gained a new name at the moment of the construction of the harbour town of Nea Paphos. The pre-existing town of Paphos – which remained active mainly as a religious centre – was then renamed '*Palaia Paphos*' (Papuci-Władyka 2020, 73; Młynarczyk 1990, 23–25), contracted in Palaepaphos (Iacovou 2019; 2010; Georgiou 2017); however, not all historical sources cite the full name of the settlement, and distinguishing the two towns is often a matter of great complexity (for a full discussion on the topic see Młynarczyk 1990).

The site of Palaepaphos, located in the district of the modern-day village of Kouklia, was established at the beginning of the Late Bronze Age, ca. 1600 BCE, and had acquired a predominant role as a regional polity by the beginning of the 13th century BCE (Papuci-Władyka 2020; Iacovou 2019, 214; Georgiou 2017). It retained the function of administrative and political centre until the 4th century BCE (Iacovou 2023, 63; Crewe, Georgiou 2018, 55; Iacovou 2010). Largely, the prosperity of the town of Palaepaphos in the earliest phases of its long history depended on its landscape, specifically – as was valid for several other Cypriot cities – on the accessibility to raw material resources (copper and wood) and on the presence of a harbour (Papuci-Władyka 2020, 73; Iacovou 2019, 216; Crewe, Georgiou 2018, 64). The location of this fluvial harbour remains unknown to date (Iacovou 2019, 216–218), nevertheless its silting up at some point during the 4th century BCE is cited as the main reason behind the foundation of the coastal site of Nea Paphos (Crewe, Georgiou, 2018; von Rüden 2016a, 13; Iacovou 2014). Palaepaphos represented the last ring of the chain of copper export, which started with extraction of raw materials on the Troodos foothills, exploited the Diarizos and Ezousas rivers as means of transportation, and took advantage of the fluvial harbour of Palaepaphos as gateway to the Mediterranean Sea routes (Iacovou 2023, 63; Georgiou 2017, 212; von Rüden 2016a, 16).

The settlement of Palaepaphos is constructed on a system of plateaus spaced out by steep valleys on a vast area of around two squared kilometres (von Rüden 2016a, 11) (**fig. 7**). According to the findings of the most recent excavations, it appears that these plateaus responded to different needs and functions, and possibly they were not all contemporarily in use.

The Sanctuary of Aphrodite, the main archaeological landmark, is weaved in the urban pattern of modern-day Kouklia and was built on the hilltop of *Alonia* (Iacovou 2023, 66) to answer to the religious, administrative and economic needs of the town. It oversaw the ancient harbour and hosted a number of economic enterprises within its premises (Iacovou 2010). To the North-East of the Sanctuary lies at an elevation of 120 m a.s.l., the plateau of *Marchello*, where the North Gate sits; while to the East it is possible to observe the man-made hill of Laona and the natural acropolis area known as *Hadjiabdoulla*, 112 m a.s.l. Further archaeological areas of interest, mainly tomb clusters and wells, have been located to the South-East in the localities of *Evreti* (an unpublished group of 44 tombs, von Rüden 2016a, 18) and *Teratsoudhia* (Crewe, Georgiou 2018, 53; von Rüden 2016a); a necropolitan area is also located in *Skales* (Karageorghis, Raptou 2016; 2014).

Trench excavations have interested the area of *Arkalon* – where only few Classical remains of earthen architecture (Iacovou 2010) and the tomb complex known as *Spilaion tis Regainas* have been found. A Classical peristyle house was unearthed at the locality of *Evreti* (Iacovou 2019, 209). All the above-mentioned sites were object of archaeological work in the 1950s, although they largely remained unexcavated until the early 2000s.

Before the foundation of Nea Paphos, Palaepaphos functioned as an administrative centre and last post in the trade of copper (Crewe, Georgiou 2019). Once the harbour and administrative facilities were moved to the new settlement on the south-western coast, Palaepaphos remained active as a religious site (Papuci-Władyka 2020, 73), with the temple being destination of pilgrimages until the Late Roman times. The cult of Aphrodite was so strongly associated with the temple in Palaepaphos that a new epithet started circulating for the goddess: Paphian Aphrodite.

Excavation history

The Sanctuary area has always been well visible (Iacovou 2023, 67; von Rüden 2016a, 14) and often became object of interest for travellers since well before the first proper excavations, or even descriptions. Excavations begun in 1888 with the archaeological mission led by D.G. Hogarth under the Cyprus Exploration Fund (von Rüden 2016a, 14). During this first campaign, scattered remains of pottery dated back to the transitional period between MC and LC were unearthed. In the 1950s, the British Kouklia Expedition uncovered LC funerary material in the localities of *Evreti* and *Asproyi*; unfortunately, the results of these excavations remain to date only partially published in form of preliminary reports (Crewe, Gerogiou 2018, 55). A German Swiss expedition led by F.G. Maier, in 1966, resumed working in a vast area around the Sanctuary of Aphrodite, deepening the understanding of the earliest phases of the settlement, other than of other aspects connected to the site (Crewe, Georgiou 2018; von Rüden 2016a, 14; Maier 1984). Excavations of Palaepaphos after the 70s proceeded mostly in the form of rescue works under the direction of the Department of Antiquities. These short-time expeditions uncovered relevant, but fragmentary, evidence for both the early history of the site, and its subsequent developments (see Crewe, Georgiou 2018, 55–56 for a detailed presentation of the excavation history). Between the 70s and the early 2000s, several survey projects have investigated the history of the site, unlocking information concerning the Late Bronze Age levels and the general hinterland (for a complete summary of the expeditions, see von Rüden 2016a, 14–15). In 2002, a large-scale project under the auspices of the Department of Antiquities and led by professor M. Iacovou of the University of Cyprus, started investigating the already known archaeological landmarks in the polity of ancient Paphos, and further worked to enhance the knowledge of the town's history (von Rüden 2016a, 15). This project aimed at acquiring a comprehensive view of the settlement both from a synchronic and diachronic perspective, with a specific interest in the conservation and preservation of the cultural heritage. The Palaepaphos Urban Landscape Project (PULP) has led target excavations, geological surveys and prospections, along with study seasons, acquiring priceless information about the site development.

The starting point of the PULP project was the re-examination of F.G. Maier's interpretation of Palaepaphos diachronic history. Although his recollection and systematic analysis of the evidence excavated in the 1950s and 60s "remains the most valuable guide to the cultural horizons of Palaepaphos" (Iacovou 2019, 210), the recent excavations have refuted his interpretation of the functions and relationships of the monuments he listed, in particular, the site of *Marchello*.

The Sanctuary

The sanctuary of Aphrodite is by far the most long-lived temple of Cyprus (Iacovou 2023, 67), and equally one of the most renowned and famous. Its foundation lays at the end of the Late Bronze Age (ca. 1200 BCE) (Iacovou 2023, 67; von Rüden 2016a,17), around 500 years after the site's foundation; the slow process of abandonment begun during the 4th century CE, with the progressive affirmation and spread of Christianity on the island (Iacovou 2019; Georgiou 2017). The foundation date of the site is documented only by the presence of scanty LBA pottery fragments unearthed in pits around the Sanctuary site (von Rüden 2016a, 17–18); thus, it is best to consider 1200 BCE as a *terminus post quem* for the foundation of the site. Interpretation of this monument has been strongly affected by two relevant biases. The first misconception is caused by the scarce knowledge of the urban fabric surrounding this sacred building: most of the settlement of Palaepaphos is known and documented only by funerary evidence and scarce traces of poorly understood buildings located at a discrete distance from the sanctuary. The connections between these poles and the interrelations between the social, economic and political spheres had remained almost non-investigated until the start of the PULP project. However, even more relevant perhaps, is the second prejudgment. Epigraphic evidence and written sources pointed out the prominent role of the Sanctuary as a pilgrimage destination and as the most influential centre of aggregation of the whole Cyprus. Although this is certainly true, it must be kept in consideration that this role was not assumed any time before the foundation of Nea Paphos, estimated around the 4th century BCE (see following chapters). Before this moment, the temple served the polity of Paphos and retained functions that went beyond the exclusive religious character.

As mentioned in the previous section, Palaepaphos was built on a system of plateaus separated by steep valleys, the sanctuary site occupies the plateau of *Alonia* (Iacovou 2023, 66), which was interested since the earliest phases of Palaepaphos' history by a number of different activities. The earliest use of the plateau, dating to the transitional phase from the Middle to the Late Bronze Age, alongside with the presence of rich burial clusters partially coexisting with the sanctuary, suggest that this hill was possibly the first to see settling activities (Iacovou 2019), and thus must have been close to the harbour facilities, as Palaepaphos was rising as a gateway seascape town (von Rüden 2016a, 16). The site must have been located in direct connection with the fluvial harbour – current hypotheses locate it in the area of *Loures* (Iacovou 2023, 69; 2019) – mirroring the structure at coeval Kition.

The first excavation at the Sanctuary site started in 1887 at the expenses of the Cyprus Exploration Trust. However, the complex architecture and the difficult comprehensibility led the excavators to

abandon the area after just a few months (Iacovou 2019, 206). Improper archaeological methodology adopted by the British excavation led to further damage to the already decaying temple. Before 2002, no other significant excavations were conducted in the area (Iacovou 2019, 208), and most of the work was focused on an extensive publication of all the epigraphic and literature evidence collected in and around the temple (other than the complete publication of the Cyprus Exploration Trust, T.B. Mitford and O. Masson published several collections of epigraphic record between 1950s and 1990s; see Iacovou 2019 for full references). Aside from the Medieval Manor House, few Roman buildings, and the *ashlar* temenos, no other building is visible on the sanctuary hill.

In regard to the architectural structure, the complex stratigraphy and the scanty traces of the earliest phases of the temples have led to different tentative interpretations and reconstructions of the temple original plan. A recent hypothesis of reconstruction, illustrated by Dr. A. Georgiou (2017, 213–214), includes two different spaces: a large open temenos and a colonnaded building, most likely roofed, located to the North. The fine masonry, consisting of massive limestone orthostats, as well as the material associated to this structure, suggest a high-end construction. The temenos wall is preserved to a maximum length of 28 m and to a height of 2 m (von Rüden 2016a, 16), highlighting the impressive construction effort behind this religious site. The foundation of this site and the contemporary Temple 1 in Kition (Iacovou 2019; Georgiou 2017) are remarkable proofs of the empowerment and flourishing economy of Cyprus – or at least of the polities of Paphos and Kition – during the so-called "crisis years" that saw many of the Mediterranean kingdoms and Empires perish.

Before the 4th century BCE, no epigraphic or written evidence except for Homer (*Odyssey* 8.363) identifies the worshipped goddess with Aphrodite (Georgiou 2017). In the pre-Ptolemaic inscriptions, the goddess is referred to as *wanassa* or *theos*, terms used eventually by the kings of Paphos to highlight their double function of king and priest (Iacovou 2019). It appears evident that the original function of the temple was that of an urban sanctuary, rather than "a pan-Cypriot […] site of pilgrimage" (Iacovou 2019, 215).

Marchello

Partial excavations on the plateau took place between 1950 and 1955 under the British Kouklia Excavation (Kopanias 2021) and during the Swiss-German expedition led by F.G. Maier in the 1980s and 1990s. Part of the unearthed structures were erroneously identified as a rural sanctuary. After conducting a geological prospection study, the PULP project resumed field seasons on the site of *Marchello* in 2006, unearthing large part of an entrance gate and a fortifying wall. A preliminary hypothesis wanted this gate, along with the fortifications associated, to be connected to the fortifying wall uncovered in the *Hadjiabdoulla* area (Iacovou 2019). Remarkable similarities, both in terms of masonry and dimensions, easily led to this interpretation. However, the excavation seasons of 2006 and 2007 revealed how these two fortifications systems could not be linked, as they followed a different orientation and would have needed to cross a very steep valley. This

construction seems to be connected, instead, with the so-called rural sanctuary excavated before 2000, which thus was correctly identified as an urban sanctuary (see more on the PULP project website at https://websites.ucy.ac.cy/ariel/). Underneath the foundation of the fortification wall lay a series of LBA tombs, which serves as a *terminus post quem* for the dating of the *Marchello* complex. A plausible date of foundation was believed to fall between the Late Archaic and the Early Classical period (Iacovou 2019), while the site was likely dismissed around 500 BCE after a violent siege. The sacred and secular buildings were never rebuilt, signifying that their function was no longer needed or had been taken over by a different site. This hypothesis is further strengthened by the rise of the acropolis of *Hadjiabdoulla*, just 1 km from *Marchello*, as main administrative and political centre. The violent confrontation registered at *Marchello*, could have thus mirrored a change in the town's leading force.

In September 2021, the National and Kapodistrian University of Athens (NKUA) took over the excavation project, uncovering material associated with the foundation strata dating as early as the Late Cypriot II, between the 17th and 18th centuries BCE (Kopanias 2022; Kopanias 2021). The preliminary character of the reports does not allow for further discussions on the use and construction of the site, which was not among the selected sampled areas for this PhD project. However, it is noteworthy to mention that the first press releases available on the website of the Department of Antiquities of Cyprus announce the discovery of a 12th century tomb with two individuals, the study of whom might provide insightful information concerning the socio-economic situation in Palaepaphos during the so-called "crisis years".

Hadjiabdoulla

The monumental administrative centre of *Hadjiabdoulla* was first unearthed by the British Kouklia Expedition in the 1950s. However, serious structural damages due to the conditions of preservation prompted the start of a new systematic excavation on the Acropolis hill. Extensive digging started in the area of the preceding excavations, and new trenches were opened around the so-called Fortress in order to identify structures related or associated with it. The data presented in this chapter have been collected from the press releases, the PULP project website (https://websites.ucy.ac.cy/ariel/) and personal communications from the excavator, professor M. Iacovou.

On this plateau two main administrative centres lie in proximity one to the other, and possibly represent the rise of different elites. The *ashlar* building, called Fortress, dates to the Late Bronze Age period. The attribution to this chronological phase was exclusively based on the architectural fashion; however, a test trench opened by the PULP excavators inside this area, where LC material evidence was unearthed (Iacovou 2019), confirmed the accountability of the LC dating. The second administrative building (**fig. 8**) can be dated to around 500 BCE, contemporary with a fortress-like structure on top of the neighbouring terrace of *Laona* (Iacovou 2019, 223–225; for further information on the site see *infra*). This former building, also called Western Complex, was a storage and industrial multifunctional centre. A vast assemblage of storage vessels, a bathtub with a

complete drainage system, olive presses, a large deposit of murex shells, as well as other industrial-like features have been unearthed in the identified rooms (as of 2022, at least ten rooms have been identified and excavated).

The *Laona* rampart

The natural plateau of *Laona* rises at an elevation of 105 m a.s.l. It is located 70 m to the North of the *Hadjiabdoulla* terrace and was never identified as an archaeological construction, until the geological prospections and excavations of the PULP started in 2009. The 105 m of natural sediments are, in fact, capped by additional 9 m of man-made mound, generating a *tumulus* structure completely unfamiliar to the archaeological record of Cyprus (Gkouma *et al.* 2021; Lorenzon, Iacovou 2019). The man-made mound is formed by a sequence of terra rossa strata and local geological marl, all gathered from areas in the proximity of the site. The terra rossa layers contained a small percentage of artefacts ranging in date from the LBA to the 3rd century BCE, offering a *terminus post quem* for the construction of the hill (Gkouma *et al.* 2021, 605; Lorenzon, Iacovou 2019, 351).

During the excavation campaign of 2014, under the layers of the 3rd century geological material, a monumental rampart built in mudbricks has been identified and dated to a period comprised between the 6th and 5th century BCE (Lorenzon, Iacovou 2019, 319), thus contemporary to the second administrative building on the *Hadjiabdoulla* hill. This fortification's elevation varies according to the natural hill conformation, but the discovery of two staircase has led to hypothesize the presence of towers. The architectural layout is as follows: a stone foundation of limestone blocks worked only on the outer surface and joint by red clay is topped by several rows of mudbricks of apparent standard dimension. The shell wall appears empty inside, with a filling constituted exclusively of marl (Gkouma *et al.* 2021).

A pilot study on the earthen architecture of the fortification system, in particular on the mudbricks (Lorenzon, Iacovou 2019), unlocked two relevant information related to this structure: the mudbricks were mass-produced following local traditions, meaning that a central administrative power was in control of financing and administrating the construction; no evidence of repairs were documented, highlighting a short life span for the rampart, which was possibly already dismissed during the 4th century BCE.

Leaving the earthen fortification system aside, the construction of such an impressive feature like a 9 m mound is an unmistakable sign of deep knowledge of the geological landscape, and centralised administrative efforts (Gkouma *et al*. 2021, 601). The estimated amount of material imported on the site for the completion of the mound is around 9,500 m³ of soil and marl (Gkouma *et al.* 2021, 605), a quantity that certainly required careful planning.

Keeping this into consideration, it is possible to hypothesise that the fortification system with the impressive rampart and watchtowers was built contemporary to the administrative complex on *Hadjiabdoulla* and was likely part of a monumental project promoted by the same ruling dynasty (Gkouma *et al.* 2021, 606), possibly the last to rule in Ancient Paphos before the transition to Nea

Paphos. This would also pair up perfectly with the abandonment date, which corresponds to the 4th century BCE, estimated time of foundation of Nea Paphos.
After the abandonment of this fortification complex, a second monument, an uncompleted stone building identified as a pseudo-grave, was built, possibly to divert the attention of eventual grave robber from a possible actual grave (yet to be discovered). The mound itself was then carefully constructed to cover the pseudo-tomb and to possibly function as funerary monument, no earlier than during the 3rd century BCE. If the pseudo-grave, found completely empty, was part of the same architectural plan as the mound, it would be logical to suppose it is also dated to the same period. In regard to the mound building system, M. Gkouma reconstructs a sequence of construction phases based on the micromorphological analysis of the deposited sediments (Gkouma *et al.* 2021, 612–613). Her reconstruction lists a minimum of three macro-phases: the first step was the construction of the pseudo-grave and a relatively small red-soil mound on top of it; then, the central part of the *tumulus* was built following the freefall and wetting techniques and using a system of inclined ramps to contain the soil; the last phase included maintenance and repairs to the mound.
Interpreting this monument is still a tough challenge. Some elements must be underlined: *tumuli* are allochthonous monuments, unprecedented in Cyprus. The specific mound of *Laona* was carefully pre-planned, and it was built by skilled workers with consistent knowledge of the materials with which they were working. Finally, the *tumulus* was built in an uncertain period of time, which does not pre-date the 3rd century BCE. The function and the scope of such a demanding construction are still subject to change with the proceeding of archaeological excavations.

Chapter 1.2.4: The Hellenistic-Roman Theatre in Nea Paphos

Introduction and excavation history

The Hellenistic Theatre is located in the area of Fabrika Hill, the North-Eastern quarter of the ancient city of Nea Paphos, near to where the N-E entrance gate to the city is supposed to have been located (**fig. 9**). The theatre has been in function as a spectacles' venue for almost seven centuries (Lindberg 2017; Barker 2015, 38; Green *et al.* 2015; paphostheatre.org) and was used continuously for different purposes for at least three more. At its maximum capacity, the theatre could host up to 8500 viewers distributed on a length of 90 m from side to side (Lindberg 2017, 313; Barker 2015, 35).
The first excavations on the site of the Hellenistic Theatre date back to the 60s, when archaeologist K. Nicolaou discovered the top rows of the seating (Nicolaou 1966, 583–584). The presence of the theatre, however, remained merely a hypothesis until 1987, when the University of Trier opened a test trench in the orchestra area (Barker 2015, 33–34). The Paphos Theatre Archaeological Project, an Australian research team, resumed excavations in 1995, and has since directed over two decades of successful working seasons. The methodology adopted by the PTAP project involves stratigraphic excavations in trenches, although the whole area is nowadays mostly uncovered (paphostheatre.org).

The plan of the Nea Paphos' theatre differs from the standard Hellenistic models – characterized by a horseshoe shape – by displaying a semi-circular implant (Barker 2015, 34); it is likely that the original shape followed the Hellenistic tradition and was modified under development during the 1st century BCE, in order to follow the Roman standards (on the theatre Hellenistic phases see Green *et al.* 2015). The date of foundation is still under discussion up to this day. Pottery findings in the area have been dated as early as the 4th century BCE, suggesting that the theatre was built for a settlement pre-dating the foundation of Nea Paphos, the presence of which has been long hypothesised and discussed by archaeologists and historians (Green *et al* 2015, 321; Hayes 1991, 5; Młynarczyk 1990, 76, 85–94). Furthermore, a carved inscription unearthed on top of the cavea has been dated by epigraphists to around 300 BCE (Green *et al.* 2015, 323). More definite data concern the abandonment phase of the structure: after several major and minor refurbishments and reworks, the theatre was definitively abandoned during the 4th century CE, most likely due to heavy damages caused by a devastating earthquake (Barker 2015, 38). The increasing spread of Christian religion might have contributed to the decline of the theatre venue, as the difficult relationship between these two institutions is well documented in several areas of the Empire (Davis 2010). After the abandonment, the theatre was used as primary source for building materials, especially for the construction of the neighbouring Chrysopolitissa Basilica. Quarrying activities ceased around the 7th century CE, as testified by the complete absence of deposits between this latter phase and the Medieval one. During Medieval times, the site on Fabrika Hill was interested by extensive productive activities, with the presence of structures related to metallurgic activities and even a sugar can factory.

Although the basic architectural plan of the theatre did not undergo any fundamental change over the six and a half centuries of life, the spectacles' venue often underwent minor repairs, refurbishments, or restyling, according to changes of purpose or fashion. Dating these several phases was possible thanks to the analysis of associated materials, especially pottery and epigraphic inscriptions.

Despite the theatre is still known as "Hellenistic", not much of this first phase is currently visible (Barker 2015, 38; Green *et al.* 2015, 320).

The foundation

Archaeological evidence suggest that the theatre might have been one of the first building to see the light in the newly found settlement of Nea Paphos. As mentioned in the previous chapter, legend says that Nea Paphos was founded by King Nikokles as the new capital of his kingdom, after the preexisting fluvial harbour in Palaepaphos had silted up (Barker 2015, 31). However, archaeologists and historians had argued about the possibility of a Ptolemaic foundation during the early decades of the 3rd century BCE (Green *et al.* 2015) or even the possibility of an antecedent pre-settlement (Papuci-Władyka 2020, 73). Aside from the discussion concerning the foundation of the town, several elements point to the early construction of the theatre: first and foremost, the deviating orientation of the structure from the Hippodamian road grid (Barker 2015, 59). Following

the geological profile of the Fabrika hill, the theatre was built directly facing the ancient harbour (Barker 2015, 34) and with an approximately 10 degrees angle from the main road grid. It was located in close proximity to the North-Eastern entrance gate to the city, where the processional road leading to the sanctuary of Aphrodite would have started. This strategical positioning inside the urban fabric reveals the clear emphasis put on the theatre building for the settler(s), whether they be king Nikokles or the Ptolemies.

Up to date, archaeologist do not dispose of enough elements to certainly date the foundation of the theatre. It is well known, both from archaeological record and from written sources, that theatre as an institution was familiar to Cypriots since as early as the 4th century BCE. In fact, a conspicuous production of theatrical terracotta (Barker 2015, 36; Green *et al.* 2015, 323), as well as ancient texts (Plutarch*, Life of Alexander* 29), testify how theatrical performances were popular in Cyprus in this period. An inscription located in the upper part of the cavea has been identified during the excavations, and it possibly represents the key element to date the earliest construction phase of the theatre. Although it is no longer possible to piece together the carved letters, palaeographic studies confirm that the script is dated to around 300 BCE. The location of the inscription, towards the upper part of the seating rows, could also suggest the extension of the theatre at the time of foundation, with the additional seating rows located on top dating to successive expansions. In general, the dimensions and shape of the first building remain in most part unknown today. Traditionally speaking, Hellenistic theatre presented a horseshoe shape, while the current Paphian theatre displays a semi-circular one (Barker 2015, 34). Following the strata sequence, it appears plausible that the semi-circular shape came to be not earlier than the 1st century BCE, likely in connection to the extensive repairs after the earthquake of 15 BCE. Whether it had a horseshoe or linear shape before, however, is yet to be defined. Straight-lined seats with back supports have been considered persuasive evidence of the cavea and orchestra having a rectilinear shape.

Very little is left of the original stage building too. A series of post-holes and the lack of foundation walls related to this phase have led the excavators to assume that the first stage building was constructed with perishable materials – possibly wood, considering timber was one of the main local resources (Papuci-Władyka 2020, 73; Iacovou 2019, 216).

The Hellenistic phases: influence of the Ptolemies

In 1927 a now lost inscription was found in the proximity of the theatre (Greene *et al.* 2015). The inscription, located on the base of a statue, belonged to the Guild of Artists of Dionysus, and dated to ca. 142 BCE. This is key evidence to support the existence of an active and flourishing theatre community and culture in Cyprus already in the 2nd century BCE. To further corroborate this hypothesis, large deposits of ceramic material dating back to half-2nd century BCE have been unearthed in concurrence with the embankment walls of the *cavea* (Greene *et al.* 2015, 325). The full architectural prospect plan of the theatre during this phase, however, largely remains hypothetical. The *cavea* was certainly enlarged, as testified by the presence of the above-mentioned embankment walls. The construction of this particular feature was a strategic solution to the scarce

accommodating possibilities due to the relatively reduced dimensions of Fabrika hill. As a matter of fact, Hellenistic theatres, differently form Roman ones, were hewn directly from hills, creating issues of lodging for a large amount of public in case of naturally restrained ridges. To resolve this hitch, the western and eastern sides were indeed built using *analemmata* and containment walls (Barker 2015, 35).

Concerning the shape, parallels with other Hellenistic theatres, including the ones in Alexandria, Philadelphia (modern day Amman, Jordan) and Megalopolis have been noted (Greene *et al*. 2015, 328). The shape and size of the orchestra remain unknown; a thick soil stratum lying beneath the 3rd century CE floor level is the only remnant of the Hellenistic pavement in the orchestra area.

To this period dates the so-called Charonian tunnel, a passage that run underground from the stage building until the central area of the orchestra. This mechanism, possibly used as gimmick for the appearance of characters on stage (Barker 2015, 40), has been identified in several other Hellenistic theatres. In all cases, the usage and abandonment of the passages is still largely under debate, as the relative chronology associated with them. The Charonian tunnel in Paphos was sealed during the Augustan refurbishment of the theatre, and later reused as part of a drainage system in the 3rd century CE, when the theatre was turned into a venue for *naumachiae*. Likewise, the pipelines were reused, as proved by the presence of pre-existing limescales. At any rate, they do not pre-date the 3rd century CE.

The architectural profile of the tunnel is indicative of the possible orientation of the stage building, which was built in stone, although the foundations are not preserved. Information concerning this building derive from scattered architectonic elements unearthed in the southern area of the orchestra. The limestone blocks present in some cases traces of stucco decoration (for instance, see inv. 3767). Alexandrian decorative style is distinctively visible in these fragments, strengthening once again the parallels between Ptolemaic theatres and the Paphian one (as noted by Dr. C. Barker these elements remind of the architecture at the neighbouring site of the Tombs of the Kings – see Barker 2015, 40). The stage building hypothesised from the analysis of these architectural elements consists of a two-storey stone building with movable wooden panels and rich, colourful stucco decorations. The hypothesised orientation of the stage is similar to the one of the Augustan phase. In particular, the Augustan renovations closely followed the architectural model of the Hellenistic phases, leading to questions concerning the dating of the above-mentioned architectural elements.

<u>The Augustan phase</u>

The Roman Age in Cyprus is characterized and constellated by a series of devastating earthquakes that struck the island in different moments, damaging in particular the southern coast. One of these first cataclysms occurred in 15 BCE (Lindberg 2017, 313; Barker 2015, 40; Green *et al*. 2015, 324). The damages in Paphos were so relevant that financial aid from Emperor Augustus was deemed necessary. After the renovations and refurbishments, the town gained the epithet "Augusta". At this point, Paphos was already the administrative centre of the Roman territory and will later become the capital of the Senatorial Province.

The damages caused by the earthquake interested mostly the western *analemma*. The containment wall collapsed and was replaced by a new strengthened and thicker wall, which resulted in the slight greater than semicircle shape. Other formal changes have not been clearly identified, as possibly they mirrored the Hellenistic style.

The Antonin phase

The year 126 ca. CE was interested by a second seismic event, which resulted in the almost complete destruction of Paphos. Under the auspices of Emperor Antoninus Pius, the settlement – and particularly the public areas – were refurbished and embellished with precious materials, including marbles imported from North Africa, Italy, the Aegean, and Anatolia. The scale of import and export of marble – a resource scarcely available in Cyprus – reflects the world-scale of commerce reached during Imperial Roman times (Barker 2015, 42).

The theatre was greatly enriched, and the restoration works were commemorated in a surviving inscription dating back between 136 and 142 CE. The inscription mentions both Emperors Antoninus Pius and his successor, Marcus Antonius; the marble slab, possibly part of the stage building façade, was retrieved during two different excavation seasons, respectively in 1916 and 2002 (Barker 2015, 43–44). The size, quality and workforce invested in this project highlight the key role Paphos played for the Romans in managing oriental ship commerce and the island's administration.

For what concerns the theatre building, archaeological evidence testifies an expansion of the capacity of seats, obtained through extending the eastern part of the *cavea*, towards the Nymphaeum. At this point, both the Nymphaeum and the Hippodamian grid fully existed, causing a complex architectural development on this side of the theatre, which surely required careful and skilful planning. On top of the *cavea*, *vomitoria* were added to ease the access in and out of the theatre. Up to date, only the western one has been unearthed and studied. The stage building was enlarged and consisted of a two-storey stone building covered in marble slabs and marble veneering stuccoes. The *parodoi* were closed with barrel vaults – typical of Roman architecture – and decorated with frescoes partially surviving up to date. The theatre reached its maximal seat capacity during this phase.

Final stage

Following a common trend in the Roman Empire, during the 3rd century CE the purpose of the theatre was altered, privileging hosting spectacles over dramas (Barker 2015, 44). The shift in performance preference required significant modifications and repurposing of the theatre traditional elements. The theatre was designed to host *naumachiae*, the famous small-scaled naval battles. For this reason, the marble floor was substitute by a thick layer of waterproofing pink "cement" (as to why the noun is under quotations, please check the Introduction chapter). A parapet wall, approximately one metre tall, was erected between the orchestra and the *proedria*, in order to protect the audience sitting in the front rows. The *parodoi* were partially sealed and used for the

management of water flow inside the orchestra. Access to the theatre was possible from the top of the hill or from the *vomitoria*. The Charonian tunnel was repurposed to function as drainage system, with ceramic pipelines inserted vertically in the narrow passage. This refurbishment is possibly the last one before the theatre slowly fell in disuse and was abandoned.

Abandonment and reuse

Between 365 and 370 CE Cyprus is interested by severe and constant seismic activity, which proved to be particularly detrimental for the southern coastal sites like Nea Paphos and Kourion (Barker 2015, 45; Ambraseys 2009). Although previous earthquakes had already damaged the theatre (see the events of 15 BCE and 126 CE mentioned above), the socio-economic situation in the IV century CE had significantly changed, compromising the rebuilding of the theatre. As mentioned by Dr. C. Barker in his summary of the 20 years of excavation at the theatre site, 4th century Paphos was facing a period of "economic downturn" enhanced by the designation of Salamis as new capital of the Roman province (Barker 2015, 45–48). Furthermore, the ascent of Christianity in Cyprus played a significant role in the missed reconstruction of the Paphian theatre. The building slowly fell in disuse and the refined and precious building materials were subsequently employed in the construction and embellishment of other neighbouring sites, including the Chrysopolitissa Basilica.

The town of Paphos faced centuries of decline, maintaining a marginal role while the main economic, politic, and commercial activities took place in Salamis, the now capital of the island. The situation changed with the occurrence of the crusades. During the 11th and 12th centuries, the harbour of Paphos regained the status of central trade post in the route towards Jerusalem (Barker 2015, 48). The increased commercial activities resulted in a flourishing manufacturing industry that found its prosper ground in the now soil-covered theatre site. Around this time, the hill and area surrounding it gained the name "Fabrika", which comes from the Medieval Latin word "*fabbrica*" meaning "factory". Farmsteads, a glazed pottery workshop and other metallurgic activities took place in the premises of the ancient theatre (Barker 2015, 48–50), contributing to a rich archaeological stratigraphy.

This brief parenthesis of "late renaissance" (Barker 2015, 49) ended with a series of earthquakes, which resulted in the silting up of the harbour to only one third of its original size. As the core of socio-economic prosperity of the town had lost most of its capacity, Paphos slowly lost ground in favour of other coastal centres in the island. Nonetheless, settling activities continued, both in the settlement area and specifically in the theatre, up until the first excavations took place in the 1980s. Nowadays, the theatre stands in between of houses and private properties, perfectly nestled in a modern urban patter.

Chapter 1.2.5: Nea Paphos

Introduction

Although the Hellenistic Theatre is part of the archaeological site of Nea Paphos, it represented a stand-alone case for the present research. As a matter of fact, the public nature of the building, along with the extraordinary longevity, allowed to formulate hypothesis on the plaster industry in a diachronic perspective. Other areas of the archaeological site of Paphos did not offer a similar possibility, either due to scarcer documentation or to the lack of long stratigraphic sequences easily accessible. In the case of the *Maloutena* district, especially, the presence of fully preserved Late Roman private structures completed with extraordinary mosaic floors did not allow an extensive excavation of the pre-existing Hellenistic layers. Even in the Agora area, where Hellenistic layers have been successfully unearthed, the amount of securely dated and contextualized plaster samples was not sufficient to draw sound conclusions in a diachronic perspective. This chapter will briefly outline the complexities of the extensive archaeological site of Nea Paphos, a town that offers centuries of history across multiple sovereign, religions, cultures and populations.

Nea Paphos was founded during the 4th century BCE by King Nikokles as the new central harbour town of the region. The pre-existing seat of Nikokles' dynasty was the town of Paphos, located in the modern-day village of Kouklia. There are diverging sources about the foundation history of Nea Paphos: both Strabo and Pausanias refer the foundation to king Agapenor, part of a pre-Hellenistic dynasty ruling over Palaepaphos and also responsible for the foundation of the Aphrodite's temple in this latter site. Arrian and Diodorus, on the other hand, mention Nikokles as a prominent Ptolemaic supporter during the Diadochi wars and they designate his seat in Paphos, likely meaning the harbour town of Nea Paphos (Młynarczyk 1990, 26–27). The first archaeologist to connect the foundation of the town to the figure of king Nikokles is T.B. Mitford (Młynarczyk 1990, 67), who based his assumption on the epigraphic record being written in the Greek alphabet for the first time in the history of the Paphian kingdom. Combining the epigraphic evidence with the written sources mentioning king Nikokles, the outlining picture is that of the last independent king of the kingdom of Paphos, active supporter of Ptolemy in the Diadochi wars and strongly connected to the religious aspect of the Paphian society (he is defined as "king of Paphos Nikokles, priest of Anassa"; Młynarczyk 1990, 68).

Besides the blurred origin of Nea Paphos and the open questions pertaining the death of its last king (Młynarczyk 1990, 72–73), it appears clear how the large, new settlement, counting at its maximum extension about 1 kilometre squared, held a predominant role over the region surrounding. As a matter of fact, a number of important public buildings were erected within and outside of the fortification wall, with impressive architecture and lavish decorations. The site served as main trading port for the easily and readily available geological and mineralogical resources of the region. Nea Paphos boasts access to the copper outcrops on the Troodos foothills, as well as lavish timber forests (Papuci-Władyka 2020, 73).

The site of Nea Paphos, built on the basis of the Hyppodamian road grid, counts six major areas that responded to different functional needs of the city (**fig. 10**): the heart of the town is occupied

by the complex of the Agora-Odeon-Asclepeon, located at the feet of Fanari Hill, the seat of the *strategos* palace and the urban sanctuary of Aphrodite; to the South of the Agora, the residential quarter occupies the topographic areas of *Ktitso* and *Maloutena,* displaying a series of houses and villas dated from the Late Hellenistic to the Late Roman periods; to the N-E of the Agora it is possible to observe Fabrika Hill with the Hellenistic Theatre and several Medieval industrial buildings; lastly, still embedded in the urban fabric is the site of *Toumpallos*, also known as the Garrison's Camp, mainly interested by Early Christian activities. A fortification wall encompasses these areas, while just outside of it lay the harbours and necropoleis. The most relevant cemetery associated with Nea Paphos, at least in terms of impressive funerary architecture and tombs' richness, is the site of the Tombs of the Kings, located about 1 kilometre N-W from the town.
In addition to the above-mentioned archaeological areas, a number of buildings dating from across the Late Hellenistic to Byzantine periods are scattered around the modern-day town of Paphos, amidst and beneath modern buildings. Worth mentioning are the Medieval fortress of Saranta Kolones, and the Christian Basilica of *Ayia Kyiriaki-Chrysopolitissa* dated to the Early Byzantine period – approximately between the 4th 7th century CE (Młynarczyk 1990, 64).
One issue encountered while approaching this vast archaeological site is the fragmentation of the information available. Permits to excavate in Nea Paphos are currently held by four different archaeological teams from Europe and outside; each team focusing on a different area and chronological period, applying different methodologies and answering different questions. Currently, the Agora and part of the *Maloutena* district are excavated by a Polish mission under the initiative of the Jagellonian University (Papuci-Władyka 2020, 92); the Theatre has been studied for over two decades by an Australian team led by the University of Sidney (see Chapter 1.3.5); the Avignon University leads a project on the fortification wall (MafaP); and an Italian mission from the University of Catania excavates the area of the so-called Garrison's Camp.

Excavation history

A detailed chronicle of the excavation history of Nea Paphos has been published in 2020 by E. Papuci-Władyka (2020, 92–102), what is offered here is but a brief summary of a complex and intricate sequence of projects unearthing the structures of this site in a constant and compelling developing socio-political frame. The discovery that led to the opening of excavation seasons in Nea Paphos happened in 1962, when one of the mosaic floors of the House of Dionysus was unearthed. Although the ancient settlement of Nea Paphos had been already recognized at the dawn of the 20th century, until the Department of Antiquities' foundation in 1935, no significant excavations were carried out. After WWII, excavations uncovered important buildings in the area of *Maloutena* (House of Orpheus), *Toumpallos* (an underground sanctuary) and the north-western necropolis now known as The Tombs of the Kings. Despite the results of these trial excavations were significant and key for the interpretation of the entire site, no effective publication was ever printed, and the study of this site is still heavily affected by the lack of detailed information up to date. The Kouklia Expedition, a British mission funded by the University of St. Andrews and the

Museum of Liverpool, initiated a survey campaign through test-trenches in order to establish chronological sequences and the correlation between Nea Paphos and Kouklia (Papuci-Władyka 2020; Młynarczyk 1990, 57). Excavations through trenches located in strategical positions (Basilicas, amphitheatre, harbour and so on) continued until the late 1960s with, again, no significant summary publication (Papuci-Władyka 2020). The survey of the Kouklia Expedition, however, produced interesting results by stating that most of the findings were Hellenistic to Roman in date, and that very little was uncovered after the earthquakes of the 4th century CE. When, in 1962, archaeologist K. Nicolaou started working on the first systematic excavations on Nea Paphos, large part of his work focused on the collection of all the available data in order to create an organic picture of the town, including a first tentative reconstruction of the city plan and fortification system (Młynarczyk 1990, 61; **fig. 11**). The remarkable work of Nicolaou has been reprised and enhanced by E. Papuci-Władyka resulting in a complete and updated overview of the unearthed material and buildings. Nicolaou's excavations mainly interested the House of Dionysos and part of the Agora-Asclepeon-Odeon area, with a particular focus on the two latter buildings.

The residential quarter

The most extensively excavated area is the vast residential quarter comprised between the localities of *Maloutena* and *Ktitso*; other than being the most widely investigated area, this district was also the place of uncovering of the mosaic floor that, in 1962, led to an increased interest in investigating the ancient past of the Paphian town. The mosaics, which also name the roman house they are hosted into, were discovered in the locality of *Ktitso* by the Cypriot mission led by archaeologist K. Nicolaou (Młynarczyk 1990, 59). The Department of Antiquities' excavations proceeded until 1969 under the direction of K. Nicolaou. The results of the excavation have not been published (Papuci-Władyka 2020, 94), leading to a partial interpretation of the outstanding villa. The building has been dated initially to the 2nd century CE, although further analytical work on the mosaics has revealed that the so-called House of Dionysos cannot be dated any time earlier than the 3rd century CE. Nonetheless, beneath the large Roman building, the underneath insula bears signs of inhabitation and construction pertaining to as early as the 3rd century BCE (Młynarczyk 1990, 60), including the most ancient pebble mosaic ever discovered in Cyprus (Papuci-Władyka 2020, 94). The insulae of the *Ktitso* area leave several open questions, mainly due to the only partial publication and to the heavy reconstruction work executed on the House of Dionysos. More readily understandable are the insulae located in the area of *Maloutena*, where up to seven different housing complexes, dated to diverse chronological periods, have been unearthed. Most of these buildings have been excavated by the Polish mission led by the University of Warsaw's Centre of Mediterranean Archaeology since 1965. In chronological order, the first building of this insula is the so-called Hellenistic House (HH), now dated to the Early Roman period, possibly built after the devastating earthquake of 15 BCE. Contemporary and contiguous to the HH lies the Early Roman House. The North-West House (NWH), located in the same insula, dates to the 1st or 2nd century CE. On the ruins of the HH and the NWH, a superimposing massive villa was built around

the 3rd century CE and is nowadays named the Villa of Theseus (VT) after the theme of one of the mosaics unearthed inside the rooms. On the eastern insula across the VT, a smaller and yet richly decorated villa was built during the 4th century CE and abandoned during the 5th; this construction was named after the main decorative theme "the House of Aion" (HA). Erroneously, during the first excavation seasons, the HA was believed to extend until the northern end of the insula; however, successive years of research revealed how the northern part of the complex was a separate building, temporarily named the North-Eastern House (NEH). A seventh residential complex just West of the VT was unearthed between 1982 and 1998 by D. Michaelidis from the Department of Antiquities. The house, initially known as House of Heracles and later renamed House of Orpheus (HO), displayed several phases of occupation, the latest of which dated to the early 3rd century CE. A series of other complexes around the HO have been unearthed, including at least one more undated house. The overview of the residential district is completed by the presence of a Late Roman house, located halfway between the *Maloutena* and *Ktitso* areas, and an Early Christian one.

Fanari Hill and the Agora-Odeon-Asclepeon complex

Although in terms of extension and decorations very few buildings of Nea Paphos could rival the residential quarter, a second relevant area of excavation is the Agora-Odeon-Asclepeon complex, located on the foothills of Fanari. The Fanari, or Pharos, Hill has been strongly eroded throughout the centuries and nothing of the ancient structures located here remains visible today. Furthermore, the presence of the modern lighthouse has made archaeological investigations on the hill considerably more complicated.

Architectural and decorative parts of a temple, compatible with what the ancient sources described, have been collected scattered on the flanks of the hill (Papuci-Władyka 2020; Młynarczyk 1990, 202). The sacred structure has been associated with a temple in honour of the goddess Aphrodite, however the scarce documentation concerning the architectural fragments retrieved does not allow for a more in-depth interpretation of the chronology of this structure. The association between the religious building and the cult of Aphrodite, reportedly advanced by I. Peristianis, was solely based on the strategic placement of the temple, while no archaeological data support this interpretation (Młynarczyk 1990, 203). Archaeologists believe that the *strategos* palace would have been located on this hill, overlooking the Agora and the harbour (Papuci-Władyka 2020; Młynarczyk 1990, 204-205), and J. Młynarczyk (1990, 59) mentions "Hellenistic remains of a monumental nature" on the site, highlighting the presence of passages and cisterns connected to these.

On the south-eastern flank of Fanari a series of three structures were uncovered by K. Nicolaou during the campaigns of 1968-1980 (Papuci-Władyka 2020, 98; Młynarczyk 1990, 63). His work focused on two of the buildings of the complex, the Odeon and Asclepeon, with the former being subjected to heavy reconstruction to host public performances. Nicolaou did not uncover extensively the Agora, which remained known only by a few trenches dug between the late 70s and the 80s. This complex was even erroneously dated to the 2nd century CE and identified as a

gymnasium (Młynarczyk 1990, 63 and 213). The Asclepeion-Odeion complexes were built directly over the bedrock signifying the absence of a pre-existing phase or the complete clear out of it (Młynarczyk 1990, 64). In 2011, the Paphos Agora Project officially started and resumed work in the square, with the bigger scope of understanding this key building for the life of ancient Paphos. The Jagellonian University excavations initially focused on the earlier stages of the Agora, aiming at uncovering the suspected Hellenistic layers covered by consistent Roman architecture. The excavations proceeded, and still proceed, in three main trenches located, respectively, in the central part of the Agora, in the East Portico, and in the southern entrance to the square. In 2015 a fourth trench was opened in the South-East corner of the Agora, intending to later unify it with the East Portico one, uncovering the entirety of the eastern *stoa*. The project is still undergoing excavation with some of the material or more recent discoveries not entirely published. The results presented in this thesis, especially considering the archaeological side, are to be considered preliminary and thus subject to interpretative changes in the future.

One of the major points of the project was the establishment of a reliable chronological sequence for the site. The nearby *Maloutena* area had been subjected to a pottery typology study, at least for what concerned the Hellenistic phases. These pre-existing data were compared with the unearthed pottery and coins of the Agora, and, in combination with stratigraphic analyses it was possible to revise the chronology and define a time frame for the construction and development of the Agora. It is important to note that no building dating later than the 2nd century CE has been unearthed yet, and the Late Roman and Byzantine material is exclusively consisting of pottery and movable architectural pieces. The results of the PAP studies concerning the chronological phases of the Agora are summarized in the following table. From this schematic summary it is evident that the square was interested by building activities since as early as the 4th century BCE and was kept in use – with different purposes and functions – until at least 649 CE. The agora specifically is squared in shape, it had porticoes on all sides and a central building in the middle of the square. A series of other facilities were associated with the porticoes, although only a minimal part of them is today under excavation, as the other three were covered by modern traffic road for tourists. Recent excavations established a foundation date for this complex during the 2nd century BCE (Papuci-Władyka 2020, 75).

Toumpallos

In 1988 an Italian archaeological mission from the University of Catania begun work on the area of *Toumpallos*, on the north-eastern part of the old town. The site was initially interpreted as a Ptolemaic Garrison's Camp dated to the mid-3rd century BCE (Młynarczyk 1990, 111), hence the alternative name often provided in publications. However, excavations highlighted elements compatible with a religious area, possibly in association with the cult of Apollo. The site is still partially published, and significative information regarding its chronology are still under discussion (Papuci-Władyka 2020). Epigraphic evidence associated with the existence of the garrison's camp and a gymnasium have been retrieved in the archives of the temple of Aphrodite in Palaepaphos

(Młynarczyk 1990, 112). In regards of the possible location of the gymnasium, K. Nicolaou had identified an optimal spot in the area known as *Loukkarka* and currently occupied by the Agora (Młynarczyk 1990, 213). There are no conclusive evidence as to where this structure might have been placed in Nea Paphos, it is worth mentioning that only one gymnasium has been unearthed in Cyprus, specifically in Salamis (Młynarczyk 1990, 213).

Necropoleis

There are several funerary areas associated with Nea Paphos, and – as most often happens with necropolis – they have been systematically excavated during the course of rescue operations (Młynarczyk 1990, 65). However, one astonishing funerary area lies about one kilometre North of the city wall, hosting several funerary buildings from the Late Hellenistic to the Roman times so majestic that they earned the nickname of "Tombs of The Kings". The tombs present singular or multiple underground chambers accessible through a long *dromos* or steep staircases; on the outside carved stone buildings lavishly decorated with stuccoes stand out against the modern sandy, dry landscape. The burials contained rich grave goods, which highlight the presence of a powerful and wealthy elite in ancient Nea Paphos. This site, formerly known as *Paleokastro* was excavated since 1977 by the Department of Antiquities, under the leadership of S. Hadjisavvas (Młynarczyk 1990, 64).

Other funerary clusters have been identified in the localities of *Ammoi* and *Glyky Nero*, in the upper city and to the East of the town fortifications. The latter necropolis is believed to have served a Hellenistic settlement pre-existing the foundation of Nea Paphos by King Nikokles (Papuci-Władyka 2020; Hellenistic findings also mentioned in Młynarczyk 1990, 65), although according to J. Młynarczyk (1990, 65) a built tomb of the Imperial Roman period was also discovered on site. Additional Roman tombs have been discovered in the vicinity of the *Glyky Nero* site, close to the Hassandjik stream (Młynarczyk 1990, 65).

Between 1951 and 1952 excavations led by the Museum of Paphos uncovered the necropolis of *Ayios Lambrianos*, in the Fabrika Hill area (Młynarczyk 1990, 57), dating the hypogeum to the Hellenistic period. Successive campaigns extended in the area of the Garrison's Camp and have now been reprised by the University of Catania, to which goes the merit of recognizing Early Christian catacombs in the site.

Period /relative chronology	Absolute chronology (with the earthquakes[62] which could have had a strong impact on the city's development)	Architecture of the Agora — main development phases[63]	Some basic observations resulting from PAP's research
Transitional	Late 4th/early 3rd century BCE	Erection of Building B — phase B1 (?)	LCl pottery together with H
EH	3rd century BCE	Building B — phases B1 and B2 Erection of Building A (?)	LCl pottery disappears by the mid-3rd century. Increasing number of CCW pottery
MH	2nd century BCE	Building A Erection of East and South Porticos	CCW most common
LH	Late 2nd century – ca 30 BCE	End of Building A Erection of Building C East Portico South Portico	CCW still common
ER	30 BCE – 2nd century CE		With sub-phases clearly visible in architecture's development
ER I	27 BCE – 68 CE Julian-Claudian dynasty 17/15 BCE earthquake	East Portico South Portico	The Augustan period is best captured in architecture and especially in its connection with the 17/15 BCE earthquake and rebuilding of the city. The Augustan period is characterised by the presence of TW pottery whose production originates in the H period (mainly CCW) along with pure R pottery (mainly TS).
ER II	69–96 CE Flavian dynasty 76–77 CE earthquake	East Portico South Portico	Scanty architectural remains
ER III	96–192 CE Antonine dynasty 126 (?) CE earthquake	End of ER III phase at the Agora, end of East Portico — probably after the earthquake of 126 (?) CE	There are no architectural remains in the PAP's research on the Agora after Hadrian's reign[64], but later pottery has been discovered
MR	193–284 CE Sewers dynasty and the Crisis of the Imperium		Small amount of pottery
LR	284–491 CE Several earthquakes in 4th century CE		Much more pottery, especially amphorae, than in the 3rd century
Byz	491–649 CE		Presence of 6th century pottery, rather scanty 7th century material

Harbour or Harbours?

To the South of the archaeological park the city harbour lies underneath the modern shoreline. This site has been interested by an extensive American survey project between 1993 and 1996, called the Paphos Ancient Harbor Exploration Project. The results of this study were never fully published and no conclusive point, beside the subdivision of the port in distinct parts, were ever outlined. According to archaeologist J. Młynarczyk (1990, 177) during Hellenistic times, Nea Paphos had two ports serving different purposes: one was to fulfil the commercial needs of the town, while the second was dedicated to war operations. Researchers have been suggesting a possible additional harbour in the north-western bay (Młynarczyk 1990, 177), area currently under the investigation by a joint Polish French team (Papuci-Władyka 2020, 101).

For what concerns the Hellenistic harbour, no buildings have been retrieved up to now (Młynarczyk 1990, 182). The monumental constructions unearthed belong to the Roman or even Late Roman period; although one must consider it was a frequent practice to restore buildings after earthquakes (see the above chapter on the theatre). Another pressing issue concerns the lack of a visible lighthouse.

In the reconstruction of the Hellenistic layers of Nea Paphos, J. Młynarczyk (1990, 183) brings attention to an interesting aspect concerning the dimensions of the port of Nea Paphos. The whole complex occupies an area of about 0.23 to 0.24 square kilometres, which is relatively small and not comparable to the Egyptian ports such as Alexandria. However, in relation to the total dimension of the settlement, the ratio between harbour area and town area in Nea Paphos is very close to the Alexandrian one. This consideration alone highlights the relevance of the Cypriot settlement even in the earliest phases of its foundation.

Chapter 1.3: Geological Context

As visible from the geological maps of Paphos (**fig. 12**), the vast majority of the sites considered on this thesis lays on Pleistocene terrace deposits, consisting of calcarenites, sands and gravels. Solely the site of Palaepaphos, in the proximity of modern-day Kouklia, lays on a Middle Miocene Pachna formation area, where chalks, marls and calcarenites are predominant. Other than these main geological deposits, there are a number of other formations located in the vicinity of the archaeological sites, including the Lower Miocene Pachna formation, the Upper Cretaceous Kannaviou formation, the Agyos Photios and Diarizos groups (respectively Middle Cretaceous and Middle Triassic), the Lefkara formation, and Holocene Alluvium and Colluvium deposits. These specific sedimentary formations include rocks such as chalks, marls, reef limestone, recrystalised limestones, pillow lavas and cherts.

Limestones

As limestone is a widely available commodity around the South-Western part of Cyprus, a geological survey to identify and sample as many different typologies of limestones as possible was conducted. During the survey, an area of approximately 5 km radius from the sites was circumscribed; modern-day mining sites were identified, and samples were collected from the surrounding areas.

The majority of the collected samples consist of biomicrites (**fig. 13**) with significant presence of shells, specifically planktonic foraminifera and corals. Inclusions of metamorphic rocks are often present, particularly serpentine; radiolarian chert, quartz and feldspars are other common components. Clay infills are occasionally spotted, mostly due to the deposition area being characterised by terra rossa soil. The macroscopic appearance of the samples, and especially the colour(s), frequently varies; overall, this type of limestones is slightly brittle, relatively light, and quite porous.

A smaller percentage of samples, on the other hand, corresponds to micritic, fine limestone with little to no inclusions, nearly purely made of calcium carbonate (**fig. 14**). These samples are usually denser and more compact, with all the pores completely recrystallised by large sparitic calcite crystals. Macroscopically, these samples appear as hard, heavy, and dense rocks with a dusty consistency typical of chalks.

Gypsiferous stones

The gypsum deposits closest to the archaeological sites are located in the Upper Miocene Kalavasos formation, in the circum-Troodos area. Both the alabaster and selenite gypsum variations appear frequently and share similar properties. The gypsiferous stones are macroscopically characterized by a white to light-grey colour and large crystals that immediately distinguish them from the surrounding rocks. Microscopically, the samples are composed of pure gypsum with occasional flakes of anhydrite, distinguishable thanks to the high refractive colours in XPL (see **fig. 15**).

Fossils and palaeontological data

The paleontological record in the area shows a constant presence of microfossils in the calcareous stones. The vast majority of the formations of Cyprus was formed in marine environment; thus, the fossils belong to the marine flora and fauna. Sediments in the Circum Troodos terrain contain high quantities of radiolarians, which are also present – although in lower amounts – in the Lefkara formation. However, this latter terrain is better characterized by the presence of abundant foraminifera of diverse species (Globorotalia, Globigerina, Globigerinoides, Globoquadrina). Pachna formations are rich in foraminifera, but also present a higher presence of macrofossils, mainly bivalve, gastropods, and echinoids; occasionally, larger fossils such as fish bones and marine flora remains can be spotted. The reef limestones in the Terra and Koronia deposits of the Pachna formation are especially rich in macrofossils, featuring corals such as bryozoans – detected in significant quantities in the archaeological samples.

ILLUSTRATION PLATES

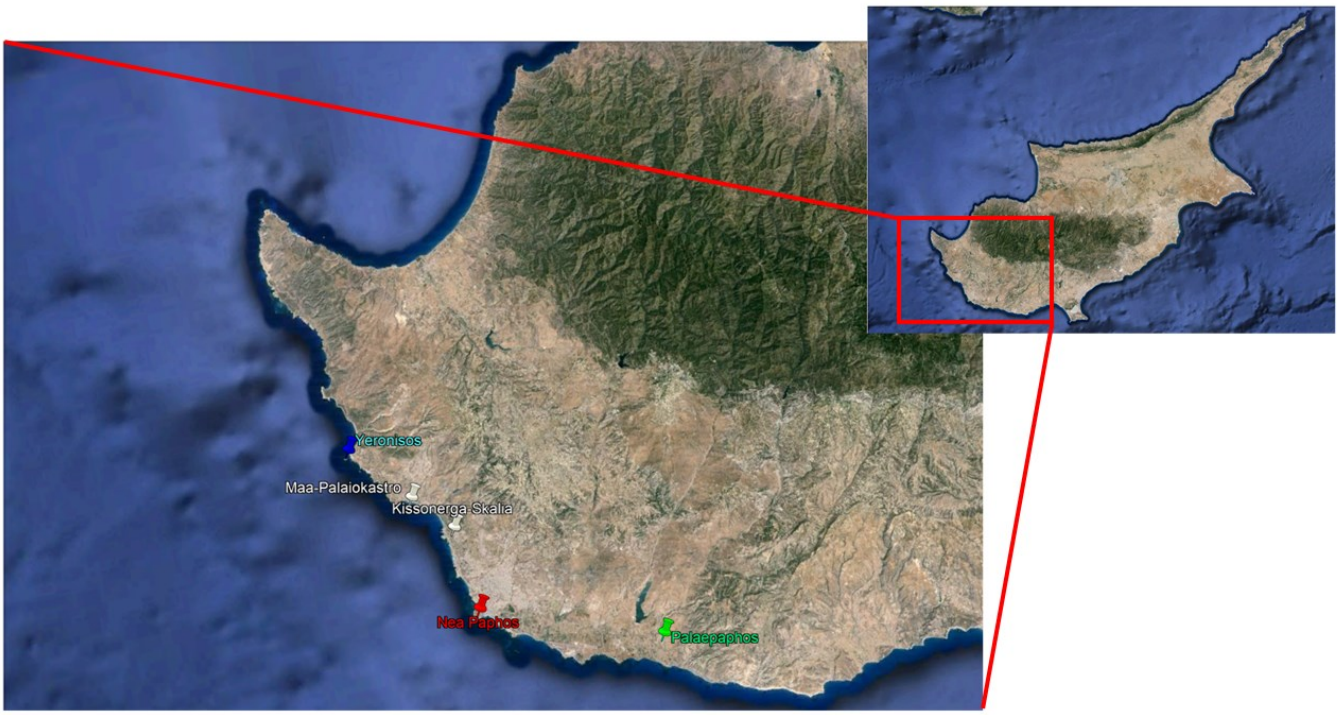

Figure 2) *Location of the sites object of study, map by author. Assorted colours correspond to different chronological periods: white – LBA; green – IA; blue – Hellenistic; red – Roman.*

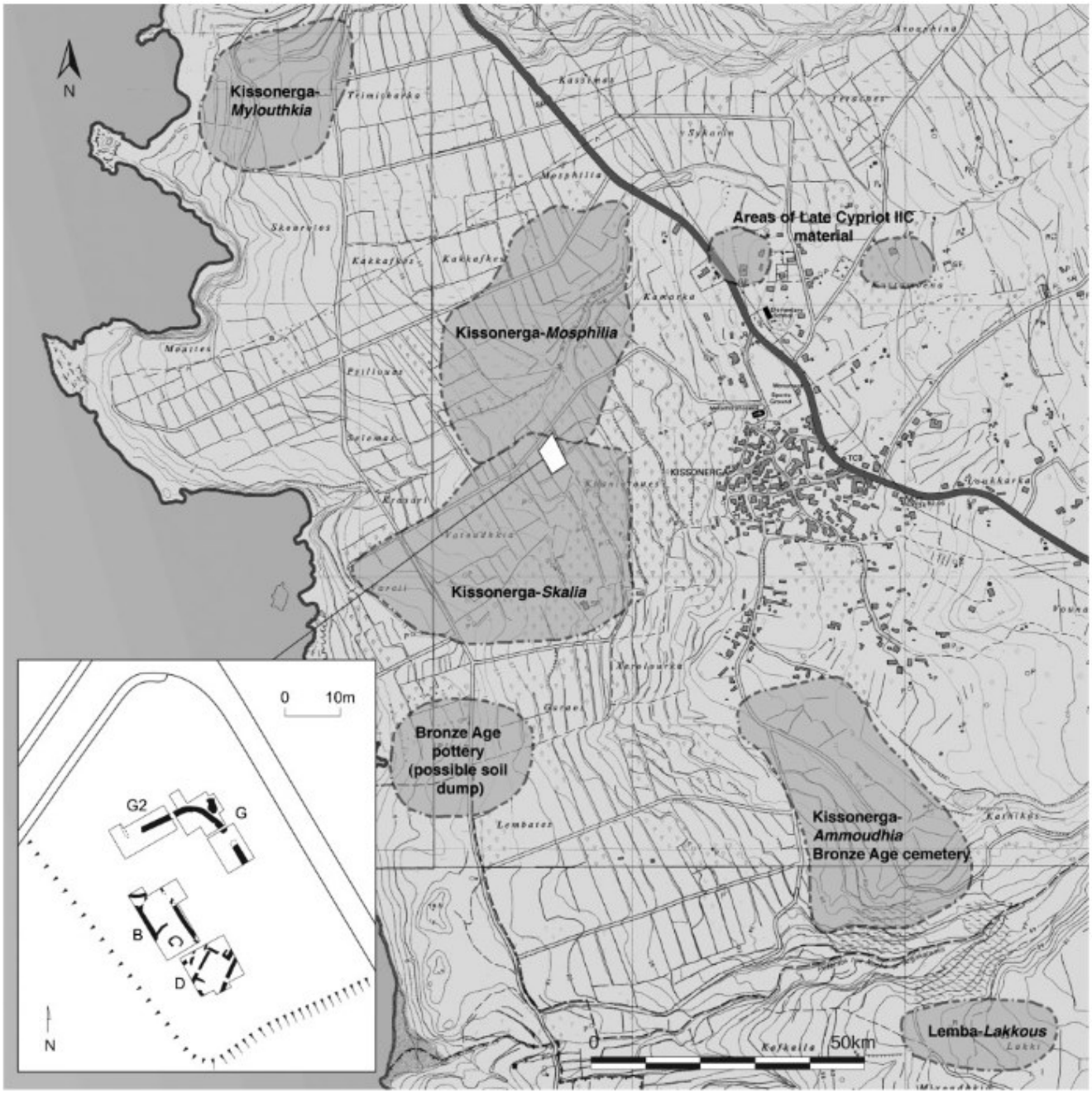

Figure 3*) Map of the area of Kissonerga with traced outlines of the expected extents of the archaeological sites discovered in the area. In the bottom left corner, an earlier drawing of the excavated areas in Plot 199 (Kissonerga-*Skalia*) up to 2012. Picture after Crewe, Hill (2012, 208, figure 2).*

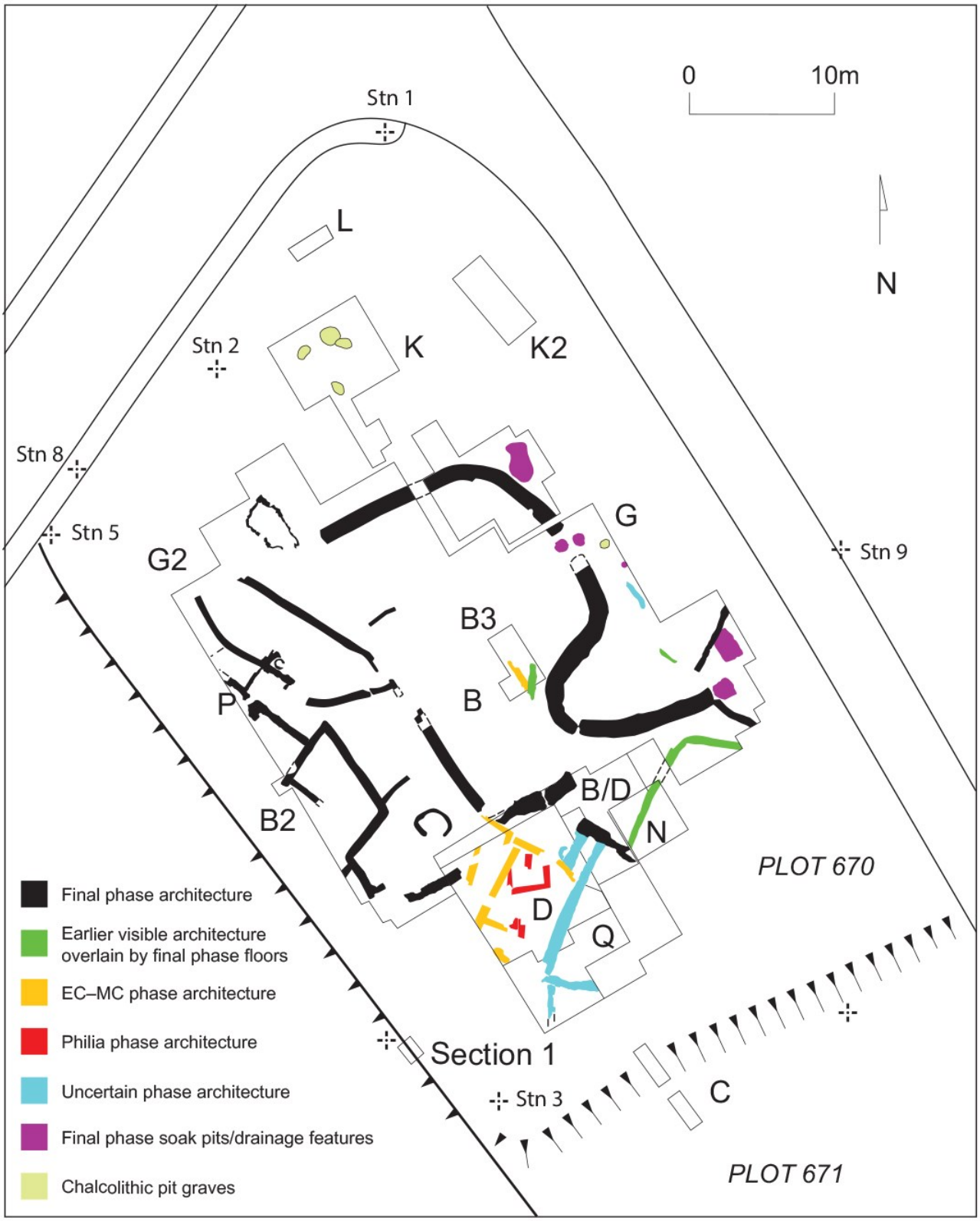

Figure 4*) Plan of the ongoing excavations at the site of Kissonerga-*Skalia*; drawing by L. Crewe, shared under her permission.*

Figure 5*) Aerial picture of Yeronisos Island and Maniki harbour, from Yeronisos' excavations press release 2013 (Department of Antiquities, Cyprus).*

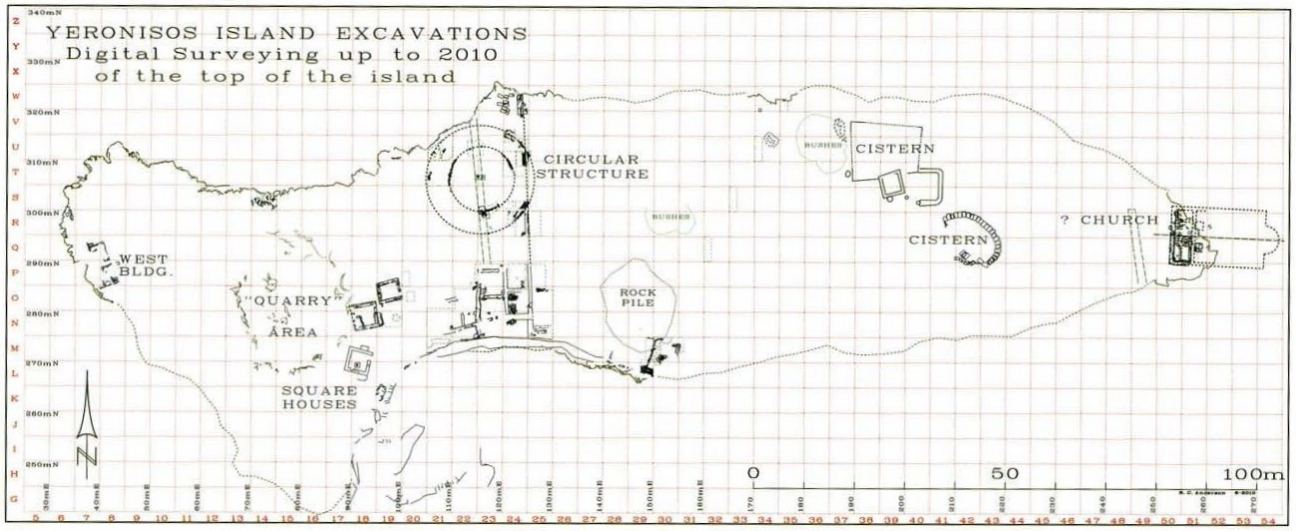

Figure 6*) Map of Yeronisos Island by R. Anderson with the excavated structures up to 2010.*

Figure 7) *Aerial view of the surroundings of modern-day village of Kouklia. Marked and highlighted are the structures excavated and documented by the PULP project. Background: aerial orthophoto of 2008; source: Department of Lands and Surveys, Cyprus. Map drafted by A. Agapiou for the PULP website.*

Figure 8) *Orthophoto of the site of Palaepaphos-*Hadjiabdoulla*with annotated units' plans. Picture courtesy of Professor M. Iakovou, director of the PULP project.*

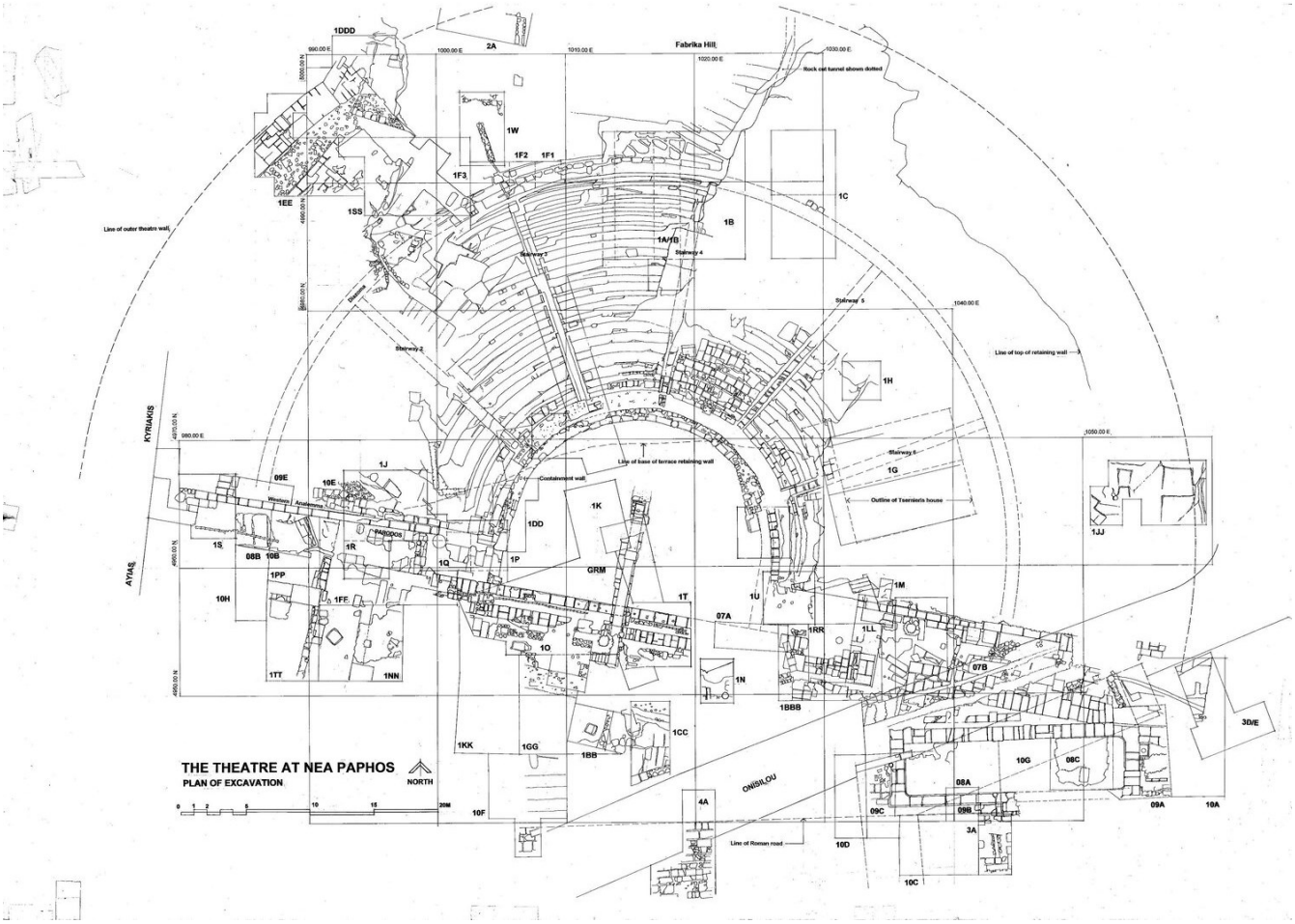

Figure 9*) Plan of the Theatre in Nea Paphos with excavated areas and reconstructed outlines as drawn by G. Stennett; courtesy of C. Barker, director of the Paphos Theatre Archaeological Project.*

Figure 10*) Satellite picture (Google Earth) of the archaeological park of Nea Paphos, cropped and altered by author. The red square includes the Agora-Odeon-Asclepeon complex – where the samples coded NPA were collected; the blue rectangle covers the area of the residential quarters – from which samples NPVT-NPHH-NPER were collected; finally, the yellow area correspond to the fortress* Saranta Kolonnes *– not included in this study.*

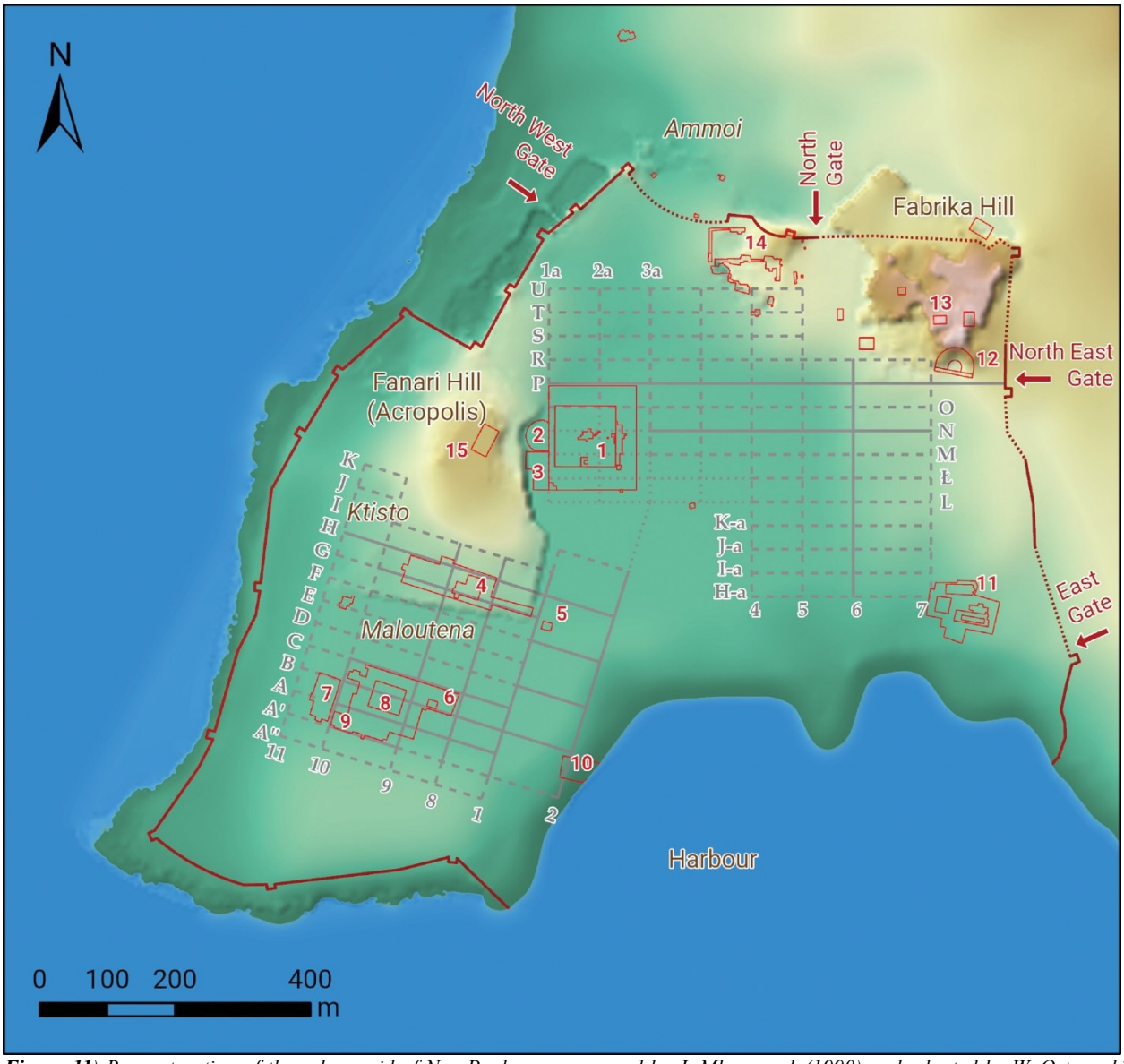

Figure 11*) Reconstruction of the urban grid of Nea Paphos as proposed by J. Młynarczyk (1990) and adapted by W. Ostrowski (Papuci-Władyka 2020, 83: pl.5). Legend: (1) Agora; (2) Odeon; (3) Asclepeon; (4) House of Dyonisus; (5) podium; (6) House of Aion; (7) House of Orpheus; (8) Villa of Theseus; (9) "Hellenistic" House and Early Roman House complex; (10) Limeniotissa Basilica; (11) Chrysopolitissa Basilica; (12) Theatre; (13) Temple of Aphrodite; (14) "Garrison's Camp"*-Toumballos*; (15) Phanari Hill. Not featured:* Saranta Kolonnes.

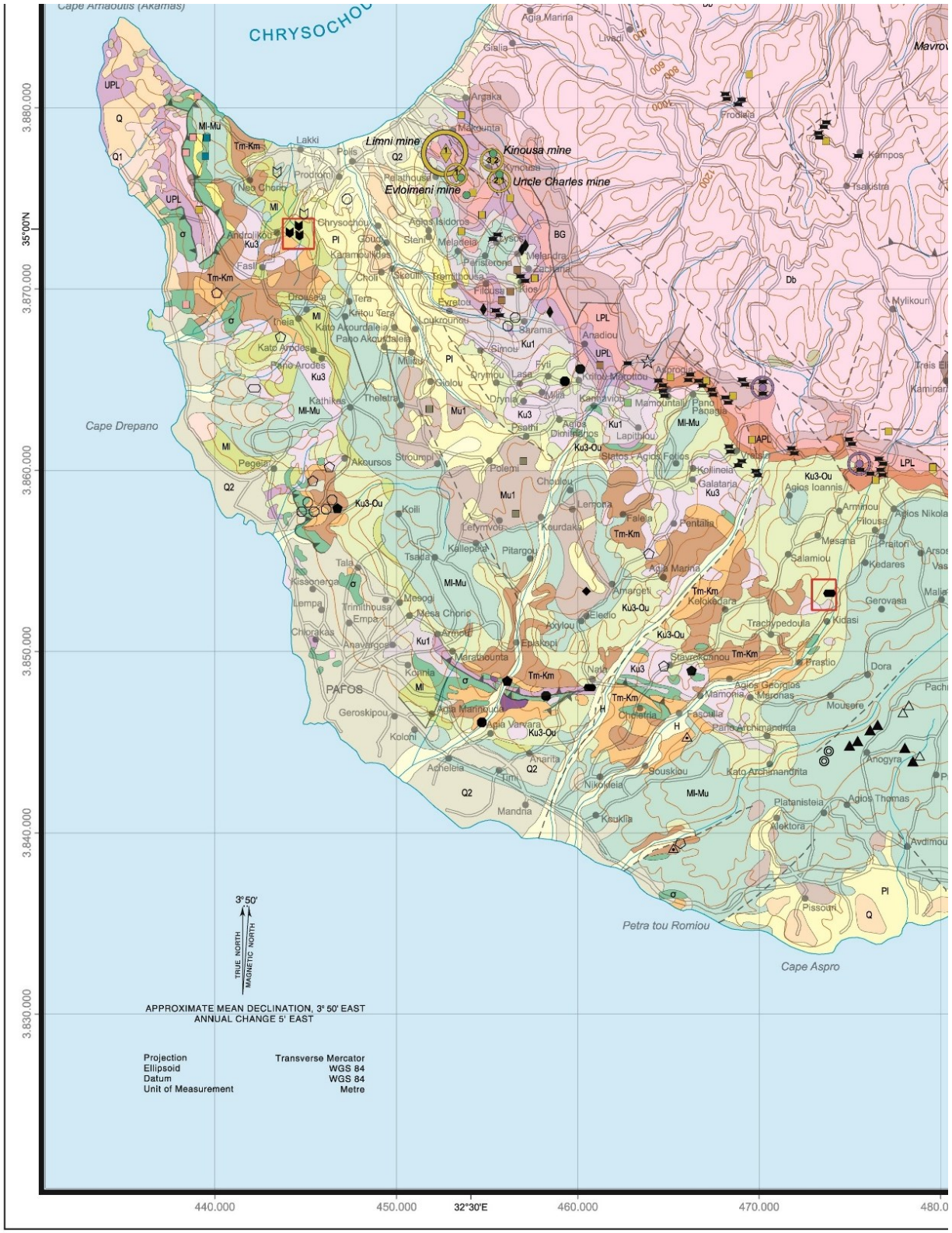

***Figure 12**) Geological map of the mineral resources of Cyprus, cut-out area of Paphos. Map compiled and designed by the Geological Survey Department, Cyprus (Economic Geology and Regional Geology, GIS and Cartography sections) under director Dr. P. Michaelides – cut-out by author. Information on the map is based on the archives of the Geological Survey Department and the Mines Service of the Republic of Cyprus, and it was revised in 2007. Further information and maps can be viewed at Geological Survey Department | Map Publications (moa.gov.cy).*

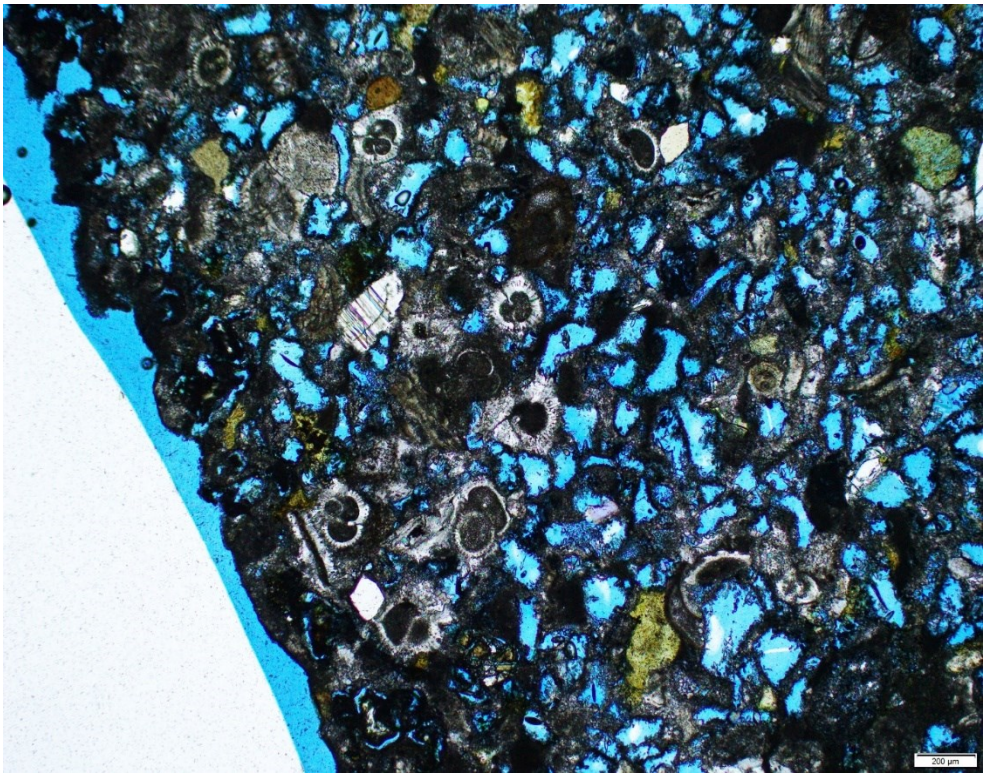

Figure 13) *Photomicrograph of a packed biomicrite sample in PPL, with focus on the planktonic foraminifera and serpentine fragments (yellow particles). Picture scale = 200 µm.*

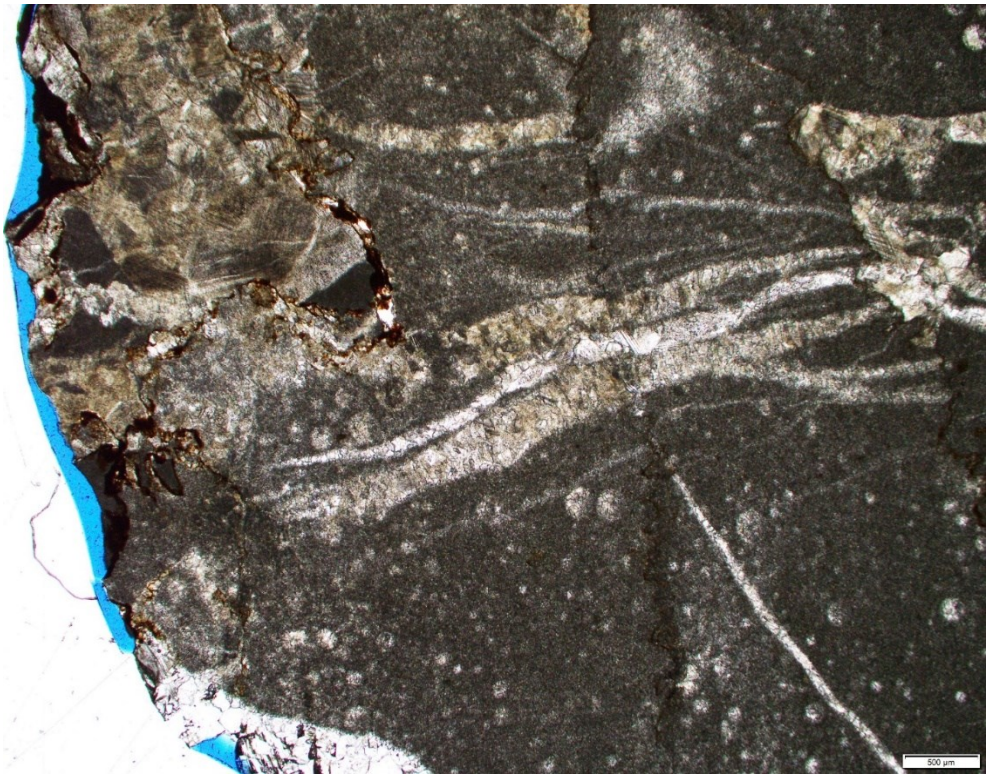

Figure 14) *Photomicrograph of a chalk sample in thin section, with focus on the sparitic calcite crystals infills in the cracks and pores. Red haloes are due to the presence of iron oxides penetrating the stone from the soil. Picture scale = 500 µm.*

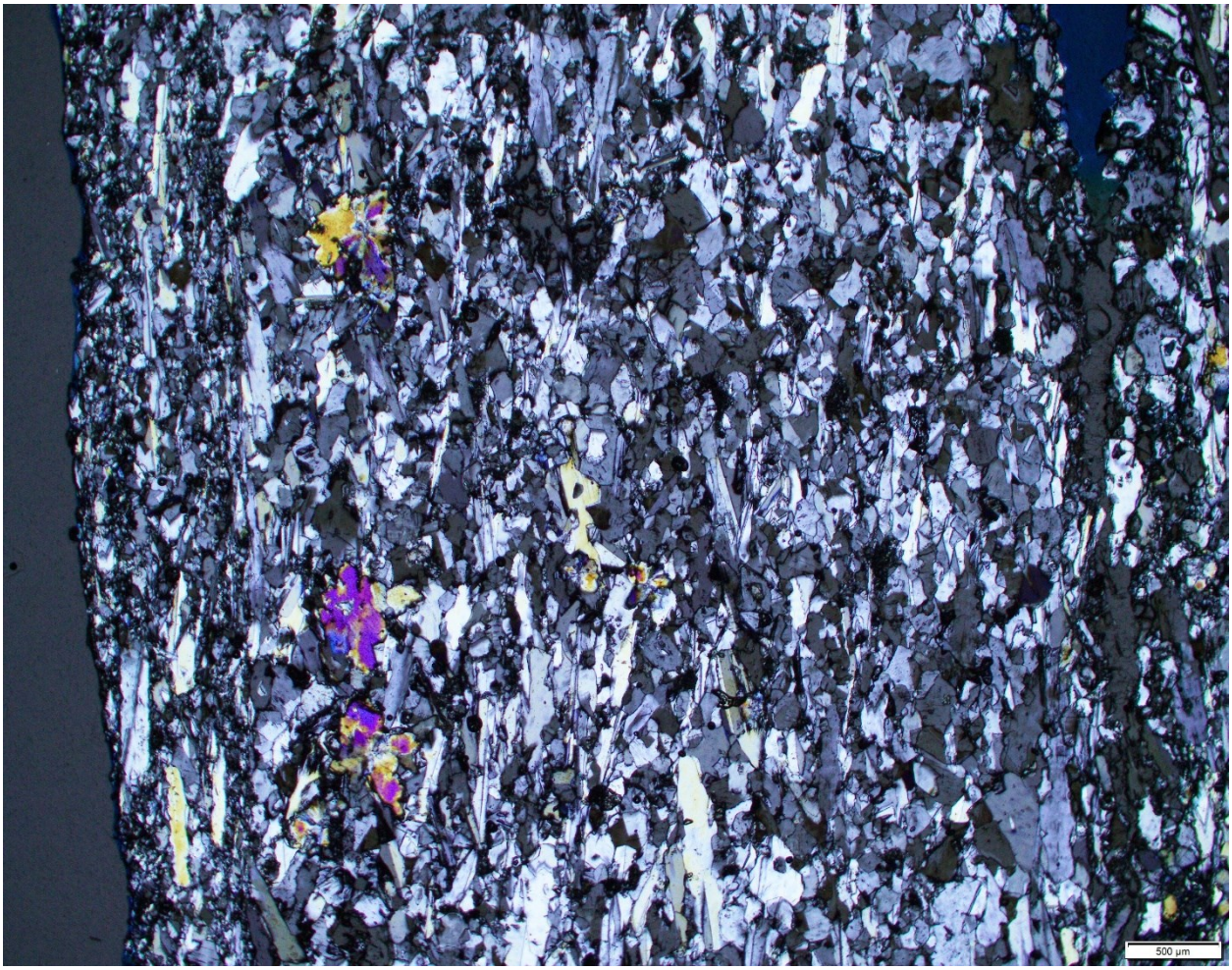

Figure 15*) Photomicrograph of gypsiferous stone (alabaster variety) in XPL, with focus on the anhydrite flake-shaped crystals. Picture scale = 500 µm.*

References

AMBRASEYS, N.

2009. *Earthquakes in the Mediterranean and Middle East: A Multidisciplinary Study of Seismicity up to 1900,* Cambridge: Cambridge University Press.

ARIZZI, A., G. CULTRONE

2021. Mortars and plasters-how to characterise hydraulic mortars. *Archaeological and Anthropological Sciences* 13, 144. https://doi.org/10.1007/s12520-021-01404-2

ARTIOLI, G., M. SECCO, A. ADDIS

2019. The Vitruvian legacy: Mortars and binders before and after the Roman world. *EMU Notes in Mineralogy* 20, pp. 151–202.

BARKER, C.

2015. Twenty Years of the University of Sydney Excavations of the Theatre Precinct in Nea Paphos in Cyprus. *Australian Archaeological Fieldwork Abroad III, Ancient History Resources for Teachers* 45, pp. 26–63.

CALZOLARI, L., L. MEDEGHINI, I. BAIOCCHI, G.L. ZANZI, S. MIGNARDI

2023. Aqua Alexandrina and Fragole cistern: characterization of mortars from Roman constructions, Rome (Italy). *Archaeological and Anthropological Sciences* 15, 183. https://doi.org/10.1007/s12520-023-01885-3

CENTAURO, I., E. CANTISANI, C. GRANDIN, A. SALVINI, S. VETTORI

2017. The Influence of Natural Organic Materials on the Properties of Traditional Lime-Based Mortars. *International Journal of Architectural Heritage* 11(5), pp. 670–684. https://doi.org/10.1080/15583058.2017.1287978

COLLEPARDI, M.

1990. Degradation and Restoration of Masonry Walls of Historical Buildings. *Materials and Structures* 23, pp. 81–102. https://doi.org/10.1007/BF02472568

CONNELLY, J.B.

2002. Excavations on Geronisos (1990- 1997): First Report. *RDAC*, pp. 245–268.

2005. Excavations on Geronisos Island: Second Report, The Central-South Complex. *RDAC*, pp. 149–181.

2007. Ptolemaic Sunset: Boys Rites of Passage on Late Hellenistic Geronisos, in P. Flourentzos (ed.) *From Evagoros I to the Ptolemies: The Transition from the Classical to the Hellenistic Period*, Nicosia: Dept. of Antiquities of Cyprus, pp. 35–51.

2009. Hybridity and Identity on Late Ptolemaic Yeronisos. *Centre d'Etudes Chypriotes Cahier* 39, pp. 69–88.

2010A. Excavations on Geronisos Island, Third Report: The Circular Structure, The Square House, And East Building. *RDAC*, pp. 295–348.

2010B. Yeronisos: Twenty Years on Cleopatra's Isle. *Explorers Club Journal*, pp. 18–25.

CONNELLY, J.B., C. MCCARTNEY

2004. The Chalcolithic Occupation of Geronisos Island. *RDAC* 2004, pp. 19–50.

CONNELLY, J.B., A.I. WILSON, C. DOHERTY

2002. Hellenistic and Byzantine Cisterns on Geronisos Island. *RDAC* 2002, pp. 269–292.

CREWE, L.

2013. Regional Connections during the Middle-Late Cypriot Transition: New Evidence from Kissonerga-Skalia. *Pasiphae. Rivista di Filologia e Antichità Egee* VII (2013), pp. 47–56.

2015. An Early-Middle Cypriot Bronze Age zoomorphic figurine from Kissonerga-Skalia. *Cahiers du Centre d'Études Chypriotes* 45, pp. 351–361. https://doi.org/10.3406/cchyp.2015.1649

2017. Interpreting Settlement Function and Scale during MC III– LC IA Using Old Excavations and New: Western Cyprus and Kisonerga (Kissonerga) *Skalia* in Context, in D. Pilides and M. Mina (eds.), *FOUR DECADES OF HIATUS IN ARCHAEOLOGICAL RESEARCH IN CYPRUS: TOWARDS RESTORING THE BALANCE. Proceedings of the international one-day workshop, held in Lefkosia (Nicosia) on 24th September 2016, hosted by the Department of Antiquities, Cyprus*, Wien: Verlag Holzhausen, pp. 140–153.

CREWE, L., I. HILL

2012. Finding Beer in the Archaeological Record: A Case Study from Kissonerga-Skalia on Bronze Age Cyprus. *Levant* 44 (2), pp. 205–237. https://doi.org/10.1179/0075891412Z.0000000009

CREWE, L., A. GEORGIOU

2018. Settlement nucleation at the beginning of the Late Bronze Age in Cyprus: the evidence from Palaepaphos. *SIMA PB* 187, *Structures of Inequality on Bronze Age Cyprus. Studies in Honour of Alison K. South,* pp. 53–70.

CREWE, L., E. SOUTER
2023. Strategies for success during the transition to the Late Bronze Age at Kissonerga-Skalia, in T. Bürge, L. Recht, *Dynamics and Developments of Social Structures and Networks in Prehistoric and Protohistoric Cyprus*, pp. 179–195, United Kingdom: Routledge. https://doi.org/10.4324/9781003320203-10

DARVILL, T.
2009. *The Concise Oxford Dictionary of Archaeology, 2nd Edition.* Oxford: Oxford University Press.

DAVIS, T.W.
2010. Earthquakes and the Crisis of Faith: Social Transformation in Late Antique Cyprus. *Buried History* 46, pp. 5–16.

DELOYE, F.X.
1993. Hydraulicité et pouzzolanicité. *Bulletin de liaison des Laboratoires des ponts et chaussées* 184, pp. 94–95.

DI BELLA, G., V. FIORE, G. GALTIERI, C. BORSELLINO, A. VALENZA
2014. Effects of natural fibres reinforcement in lime plasters (kenaf and sisal vs. Polypropylene). *Construction and Building Materials* 58, pp. 159–165. https://doi.org/10.1016/j.conbuildmat.2014.02.026

DIEKAMP, A., R. STALDER, J. KONZETT, P.W. MIRWALD
2012. Lime Mortar with Natural Hydraulic Components: Characterisation of Reaction Rims with FTIR Imaging in ATR-Mode, in J. Válek, J.J. Hughes, C.J.W.P Groot (eds.), *Historic Mortars. Characterisation, Assessment and Repair, RILEM Bookseries* 7, pp. 105–114, Springer.

DOLEŽELOVÁ, M., J. KREJSOVÁ, A. VIMMROVÁ
2018. Influence of fine aggregate on some properties of gypsum mortars. *IOP Conf. Ser.: Material Science and Engineering* 379, 012005. https://doi.org/10.1088/1757-899X/379/1/012005

ELSEN, J., K. VAN BALEN, G. MERTENS
2012. Hydraulicity in Historic Lime Mortars: A Review, in J. Válek, J.J. Hughes, C.J.W.P Groot (eds.), *Historic Mortars. Characterisation, Assessment and Repair, RILEM Bookseries* 7, pp. 125–140, Springer.

EN 16572 (2015) *Conservation of cultural heritage. Glossary of technical terms concerning mortars for masonry, renders and plasters used in cultural heritage*. Brussels: European Committee for Standardization.

ERGENÇ, D., R. FORT, M.J. VARAS-MURIEL, M. ALVAREZ DE BUERGO
2021. Mortars and plasters - How to characterize aerial mortars and plasters. *Archaeological and Anthropological Sciences* 13, 197. https://doi.org/10.1007/s12520-021-01398-x

GEORGIOU, A.
2017. Flourishing amidst a 'Crisis': The Regional History of the Paphos Polity at the Transition from the 13th to the 12th Centuries BCE, in P.M. Fischer, T. Burge (eds.), *SEA PEOPLES UP-TO-DATE. New Research on Transformations in the Eastern Mediterranean in the 13th–11th Centuries BCE*, Wien: Austrian Academy of Science Press, pp. 207–228. https://doi.org/10.2307/j.ctt1v2xvsn

GKOUMA, M., P. KARKANAS, M. IACOVOU
2021. A geoarchaeological study of the construction of the Laona tumulus at Palaepaphos, Cyprus. *Geoarchaeology* 36, pp. 601–616. https://doi.org/10.1002/gea.21850

GREEN, J.R., C. BARKER, G. STENNETT
2015. The Hellenistic Phases of the Theatre at Nea Paphos in Cyprus: the Evidence from the Australian Excavations, in R. Frederiksen, E.R. Gebhard, A. Sokolicek (eds.), *The Architecture of the Ancient Greek Theatre. Monographs of the Danish Institute at Athens* 17, Aarhus: Aarhus University Press, pp. 319–334.

HADJISAVVAS, S.
1983. An Archaeological Survey and Trial Excavations on the Small Island 'Geronisos', off the Paphos Coast. *RDAC* 1983, pp. 39–40.

HAYES, J.W.
1991. *Paphos III: the Hellenistic and Roman Pottery*, Nicosia: Department of Antiquities.

HOMER, *Odyssey*, translation by A.T. Murray, Harvard University Press, 1919.

IACOVOU, M.
2002. From ten to naught. Formation, consolidation and abolition of Cyprus' Iron Age polities. *Cahiers du Centre d'Etudes Chypriotes* 32, pp. 73–87.
2008. 'The Palaepaphos Urban Landscape Project': Theoretical Background and Preliminary Report 2006–2007. *RDAC* 2008, pp. 1–17.
2010. Kouklia-Palaepaphos: the Palaepaphos Urban Landscape Project: University of Cyprus, press release on the website of the Department of Antiquities, Cyprus Department of Antiquities - Excavations (culture.gov.cy)

2014. Political economies and landscape transformations. The case of ancient Paphos, in J.M. Webb (ed.), *SIMA* 143, *Structure, measurement and meaning: Insights into the prehistory of Cyprus. Studies on prehistoric Cyprus in honour of David Frankel*, Uppsala: Åströms Förlag, pp. 161–174.

2019. Palaepaphos: Unlocking the Landscape Context of the Sanctuary of the Cypriot Goddess. *Open Archaeology* 5, pp. 204–234. https://doi.org/10.1515/opar-2019-0015

2023. The First Urban Landscape of Southwest Cyprus: Paphos in the 'Age of Transformation', in T. Bürge. P.M. Fischer (eds.), *SIMA* 154, *The decline of Bronze Age civilisations in the Mediterranean: Cyprus and beyond*, Nicosia: Åströms Förlag, pp. 63–80.

JAYASINGH, S., J. BABY

2022. Influence of organic addition on strength and durability of lime mortar prepared with clay aggregate. *Materials Today: Proceedings* 64, pp. 1006–1013. https://doi.org/10.1016/j.matpr.2022.05.088

KARAGEORGHIS, V., E. RAPTOU

2016. *PALAEPAPHOS*-SKALES. *Tombs of the Late Cypriote IIIB and Cypro-Geometric Periods (Excavations of 2008 and 2011)*, Nicosia: The Cyprus Institute.

2014. *Necropoleis at Palaepaphos from the end of the Late Bronze Age to the Cypro-Archaic Period,* Nicosia: The Cyprus Institute.

KOPANIAS, K.

2021. Excavations at Kouklia-*Marchello* 2021, press release on the website of the Department of Antiquities, Cyprus, Department of Antiquities - Excavations (culture.gov.cy)

2022. Excavations at Kouklia-*Marchello* 2022, press release on the website of the Department of Antiquities, Cyprus, Department of Antiquities - Excavations (culture.gov.cy)

LINDBERG, J.

2017. Floor Mosaics from the Greco-Roman Theatre at Nea Paphos, in D. Michaelides, A.M. Guimier-Sorbets (eds*), Managing Archaeological Sites with Mosaics: From Real Problems to Practical solutions*. *Proceedings of the 11th ICCM Conference, Meknes, Morocco 2011*, Firenze: EDIFIR-Edizioni Firenze, pp. 313–318.

LORENZON, M., M. IACOVOU

2019. The Palaepaphos-Laona rampart. A pilot study on earthen architecture and construction technology in Cyprus. *Journal of Archaeological Science: Reports* 23, pp. 348–361. https://doi.org/10.1016/j.jasrep.2018.11.004

LUND, J.

2015. *A Study of the Circulation of Ceramics in Cyprus from the 3rd Century BC to the 3rd Century (Gosta Enbom Monographs).* Aarhus: Aarhus University Press.

MAIER, F.G.

1984. *Paphos: History and Archaeology*, Nicosia: A.G. Leventis Foundation.

MARINOWITZ, C., C. NEUWALD-BURG, M. PFEIFER

2012. Historic Documents in Understanding and Evaluation of Historic Lime Mortars, in J. Válek, J.J. Hughes, C.J.W.P Groot (eds.), *Historic Mortars. Characterisation, Assessment and Repair, RILEM Bookseries* 7, pp. 15–24, Springer.

MŁYNARCZYK, J.

1990. *Nea Paphos III – Nea Paphos in the Hellenistic Period*, Warsaw: Éditions Géologiques.

NICOLAOU, K.

1966. The Topography of Nea Paphos, in M.L. Bernhard (ed.), *Mélanges offert á Kazimierz Michalowski*, Warsaw: PWN, pp. 561–601.

PAPUCI-WŁADIKA, E.

2020. *Paphos Agora Project (PAP): Interdisciplinary Research of the Jagiellonian University in NEA PAPHOS UNESCO World Heritage Site (2011-2015). First Results* (1), Krakow: Historia Iagellonica.

2018. Paphos – Mystery of the City of Aphrodite: Introductory Note, in E. Papuci-Władyka (ed.), *Paphos – Mystery of the City of Aphrodite*, pp. 17–24, Krakow: Fundacja Archaeologica.

PEDERGNANA, M., S.T. ELIAS-OZKAN

2021. Impact of various sands and fibres on the physical and mechanical properties of earth mortars for plasters and renders. *Construction and Building Materials* 308, 125013. https://doi.org/10.1016/j.conbuildmat.2021.125013

PELTENBURG, E.J.

2003. The Colonisation and Settlement of Cyprus. Investigations at Kissonerga-Mylouthkia, 1976-1996. *SIMA* 70 (4), Sävedalen: Åströms Förlag.

PELTENBURG, E.J., D.R. BOLGER

1998. *Excavations at Kissonerga-Mosphilia*, 1979-1992, Jonsered: Åströms Förlag.

PHILOKYPROU, M.

2012a. The Earliest Use of Lime and Gypsum Mortars in Cyprus, in J. Válek, J.J. Hughes, C.J.W.P. Groot (eds.), *Historic Mortars. Characterisation, Assessment and Repair, RILEM Bookseries* 7, pp. 25–36, Springer.

2012b. The Beginnings of Pyrotechnology in Cyprus. *International Journal of Architectural Heritage* 6, pp. 172–199. http://dx.doi.org/10.1080/15583058.2010.528145

PLINY THE ELDER, *Naturalis Historia,* J. Bostock, H.T. Riley, K.F.T. Mayhoff, Perseus Digital Library 2006.

PLUTARCH, *Lives (Alexander)*, translation by B. Perrin, in W. Heinemman (ed.) *Lives of Plutarch*, Harvard University Press 1959.

QUINN, P.S.

2022. *Thin Section Petrography, Geochemistry and Scanning Electron Microscopy of Archaeological Ceramics.* Oxford: Archaeopress.

2013. *Ceramic Petrography, the Interpretation of Archaeological Pottery and Related Artefacts in Thin Section*. Oxford: Archaeopress.

STEFANIDOU, M., I. PAPAYIANNI

2005. The role of aggregates on the structure and properties of lime mortars. *Cement & Concrete Composites* 27, pp. 914–919. https://doi.org/10.1016/j.cemconcomp.2005.05.001

STRABO, *Geography*, in H.L. Jones (ed), *The Geography of Strabo*, Harvard University Press 1924.

THEODORIDOU, M., I. IOANNOU, M. PHILOKYPROU

2013. New evidence of early use of artificial pozzolanic material in mortars. *Journal of Archaeological Science* 40, pp. 3263–3269. https://doi.org/10.1016/j.jas.2013.03.027

TURCO, F., P. DAVIT, F. CHELAZZI, A. BORGHI, L. BOMBARDIERI, L. OPERTI

2016. Characterization of Late Prehistoric Plasters and Mortars from Erimi – Laonin tou Porakou (Limassol, Cyprus). *Archaeometry* 58, pp. 284–296. https://doi.org/10.1111/arcm.12168

VON RÜDEN, C.

2016a. Introduction: the Late Bronze Age Context in Palaepaphos, in C. Von Rüden, A. Georgiou, A. Jacobs and P. Halstead (eds.), *Feasting, Craft and Depositional Practice in Late Bronze Age Palaepaphos*, pp. 11–22, Rahden: VLM.

VON RÜDEN, C.

2016b. Conclusion: Feasting, Craft and Depositional Practice in Evreti/Palaepaphos, in C. Von Rüden, A. Georgiou, A. Jacobs and P. Halstead (eds.), *Feasting, Craft and Depositional Practice in Late Bronze Age Palaepaphos*, pp. 419–423, Rahden: VLM.

WEINER, S.

2010. *Microarchaeology. Beyond the Visible Archaeological Record*. Cambridge: Cambridge University Press.

PART 2. METHODOLOGY

Introduction

The principal aim of this project is to characterise the binders of the Paphian plasters. In order to achieve this goal, a multidisciplinary and multiscale approach was adopted, following well known studies (see Kozlovcev *et al.* 2023; Kozlovcev, Válek 2021; Singh *et al.* 2014; Letourneux, Feneuille 2012; Philokyprou 2012a, b) as well as proceedings of the RILEM Technical Committees (see Groot *et al.* 2004; Middendorf *et al.* 2007). After preliminary macroscopic assessments, petrographic studies in optical microscopy (hereinafter PLM) – combined, when necessary, with cathodoluminescence – were the first and most substantial step for the characterization and technological appraisal of the plasters. To complete the overview, geochemical and mineralogical information were gathered combining x-ray powdered diffraction (XRD) and thermal analysis (TA). Scanning electron microscopy (SEM) was employed to collect elemental information about the chemical composition and to acquire high resolution images of the microstructures of the samples. In addition to this relatively standard procedure, a variety of chemical and mechanical tests was performed on selected samples to enhance understanding and corroborate interpretations. For instance, RAMAN spectroscopy was employed to identify pigments; Fourier-transform infrared spectroscopy (FTIR) was applied to identify suitable samples on which to perform organic residue analysis; and, finally, porosity and water absorption tests completed the overview of the samples' performance. The graph below (**fig. 16**) synthesizes the analytical procedure.

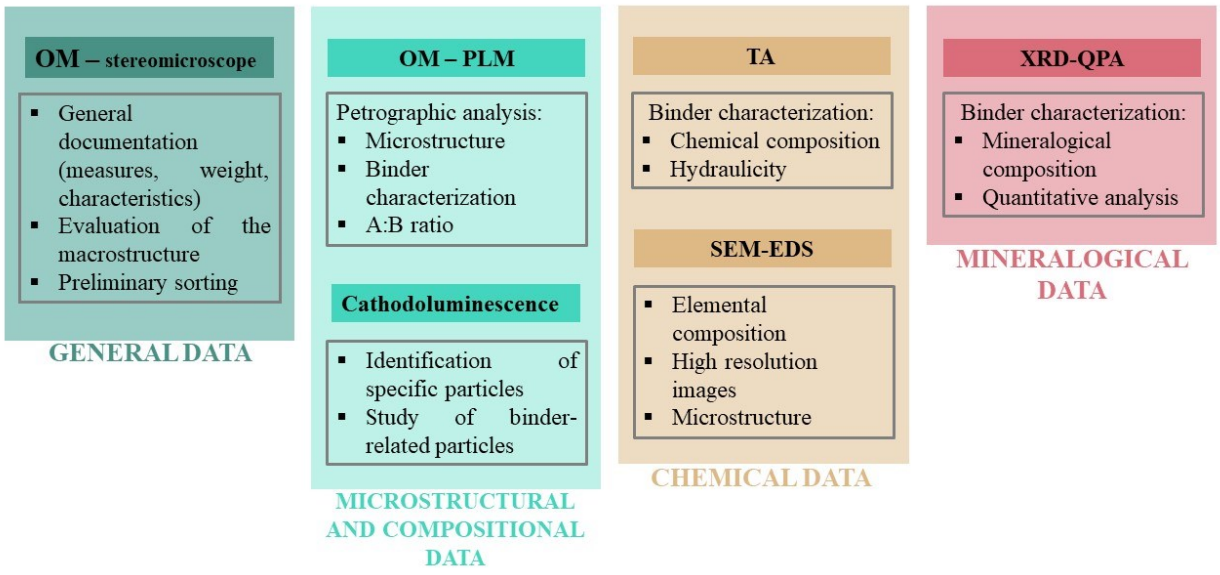

Figure 16 *schematically represents the analytical procedure followed to process the samples. The graph highlights the standard set of techniques employed and for each illustrates the information and data acquired.*

Chapter 2.1: Criteria for site selection

As mentioned in the previous chapters, the area of Paphos had been scarcely investigated from the point of view of plaster production. While several studies have been conducted in other regions of the island – for instance in Erimi-*Laonin tou Porakou* (Amadio 2018; Turco *et al.* 2016) and Kalavasos – the research concerning the Paphian district was limited to in-passing mentions and comments (with the exception of the study of Yeronisos cisterns' plasters conducted by J.R. Connelly (Connelly *et al.* 2002)).

Initially, it was decided to collect samples from at least two sites for each macro-chronological period considered in this research. Thus, for the Late Bronze Age, the settlement of Kissonerga-*Skalia* and the neighbouring town of Maa-*Palaiokastro* were selected; while for the Iron Age – due to the scarcity of archaeological data – the focus was exclusively on the site of Palaepaphos; for the Hellenistic period, samples were collected from relevant strata at Yeronisos Island, and from selected buildings in Nea Paphos; while for the Early Roman stage, public and private areas of Nea Paphos and targeted buildings in the Sanctuary precinct at Palaepaphos were considered. However, at the present moment, two of the above-mentioned archaeological sites are not included in the study: namely, Maa-*Palaiokastro* and the Sanctuary area in Nea Paphos. The settlement of Maa-*Palaiokastro* was systematically excavated by an archaeological mission of the Department of Antiquities of Cyprus lead by V. Karageorghis between 1979 and 1985 (Karageorghis, Demas 1988). Due to the early time of excavation, the collected plaster samples were stored without properly documented relevant information, such as context, description or processing of the samples. After visiting the storage rooms of the Paphos Museum and appraising the status of the documentation and samples, the site was discarded from the project. In fact, although it would have been possible to perform the standard analytical procedure on the samples, important knowledge on the contextualization would be missing. For similar reasons, the originally planned sampling at the Sanctuary precinct was postponed and ultimately not performed at all. Indeed, published records concerning this site are already scarce and lacking key information for a proper contextualization. Thus, it was decided to not inspect the available material at all, if not for a simple appraisal of the macroscopic characteristics of the samples.

Chapter 2.2: Sampling strategies and collected samples

Whenever possible, samples were collected from all the plastered features of each site, avoiding aesthetical or structural damages to the buildings. Considering that one of the key questions of the project was whether distinct types of plasters were produced to fulfil specific functions, samples were collected from each functional category (specifically, masonry mortars, waterproofing mortars, wall plasters and floor structures).

Samples were not collected in a standardised quantity, but proportionally to the preserved amount *in situ*. When possible, small blocks of around 5 cm in length and 2 cm in thickness were collected and stored in sealed plastic bags. For each sample, the specific location of collection, including –

if available – the geo-coordinates, was documented. Relevant information concerning the associated structure, such as the preservation extent and status, masonry characteristics and chronological data were recorded as well.
Thanks to the permission of the Department of Antiquities of Cyprus, 90 samples in total were collected from the selected archaeological sites. Chronologically speaking, Roman and Hellenistic plasters are by far the most present, constituting up to 75% of the samples (see illustration plates, **gr. 1**); scarcer are the data concerning the preceding phases. In terms of binder types, 75% of the considered plasters are lime-based, 11% are natural hydraulic lime-based (NHL), 14% are gypsum-based, and only 1% is constituted by a mixture of different binders (illustration plates, **gr. 2**). Lime binder is used to produce mainly wall plasters (56% of the whole lime-plaster assemblage), waterproofing mortars (15%) and floors (17%); gypsum binder is employed mostly for masonry mortar (64%) and, in rarer occasions, for the production of wall plasters (36%); NHL is mostly utilized for the production of waterproofing mortars or, more rarely, wall and floor plasters. Summarizing statistical graphs are included in the illustration plates at the end of the chapter.

Chapter 2.3: Sample processing and methodology overview

The collected samples were mechanically cleaned using simple soft brushes; in few cases (especially for the samples from Yeronisos Island), compact soil encrustations were removed with the aid of a scalpel. The cleaned samples were labelled and photographed with a standard camera. At this point, a preliminary examination under a stereomicroscope was performed in order to select the most suitable and representative samples for the subsequent analytical procedures. 68 samples were cut with a circular table saw and sent for the preparation of blue-stained, uncovered, polished thin sections. The thin sections were analysed through a standard polarized light microscope (PLM) – Olympus BX53M with an Olympus DP27 digital camera – to study the fabric, pores' structure, composition and technological features of each sample (Ergenç et al. 2021; Válek 2015; Pecchioni *et al.* 2014). A "cold cathode" type Mk 5-2 was associated with the microscope to further investigate binders and binder-related particles. High-resolution images, as well as the elemental composition, were obtained via SEM-EDS analysis on a selection of 30 thin sections. SEM-EDS analyses were performed on carbon-coated samples with two different instruments: the first half of the samples was analysed with a Tescan MIRA II LMU scanning electron microscope with an energy-dispersive analytical system (Bruker AXS) under the following conditions: back-scattered electron mode (BSE) with electron accelerating voltage corresponding to 15 kV, at a WD of 15 mm, in high vacuum. The chemical composition was quantified by Brucker Esprit 2.5 software, without standardization. The analytical results were expressed in oxide form. The second set of samples was analysed with a Carl Zeiss EVO 25 scanning electron microscope coupled with two energy dispersive analytical systems (Oxford Instruments) under the following conditions: back-scattered electron mode (BSE) with electron accelerating voltage corresponding to 20 kV, at a WD of 8.50 mm, in high vacuum. The chemical data were quantified by Aztec 5.1 software, and the results were expressed in oxide form.

To acquire mineralogical data, a small fraction of 55 selected samples was grounded to analytical fineness. Each sample was firstly gently crushed in a mortar and sieved through a set of different sieves ranging from 90 to 63 µm. The fraction above 90 µm was considered to be corresponding mainly to the aggregates, while the fraction below 63 µm was considered to be rich in binder (Diaz *et al.* 2022; Middendorf *et al.* 2007). Before the XRD analysis, an internal standard (ZnO, 10 wt.%) was homogenized with the sample. Data were collected on a diffractometer D8 Bruker Advance pro (Cu Ká radiation, 40 kV and 40 mA) with 0.01°C step size 2Θ and counting time 0.4 s/step. Quantitative phase analysis (QPA) to determine crystalline and amorphous phases was performed by the Rietveld method (1969) using Topas 4.2 software from Bruker AXS. Derivative thermogravimetry was performed on the binder-rich fraction of the samples with a TA Instruments Discovery SDT 650, under the following conditions: Nitrogen atmosphere, heat rate 20°C/minute, temperature range 50-1000°C. TG, DTG and heat flow curves were collected and analysed with MS Discovery; special focus was directed towards the regions between 50–250°C (detection of gypsum), 250~550°C (estimation of hydraulic phases) and between ~600–850°C (carbonate decomposition) (Földvári 2011; Middendorf *et al.* 2007). When the spectrum displayed possible traces of organic materials the sample was analysed again with thermogravimetry coupled with a mass spectrometer (TGA-EGA, evolved gasses analysis), measuring the eventual exothermic processes in Nitrogen and air atmospheres. The detection and identification of evolved gases were realised by quadrupole mass spectrometry MS Discovery.

Chapter 2.4: Microscopy techniques (PLM, CL, SEM-EDS)

Chapter 2.4.1: Optical Microscopy

Microscopy is a well-known technique successfully employed in the study of archaeological materials, and, in particular, usually adopted for petrographic evaluation of ceramics (Quinn 2022, 13). Normally, it is executed on thin sections (approx. 30 µm thickness) mounted on a glass microscope slide. For the present study, the thin sections were realized partly by MK Factory in Berlin (uncovered, blue-stained thin sections), partly by the Department of Geological Sciences, Faculty of Science of Masaryk University in Brno (uncovered, blue-stained thin sections), and additionally by Centrum Telč of the Czech Academy of Science (uncovered thin sections, not stained).

The observation of plasters under PLM focused on the preliminary identification of the binder type, allowing an initial sorting, and providing necessary information to correctly operate with the materials. Other data gathered through this technique focused on registering the macroporosity, aggregate to binder ratio, microstructure, and average particles size (Miriello *et al.* 2021, 4). Furthermore, by observing the specific pleochroism under crossed Nicols, it was possible to identify the single grains embedded in the binder matrix (aggregates).

68 samples were analysed with this technique, and for each the following characteristics were recorded:

- General description: this part included a general overview of the thin section slide and included data such as the presence of multiple layers, the thickness of each of them, the type and colour of the binder, the type and average size of the aggregates.
- Aggregates section: this part included the description of each aggregate grain present in the thin section. Aggregates were categorized as major, minor, and accessory components according to the percentage of content. Size – from very fine (less than 0.5 mm) to coarse (more than 1.5 mm) – and shape – well-rounded to angular – of each aggregate type were recorded as well.
- Binder section: this part included the description of the binder, focusing on the colour, fineness, compactness and pores' structure. Also included in this section were information concerning the surface finishing (polishing, coating, paint), along with a visual estimation of the binder to aggregates ratio following the grain size chart (**fig. 17**).

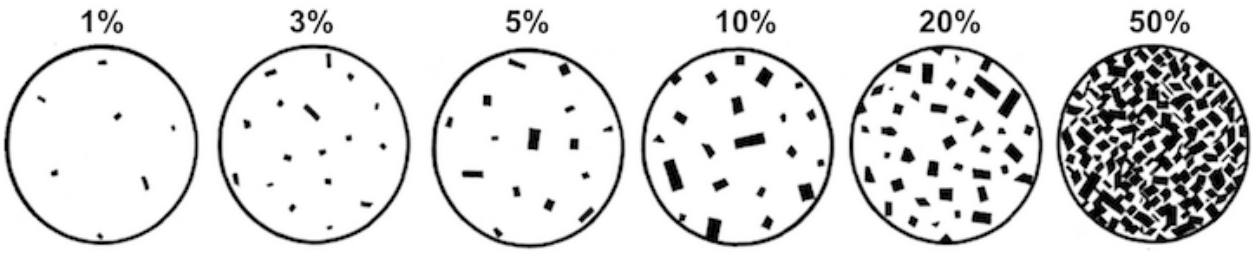

Figure 17) *This chart has been employed to visually estimate the aggregate to binder ratio. Figure modified after Earle 2015 (67) under CC-BY 4.0 International License.*

Chapter 2.4.2: Cathodoluminescence

Cathodoluminescence (CL) is an analytical technique based on the phenomenon of luminescence of materials caused by emitted electrons after the sample is electronically bombarded (Murakami *et al.* 2013, 963-964; Yacobi, Holt 1990, 55; Marshall 1988). In this study, CL was employed to estimate the degree of calcination of lime, and more specifically to distinguish un-burnt calcite (bright red in CL) from burnt particles. Furthermore, this technique enabled the identification of specific particles, such as Si-based minerals, and Na and K-feldspars. The luminescence emitted by these grains was observed and classified following Richter *et al.* (2003).

Chapter 2.4.3: SEM-EDS

Scanning Electron Microscopes (SEM) are used in the study of archaeological materials for a variety of reasons, from use-wear analysis (see for instance Borel *et al.* 2014) to compositional studies. Primarily, SEM offers high resolution and high magnification images (up to 10,000x and more), and, if coupled with an energy-dispersive spectrometer (EDS), it can provide information about the chemical composition of the analysed sample. In principle, a SEM is composed of a

chamber, an electron gun and one or more EDS detector(s): the sample is mounted in the vacuum chamber, and the electron gun shoots an electron beam that – through a variety of lenses – hits the surface of the sample. When the electrons encounter the surface, the atoms of the analysed material are brought into higher, but less stable, energy electron shells; once the excited electrons decay to the more stable electron shells, the lost energy is emitted in form of x-rays. The EDS detector(s) registers these x-rays and detect which electron shells were engaged in the process, thus enabling the identification of the single elements present in the sample; by measuring the amount of x-rays emitted, the detector is also able to precisely calculate the percent quantity of the emitting element. SEM analysis was employed in this study with the primary aim of gaining high resolution images to better understand the microstructure (*i.e.* porosity), and to identify specific particles that were not easily recognizable through PLM. Furthermore, SEM-EDS became an invaluable instrument in the identification and study of the lime-based plasters containing ceramic components. Through EDS analysis it was possible to analyse reaction rims and, occasionally, to determine the presence of NHL. As a standard procedure, for each sample analysed with this instrument a variety of spectra from the binder and the binder-related particles were collected (at least 5); in addition, for each individual sample measurements of specific particles (point analysis) or interfaces (point analysis and mapping) were also recorded. The data collected through elemental composition analysis were employed for the calculation of the cementitious index (CI, calculated according to the following formula: $CI = \frac{1.1Al_2O_3+2.8SiO_2+ (0.7Fe_2O_3)}{\mathrm{CaO}+1.4\mathrm{MgO}}$) of suspected hydraulic plasters.

Chapter 2.5: Mineralogical Analysis

The analysis of the mineral phases present in the binders was achieved, in this study, by means of x-ray diffraction analysis. The XRD machine is composed of a chamber, an x-ray tube and a detector. The x-ray tube shoots onto the powdered sample an x-ray beam, which is diffracted by the crystals. The diffracted x-rays are registered by the detector, and their angles and intensities are measured. Through a simple database search, it is possible to observe the compounds(s) best matching to each x-ray intensity at given angles. In order to gain better results, it is necessary to powder the sample, avoiding the natural preferred orientation of the crystalline structure. Furthermore, the addition of 10% of standard allows for a more refined and precise quantification of the mineral phases following the Rietveld method.

This technique is particularly useful for the identification of mineralogical phases, and thus to understand the overall composition of the samples. In the case of this study, since exclusively the binder-rich fractions of each sample were analysed, the main focus of XRD analysis was the identification of the components of the binders. In particular, attention was directed to the mineralogical phases of $CaCO_3$, SiO_2, $CaSO_4$, and the so-called amorphous phases. Thanks to XRD-QPA it was possible to detect the use of slightly different minerals associated with the chemical compound of $CaCO_3$, for instance calcite, aragonite and Mg-rich calcite. This information could only be acquired studying the mineralogical composition, as the elemental one would have

only indicated the presence of calcium carbonate. Amorphous phases and SiO_2 content were also a relevant data, as they could possibly be signalling the presence of NHL.

Chapter 2.6: Thermal analysis

Thermal analytical methods are employed to study the changes of chemical properties in a sample in relation to the variations of temperature (Cavalheiro 2019, 12; Hill, Verma 2019; Cheremisinoff 1996, 17; Hill 2005, 17). In principle, a sample is heated under controlled conditions, and its reactions to temperature increase are recorded and registered by the instrument. There are a variety of thermal analysis often combined with complementary methods to obtain a wider range of data, each of which requires different analytical equipment and sample processing methods. The diverse types of TA can be distinguished according to the measured property, and are grouped in (Cavalheiro 2019, 13):

- Thermogravimetry (TGA) for the measurement of masses;
- Differential Thermal Analysis (DTA) for temperature;
- Differential Scanning Calorimetry (DSC) for heat;
- Thermomechanical Analysis (TMA) for dimensions;
- Dynamic Mechanical Analysis (DMA) for mechanical properties (*e.g.* vitrification);
- Evolved Gas Analysis (EGA) for the characterization of volatiles.

Thermal analyses are usually performed on samples grounded to analytical fineness; the major advantage of all TA techniques is the necessity of small quantities of material, between 1 mg and 1 µg. Different and complementary TA techniques have been successfully applied to the study of cementitious materials, specifically for the quantification of the chemical composition (Cavalheiro 2019) – which were estimated following the formulas $CaCO_3 \text{ content} = \frac{\text{wt.loss\% (600–800°C)} * 100}{percentage\ of\ CO_2\ in\ CaCO_3\ (44)}$ for the calculation of the calcium carbonate content, and $CaSO_4 \text{ content} = \frac{\text{wt.loss\% (100–250°C)} * 100}{percentage\ of\ H_2O\ in\ CaSO_4 * 2H_2O\ (20.93)}$ for the calculation of gypsum content. Furthermore, TA has been successfully employed as a tool for the assessment of hydraulicity (Rizzo, Megna 2008). In this study, TA-DSC and TA-EGA were employed for the compositional characterization of the binder fractions of the Paphian samples. The data collected were also relevant for the identification of possible hydraulic and natural hydraulic plasters. In total, around 60 samples were measured by means of TA-DSC, with an additional dozen measured by TA-EGA. Around 20 µg of binder crushed to analytical fineness was measured in Nitrogen atmosphere, at a heat rate of 20°C/minute, in a temperature range of 50–1000°C.

Chapter 2.7: Water absorption and porosity tests

To complement the set of analysis, water absorption and porosity tests were performed on the samples whose function was believed to be associated with retain or disposal of liquids. For this

purpose, twenty samples were selected firstly for water absorption testing, under the following conditions: samples were dried in an oven at 60°C for 24 h, weighted, and subsequently immersed in 80 ml of distilled water. After 48 h, the samples were extracted from the water, lightly dried on a cloth, and measured (while still wet but surface dry) to calculate the percentage of weight increment and the amount of absorbed water ($water\ absorption = \frac{Weight\ of\ absorbed\ water}{starting\ sample\ weight} * 100$). After 72 h of drying in a dryer at 60°C, the weight of the sample was recorded again, in order to estimate the percentage of eventual weight loss. The open porosity of this same set of samples was measured following this procedure: the dried samples were put in a vacuum chamber under pressure for 24 h; the chamber was subsequently flooded with distilled water, so that the samples would be submerged. After 24 h the vacuum was released, and the samples were kept at atmospheric pressure for a further 24 hours. Then, the masses of the samples underwater and in air (surface dry) were determined to calculate the total volume of the samples according to Archimedes' law, and their open porosity (P) in vol. % (following the formula $P = \frac{Vv}{Vt}$, where Vv= volume of open voids, and Vt= total volume).

Chapter 2.8: Additional analysis

Chapter 2.8.1: FTIR analysis

One of the highest advantages of FTIR analysis is the necessity of only few milligrams of powdered samples, allowing for precise and micro-invasive studies. However, this technique works best when analysing a single compound and not a heterogeneous mixture, making it less suitable for the study of plasters, notoriously highly heterogeneous. Furthermore, this analytical method is also suitable for the study of organic compounds, such as pigments or their binding mediums. However, it must be considered that there are still high detection limits, thus FTIR is not well versed for the identification of trace elements or compounds under approximately 5 wt.%.

FTIR analysis can be performed on powdered samples or – with the use of a specific table-top instrument – directly on the samples' surface. This method is based on the measurement of certain wavelengths of light, which is in turn dependent on the molecular structure and chemical bonds. By analysing the wavelengths absorbed and refracted and comparing them with a library database of known materials, it is possible to identify the main component(s) (Smith 2011).

With all the limitations of the case, FTIR analysis was here employed with a double purpose: initially, it served as a screening method to distinguish between lime and gypsum-based samples. It was employed for this purpose on a pool of a dozen of samples; the results proved that our macroscopic and microscopic observations were reliable enough, thus it was not necessary to perform FTIR on all the samples. Secondly, FTIR analysis was also suitable for the study of certain pigments and to trace the possible presence of organic compounds in the binder matrix. With this secondary aim, FTIR was performed on ten samples. FTIR spectra were acquired in attenuated total reflectance (ATR) mode using the iZ10 module of a Nicolet iN10 laboratory spectrometer (Thermo Scientific), equipped with a DTGS detector and KBr beam splitter. The spectral range

covered 4000–525 cm^{-1} with a resolution of 4 cm^{-1}, and 64 scans were accumulated. Prior to measurement, the surface layer of each sample was gently scratched, and the obtained powder was deposited onto a single-reflection diamond ATR crystal.

Chapter 2.8.2: Organic analysis

Protein analysis by mass spectrometry was performed on a selected set of 10 samples with the aim of detecting possible organic residues associated with the mortar mixture or the binder for the pigment layer. The procedure was as follows:

- Protein digestion and purification

100–250 µL of 50 mM NH 4 HCO 3 containing approximately 10 µg/mL of trypsin was applied to the sample and let react at room temperature for two hours. After the trypsin digestion, the solution was taken and purified on reverse phase ZipTip. After equilibrating, binding and washing steps, target compounds were desorbed from the stationary phase. The solutions were consequently used for analyses by nano-LC-ESI-Q-TOF.

- Mass spectrometry nano-LC-ESI-Q-TOF[1]

Measurement was carried out using UHPLC Dionex Ultimate3000 RSLC nano (Dionex, Germany) connected with mass spectrometer ESI-Q-TOF Maxis Impact (Bruker, Germany). 10 µL of peptide solution were previously dried and then dissolved in 97:3:0.1% mixture of water:acetonitrile:formic acid. Consequently, they were loaded on trap column Acclaim PepMap 100 C18 (100 µm x 2 cm, size of reverse phase particles 5 µm, Dionex, Germany) with flow rate of mobile phase A 5 µL/min for 5 min. The peptides were eluted from trap column to analytical column Acclaim PepMap RSLC C18 (75 µm x 250 mm, size of reverse phase particles 2 µm) using following gradient: 0 min 3 % B, 5 min 3 % B, 85 min 50 % B, 86 min 90 % B, 95 min 90 % B, 96 min 3 % B, 110 min 3 % B. Mobile phase A was 0,1% formic acid in water and mobile phase B was 0.1 % formic acid in acetonitrile. The flow rate during gradient separation was set to 0.3 µL/min. Peptides were eluted directly to the ESI source – Captive spray (Bruker Daltonics, Germany). Measurement was carried out in positive ion mode with precursor selection in the range of 400–2200 Da; from each MS spectrum up to ten precursors were selected for fragmentation.
Peak lists were extracted from raw data by Data Analysis (Bruker Daltonics, Germany). Proteins were identified using Mascot version 2.2.04 (Matrix Science, UK) by searching protein database Uniprot version 20110–12. Parameters for database search were set as follows: Oxidation of methionine and hydroxylation of proline as variable modifications, tolerance 50 ppm in MS mode and 0.05 Da in MS/MS mode.

[1] It is important to notice that the author carried on only the protein digestion of the procedure, while the rest of the analysis was carried out by Dr. Štěpánka Kučková of the Department of Biochemistry and Microbiology of UCT, whom we acknowledge and thank; the paragraph following is an excerpt of Dr. Kučková analytical report.

Chapter 2.8.3: RAMAN spectroscopy

Raman spectroscopy (RS) is less common in the study of archaeological materials due to a series of limitations imposed by the method itself, and to the cost of the instrumentation (Smith, Clark 2004, 1137). Similarly to FTIR, Raman spectroscopy is based on the detection of the molecular vibrations, and allows to simultaneously observe composition, crystalline phase and bonding of the specimen in any physical form (Smith, Clark 2004). This analytical procedure starts with shooting on the sample a monochromatic photon beam, which causes the molecules of the samples to shift to unstable excited states. The majority of the scattered electrons decay following the so-called Rayleigh effect (Young 1981) bearing no information "on the vibrational energy levels of the sample" (Smith, Clark 2004, 1138). However, a minor quantity of scattered photons – therefore called Raman photons – vibrates at different energies, which are detected by the Raman spectroscope and recorded. The identification of the elements happens by comparison with existing databases. The major advantage of this technique is the possibility to connect the Raman spectroscope to a microscope, obtaining high-resolution and point-related information on a microscopic scale. Furthermore, through RS it is possible to analyse not fully crystalline materials, such as glass or glazes.

In this study, RS was performed on a small pool of eleven samples with the specific purpose of identifying the pigments contained in the thin, superficial layer. Three samples (NPA 27, NPA 28, NPA 29) were analysed using a Raman microscope DXR3xi (Thermo Scientific) with an excitation laser at a wavelength of 532 nm and a power of 0.5–10 mW on the sample (the power was adjusted to avoid sample damage), in the spectral range of 1800-50 cm^{-1}. Maps and points were measured from various parts of the samples' surface with a measurement step of 2–5 μm. The remaining seven samples were analysed at the Faculty of Chemistry of the University of Warsaw: the spectra were obtained on a Dispersive Raman Spectrometer Nicoled Almega equipped with confocal microscope. All spectra were recorded with use of the 780 nm laser and high-resolution grating (1200 line/mm). The power of the laser on the sample was reduced to 30–50% in order to avoid sample overheating and consequent damage. The exposure time was set to 30 s; each spectrum was a sum of two independent scans.

Samples were placed on the microscope stage and the laser was focused on the selected spot with a diameter of 1–2 μ^2. FTIR spectra were recorded on IS5 Nicolet Infrared Spectrometer equipped with GladiATR accessory with diamond crystal. Each spectrum was averaged from 128 scans. The spectral resolution was 2 cm^{-1}.

Chapter 2.8.4: Burning and slaking

In addition to the archaeological samples, 30 geological samples were collected. These stones were analysed with XRD and TA (following the same procedure employed for the archaeological materials); in addition, burning and slaking experiments were performed in order to assess the quality of the produced lime and to estimate the suitability of the stones for their production.

The limestone samples were crushed to a particle size of 10 to 30 mm and calcinated in a laboratory electric muffle furnace (type LAC LMH04/12). The furnace was set to rise from 20°C to 1050°C over a period of 6 hours (i.e. 170 °C/hour) and then to maintain a constant temperature of 1050°C for 1 hour. The particular temperature and dwelling time were set to create conditions for maximising possible compound combinations (Válek *et al.* 2014). The burnt material was slaked following the standard ČSN EN 459-2 (722201). Slaked lime was left to cure underwater for 12 months.

ILLUSTRATION PLATES

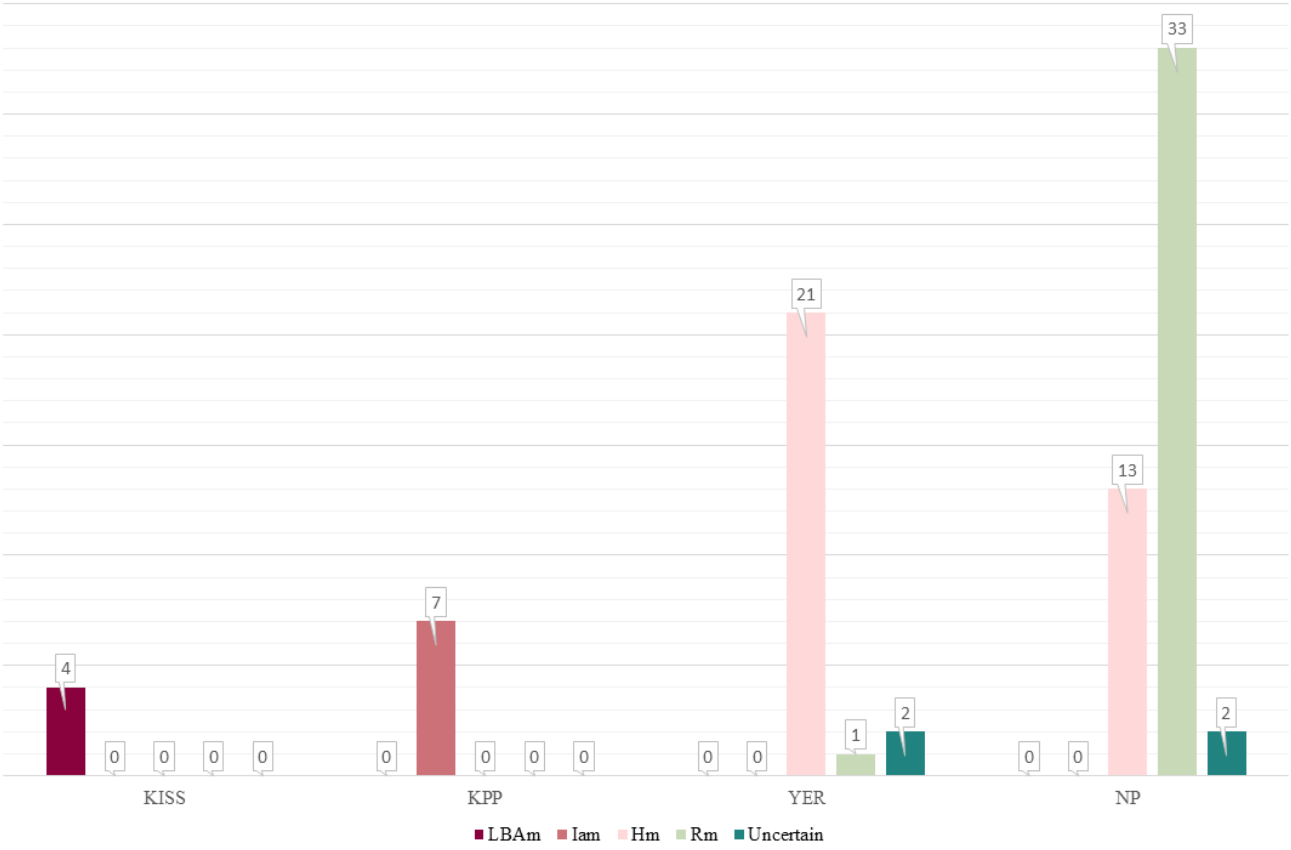

Graph 1 *illustrates the distribution of the collected samples in each site, highlighting the amount of samples collected for each chronological period considered in this study. As evidenced by this graph, the majority of the samples were collected in Yeronisos and Nea Paphos, thus covering extensively the Hellenistic and Roman periods. Legend: LBAm=Late Bronze Age mortars; Iam= Iron Age mortars; Hm= Hellenistic mortars; Rm= Roman mortars.*

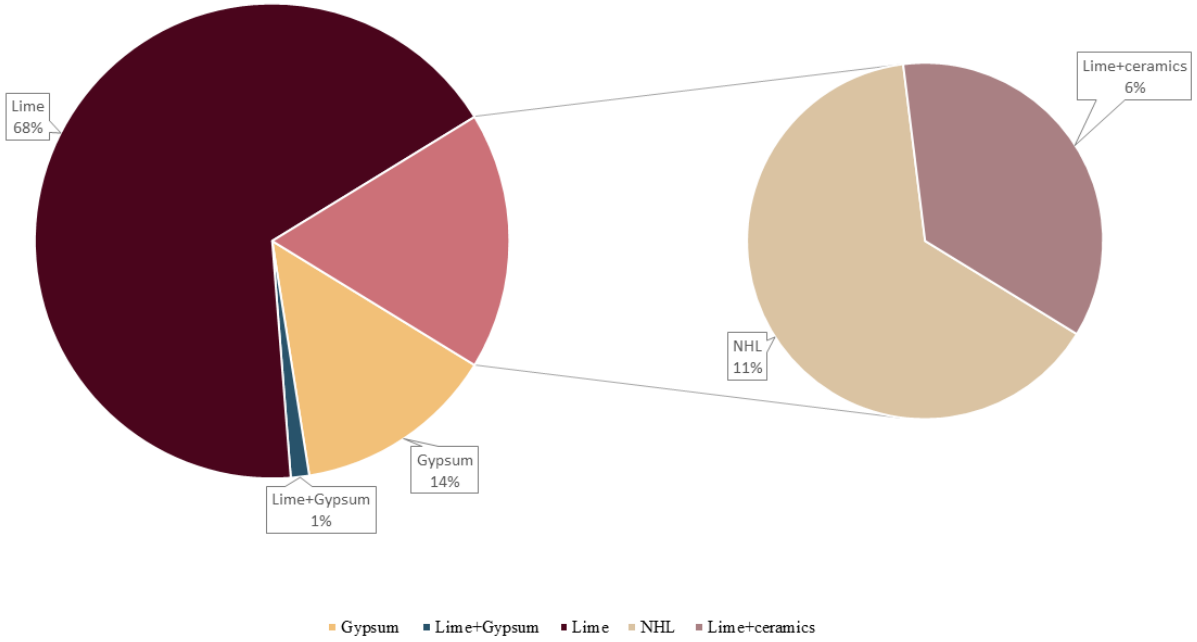

Graph 2 *highlights the distribution of samples according to their main binder type. NHL and Lime+Ceramics binder constitute a special category, here nominated "possibly hydraulic" binders.*

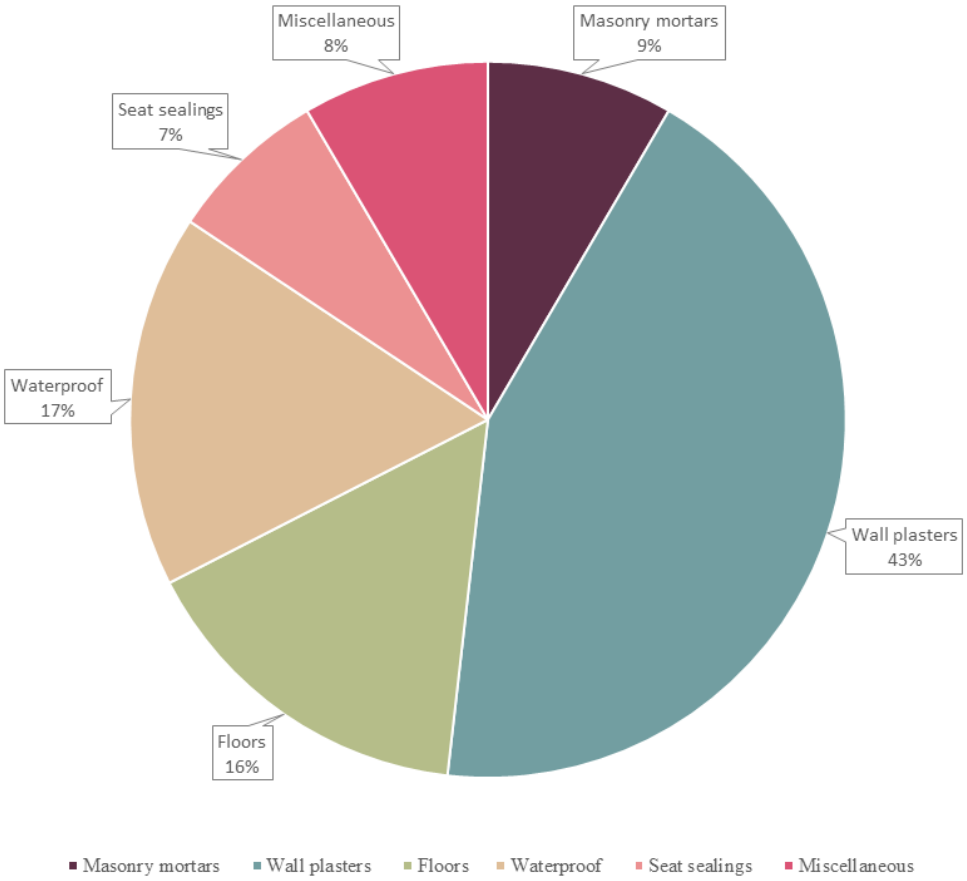

Graph 3 *displays the distribution of samples according to their functional categories.*

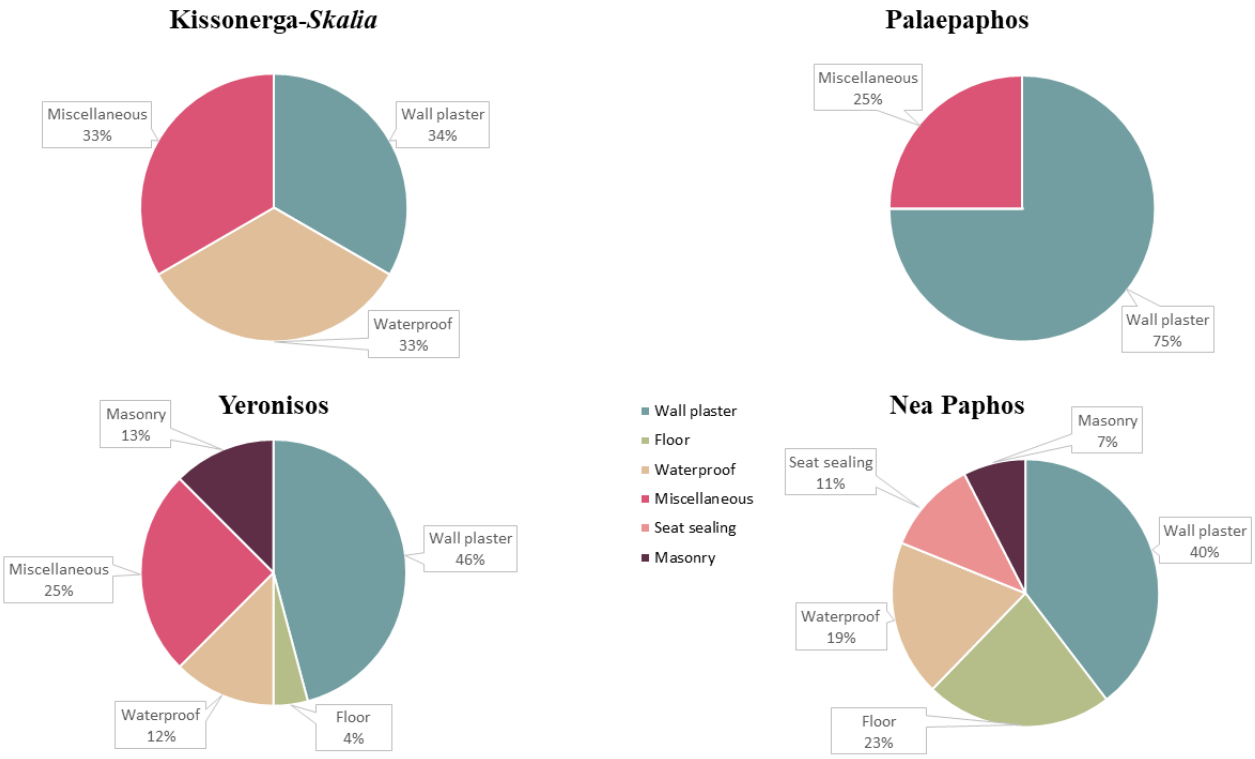

Graph 4 *displays the distribution of samples according to their functional categories per each archaeological site.*

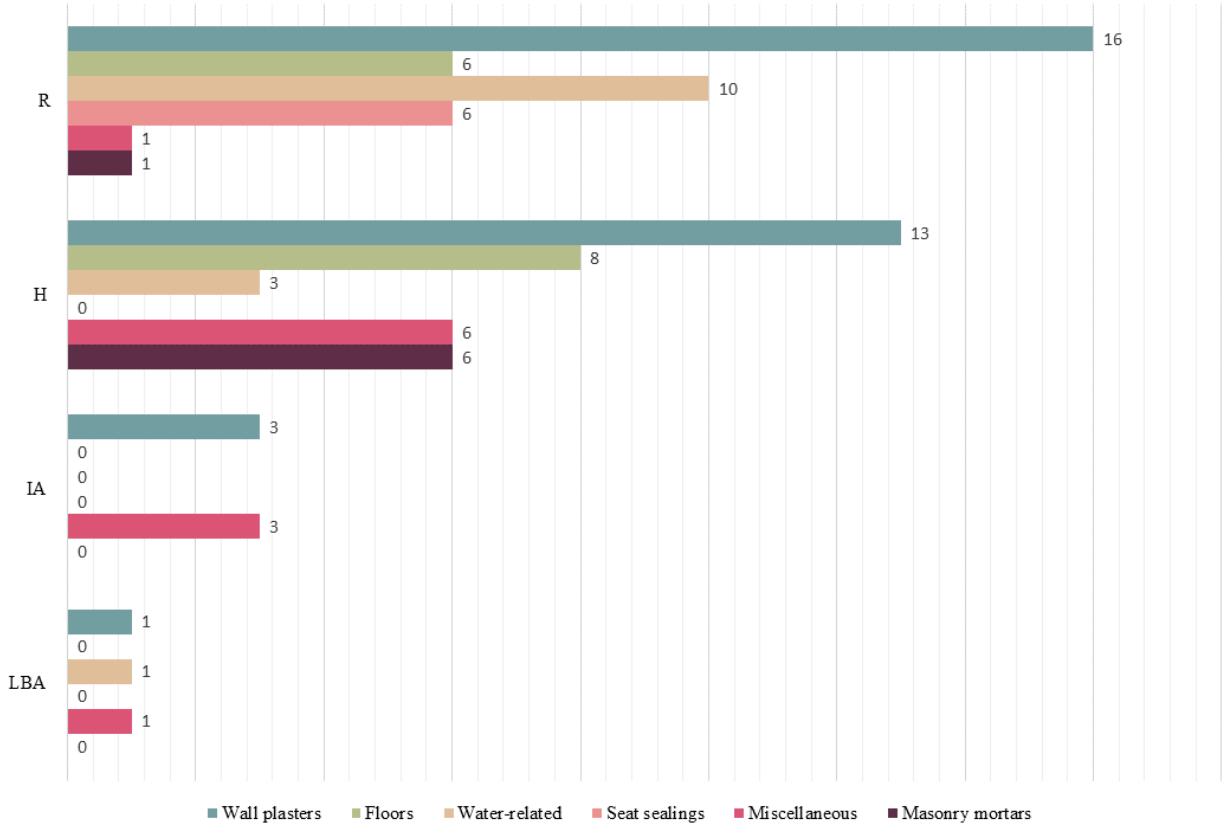

Graph 5 *displays the distribution of samples according to their functional categories per chronological period.*

REFERENCES

AMADIO, M.

2018. From deposits to social practices: Integrated micromorphological analysis of floor sequences at Middle Bronze Age Erimi-Laonin tou Porakou, Cyprus. *Journal of Archaeological Science: Reports* 21, pp. 433–449. https://doi.org/10.1016/j.jasrep.2018.07.023

BORELL, A., A. OLLÉ, J.M. VERGÈS, R. SALA

2014. Scanning Electron and Optical Light Microscopy: two complementary approaches for the understanding and interpretation of use wear and residues on stone tools. *Journal of Archaeological Science* 48, pp. 46–59. https://doi.org/10.1016/j.jas.2013.06.031

CAVALHEIRO, E.T.G.

2019. Thermal Analysis | Overview. *Encyclopaedia of Analytical Science, 3rd edition, v.* 10, pp. 12–16. https://doi.org/10.1016/B978-0-12-409547-2.14380-X

CHEREMISINOFF, N.P.

1996. Thermal Analysis, in N.P. Cheremisinoff (ed.), *Polymer Characterization: Laboratory Techniques and Analysis*, Westwood: Noyes Publications, pp. 17–24. https://doi.org/10.1016/B978-081551403-9.50004-2

CONNELLY, J.B., A.I. WILSON, C. DOHERTY

2002. Hellenistic and Byzantine Cisterns on Geronisos Island, *RDAC* 2002, pp. 269–292.

DIAZ, J., R. ŠEVČÍK, P. MÁCOVÁ, B. MENÉNDEZ, D. FRANKEOVÁ, Z. SLÍŽKOVÁ

2022. Impact of nanosilica on lime restoration mortars properties. *Journal of Cultural Heritage* 55, pp. 210–220. https://doi.org/10.1016/j.culher.2022.03.014

EARLE S.

2015. *Physical Geology*. Victoria: BC Campus.

ERGENÇ, D., R. FORT, M.J. VARAS-MURIEL, M. ALVAREZ DE BUERGO

2021. Mortars and plasters—How to characterize aerial mortars and plasters, *Archaeological and Anthropological Sciences* 13, 197. https://doi.org/10.1007/s12520-021-01398-x

FÖLDVÁRI, M.

2011. *Handbook of Thermogravimetric System of Minerals and Its Use in Geological Practice*. Budapest: Geological Institute of Hungary.

GROOT, C.J.W.P., G.J. ASHALL, J.J. HUGHES, P.J.M. BARTOS
2004. Characterization of old mortars with respect to their repair: A state of the art, in C. Groot, G. Ashall, J. Hughes (eds.), *Characterization of Old Mortars with Respect to their Repair, RILEM TC 167-COM*, pp. 1–8.

HILL, J.O.
2005. Thermal Analysis | Overview. *Encyclopaedia of Analytical Science, 2nd edition*, pp. 17–22. https://doi.org/10.1016/B0-12-369397-7/00613-0

HILL, J.O., R.K. VERMA,
2019. THERMAL ANALYSIS | COUPLED TECHNIQUES. *Encyclopaedia of Analytical Science, 3rd edition, v.* 10, pp. 6–12. https://doi.org/10.1016/B978-0-12-409547-2.14380-X

KARAGEORGHIS, V., M.V. DEMAS,
1998. *Excavations at Maa-Palaeokastro: 1979-1986*. Nicosia: Cyprus Dept. of Antiquities.

KOZLOVCEV, P., K. KOTKOVÁ, D. FRANKEOVÁ, J. VÁLEK, A. VIANI, J. MAŘIKOVÁ-KUBKOVÁ
2023. Characterisation of Historic Mortars Related to The Possibility of Their Radiocarbon Dating, Mikulčice and Pohansko Archaeological Sites, in V. Bokan Bosiljkov, A. Padovnik, T. Turk (eds), *Conservation and Restoration of Historic Mortars and Masonry Structures. HMC 2022. RILEM Bookseries* (42), Springer Nature, pp. 172–190.

KOZLOVCEV, P., J. VÁLEK
2021. The micro-structural character of limestone and its influence on the formation of phases in calcined products: natural hydraulic limes and cements, *Materials and Structures* 54, 217. https://doi.org/10.1617/s11527-021-01814-7

LETOURNEUX, J., S. FENEUILLE
2012. Mineralogical and Microstructural Analysis of Mortars from Kushite Archaeological Sites, in J. Válek, J.J. Hughes, C.J.W.P. Groot (eds.), *Historic Mortars. Characterisation, Assessment and Repair*, *RILEM Bookseries* 7, pp. 37–48.

LUND, J.
2015. *A Study of the Circulation of Ceramics in Cyprus from the 3rd Century BC to the 3rd Century (Gosta Enbom Monographs).* Aarhus: Aarhus University Press.

MARSHALL, D.J.
1988. *Cathodoluminescence of Geological Materials.* London: Unwin Hyman Ltd.

MIDDENDORF, B., J.J. HUGHES, K. CALLEBAUT, G. BARONIO, I. PAPAYANNI

2007. Mineralogical characterization of historic mortars, in C. Groot, G. Ashall, J.J. Hughes (eds.), *Characterization of Old Mortars with Respect to their Repair, RILEM* TC 167-COM: 37–54, Bagneux: RILEM Publications S.A.R.L.

MIRIELLO, D. L. BARBA PINGARRÓN, A. BARBA PINGARRÓN, D. BARCA, A. BLOISE, J.R. GONZALES PARRA, G. CRISCI, R. DE LUCA, G. GIRIMONTE, J.L. RUVALCABA-SIL, A. PECCI

2021. Hydraulicity of lime plasters from Teotihuacan, Mexico: a microchemical and microphysical approach. *Journal of Archaeological Science* 133, 105453. https://doi.org/10.1016/j.jas.2021.105453

MURAKAMI, T., G. HODGINS, A.W. SIMON

2013. Characterization of lime carbonates in plasters from Teotihuacan, Mexico: preliminary results of cathodoluminescence and carbon isotope analyses. *Journal of Archaeological Science* 40, pp. 960–970. http://dx.doi.org/10.1016/j.jas.2012.08.045

PECCHIONI, E., F. FRATINI, E. CANTISANI

2014. *Atlas of the Ancient Mortars*. Firenze: Nardini Editore.

PHILOKYPROU, M.

2012a. The Earliest Use of Lime and Gypsum Mortars in Cyprus, in J. Válek, J.J. Hughes, C.J.W.P. Groot (eds.), *Historic Mortars. Characterisation, Assessment and Repair, RILEM Bookseries* 7, pp. 25-36, Springer.

2012b. The Beginnings of Pyrotechnology in Cyprus. *International Journal of Architectural Heritage* 6, pp. 172–199. https://doi.org/10.1080/15583058.2010.528145

QUINN, P.S.

2022. *Thin Section Petrography, Geochemistry and Scanning Electron Microscopy of Archaeological Ceramics*. Oxford: Archaeopress.

RICHTER, D.K., TH. GÖTTE, J. GÖTZE, R.D. NEUSER

2003. Progress in application of cathodoluminescence (CL) in sedimentary petrology. *Mineralogy and Petrology* 79, pp. 127–166. https://doi.org/10.1007/s00710-003-0237-4

RIETVELD, H.M.

1969. A profile refinement method for nuclear and magnetic structures. *Journal of Applied Crystallography* 2, pp. 65–71.

RIZZO, G., B. MEGNA
2008. Characterization of Hydraulic Mortars by Means of Simultaneous Thermal Analysis. *Journal of Thermal Analysis and Calorimetry* 92, pp. 173–178. http://dx.doi.org/10.1007/s10973-007-8757-5

SINGH, M., S. WAGHMARE, S. VINODH KUMAR
2014. Characterization of lime plasters used in 16th century Mughal monument. *Journal of Archaeological Science* 42, pp. 430–434. https://doi.org/10.1016/j.jas.2013.11.019

SMITH, G.D., R.J.H. CLARK
2004. Raman microscopy in archaeological science. *Journal of Archaeological Science* 31, pp. 1137–1160. https://doi.org/10.1016/j.jas.2004.02.008

SMITH, B.C.
2011. *Fundamentals of Fourier Transform Infrared Spectroscopy.* Boca Raton: CRC Press.

TURCO, F., P. DAVIT, F. CHELAZZI, A. BORGHI, L. BOMBARDIERI, L. OPERTI
2016. Characterization of Late Prehistoric Plasters and Mortars from Erimi – Laonin tou Porakou (Limassol, Cyprus). *Archaeometry* 58, pp. 284–296. https://doi.org/10.1111/arcm.12168

VÁLEK, J., E. VAN HALEM, A. VIANI, M. PÉREZ-ESTÉBANEZ, R. ŠEVČÍK, P. ŠAŠEK
2014. Determination of optimal burning temperature ranges for production of natural hydraulic limes. *Construction and Building Materials* 66, pp. 771–780. https://doi.org/10.1016/j.conbuildmat.2014.06.015

VÁLEK, J.
2015. *Lime Technologies of Historic Buildings*. Prague: Ústav teoretické a aplikované mechaniky, Akademie věd České republiky, v.v.i.

YACOBI, B.G., D.B. HOLT
1990. *Cathodoluminescence Microscopy of Inorganic Solids*. Boston: Springer. https://doi.org/10.1007/978-1-4757-9595-0_4

YOUNG, A.T.
1981. Rayleigh scattering. *Applied Optics* 20, pp. 533–535. https://doi.org/10.1364/AO.20.000533

PART 3. SUMMARY OF RESULTS

Introduction

This chapter focuses on the results of the analytical work described in the previous section of the present thesis. As around 90 samples were analysed through different techniques, it was not possible to incorporate all the results in a cohesive and clear manner. The present chapter contains representative and carefully selected results, to highlight how certain conclusions have been drawn. The complete list of analysis is synthesized in the Appendix.

Chapter 3.1: Microscopy (PLM-CL-SEM)

Chapter 3.1.1: Optical Microscopy and cathodoluminescence

Optical microscopy was the first step for the identification and classification of the pool of samples under study. Observing the thin sections under a polarized light microscope, in combination with different LED and UV lights, allowed for a systematization of the specimens into categories – called systems – based on a combination of their functionality and micromorphological properties. The primary characteristic elements observed under the microscope were aggregates, binders and pores' structure.

Aggregates

As an important reminder, in the present thesis the term "aggregate" indicates all the materials intentionally added in the mixture.

In terms of aggregates, it is possible to distinguish two principal groups of components based on the frequency of occurrence: primary and secondary. Primary components are typically sedimentary limestone and calcarenite, variety of bioclasts, chert and quartz; while secondary components are covered by different typologies of metamorphic rocks and minerals, ceramic fragments, and feldspars; charcoal is considered an additional component (**tab. 2**).

Bioclasts and limestones are the predominant aggregates in the samples under study, occurring in almost 95% of the specimens (**tab. 3**), as primary or secondary components. Limestones are predominantly biomicrites, with rarer occurrences of chalks and calcarenites; bioclasts occur in several typologies, with a predominance of planktonic and benthic foraminifera, gastropods, bivalves and echinoderm spines. Notably, specific classes of bioclasts – in particular, benthic foraminifera and bryozoans (corals) – are selected as primary aggregate in the finishing layers of wall plasters.

Chert is another typical primary or secondary component, with an occurrence rate of ca. 85%; most of the radiolarian chert includes iron oxides pollutants. Quartz, feldspars and metamorphic rocks occur in more than half of the samples; among the metamorphic rocks the most common is serpentine, with mica, basalt, diorite, and olivine occurring less frequently.

Type	Variants	Reference picture	Description
Limestone and Calcarenite	*Bioclast variant*	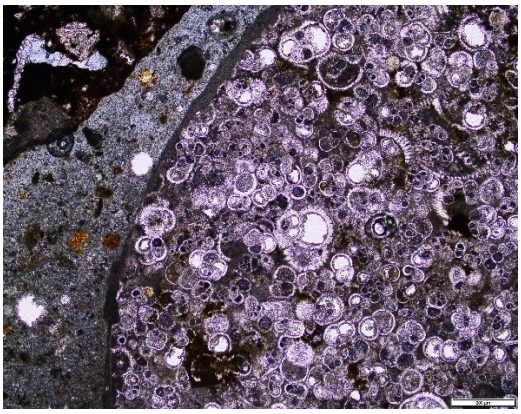 Sample NPT 3A_micritic limestone filled with planktonic foraminifera, PPL. Scale = 200 µm	Usually well-rounded, fine to coarse fragments of micritic limestone rich in bioclastic content (predominantly planktonic foraminifera and/or gastropods*). This type of aggregate is almost omnipresent in the mortar mixtures observed. **High concentration of planktonic foraminifera in some lime binders might be due to the burning process of this typology of geological limestone.*
	Micritic variant	 Sample NPT 3A_micritic limestone aggregate with large calcite crystals infills, PPL. Scale = 200 µm	Angular or sub-angular, usually present in coarser fractions, this type of aggregates is well compatible with the geological limestone of the region. It is characterized by large calcite crystals originating from the recrystallization of channels and large voids.
Bioclasts	*Gastropods*	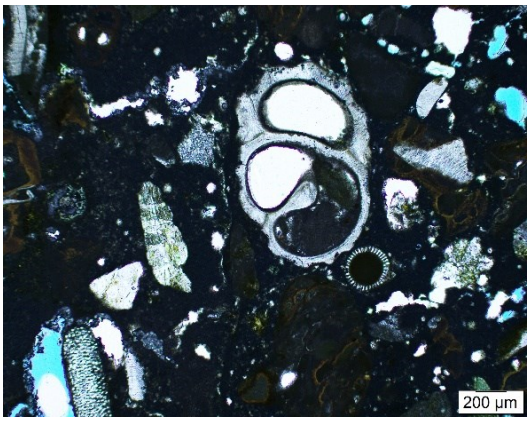 Sample NPT 1_well-preserved gastropod shell, PPL.	Gastropods are the most common types of bioclasts observed in the samples. Dimensions and shapes significantly vary, but overall correspond with the fossils observed in the local rock formations.

	Bivalves	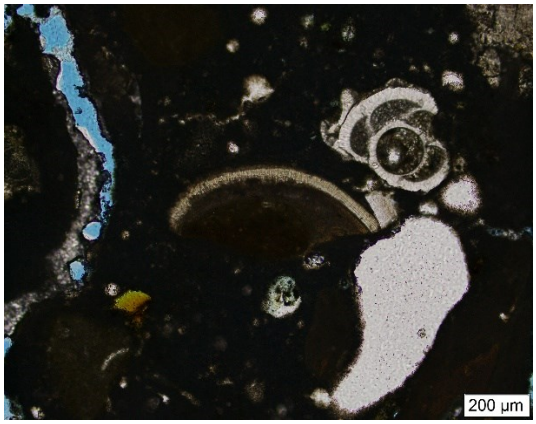 NPT 1_fragment of bivalve shell with the typical C-shape (or parenthesis-shape), PPL.	Bivalves are the second most common bioclasts types in the analysed samples. They usually appear in form of rounded, C-shaped particles. Often broken and not fully preserved.* **Suggesting that they were possibly crushed before being added to the mixture.*
	Brachiopods	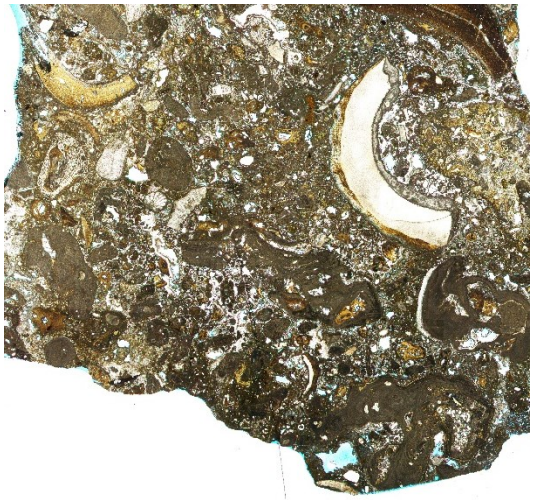 Sample LCY012_fragment of brachiopod shell embedded in a geological calcarenite sample, PPL. Scale = 2 mm	Brachiopods are detected less frequently. They appear as partial fragments of C-shaped shells with typically one wavy side.
	Ammonites	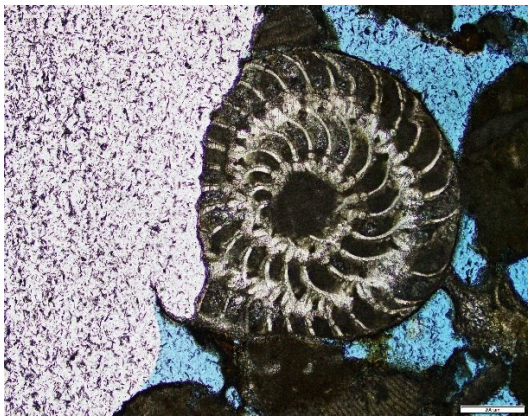 Sample YSC 18_section of ammonite embedded in a stone fragment, PPL. Scale = 200 µm	Ammonites are usually not as well preserved as in the picture attached. They are preserved to such extent in fewer instances, and normally appear in just small fragments.

	Corals (planktonic and benthic foraminifera, echinoderm spines, bryozoan colonies)	 Sample NPA 23_fragment of algae fossil (possibly *Paulsivella Antiqua*), PPL.	Corals are predominant aggregates in the finishing layers of the double-layered plaster systems. There is an evident choice and careful selection of aggregates for these layers, which mostly consists of corals – specifically the bryozoan colonies.
Chert	*Radiolarian*	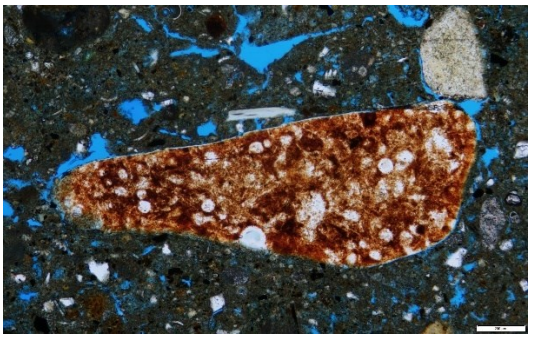 Sample KISS 4_well-rounded fragment of radiolarian chert with typical red colour, PPL. Scale = 200 µm.	Radiolarian chert is typically found in the Diarizos river basin, and it originates in the Troodos range (see Chapter 1.3). It is characterized by a typically well-rounded shape – as opposite to the more angular fragments not deriving from river sands – and by a distinctive red colour and spot-like texture, which is due to the radiolarian origin.
	Non-radiolarian	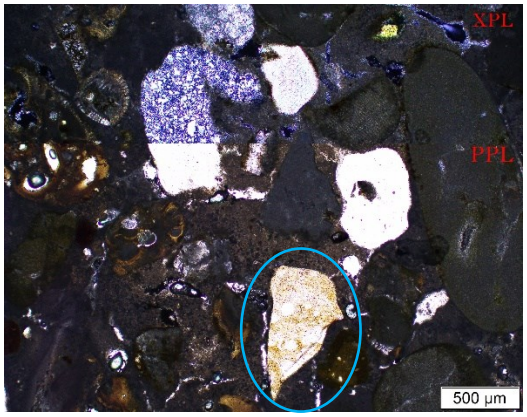 Sample NPA 7_fragments of chert of non-radiolarian origin as seen in XPL (top) and PPL (bottom). Circled in blue is a fragment of radiolarian chert.	In PPL this type of chert appears fully transparent and perfectly compatible with the appearance of quartz or feldspars. However, in XPL, chert presents a characteristic foggy texture that distinguishes it from quartz' usual refractivity.

Quartz		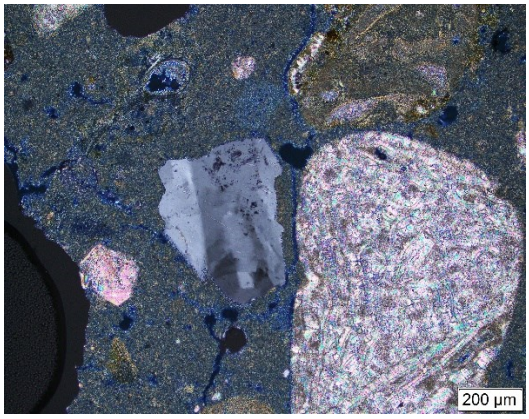 Sample NPA 23_quartz crystal in XPL with the typical grey colours. Undulous extinction can indicate an origin from a metamorphic rock.	Quartz particles present a sharp, angular shape and a colourless appearance in PPL, while the refractive colours vary in the shades of grey in XPL. It is a quite common aggregate and it was recorded in the majority of the samples, as well as in the geological stones.
Clay		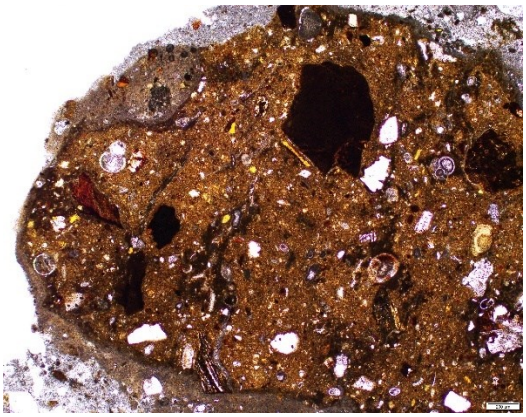 NPT 3A_fragment of coarse crushed fired ceramic embedded in lime plaster matrix, PPL. Scale = 200 µm.	Fired ceramics and bricks fragments are common aggregates in the samples associated with water-retaining properties. Occasionally, they can appear in other samples as well – but rather as an accidental addition, than a planned one. Ceramic fabrics vary from very fine to coarse ones but are overall compatible with the studied ware typologies of Cyprus for the period of interest. Multiple fabrics can be added to the same mixture.
Metamorphic rocks	*Serpentine*	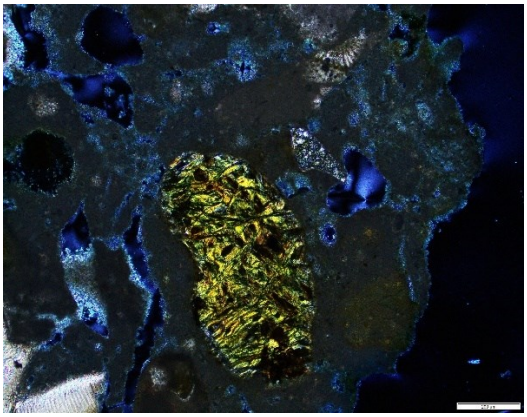 Sample NPT 11a_fragment of serpentine, XPL. Scale = 200 µm.	Among the metamorphic rocks, serpentine is the most common in the Paphian samples. In particular, it seems to be more common in the samples from Nea Paphos site, and scarcer in the other archaeological contexts. Characteristic is the roundness of the fragments, suggesting it was included in river sand.

	Mica	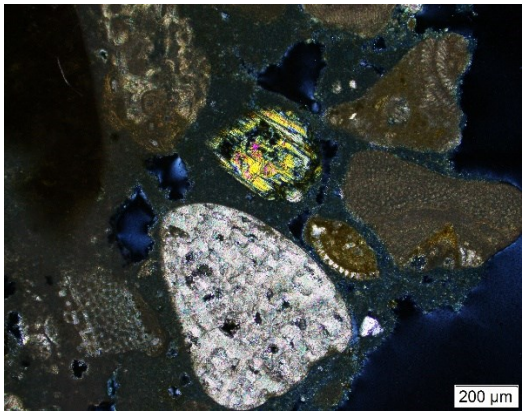 NPT 1_fragment of mica in XPL, with the typical needle-shaped crystals.	Mica appears rarely and in the form of very fine (< 0.5 mm), needle-shaped crystals with bright refractive colours. It is more common in the geological samples.
	Basalt	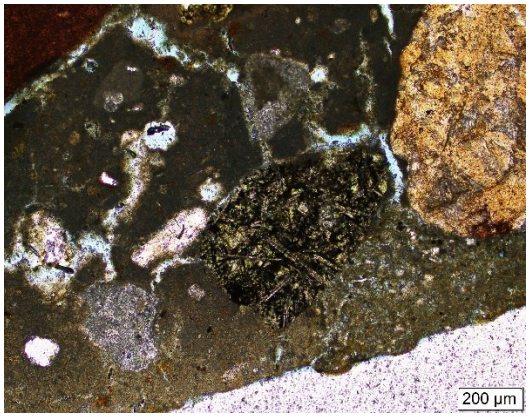 Sample YSC 4_fragment of very fine basalt, PPL.	Basalt is the least common of the metamorphic rocks in the analysed samples. It always appears in the form of well-rounded, usually large (above 1.5 mm) fragments with fine texture and a characteristic dark-green colour.
	Olivine	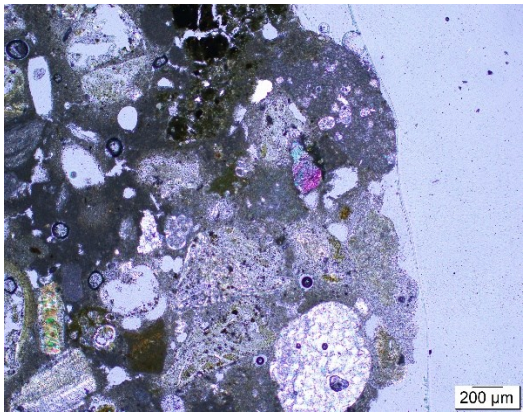 Sample NPA 17_fragment of olivine with characteristic pleochroism between green and pink, XPL.	Olivine is also relatively scarce and has been detected in the form of very fine (< 0.5 mm), singular crystals, suggesting more of an accidental inclusion rather than an intentional addition.

Feldspars		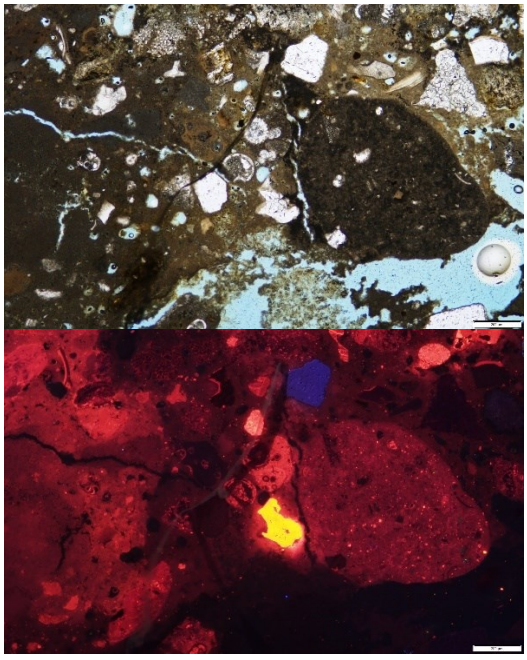 Sample NPT 11B_PPL photomicrograph of a feldspar (top), and same view in CL (bottom). Scale = 200 µm.	Feldspars appear as sharply angular, fine, colourless particles in PPL. They are usually contained in small percentages in most of the samples, however in certain instances they are extremely fine and cannot be detected at the naked eye. Feldspars can be recognized in CL, where they display bright colours, such as blue (K-feldspars) or green.
Charcoal		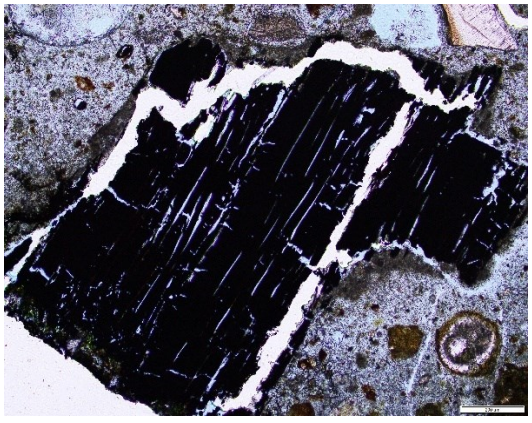 Sample NPT 3A_charcoal fragment of wood, possibly of conifer family, PPL. Scale = 200 µm.	Charcoal is the least common of the aggregates. It is preserved only in a handful of samples (less than 10). The dimensions are usually inferior to 1 mm, causing issues in the identification of the original species.

***Table 2**) List of the principal components detected in the archaeological samples under study. For each aggregate are recorded sub-variants, a reference picture and a brief description. In pink are highlighted the primary components, while the secondary are highlighted in green; in grey the accessory components*.

Aggregate	%
Limestone	93.3%
Bioclasts	93.3%
Chert	84.4%
Quartz	66.7%
Metamorphic rocks	60.0%
Ceramic fr./clay powder	51.1%
Feldspars	33.3%
Gypsum	4.4%
Organic materials	9.5%

Table 3*) The table includes a list of the major types of aggregates and the percentages in which they occur in the samples; it is important to note that gypsum samples do not have aggregates in the mixture, thus are not included in the calculations. As observable, limestone and bioclasts are predominant, being present almost all the samples.*

Binders

With optical microscopy it was possible to identify two major groups of binders: the lime-based and the gypsum-based. Within the lime group there is considerable variability in terms of micromorphology and general composition; the distinctions between these sub-categories will be discussed further in Chapter 4.

Lime-based samples are characterized by a generally fine binder, compact and usually well preserved. The colour of the lime matrix varies between yellow, light grey and dark grey. Variations of colours in lime can be due to several factors: firstly, the chemical composition of the geological raw material, but secondly – and not less importantly – the depositional context can influence the colour of the matrix, due to the presence of organic microorganisms, contaminating agents and infiltration of water.

On average, the lime samples present a well-mixed binder, without considerable heterogeneity; darker areas are observed in some specimens and could be ascribed to the presence of organics, or defects in the sample processing (*i.e.* different thickness of the thin section). Binder-related particles (hereinafter BRP) are observed mostly in the samples from Kissonerga-*Skalia* and on an exceptional basis in the samples from Nea Paphos. BRP are documented in two forms: as lighter, less compact, circular areas with different optic properties; or as darker and denser particles (see **fig. 18** and **19**). In the majority of cases, BRP are unmixed lime lumps or under-burnt lime/limestone particles (**fig. 20**). Cathodoluminescence on a set of three trial samples (NPA 7, NPA 19 and NPA 20) revealed that unburnt particles of calcite are present in the bulk samples, as well as in the binder fraction, in the form of extremely fine (10 μm) particles. The ratio of non-burnt calcite versus lime is, on average, lower than 2%, with higher percentages in the coarse fraction of the sample (/a fraction).

Gypsum-based samples present a much coarser texture, with irregularly shaped gypsum crystals bound together with fine lime particles and yellowish siliceous components. In terms of colouration, gypsum samples appear typically grey or whitish. The samples are not compact, and

often present large voids, which could possibly be due to the preparation of the thin section and excessive polishing. There are remarkable similarities in terms of microstructures on a synchronic level: all the gypsum-based mortars, be they dating to the Iron Age or the Late Roman period, share similar characteristics. Despite the restrained pool of samples, this phenomenon cannot be overlooked as a simple coincidence but could rather suggest a consistency in the productive industry.

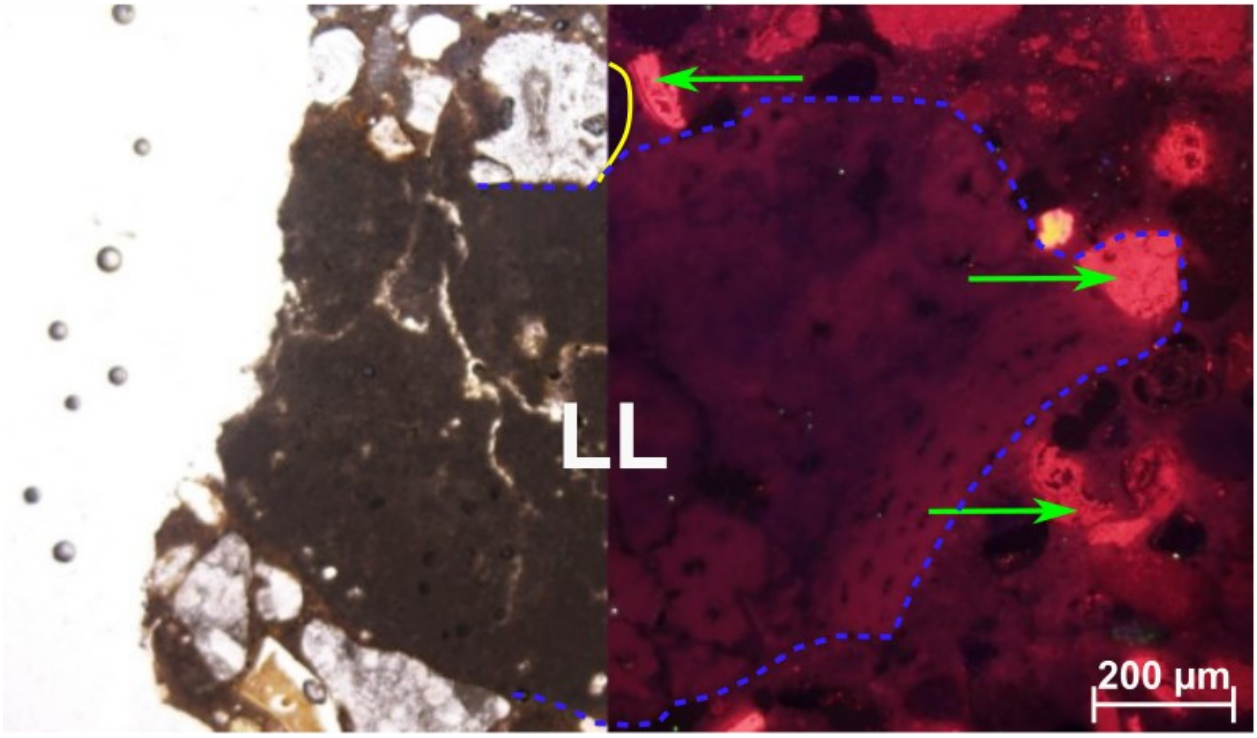

Figure 18*) Binder related particle of the denser type, as seen in PPL (left) and CL (right). Bright red colours in CL signify the presence of unburnt or partially burnt calcium carbonate particles: in particular, in this picture, it is possible to observe bright fragments of calcite/aragonite-based bioclasts (indicated by green arrows). Silica particles, on the other hand, have no fluorescence in CL, resulting in black areas (part of a Si particle are highlighted in yellow); for this reason, at times, in CL, it is not immediately possible to distinguish between Si particles and voids. A blue dotted line outlines the border of a lime lump particle.*

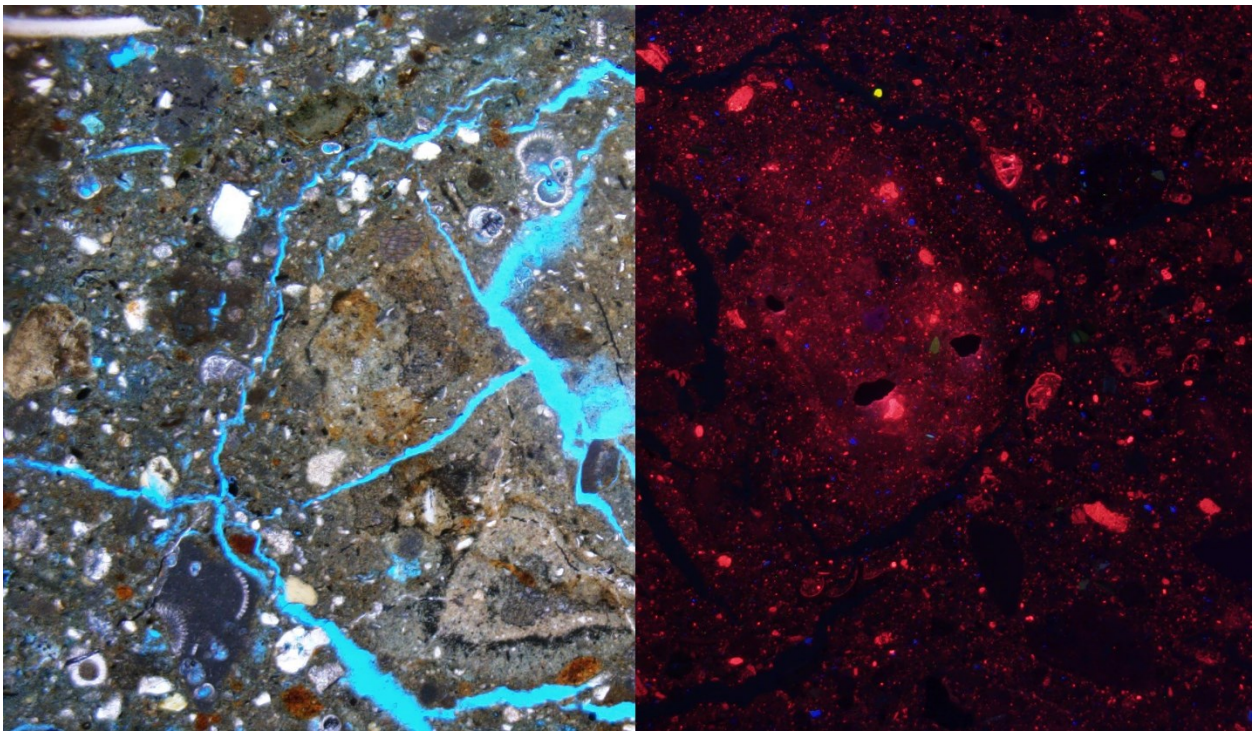

***Figure 19**) Binder related particle of the less compact type as seen in PPL (left) and CL (right). Other than the brighter red calcium carbonate particles, which are mostly bioclasts' fragments or small unburnt limestone remnants, it is possible to observe bright blue and yellow spots, which are identified as feldspars (K and Na respectively).*

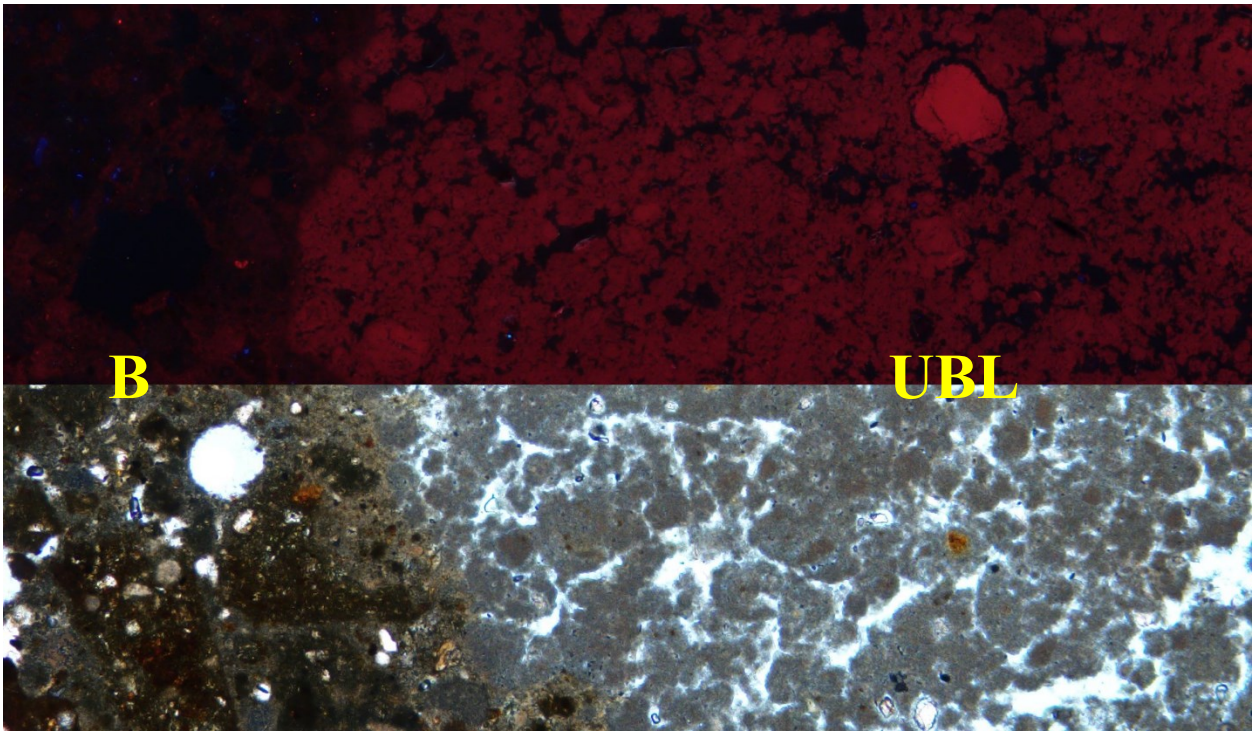

***Figure 20**) Under-burnt limestone particle as seen in CL (top) – with bright red luminescence – and in PPL (bottom). B = binder; UBL = under-burnt limestone particle.*

Pore structure

Porosity and pore structure are properties which influence the mechanical and physical performances of a plaster. Gypsum samples' porosity cannot be correctly estimated, and the visualisation of the pores' structure is heavily biased. This is due to an intrinsic issue when preparing thin sections of gypsum-based samples; gypsum is soluble in water and thus subject to dissolve during the polishing process. Therefore, the description in this paragraph will exclusively concern porosity in relation to the lime-based plasters.

In general, the Paphian samples are significantly porous. Most of the pores consist of microvoids caused by the decomposition of bioclasts and bioclastic materials; thus, these pores are not considered open, but rather closed, less influencing properties such as permeability. More significant are the large voids with irregular shapes that suggest the presence of water in the mixture. Other characteristic pores are thin cracks that run parallel to the surface (tramping) or perpendicularly to it (shrinkage cracks). Shrinkage and tramping cracks occur extensively in the samples. In most of the circumstances there are at least scanty traces of recrystallization inside pores and cracks.

Another, less common, typology of pores is caused by dissolution of the binder and precipitation: these features appear as coarser, inchoate calcite crystals around large or small irregularly-shaped voids.

Chapter 3.1.2: SEM-EDS analysis

In total, 36 samples were analysed using SEM-EDS. A combination of point analysis and elemental mapping was adopted in order to obtain data relevant for the identification of specific particles and assess the eventual hydraulicity of the samples. In each thin section examined, three to five points were collected by SEM-EDS from the binder matrix, to evaluate the binder composition and ascertain a degree of compatibility with the XRD and TA estimations. Additional points were collected according to the specific questions related to individual samples. Where paint layers were visible, SEM-EDS was carried out to identify the employed pigment(s).

SEM-EDS elemental mapping was carried out for the evaluation of possible hydraulicity by verifying the presence of either hydrated phases or reaction rims around ceramic aggregates – an important chemical reaction that provides hydraulic properties to otherwise pure air lime. The most significant elements kept in consideration for the characterisation of possible reaction rims are calcium (Ca), silicon (Si) and aluminium (Al); however, the former, is present in relatively low quantities in most of the analysed samples. Ceramic fragments have a number of slightly varying chemical and mineralogical components; in the case of the Paphian samples, most of the ceramic aggregates are composed of calcium, silicon, aluminium, magnesium (Mg), iron (Fe) and occasionally manganese (Mn). In a reaction rim the elements typically reacting are Si and Al (from the ceramic particle), and Ca (from the binder side). From the perspective of chemical composition, the reaction can be identified if the levels of Si are increasing in the area around the ceramic fragment compared to the normal levels on the binder; visually – in SEM-EDS mapping – reaction

rims appear as haloes around the ceramic particles, whose borders are no longer defined and sharp (Calzolari 2023). In **figure 21** we can observe an example of different interactions between ceramic fragments and surrounding binders. **Figure 21a** is a photomicrograph of a ceramic fragment in the binder of sample YHC 1: the binder is predominantly composed of calcium (Ca-red), with larger, unreactive, silica (Si-green), while the ceramic fragment is mainly composed of silicon (green) and aluminium (not pictured). In PLM, this same point appears as indicating the presence of a reaction rim, as the binder around the ceramic aggregate displayed different colour and density. However, as seen in the figure, there is not an increased presence of silica in the outer rim of the particle, neither in the inner one. The difference in colour in PLM might thus be explained simply with the different density of the binder in proximity with this porous particle, which attracted more binder by pore suction, enhancing adhesion. On the other hand, in **figure 21b** and **21C** it is possible to verify the presence of a proper reaction rim: in both figures it is possible to observe fine Si particles migrating toward the Ca-rich binder, causing the ceramic fragment's edges to etch due to the highly alkaline environment. While the presence of reaction rims can be verified relatively easily with SEM-EDS analysis, the identification of hydraulic components in a binder is more challenging, and even more so is the identification of so-called natural hydraulic lime binders. Fine and well distributed particles of SiO_2, Al_2O_3 and Fe_2O_3, which are present in the raw material, react at high kiln temperatures forming calcium silicate/aluminate products, the most common of which is dicalcium silicate (belite). During the hydration phase, the calcium silicate/aluminate harden and form amorphous C-A-S-H phases (Alvarez *et al.* 2021), the major compounds of hydraulic and natural hydraulic binder, constituting between 15–40% of it. The degree of hydraulicity, thus, can be estimated by measuring the content of SiO2, Al2O3 and Fe2O3 within the binding matrix, according to the formula of the cementation index (CI) illustrated in chapter 2.4.3. **Tab. 4** illustrates the results of the CI estimations according to the classification of reference.

Sample ID	CI	Classification
KISS 3	6.84	N.C.
YHC 1	0.12	Air lime
NPT 3A	0.32	Feebly hydraulic lime
NPT 12	0.27	Air lime
NPA 7	0.07	Air lime
NPA 8	0.08	Air lime
NPA 12	0.47	Feebly hydraulic lime
NPA 13	6.22	N.C.
NPA 19	0.67	Eminently hydraulic lime
NPA 20	1.96	Roman cement
NPA 30A/B	6.44/2.15	N.C.
NPH 1	4.59	N.C.
NPER 1	1.28	Eminently hydraulic lime
NPVT 1	6.9	N.C.

Table 4*) Results of the CI calculations according to the formula illustrated in chapter 2. The classification is after Válek* et al. *(2014, 772). N.C.=non classifiable; the CI of Roman and natural cements is typically between the limits of 1.0 and 2.0.*

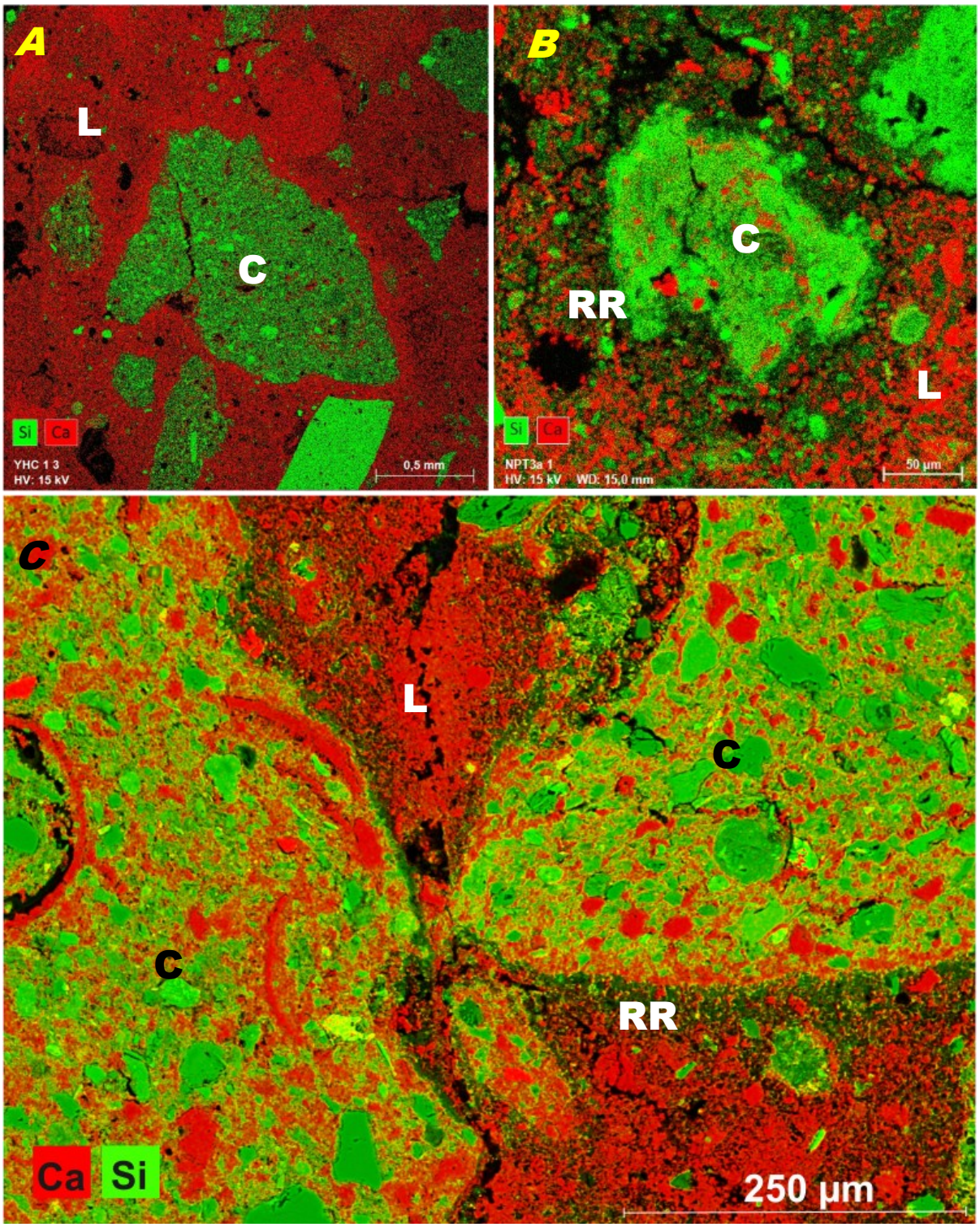

Figure 21A*) BSE image of sample YHC 1 with elemental distribution of Si and Ca, displaying a ceramic aggregate (C) surrounded by the binder matrix (L); no traces of reaction rims are visible; the binder appears denser around the ceramic particle (SEM TESCAN MIRA, EDS software Brucker Esprit 2.5).* ***B)*** *BSE image of sample NPT 3a with elemental distribution of Si and Ca, displaying a ceramic aggregate (C) in the partially hydraulic matrix (L); there are traces of a reaction rim around the ceramic particle (RR), although not as sharp and well defined as in fig. 3B (SEM TESCAN MIRA, EDS software Brucker Esprit 2.5).* ***C)*** *BSE image of sample NPA 12 with elemental distribution of Si and Ca, displaying a ceramic aggregate (C) with clear traces of reaction rims (RR) (SEM Zeiss EVO 25, EDS software Aztec 5.1).*

Furthermore, SEM-EDS analysis was employed as a tool for the identification of specific particles, especially finer aggregates and pigments; additionally, SEM high resolution images were kept in consideration for the study and identification of foraminifera (**fig. 22**) and charred plants' species (**fig. 23**). Although the attribution of the charcoal fragments to a specific plant species was not always possible due to their reduced size and scarce preservation status, comparisons between the preserved structures and the available online databases allowed in at least two cases to identify the charcoal fragments with local plant species. The identification of foraminiferas was far simpler, as there were larger amounts of them in the samples. Most of the analysed specimens belong to the family of planktonic or benthic foraminifera, organisms commonly contained in the Cypriot sedimentary rocks.

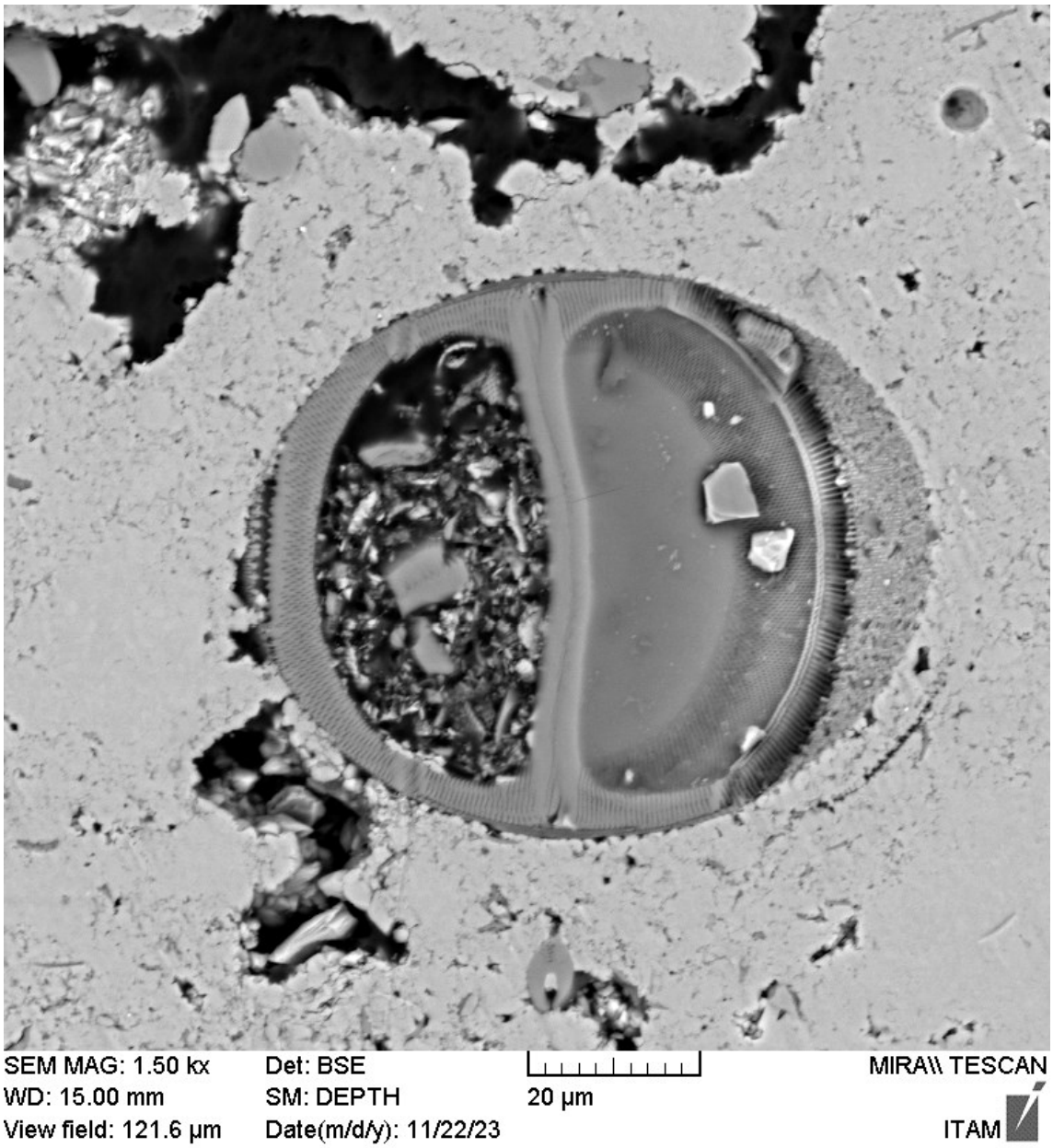

***Figure 22**) BSE image of a piece of planktonic foraminifera embedded in the matrix of the limestone sample KISS 1.*

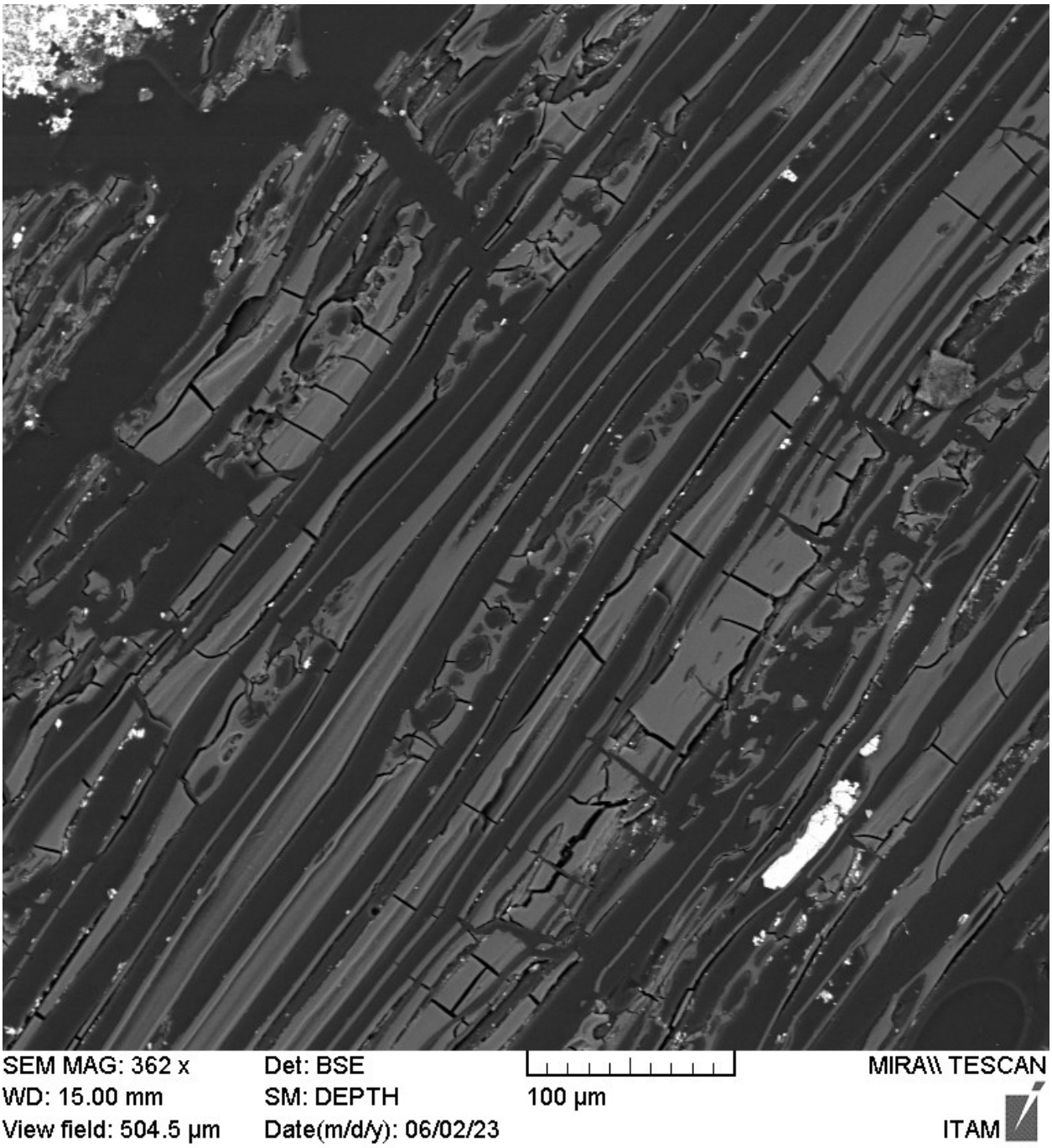

Figure 23*) BSE image of a charcoal fragment in the mortar sample NPT 3a. According to the comparison with published material (Castellano 2021, 11; Uhl, Jasper 2018, 178, 180; Carney 2016, 86) this charred wood can possibly belong to the family of conifer (picture taken in SEM TESCAN MIRA).*

Chapter 3.2: Mineralogical analysis

XRD analyses were conducted on the binder-rich fraction (/b), and, occasionally, on the binder and aggregates mixed fraction (/t). In **Tab. 5** it is possible to observe the main components analysed in each sample. Despite considering the /b fraction as binder-rich, it is important to underline that

finer aggregates' particles can still be included in it; for instance, minimal amounts of silica and clay minerals are constantly present in the analysed samples, and it is not possible to distinguish whether they are naturally present in the binder or either contamination of the aggregate fraction. The most common crystalline phases in the analysed specimens are calcite ($CaCO_3$) or gypsum ($CaSO_4$) as the main binding elements, with quartz/chert (SiO_2) and aragonite ($CaCO_3$) regularly present in minimal amounts. Feldspars are also recorded in XRD, even in instances where the particles were not identified in PLM; analysis with CL shed light on the presence of extremely fine (up to a few microns) feldspar crystals in the binder (see **Appendix II, fig. 4, fig. 13, and fig. 15**). Amorphous percentages vary based on the content of unstable silica phases, clays, and other non-crystalline components. The amorphous content signals the possible presence of NHL binders, as the hydrated phases do not have a highly crystalline form and consequently cannot be clearly identified in XRD. The evaluation of the presence of NHL must be done carefully and keeping in consideration several analytical techniques: in XRD two indicators of possible hydraulicity are the calcium-aluminium-silicate hydrate and the amorphous phases; in TA the ratio between CO_2/H_2O can suggest different hydraulic indexes; while SEM-EDS allows for the calculation of the cementation index.

Noteworthy is the presence – although in almost irrelevant percentages – of calcium-aluminium-silicate hydrate (C-A-S-H) phases in most of the gypsum binders. C-A-S-H are commonly associated with a hydraulic character and are often detected in NHL binders; gypsum-based plasters, due to the nature of the binder, are usually sensitive to water exposure, and normally do not contain such phases. Furthermore, C-A-S-H phases are usually produced at high temperatures, and their presence would imply gypsum burning at high temperatures, which would generate anhydrite (not identified in the samples). It is interesting that no C-A-S-H was detected in the possibly hydraulic samples, although it is possible that the hydrate minerals did not have a structure crystalline enough to be detected by XRD. More on this topic is discussed in the following chapter (4.5).

Unusual is the detection of halite (NaCl) and Cerussite ($PbCO_3$), although in lesser amounts. The presence of halite (NaCl) is ascribable to contaminations, possibly post-depositional, considering the proximity of the depositional environment to the coast and sea waters. Cerussite ($PbCO_3$) could be related to the use of a lead-based white pigment. All the other mineral phases detected are expected to appear in lime and gypsum plasters, other than being compatible with the minerals naturally present in the geological environment. Particular attention was also focused to the amorphous content detected by XRD. Amorphous phases are naturally present in a 15–30% ratio in lime plasters from Cyprus, while they are lower in the gypsum ones, maxing at around 20%. Whenever the amorphous content exceeds 30%, there is a reasonable possibility that the plaster is of NHL type, as the characteristic hydrated phases of this compound do not have a solidly crystalline structure (**fig. 24 and 25**).

The XRD analyses allowed the classification of the samples in three main categories: lime-based, gypsum-based, and possibly natural hydraulic plasters (**fig. 26**).

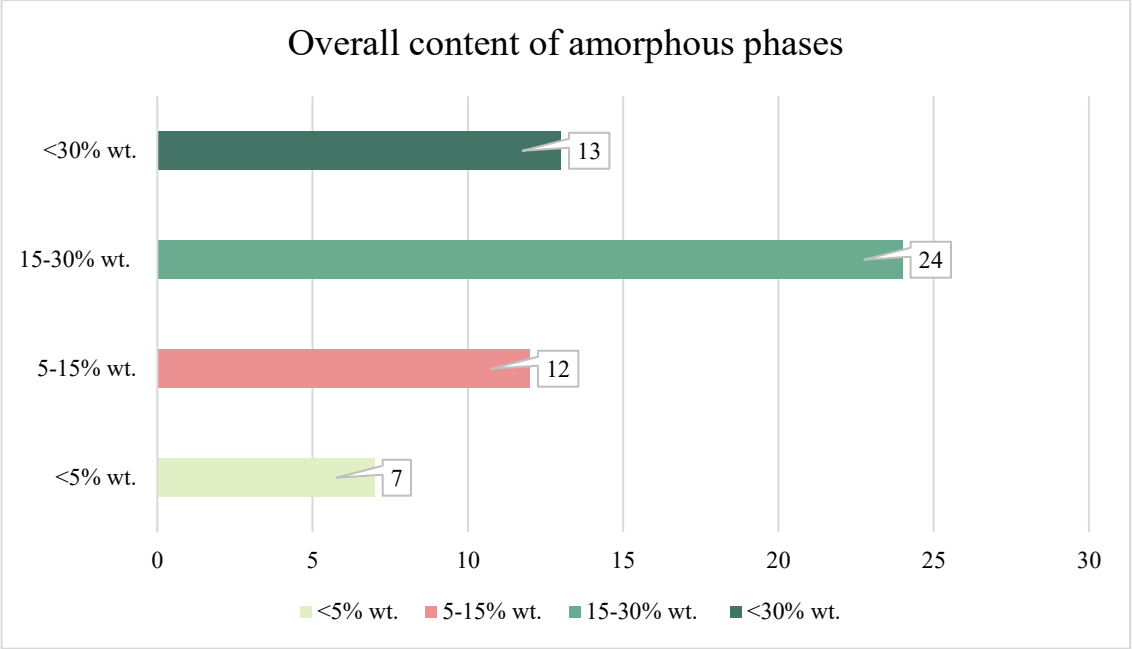

***Figure 24**) Overall content of amorphous phases in the analysed samples. A percentage between 15-30% of amorphous content is expected in lime plasters, while it is typically lower in gypsum ones. Amounts not exceeding 5% of the weight are less common and usually indicate pure aerial lime binders or pure gypsum binders. When the content of amorphous phases surpasses 30% it can be an indication of possible hydraulicity.*

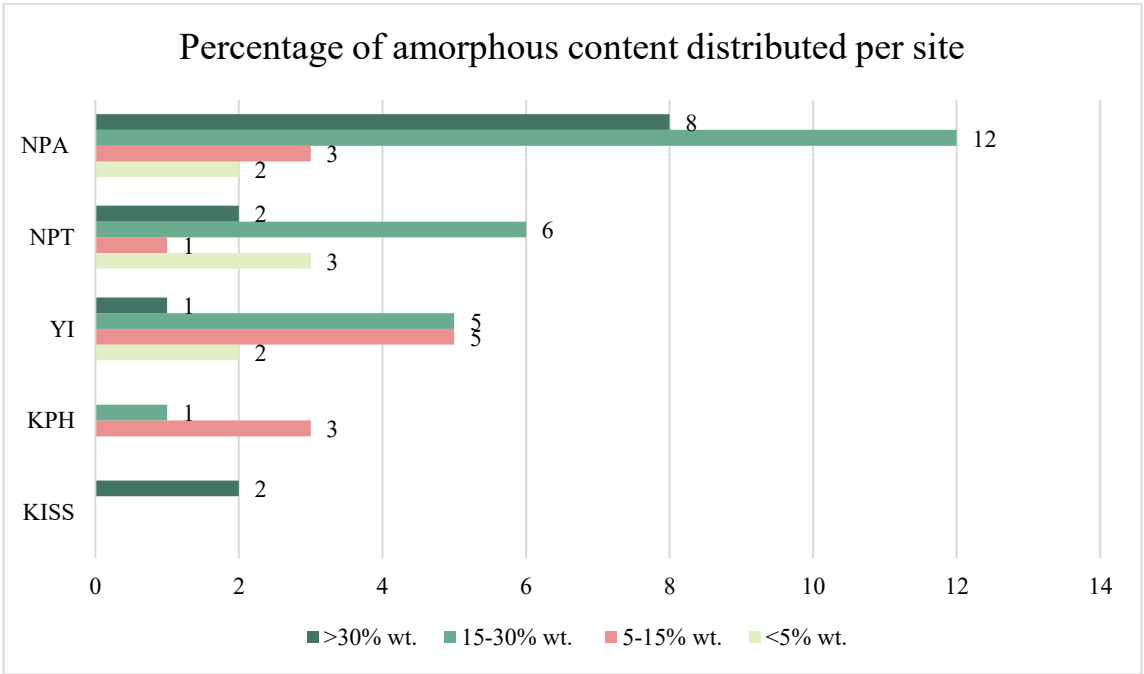

***Figure 25**) The graph illustrates the percentage of amorphous phases in the samples distributed per archaeological site. All of the analysed samples from Kissonerga (KISS) are possibly NHL, indicating that this was the preferred binder at the time; while NHL is completely lacking in the samples collected in Palaepaphos (KPH). In Yeronisos (YI) there is only one suspected case of NHL usage, however it must be noted that the site is not particularly rich in water-related features, diminishing the necessity of hydraulic materials. Finally, samples from Nea Paphos (NPT and NPA) present the highest amount of presumed NHL binders. While, on one hand, the higher percentage can be ascribed to a higher number of samples collected, it is also important to cross-reference the archaeological and chronological contexts, in order to notice a significant increase in NHL employment during the Late-Hellenistic and Roman times (periods of construction of the sampled architectonic buildings in Nea Paphos).*

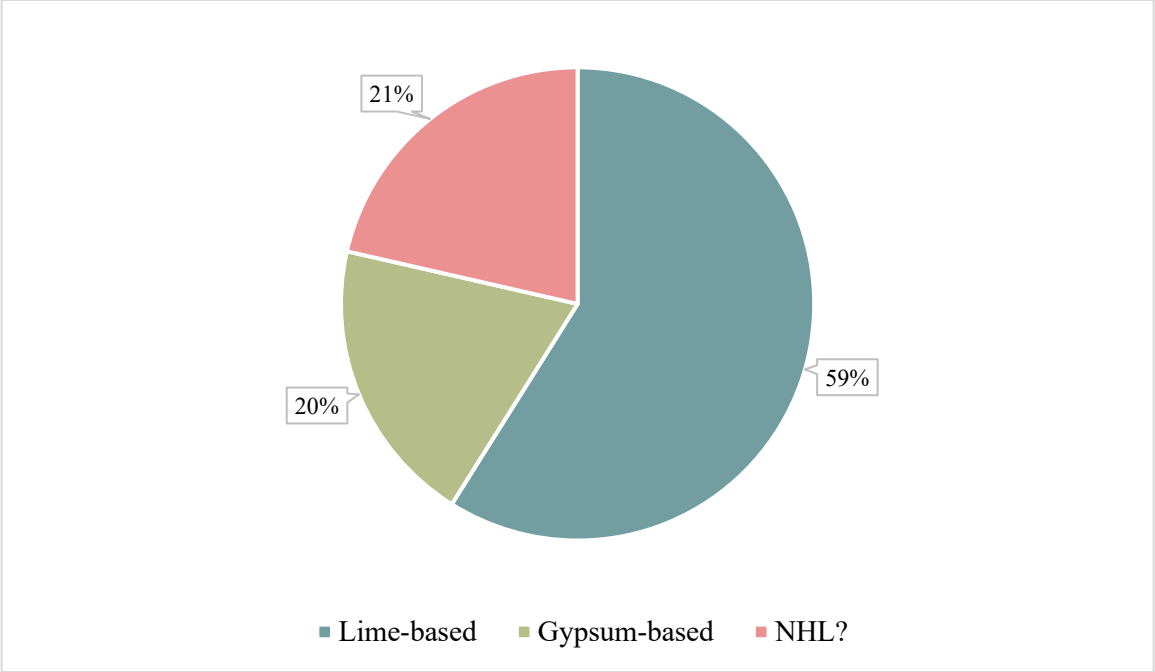

Figure 26*) Graph representing the percentages of main binders in the analysed samples according to the XRD results. It is important to note that the NHL percentage is likely overestimated with this specific analytical method, since not only hydrated phases have an amorphous structure, but also other minerals naturally present in these types of compounds – e.g. clay minerals – can present not fully crystalline forms. .*

KPH1	NPT 12	NPT 10B	NPT 10A	NPT 8	NPT 7a2	NPT 7a1	NPT 6b2	NPT 6b1	NPT 3b	NPT 3a	NPT 2	NPT 1	
/b	/b	/b	/b	/b	/b	/b	/b	/b	/b	/b	/b	/b	Measured fraction
				0.4							0.2		C-A-S-H
		<0.5				<0.5							Feldspars
<0.5	1.7	1.1	<0.5	0.7	1.5	1.2	1.1	<0.5	1.0	2.1	<0.5	1.7	Quartz
5.0	**91.3**	**61.6**	**60.1**	7.5	**77.4**	**72.5**	**75.0**	**95.0**	**71.4**	47.6	6.7	**66.1**	Calcite
		2.3			2.6							6.2	Mg-calcite
													Kaolinite
						0.5			0.7	0.7			Illite/ Muscovite
		3.3	0.8		3.1	0.6	2.0			<0.5	<0.5	0.9	Aragonite
86.7	<0.5	<0.5	0.6	**91.4**				<0.5		<0.5	**92.8**	1.9	Gypsum
												<0.5	Dolomite
						0.7							Clinochlore
		<0.5	<0.5		<0.5	<0.5							Amphibole/ serpentine
		1.1											Diopside
													Anhydrite
													Cristobalite
													Ankerite
													Halite
													Gehlenite
													Cerussite
7.8	6.4	**29.9**	**37.8**	0.0	15.0	23.6	21.9	4.5	27.0	**49.4**	0.0	23.2	Amorphous
99.9	*100.0*	*100.0*	*100.0*	*100.0*	*100.0*	*99.4*	*100.0*	*100.0*	*100.0*	*100.0*	*100.0*	*100.1*	Total

YSC 17	YSC 15	YSC 10	YSC 7	YSC 3	YSC 1	YM 2B	YM 2A	YE 1	YE 1	KPH 3	KPH 3	KPH 1	
/b	/b	/b	/b	/b	/b	/b	/b	/t	/b	/t	/b	/t	Measured fraction
			0.2		0.2								C-A-S-H
									<0.5				Feldspars
1.8	2.6	2.6	0.5	<0.5	1.0	0.8	0.7	<0.5	<0.5			0.8	Quartz
86.3	**65.1**	**71.5**	4.2	3.2	3.5	**82.0**	**98.3**	**65.7**	**85.3**	1.1	1.8	3.2	Calcite
0.7						1.0		0.8					Mg-calcite
	1.0												Kaolinite
	1.7												Illite/ Muscovite
1.1						1.8		2.2	3.6				Aragonite
<0.5		<0.5	**79.0**	**76.8**	**89.7**	<0.5	0.9	<0.5	<0.5	**79.5**	**89.5**	**84.7**	Gypsum
													Dolomite
													Clinochlore
													Amphibole/ serpentine
													Diopside
			<0.5	3.1	<0.5								Anhydrite
		<0.5											Cristobalite
	1.1												Ankerite
<0.5		0.6						0.5					Halite
													Gehlenite
													Cerussite
9.6	28.5	25.1	16.0	16.6	5.1	14.2	0.0	**30.2**	10.7	19.4	8.7	11.3	Amorphous
100.1	*100.0*	*100.1*	*99.9*	*100.1*	*99.7*	*100.0*	*99.9*	*100.1*	*99.8*	*100.0*	*100*	*100.0*	Total

NPA 13.1	NPA 12	NPA 11	NPA 9.1	NPA 8	NPA 7	NPA 6	NPA 5	KISS 3	KISS 4	YHC 1B	YHC 1A	YW 2	
/b	/b	/b	/t	/b	/b	/b	/b	/b	/b	/b	/b	/b	Measured fraction
													C-A-S-H
1.7	1.9		1.5	1.2		<0.5	1.8	<0.5	4.9		1.2		Feldspars
3.2	3.7	1.0	5.7	1.7	3.6	4.6	9.9	6.9	8.5	2.0	3.0	0.5	Quartz
43.5	**50.2**	**71.8**	**83.9**	**82.9**	**66.8**	**63.9**	37.5	34.0	38.1	**84.4**	**66.0**	4.8	Calcite
<0.5	0.6		8.2	1.5	5.1	2.5	4.8	2.3					Mg-calcite
						1.0	1.8		1.9				Kaolinite
1.6	1.1					1.0	2.4		3.5				Illite/ Muscovite
			0.7	0.5	0.9	1.8	1.5	<0.5			0.7		Aragonite
												94.7	Gypsum
									<0.5				Dolomite
									1.7				Clinochlore
							0.7	<0.5					Amphibole/ serpentine
								3.1			3.8		Diopside
													Anhydrite
													Cristobalite
													Ankerite
													Halite
								9.4					Gehlenite
													Cerussite
49.9	**42.5**	27.1	0.0	12.3	23.6	25.0	**39.5**	**43.6**	**41.2**	13.6	25.2	0.0	Amorphous
100.1	*100.0*	*99.9*	*99.97*	*100.1*	*100.0*	*100.0*	*99.9*	*100.0*	*94.9*	*100.0*	*100.0*	*100.0*	Total

NPA 30A	NPA 26	NPA 25	NPA 23B	NPA2 3A	NPA 22	NPA 21B	NPA2 1A	NPA 20	NPA 19	NPA 15	NPA 13	NPA 13	
/b	/b	/b	/b	/b	/b	/b	/b	/b	/b	/b	/t	/b	Measured fraction
										0.2			C-A-S-H
<0.5		<0.5	<0.5								8.6	2.0	Feldspars
0.6	0.7	1.1	0.8	<0.5	2.0	2.2	0.9	1.0	0.8	0.7	9.3	4.2	Quartz
69.7	**89.8**	**67.5**	**72.6**	**79.1**	**64.9**	**57.3**	**65.7**	**58.9**	**76.2**	13.2	**66.3**	43.6	Calcite
5.5		5.4	2.3		6.6	9.2	8.9	3.1	0.8		2.1		Mg-calcite
													Kaolinite
					0.6	0.8					1.9	1.6	Illite/ Muscovite
0.5	1.8	1.5	0.5		2.3	0.6	1.6				0.9		Aragonite
							<0.5	<0.5	<0.5	**78.4**			Gypsum
													Dolomite
													Clinochlore
	<0.5	<0.5	<0.5						<0.5		0.9		Amphibole/ serpentine
											8.5		Diopside
													Anhydrite
													Cristobalite
													Ankerite
													Halite
													Gehlenite
											1.4		Cerussite
23.3	7.5	23.8	23.5	20.5	23.6	**29.8**	22.7	**36.7**	21.9	7.5	0.0	**48.4**	Amorphous
99.9	*100.0*	*100.0*	*99.9*	*100.0*	*100.0*	*99.9*	*99.9*	*99.9*	*99.9*	*100.0*	*100.0*	*99.8*	Total

NPVT 1	NPH 1	NPER 1	NPA 30B	Measured fraction
/b	**/b**	**/b**	**/b**	C-A-S-H
0.5	2.3	1.1	1.2	Feldspars
1.0	<0.5	2.0	4.6	Quartz
72.8	34.3	**58.0**	48.2	Calcite
1.7		<0.5	0.6	Mg-calcite
			1.1	Kaolinite
<0.5	0.8			Illite/ Muscovite
<0.5	0.9	1.1	0.5	Aragonite
				Gypsum
				Dolomite
				Clinochlore
			1.9	Amphibole/ serpentine
				Diopside
				Anhydrite
				Cristobalite
				Ankerite
				Halite
				Gehlenite
				Cerussite
23.5	**61.2**	**37.6**	**41.9**	Amorphous
100.0	*99.9*	*100.0*	*100.0*	Total

Table 5*) Results of the XRD analysis on the Paphian samples. Legend: green=principal component of the binder is lime; blue= principal component of the binder is gypsum; orange=high amorphous phases possibly suggesting NHL binders; yellow=unexpected result; red=CASH phases in the gypsum-based binders.*

Chapter 3.3: Thermal Analysis

Thermal analyses have been performed on the binder-rich fraction (/b or /m) of the samples. The results outline peculiar tendencies in the lime-based plasters, and occasionally strengthen the suggestion of presence of NHL binders. Formulas to calculate the content of gypsum and calcium carbonate from the curves are as follows:

$$CaCO_3 \text{ content} = \frac{\text{wt. loss\% } (600 - 800°\text{C}) * 100}{percentage\ of\ CO_2\ in\ CaCO_3\ (44)}$$

$$CaSO_4 \text{ content} = \frac{\text{wt. loss\% } (100 - 250°\text{C}) * 100}{percentage\ of\ H_2O\ in\ CaSO_4 * 2H_2O\ (20.93)}$$

The gypsum TA curves (**fig. 27**) do not present particular irregularities, with the typical main double peak in the region between 100–250°C and the highest percentage of weight loss recorded in this range. Minimal records of weight loss in the region between 250–600°C occur, along with more significant ones in the region between 600–850°C. Overall, the gypsum content covers around 80–90% of the samples' weight, with calcium carbonate content not exceeding 9%.

The situation for the lime-based plasters is different, with the TA curves following two distinct paths. On one hand, in a conspicuous number of samples the standard peaks of calcium carbonate decomposition are observed in the region 600–850°C, with lower percentages of weight losses recorded in the region 50–250°C and 250–600°C (**fig. 28**). However, a substantial percentage of the samples displays lower temperatures (as low as 450–500°C) for the start of calcium carbonate decomposition (**fig. 29**). This phenomenon might be explained by the presence of biogenic carbonates, whose decomposition process starts much earlier (Milano, Nehrke 2018; Faust 1950); similar tendencies have been observed in the local geological carbonates with high content of bioclasts (**fig. 30**). The overall content of calcium carbonate in the first type (standard decomposition starting T) is above 80%, while it is relatively lower for the second type (decomposition starting at lower T) ranging between 45% and 85% (**tab. 6-7**). However, it must be noticed that the estimation of the calcium carbonate content is biased by default due to the presence of geological limestone added as an aggregate in the form of large particles and fine powder. With TA it is not possible to distinguish between geogenic and pyrogenic calcium carbonate, causing the quantification to be slightly higher. A trial test conducted on three specimens reveals that geological calcium carbonate is present not only as an aggregate, but also in the binder, in the form of a not completely burnt and processed residue of the binder production.

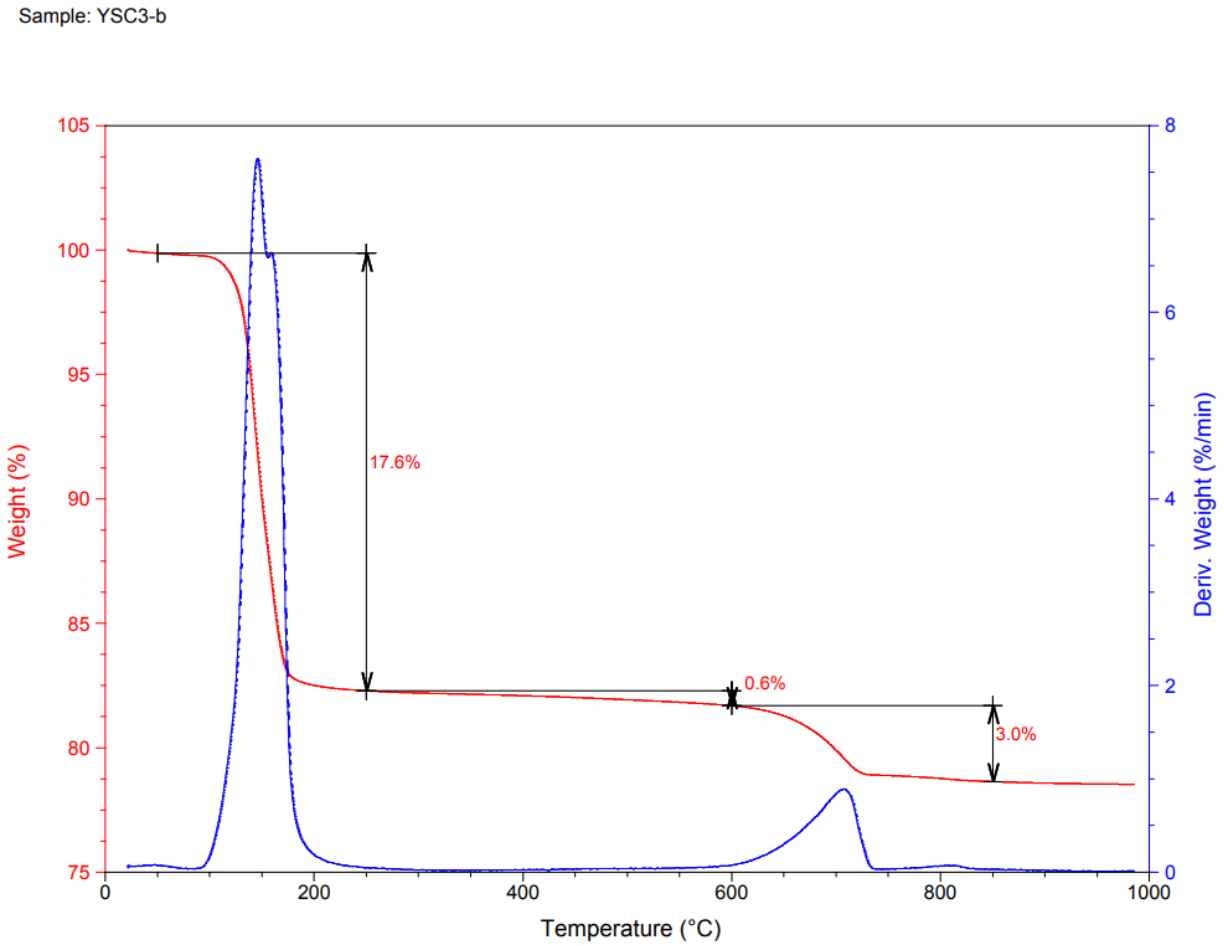

Figure 27*) TA curve of the binder-rich fraction of a gypsum-based mortar (YSC 3) from the site of Yeronisos. The weight loss in the region of 50–250°C (17.6%) corresponds to the H_2O vapour produced during the calcium sulphate main dehydration phase; the derivative curve is characterized by a double peak typical of gypsum materials. Weight loss related to the dehydration of gypsum can also occur in the region 800–1000°C. The process of decomposition of calcium carbonate starts at 600°C and ends before 800°C, with a weight loss – in form of CO_2 – corresponding to 3.0%.*

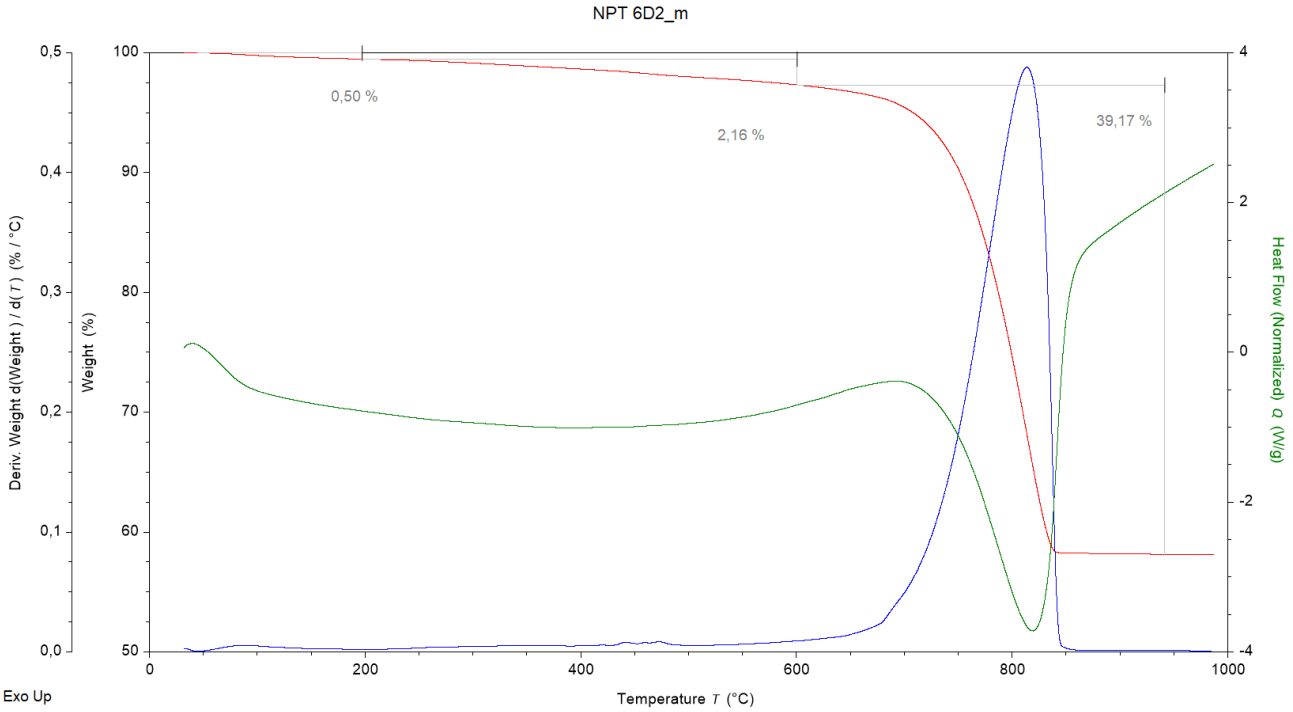

Figure 28*) TA curve of the binder-rich fraction of a lime-based plaster (NPT 6D2) from the Theatre of Nea Paphos. The decomposition of calcium carbonate starts around 650°C. The most significant weight loss is recorded in the region 650–850°C, corresponding to the process of decomposition of calcium carbonate. The total weight loss in this interval amounts to 39.2%, which allows to estimate the content of calcium carbonate at around 90%.*

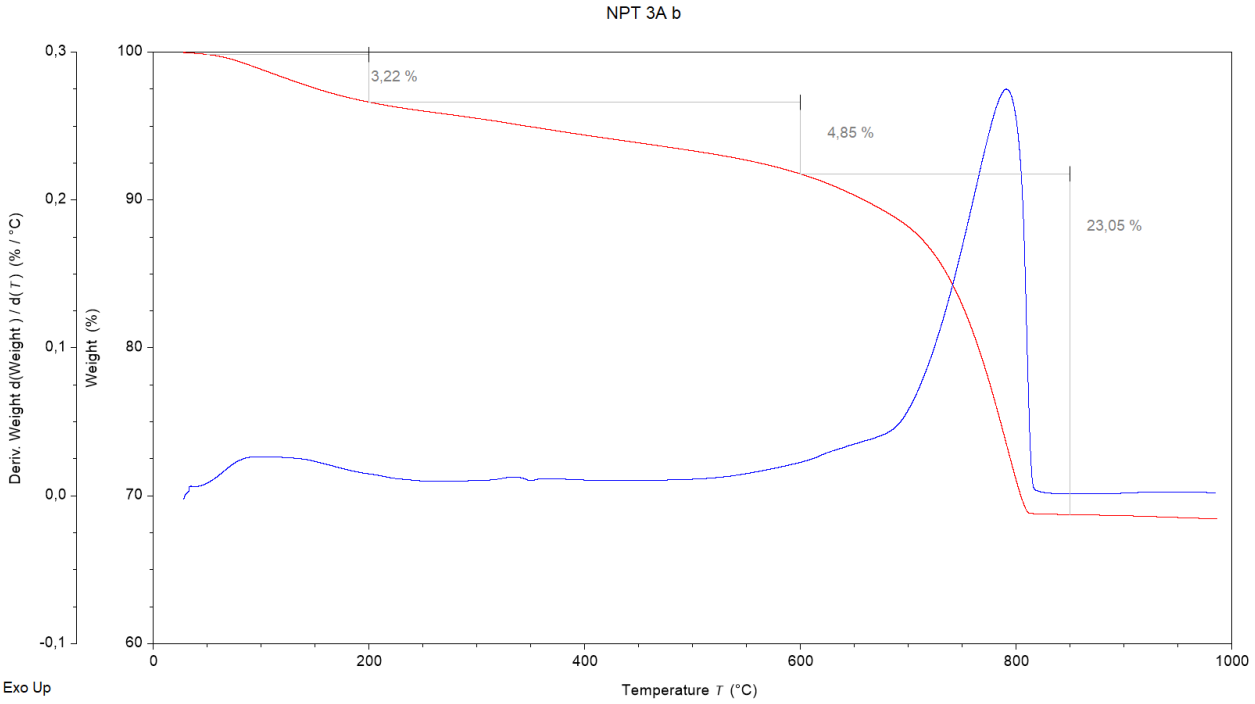

Figure 29) *TA curve of the binder-rich fraction of a lime-based plaster (NPT 3a) with anticipated calcium carbonate decomposition temperature (550°C), from the Theatre of Nea Paphos. For the estimation of the calcium carbonate content, a fixed temperature interval at 600–850°C has been set; however, singularities such as an earlier start of the $CaCO_3$ decomposition have been taken into account. The weight loss in the adjusted range (550–850°C) corresponds to 24.6%. Particularly indicative in this samples is the high percentage of weight loss in the region 200–550°C, which is an indication of possible presence of hydraulic lime.*

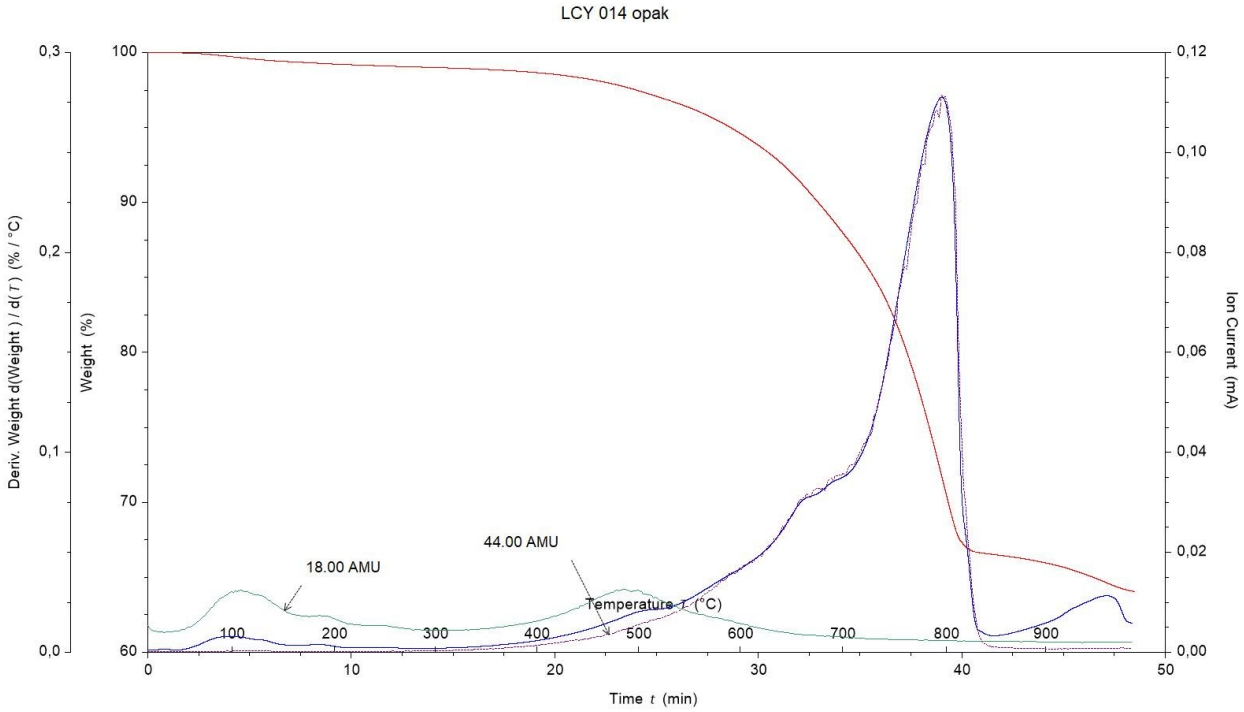

Figure 30*) TA curve of the geological sample LCY 014, corresponding to marl. This graph also contains information obtained with the EGA regarding the analysis of the gasses produced during the heating of the sample. The green line corresponds to H_2O vapour, while the purple line indicated CO_2. The initial loss of weight (region 50–200°C) is due to the loss of moisture and not chemically bound water; while the peak in the water curve in the region 400–600°C can indicate the presence of chemically bound water (in this case in hydrated phases or in clay minerals). The derivative curve presents an interesting additional peak in the range 850–1000°C, possibly associated with the presence of Sulphur.*

	50-250°C	250-600°C	600-850°C	$CaCO_3$ %	$CaSO_4$%	CO_2/H_2O
NPT 2	18.9	0.3	3.5	8.0	90.3	-
NPT 8	18.3	0.0	2.4	7.9	87.4	-
YSC 1	19.6	0.5	1.5	3.4	93.6	-
YSC 3	17.6	0.6	3.0	6.8	84.1	-
YSC 7	19.4	0.4	2.4	5.5	92.7	-
YSC 10	0.7	2.2	37.4	85.0	3.3	-
YW 2	19.4	0.3	2.4	5.5	92.7	-
YE 1	4.7		38.8	83.2	0.0*	-
KPH 1	18.4	0.7	3.2	7.3	87.9	-
KPH 3	19.8	0.4	1.5	3.4	94.6	-
NPT 7A1	1.0	3.1	37.6	85.5	0.0*	12.1
NPT 7A2	0.5	2.1	39.8	90.5	0.0*	-
NPT 6D1	0.4	1.8	41.8	95.0	0.0*	-
NPT 6D2	0.5	2.2	39.8	90.5	0.0*	-
NPVT 1	1.9	2.8	34.9	79.3	0.0*	12.5
NPA 6	0.8	2.5	35.2	80.0	0.0	14.1
NPA 7	0.6	2.6	37.3	84.7	0.0	14.3
NPA 8	1.5	4.3	34.6	78.6	0.0*	8.0
NPA 11	1.3	3.6	36.0	81.8	0.0*	10.0
NPA 12	0.5	2.2	39.6	90.	0.0	18.0

NPA 19	0.6	2.7	36.0	81.8	2.6	13.3
NPA 20	1.6	3.2	32.1	73.0	0.0*	10.0
NPA 27	0.5	2.8	39.1	88.9	0.0*	14.0
NPA 28	0.9	3.1	35.7	81.1	0.0*	11.5
NPA 29	0.5	2.0	39.3	89.3	0.0*	-
NPA 30	0.8	3.1	37.0	84.1	0.0*	11.9

Table 6*) Weight loss was measured in the above-specified regions for each sample and is here expressed in wt. percentage. Calcium carbonate and gypsum content have been calculated according to the previously mentioned formulas. Weight loss in the region between 250-600°C can be an indication of possible hydraulicity, for this reason the ratio between CO_2 and H_2O released has been calculated, and the hydraulicity index has been estimated according to the index formulated by Moroupoulou* et al. *(2005, 2004, 2000; Calzolari* et al. *2023). According to this index, samples with hydraulic characters have a ratio value comprised between 3 and 9; thus only NPA 8 can be considered hydraulic. *It is important to note that, despite weight loss has been recorded in the region between 50–250°C, it is not always associated with the presence of gypsum, but it can be ascribed to organic and/or moisture contents.*

	50-200/250°C	**250-450/500°C**	**450/500-850°C**	**$CaSO_4$ %**	**$CaCO_3$%**	**CO_2/H_2O**
NPT 1	1.0	2.7	37.6	4.8	85.5	
NPT 3a	5.0	2.2	24.6	0.0*	55.9	4.8
NPT 3b	4.3		32.7	0.0*	74.3	
NPT 10A	1.6	2.4	30.7	0.0*	69.7	
NPT 10B	1.3	1.5	36.9	1.9	83.9	
NPT 12	1.5	1.3	35.1	0.0*	79.8	27.0
YHC 1A	1.1	2.4	34.8	0.0*	79.1	14.5
YHC 1B	1.1	2.3	37.6	0.0*	85.5	16.3
YSC 15	1.3	0.8	35.9	0.0*	81.6	
KISS 3	2.4	2.4	19.3	0.0*	43.9	8.0
KISS 4	3.3	2.5	20.8	0.0*	47.3	8.3
NPH 1	6.9	3.4	16.8	0.0*	38.2	4.9
NPER 1	4.6	6.0	23.0	0.0*	52.3	3.8

***Table** 7) Weight loss was measured in the specified regions for each sample and is here expressed in wt. percentage. Calcium carbonate and gypsum content have been calculated according to the formulas mentioned previously. Weight loss in the region between 250-450/500°C can be an indication of possible hydraulicity, for this reason the ratio between CO_2 and H_2O released has been calculated and the hydraulicity has been estimated according to the index formulated by Moroupoulou* et al. *(2005, 2004, 2000; Calzolari* et al. *2023). According to this index, samples with hydraulic characters have a ratio value comprised between 3 and 9. *It is important to note that, despite weight loss has been recorded in the region between 50–250°C, it is not always associated with the presence of gypsum, but it can be ascribed to organic and/or moisture contents.*

As both XRD and TA present significant limitations in regard to a correct estimation of the chemical and mineralogical composition, a comparison between the results of the two analytical methods is beneficial for a correct evaluation of the binders. In XRD analysis the major complication is connected to the presence of the amorphous phases, which can be interpreted in various ways, and often end up hiding not well-developed crystals of calcite or other minerals. On the other hand, TA is precise in regards of the estimation of calcium carbonate and gypsum but does not allow for a clear distinction between the different forms of $CaCO_3$. **Table 8** compares the main binder contents as analysed by XRD and TA.

	$CaCO_3$		$CaSO_4*2H_2O$	
	XRD	**TA**	**XRD**	**TA**
NPT 2	6.7	8.0	92.8	90.3
NPT 8	7.5	7.9	91.4	**87.4**
YSC 1	3.5	3.4	89.7	93.6
YSC 3	3.2	6.8	76.8	**84.1**
YSC 7	4.2	5.5	79.0	**92.7**
YSC 10	71.5	85.0	<0.5	3.3
YW 2	4.8	5.5	94.7	92.7
YE 1	85.3	83.2	<0.5	0.0
KPH 1	5.0	7.3	86.7	87.9
KPH 3	1.3	3.4	89.5	94.6
NPT 7A1	72.5	85.5	0.0	0.0
NPT 7A2	77.4	**90.5**	0.0	0.0
NPT 6D1	95.0	95.0	<0.5	0.0
NPT 6D2	75.0	**90.5**	0.0	0.0
NPVT 1	72.8	79.3	0.0	0.0
NPA 6	63.9	80.0	0.0	0.0
NPA 7	66.8	**84.7**	0.0	0.0
NPA 8	82.9	**78.6**	0.0	0.0
NPA 11	71.8	81.8	0.0	0.0
NPA 12	50.2	**90.0**	0.0	0.0
NPA 19	76.2	81.8	<0.5	**2.6**
NPA 20	58.9	**73.0**	<0.5	0.0
NPA 27	92.3	**88.9**	0.0	0.0
NPA 28	86.1	**81.1**	0.0	0.0
NPA 29	78.7	89.3	0.0	0.0
NPA 30	69.7	**84.1**	0.0	0.0
NPT 1	66.1	**85.5**	1.9	4.8
NPT 3a	47.6	55.9	<0.5	0.0
NPT 3b	71.4	74.3	0.0	0.0
NPT 10A	60.1	69.7	0.6	0.0
NPT 10B	61.6	**83.9**	<0.5	1.9
NPT 12	91.3	**79.8**	<0.5	0.0
YHC 1A	66.0	**79.1**	0.0	0.0
YHC 1B	84.4	85.5	0.0	0.0
YSC 15	65.1	**81.6**	0.0	0.0
KISS 3	34.0	43.9	0.0	0.0
KISS 4	38.1	47.3	0.0	0.0
NPH 1	34.3	38.2	0.0	0.0
NPER 1	58.0	**52.3**	0.0	0.0

Table 8) *Comparative table with the estimation of calcium carbonate/calcite and gypsum content according to XRD and TA. Highlighted in green the cases in which TA estimations are higher; in red, those in which TA is lower. A margin of 10% error is tolerable due to the differences of the analytical methods (TA does not distinguish between Mg-calcite, calcite and aragonite) and the extreme heterogeneity of some of the samples; whenever the error exceeds 10% it must be carefully considered. In instances where the TA estimate higher percentages, it is safer to rely on these results, rather than the XRD; in fact, as already mentioned, some of the Calcite is hidden in the amorphous phases in the XRD measurements. However, lower estimates in TA are unexpected and more problematic.*

Chapter 3.4: Mechanical and physical tests

Water absorption and total porosity were determined on selected samples to assess properties related to their performance in wet environment. In particular, the experiments were directed at all the suspected hydraulic samples, and at those which were collected within structures related to liquid containment or disposal. The obtained results are summarised in **table 9**. Moisture content and porosity levels recorded are relatively high for samples associated with the retaining of water (or other liquids). Nonetheless, the percentage of weight loss after the testing procedure is nearly irrelevant, not measuring more than 0.5%, highlighting the fact that these plasters present solid water-resistance properties.

Water absorption under atmospheric condition at 24 h in the gypsum samples is lower (averaging at 13.5%) than in the lime-based ones, possibly due to increased density of the mortars and lack of significantly porous aggregates. The average water absorption percentage on the suspected NHL plasters, on the other hand, corresponds to 24.3% of the weight, which is higher than the observations recorded in literature (Válek, Skružná 2019); this element might suggest a degradation process which increased the volume of the open pore structure compared to when the mixture was freshly made. Another possible explanation for this high porosity levels lays in the presence of ceramic aggregates in the mixture: in fact, porous fabrics would enhance the percentage and volume of absorbed water.

As for the estimated total porosity (P), the volume of open voids (Vv) averages around 33.5% of the total volume (Vt) of the samples. Expected porosity in lime mortars averages between 26.9 and 27.4% (Ahmed 2024, 1; Fahmy *et al.* 2023; 14; Chever *et al.* 2010), while it is slightly lower for NHL (Banfill 2018, 78). Thus, the obtained result is surprising, especially considering that the supposedly NHL samples are the one presenting the highest percentages of P. However, this estimation must be cautioned by the consideration of erosion, degradation and biological decomposition of the samples: the present porosity does not correspond to the porosity at the time of production, thus there might have been a considerably lower amount of open pores. Furthermore, the overall porosity of the samples is increased by the presence of extremely porous aggregates – such as limestones, charcoal, or ceramic fragments. In conclusion, due to the degradation processes and the presence of porous aggregates, it is hard to estimate the impact of the pore structure over the water-retaining properties. In addition, water-tightness could have been further improved by application of an organic coating (i.e. wax or oil), or even by polishing the external surface closing the pores mechanically. Unfortunately, neither of these procedures could be proven to be applied in the samples under study; in fact, the state of preservation of the surfaces in particular, although relatively good in most cases, was not optimal to preserve traces of polishing or treatment with organic substances.

Table 9 highlights the results of the water absorption test, while **table 10** those of the open porosity.

Sample	material	Dry sample weight (g)	Wet sample weight (g) after 24 h	Weight of absorbed H_2O (g) in 24 h	Wt.% of water absorption at 24 h	Dry sample weight (g) after testing	Final weight loss (g)	% of weight loss
YSC 1	gypsum	2.7	2.8	0.1	**5.6**	2.6	0.10	0.5
YHC 1	lime	2.8	3.1	0.3	**12.0**	2.8	0.02	0.1
YHC 1r	lime	14.8	16.3	1.5	**10.2**	14.7	0.09	0.6
KPH 1	gypsum	6.9	8.3	1.4	**20.4**	6.8	0.10	0.4
KPH 3	gypsum	3.8	4.1	0.3	**7.5**	3.7	0.14	0.6
NPT 2	gypsum	5.2	5.5	0.3	**5.8**	5.0	0.17	0.7
NPT 8	gypsum	7.6	9.7	2.1	**28.3**	7.4	0.24	0.9
NPT 10	lime	11.3	12.8	1.5	**13.0**	11.3	0.03	0.2
NPT 12	NHL ?	7.4	10.3	2.8	**38.4**	7.3	0.08	0.3
NPT 12r	NHL ?	6.8	9.7	2.9	**42.2**	6.8	0.04	0.6
NPT 3A	NHL ?	16.2	20.9	4.6	**28.5**	16.1	0.14	0.9
NPT 3B	NHL ?	24.6	31.0	6.4	**26.0**	24.5	0.10	0.4
NPA 7	lime/NHL	6.6	7.5	0.9	**13.7**	6.6	0.03	0.4
NPA 8	lime/NHL	10.9	12.1	1.3	**11.6**	10.8	0.03	0.3
NPA 12	lime	8.8	10.9	2.0	**22.9**	8.8	0.06	0.6
NPA 13	NHL ?	4.3	5.4	1.1	**24.4**	4.3	0.04	1.0*
NPA 30	Lime	7.6	9.0	1.4	**18.4**	7.6	0.04	0.5
NPH 1	NHL ?	3.4	4.3	0.9	**27.7**	3.3	0.04	1.2*
NPVT 1	NHL ?	10.1	12.9	2.8	**27.2**	10.1	0.07	0.7
KISS 1	limestone	15.7	16.6	0.9	**6.0**	15.6	0.08	0.5
KISS 2	NHL ?	9.9	10.9	1.0	**9.6**	9.5	0.43	**4.4***

***Table 9**) Results of the water absorption tests. The dry sample weight is the starting weight. Test was performed on samples of more or less equal dimensions, the difference in weight is due to the density. The wet sample was weighted after 24h submerged in H_2O. Percentage of moisture content was calculated according to the formula:* $\text{moisture content} = \frac{Weight\ of\ absorbed\ water}{starting\ sample\ weight} * 100$. *The final dry weight was measured after 72 h since the beginning of the experiment. Final weight loss percentage in samples NPA 13 and NPH 1 is higher due to the presence of lichen on the surface; the crumbly nature of sample KISS 2 produced a significantly increased weight loss percentage. Samples YHC 1 and NPT 12 were measured from two different sub-samples of the specimens (YHC 1r, NPT 12r) due to the inhomogeneous nature of the samples; the overall performance appears comparable in both measurements. Question mark next to NHL highlights the hypothesis – preliminary to the analysis – that the samples may be NHL-based and not lime-based.*

Sample ID	Material	Vv (cm^3)	Vt (cm^3)	P vol.%
YSC 1	Gypsum	0.2	1.3	14.4
YHC 1	Lime	0.4	1.4	26.7
YHC 1r	Lime	1.9	7.4	26.0
KPH 1	Gypsum	1.8	4.8	**36.5**
KPH 3	Gypsum	0.4	2.2	17.9
NPT 2	Gypsum	0.5	2.9	17.5
NPT 3a	NHL ?	5.4	11.2	**48.5**
NPT 3b	NHL ?	7.2	16.5	**43.8**
NPT 8	Gypsum	2.7	6.1	**44.3**
NPT 10	Lime	1.7	6.3	27.2
NPT 12	Lime	3.2	6.0	**53.0**
NPT 12r	Lime	3.2	5.7	**55.1**
NPA 7	Lime/NHL	0.9	3.4	27.2
NPA 8	Lime/NHL	1.5	5.5	26.8
NPA 12	NHL ?	2.5	5.8	**43.6**
NPA 13	NHL ?	1.1	2.7	**41.5**
NPA 30	Lime	1.9	4.6	**40.9**
NPH 1	NHL ?	1.1	2.4	**45.5**
NPVT 1	NHL ?	3.1	7.0	**45.7**
KISS 1	Limestone	1.1	7.1	15.8
KISS 2	NHL ?	1.3	4.6	28.1

***Table 10**) Open porosity (P) of the samples is calculated according to the formula $P = \frac{Vv}{Vt}$, where Vv corresponds to the volume of open pores, and Vt to the total volume of the sample. Samples YHC 1 and NPT 12 were measured twice (YHC 1r, NPT 12r) due to the inhomogeneous nature of the samples; the overall performance appears comparable in both measurements, suggesting the degree of heterogeneity was not enough to disrupt the estimations.*

Chapter 3.5: Additional analyses

Chapter 3.5.1 Fourier-Transform Infrared spectroscopy

FTIR was initially used on a set of 10 samples as a testing method to identify whether the binder was lime or gypsum. In the case of samples with pigment on the surface it was additionally used to detect traces of organic binders (7 samples). Organics peaks, usually visible in the range 3100–2700 cm^{-1} and 1775–1650 cm^{-1}, were not detected in any of the analysed samples (**figs. 31-33**). It is important to notice that the absence of peaks in the above-mentioned intervals does not necessarily means absence of organic material content in the sample; indeed, it is possible that the organic content is too low to be detected by the machine, or that the suspected organic binders have completely degraded over time, not leaving traces behind.

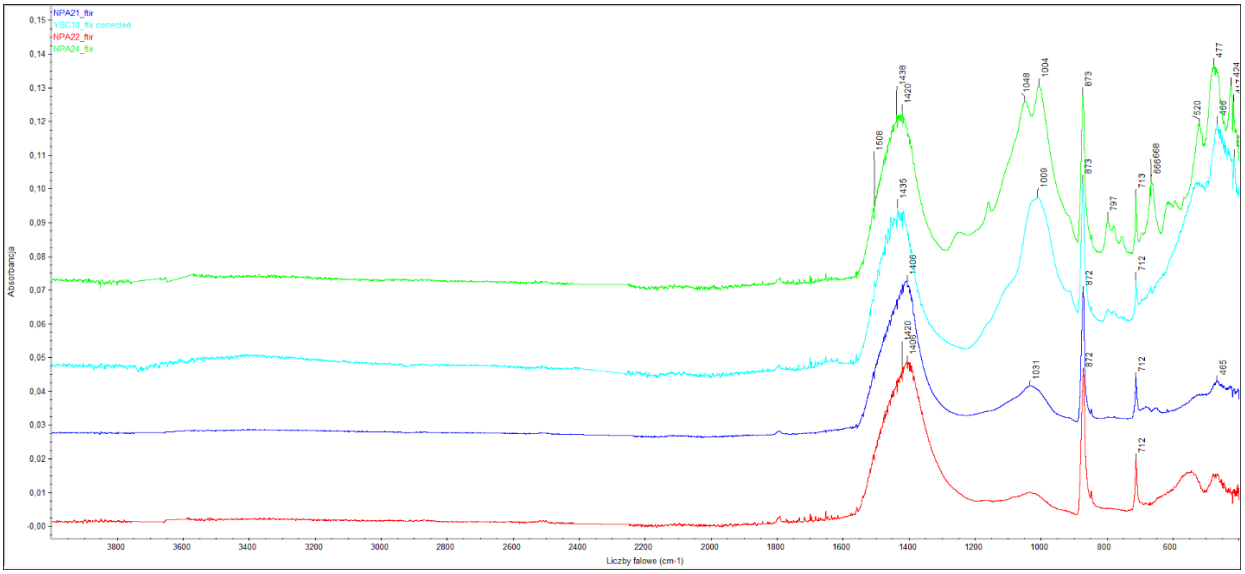

Figure 31*) A comparison of FTIR spectra recorded from the finishing layers of samples NPA 21 (blue line), NPA 22 (red line), NPA 24 (green line), and YSC 10 (turquoise line).No peaks in the regions 3100–2700 cm^{-1} and 1775–1650 cm^{-1} are present, highlighting the absence of organics.*

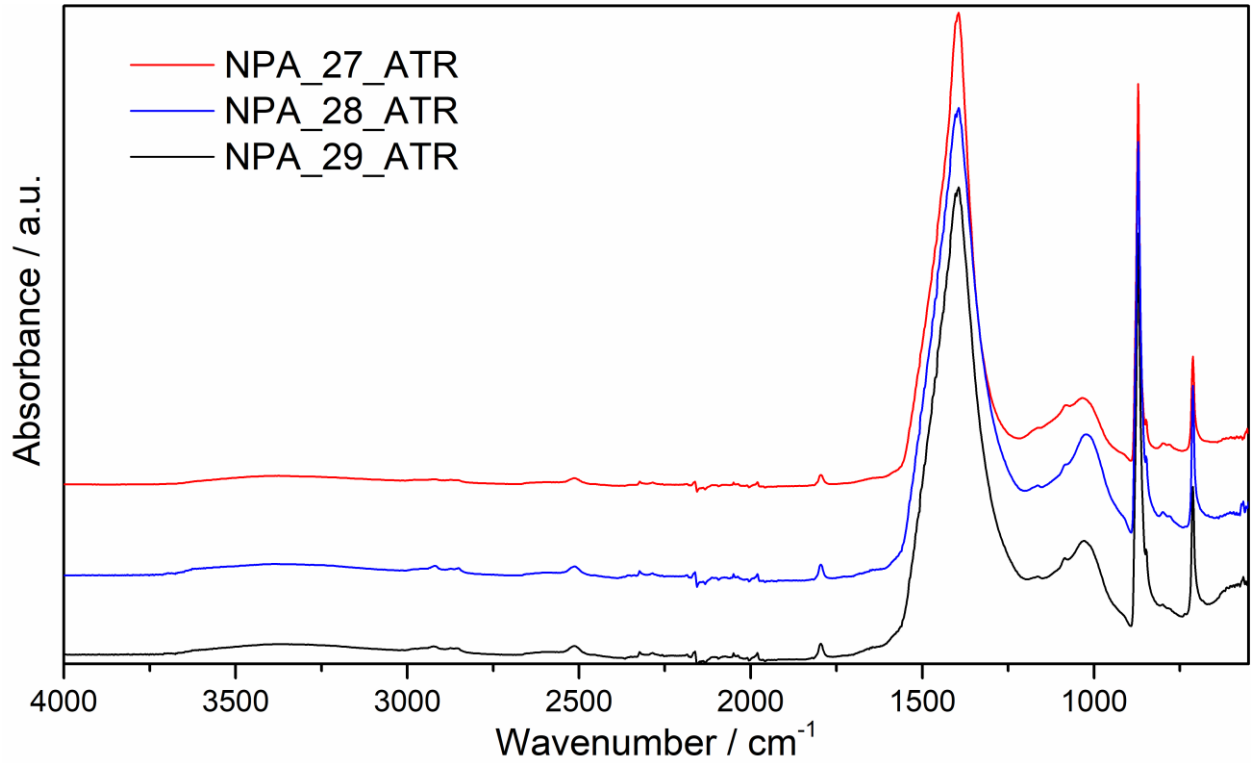

Figure 32*) Comparison of FTIR spectra recorded from the finishing layer of samples NPA 27, NPA 28 and NPA 29. As in fig. 14 there are no specific peaks in the regions 3100–2700 cm^{-1} and 1775–1650 cm^{-1}.*

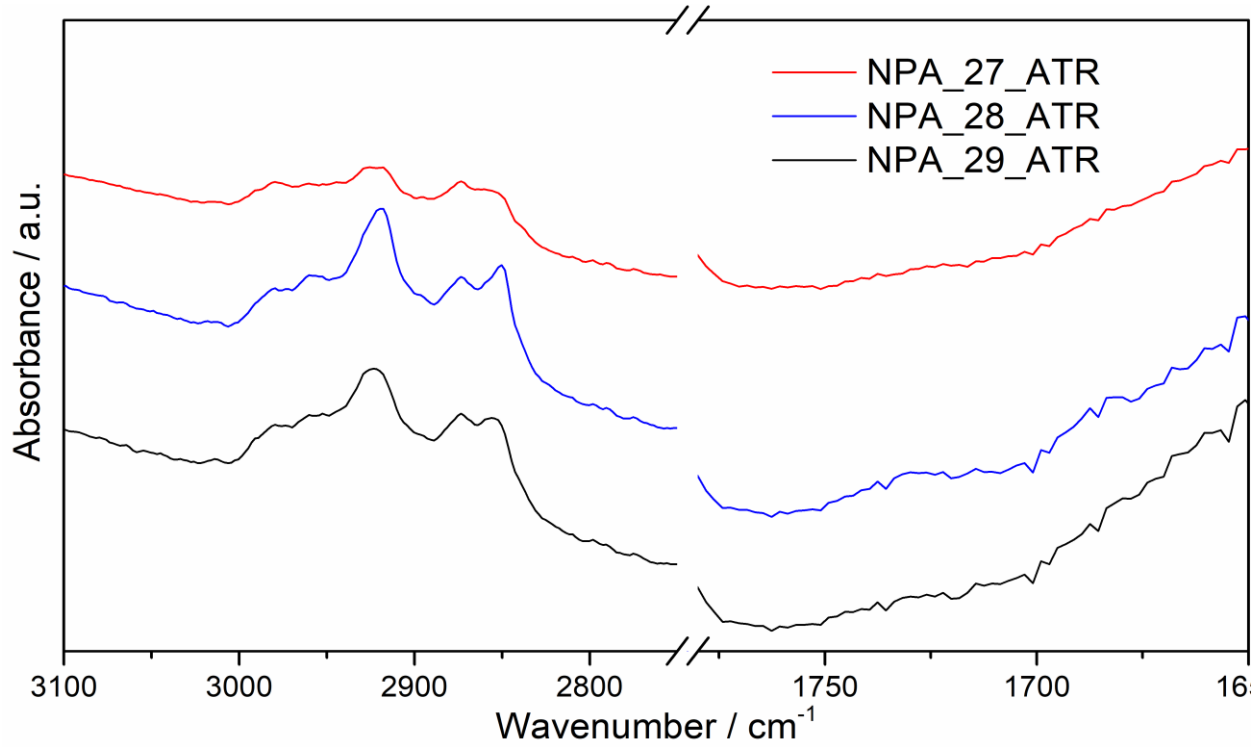

***Figure 33**) FTIR spectra of collected samples limited to the ranges of interest (3100–2700 cm^{-1} and 1775–1650 cm^{-1}) for the identification of possible organics.*

Chapter 3.5.2: Raman spectroscopy

The main objective or RS analyses was to identify the pigments on a set of 11 plasters. The main colours featured in the decorations were red, yellow, black, and white; one sample displayed traces of light blue pigmentation. The following table (**tab. 11**) and pictures (**fig. 34-39**) report the results, which were compared with existing databases for a correct identification (see Marucci *et al.* 2018; Eastaugh *et al.* 2008; Burgio, Clark 2001; Bell *et al.* 1997). Attention was specifically focused on the bands at ~ 225, 292 411, 495 and 612 cm^{-1}, characteristic for hematite (Fe_2O_3), and on the bands at ~1030, 797, 782 cm^{-1} for other clay minerals. Often observed are the peaks ascribable to calcite (~ 1086, 711, 283 and 154 cm^{-1}), and broad peaks in the region ~ 1600–1350 cm^{-1}, which related to carbon.

The pigments identified and their significance for the present study are further commented in chapter **4.2.**

Sample ID	Colour(s)	Identified pigment	Chemical formula
YSC 10	Bright red	Hematite	Fe_2O_3
NPT 1	Red	Hematite	Fe_2O_3
	Yellow	Iron oxides + anatase	$FeO + TiO_2$
NPA 21	Black	Carbon	C
NPA 22	Red + shades	Hematite: shades are realised with multilayering or mixing with calcite in different proportions.	$Fe_2O_3 + CaCO_3$ (shades)
NPA 24	Light blue	Egyptian blue	$CaCuSi_4O_{10}$
NPA 25	Red	Hematite	Fe_2O_3
	White	Calcite	$CaCO_3$
NPA 26	Red	Hematite	Fe_2O_3
	White	Calcite	$CaCO_3$
NPA 27	Red	Hematite + anatase [+ carbon]	$Fe_2O_3 + TiO_2$ (+C)
	Black	Carbon + goethite + anatase	$C + FeO(OH) + TiO_2$
	White	Calcite	$CaCO_3$
NPA 28	Red	Hematite + anatase	$Fe_2O_3 + TiO_2$
	Black	Carbon	C
	White	Calcite + anatase (impurity)	$CaCO_3 + TiO_2$
NPA 29	Red	Hematite + anatase	$Fe_2O_3 + TiO_2$
	Black	Carbon	C
	White	Calcite	$CaCO_3$
NPA 30	Black and red spots	No pigments identified.	

Table 11) *List of samples analysed with RS. For each sample, a list of the present colours is included alongside with the identified pigments and their chemical standard formula.*

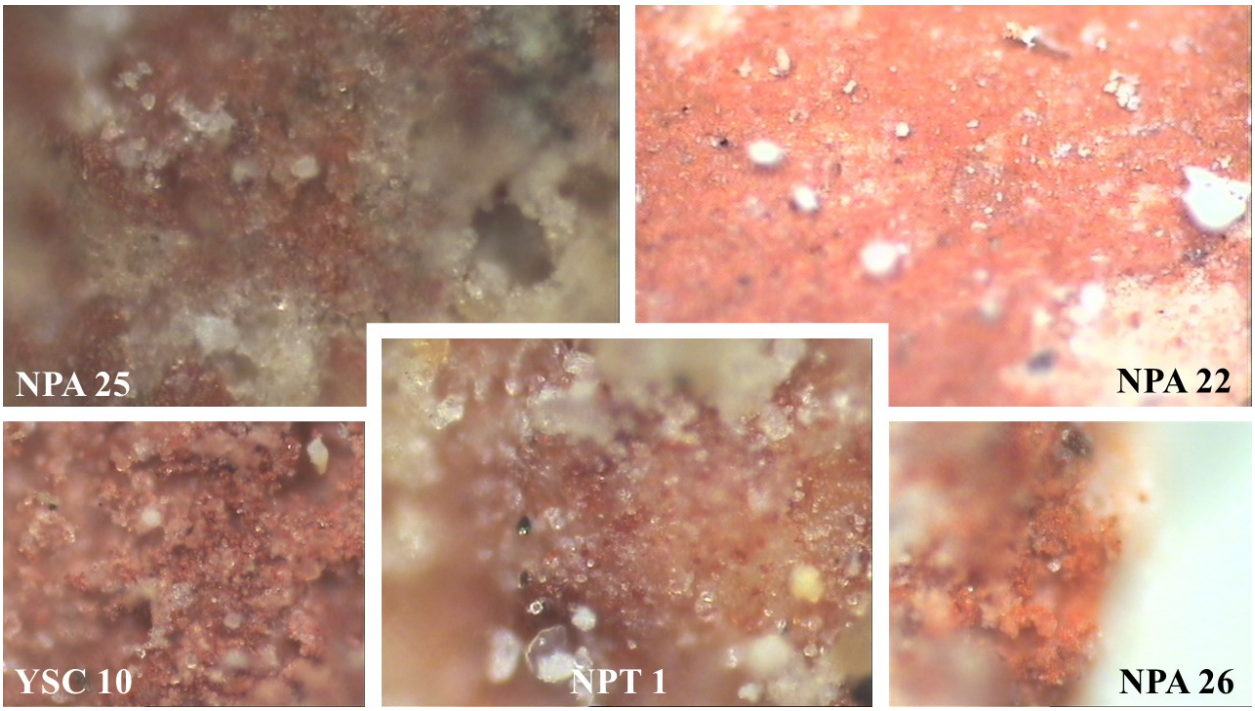

***Figure 34**) Microscope pictures (RAMAN microscope) of samples with red pigment. It is possible to observe different shades and fineness of the pigments' crystals, reflecting the stylistic, technical and aesthetic variations.*

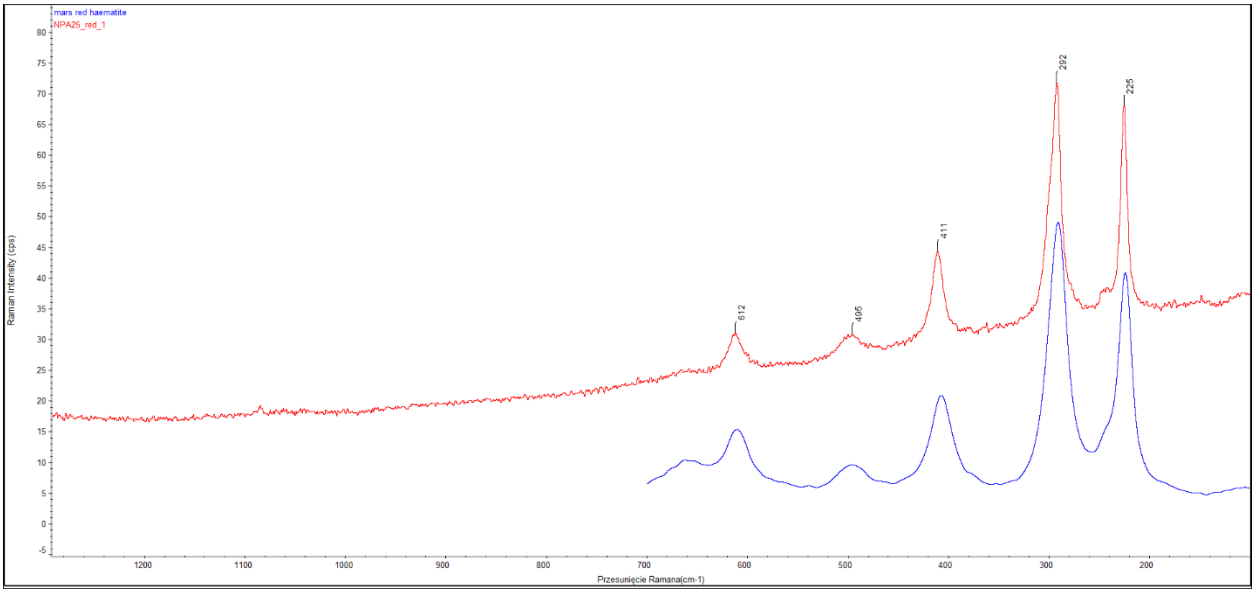

***Figure 35**) RAMAN spectra of the red pigment in sample NPA 25 (red line) with comparative reference spectra for hematite (blue line) (Burgio and Clark 2001, 1504). No peaks of calcite are recorded in this specific sample, while they appear in the RAMAN spectra of NPA 22.*

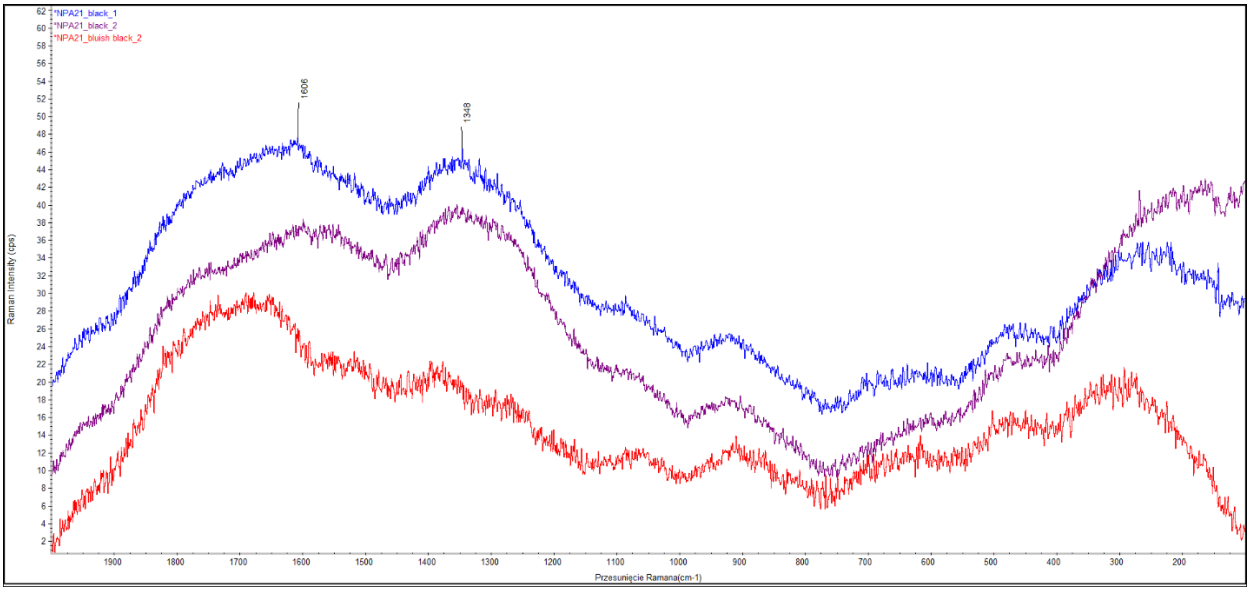

Figure 36*) RAMAN spectra of the black pigment detected on the surface of NPA 21. The strong and very broad bands with maxima at ~1600 and 1348 cm^{-1} indicate the presence of amorphous carbon.*

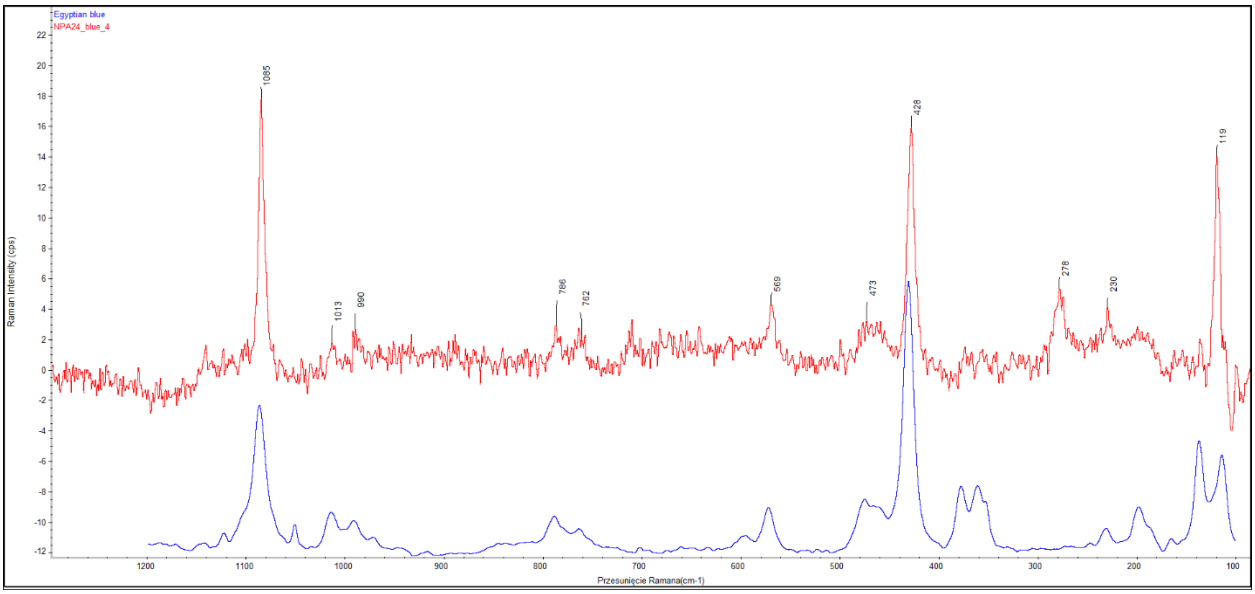

Figure 37) *RAMAN spectra of blue pigment on the surface of sample NPA 24 (red line) compared with reference spectra of Egyptian Blue (blue line) (Bell et al. 1997, online Raman Spectroscopic Library, entry: Egyptian Blue). Characteristic of Egyptian blue are the bands at 1085, 1013, 990, 786, 762, 569 and 428 cm-1.*

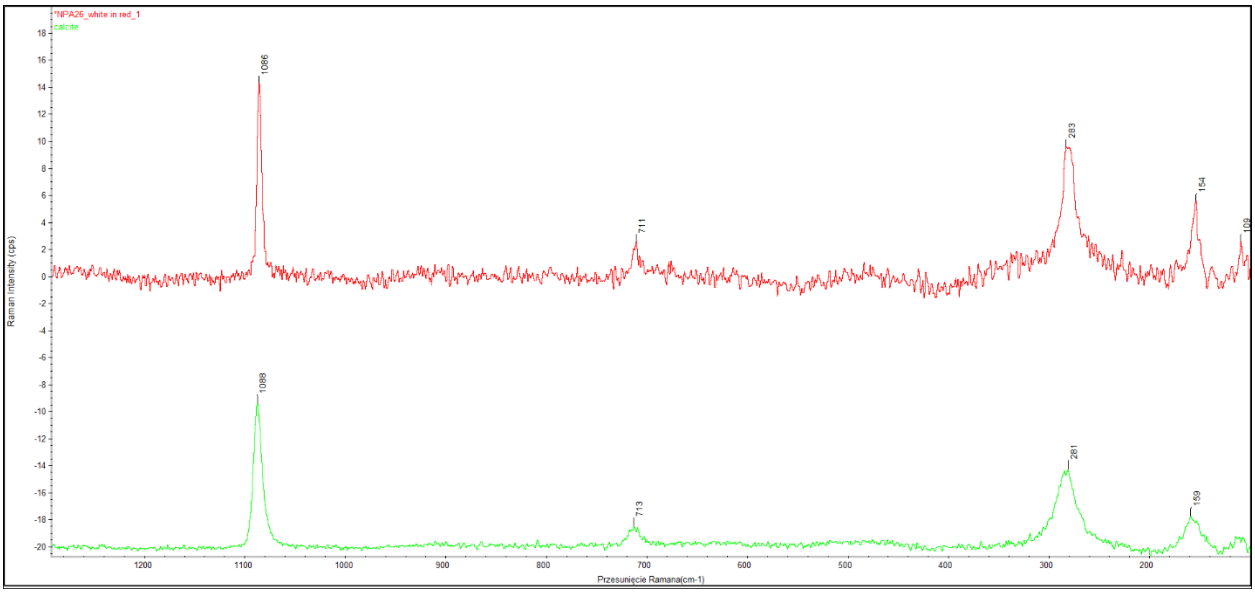

Figure 38*) RAMAN spectra of the white surface of sample NPA 26 (red line) with reference spectra of calcite (green line) with characteristics bands at 1086, 711, 283 and 154 cm^{-1}. The signal of calcite is weak in this sample.*

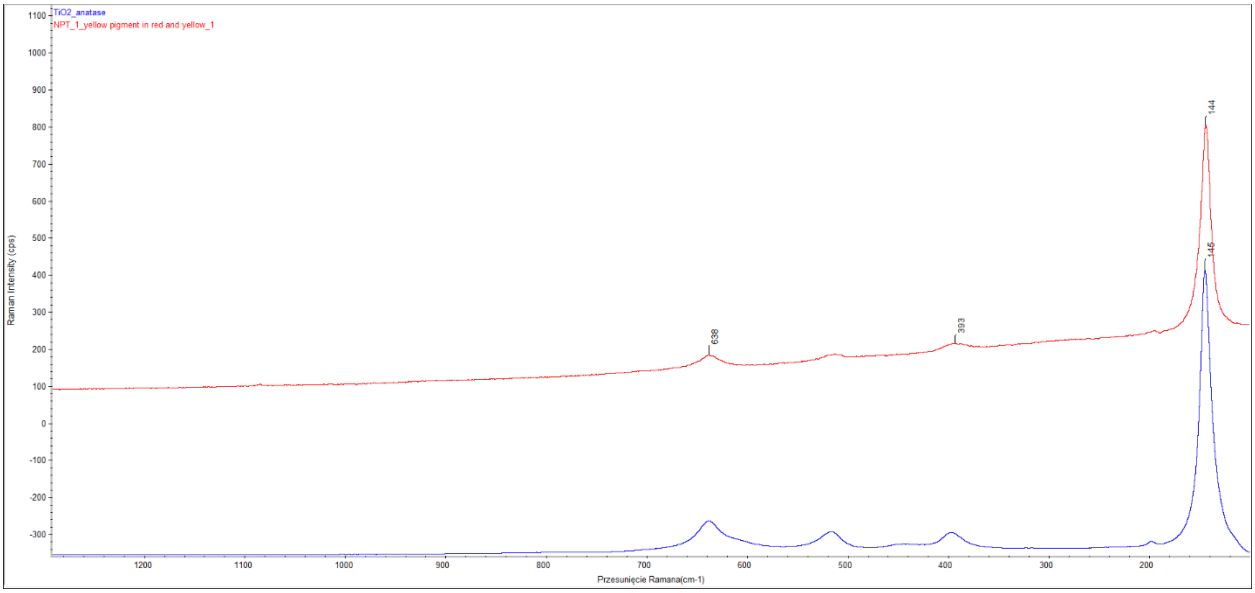

Figure 39*) Raman spectrum recorded in the yellow part of sample NPT 1 (red line) compared with spectrum of TiO_2 (anatase, blue line). Although the bands in the spectrum no doubt correspond to the bands of anatase, this compound is most likely not part of the pigment composition, but rather a natural impurity.*

Chapter 3.5.3: Organic residue analysis

The organic analysis on ten selected samples did not return positive results. This set of plasters was specifically selected for organic analysis due to a combination of factor, including the sampling context (*i.e.* proximity to cooking and food storage areas) and the microscopic observations (fluorescence in OM-UV light). Except for the presence of contaminants – such as human keratin – no relevant proteins were detected, neither from animals nor from plants. NPT 6 is the only

sample which signalled the presence of organics, specifically collagen ascribed to animal glue or gelatine. OM-UV analysis had suggested the possible use of organic binders in the pigment layer (**fig. 40**); animal glue/gelatine is a common binder for pigments in Antiquity (Duran *et al.* 2010). Following are the tables with the detected proteins.

Sample: KISS 3

Accession	Protein	#Peptides
K2C1_HUMAN	Keratin, type II cytoskeletal 1	5
K22E_HUMAN	Keratin, type II cytoskeletal 2 epidermal	3
K1C14_HUMAN	Keratin, type I cytoskeletal 14	3
TRYP_PIG	Trypsin	2
ALBU_HUMAN	Serum albumin	2
K1C18_SCYST	Keratin, type I cytoskeletal 18	2
MYSS_CYPCA	Myosin heavy chain, fast skeletal muscle	2

Sample: KISS 4

Accession	Protein	#Peptides
ALBU_HUMAN	Serum albumin	7
TRYP_PIG	Trypsin	1

Sample: KPH 3

Accession	Protein	#Peptides
K2C1_HUMAN	Keratin, type II cytoskeletal 1	7
K1C10_HUMAN	Keratin, type I cytoskeletal 10	4
K22E_HUMAN	Keratin, type II cytoskeletal 2 epidermal	4
K1C9_HUMAN	Keratin, type I cytoskeletal 9	4
K1C14_HUMAN	Keratin, type I cytoskeletal 14	3
TRYP_PIG	Trypsin OS=Sus scrofa PE=1 SV=1	2
K2C6B_HUMAN	Keratin, type II cytoskeletal 6B	2
K2C5_HUMAN	Keratin, type II cytoskeletal 5	2
ALBU_HUMAN	Serum albumin	2
NKX25_RAT	Homeobox protein Nkx-2.5	2

Sample: NPA 9

Accession	Protein	#Peptides
K2C1_HUMAN	Keratin, type II cytoskeletal 1	4
MYSA_DROME	Myosin heavy chain, muscle	3
ACTB_BOVIN	Actin, cytoplasmic 1	3
TRYP_PIG	Trypsin	2
K22E_CANFA	Keratin, type II cytoskeletal 2 epidermal	2

Sample: NPA 13

Accession	Protein	#Peptides
K2C1_HUMAN	Keratin, type II cytoskeletal 1	8
K1C10_HUMAN	Keratin, type I cytoskeletal 10	6
K22E_HUMAN	Keratin, type II cytoskeletal 2 epidermal	5
K1C14_HUMAN	Keratin, type I cytoskeletal 14	3

ALBU_HUMAN	Serum albumin	3
TRYP_PIG	Trypsin	2

Sample: NPA 24

Accession	Protein	#Peptides
ACTB_BOVIN	Actin, cytoplasmic 1	6
CUA1A_TENMO	Larval cuticle protein A1A	5
MYSA_DROME	Myosin heavy chain, muscle	4
ACTBL_HUMAN	Beta-actin-like protein 2	3
PLXA3_DANRE	Plexin A3	3
K22E_HUMAN	Keratin, type II cytoskeletal 2 epidermal	2
TPM1_BOMMO	Tropomyosin-1	2
K2C6B_HUMAN	Keratin, type II cytoskeletal 6B	2
K2C1_HUMAN	Keratin, type II cytoskeletal 1	2
H2A1A_HUMAN	Histone H2A type 1-A	2
AMY_TENMO	Alpha-amylase	2
RM51_XENLA	39S ribosomal protein L51, mitochondrial	2
TRYP_PIG	Trypsin	1

Sample: NPT 6

Accession	Protein	#Peptides
CO1A2_ONCMY	Collagen alpha-2(I) chain	24
K1C10_HUMAN	Keratin, type I cytoskeletal 10	8
K22E_HUMAN	Keratin, type II cytoskeletal 2 epidermal	8
K2C1_HUMAN	Keratin, type II cytoskeletal 1	7
K1C9_HUMAN	Keratin, type I cytoskeletal 9	6
G3P_DANRE	Glyceraldehyde-3-phosphate dehydrogenase	4
K2C5_BOVIN	Keratin, type II cytoskeletal 5	2
CO1A1_MOUSE	Collagen alpha-1(I) chain	2
CO2A1_BOVIN	Collagen alpha-1(II) chain	2
TRYP_PIG	Trypsin	1

Sample: NPT 8

Accession	Protein	#Peptides
TRYP_PIG	Trypsin	1
M3K6_MOUSE	Mitogen-activated protein kinase kinase kinase 6	1
ALBU_BOVIN	Serum albumin	1
SRP09_HUMAN	Signal recognition particle 9 kDa protein	1

Sample: NPT 12

Accession	Protein	#Peptides
TRYP_PIG	Trypsin	1
ARCH_DROME	Protein archease-like	1
ACTA_BOVIN	Actin, aortic smooth muscle	1
DCOR1_XENLA	Ornithine decarboxylase 1	1

Sample: YSC 10

Accession	Protein	#Peptides
K2C1_HUMAN	Keratin, type II cytoskeletal 1	7
K1C10_HUMAN	Keratin, type I cytoskeletal 10	5
K22E_HUMAN	Keratin, type II cytoskeletal 2 epidermal	4
K2C6A_HUMAN	Keratin, type II cytoskeletal 6A	4
K2C6B_HUMAN	Keratin, type II cytoskeletal 6B	3
K1C14_HUMAN	Keratin, type I cytoskeletal 14	3
K1C9_HUMAN	Keratin, type I cytoskeletal 9	3
K1C42_MOUSE	Keratin, type I cytoskeletal 42	2
K2C5_HUMAN	Keratin, type II cytoskeletal 5	2
TRYP_PIG	Trypsin OS=Sus scrofa PE=1 SV=1	1

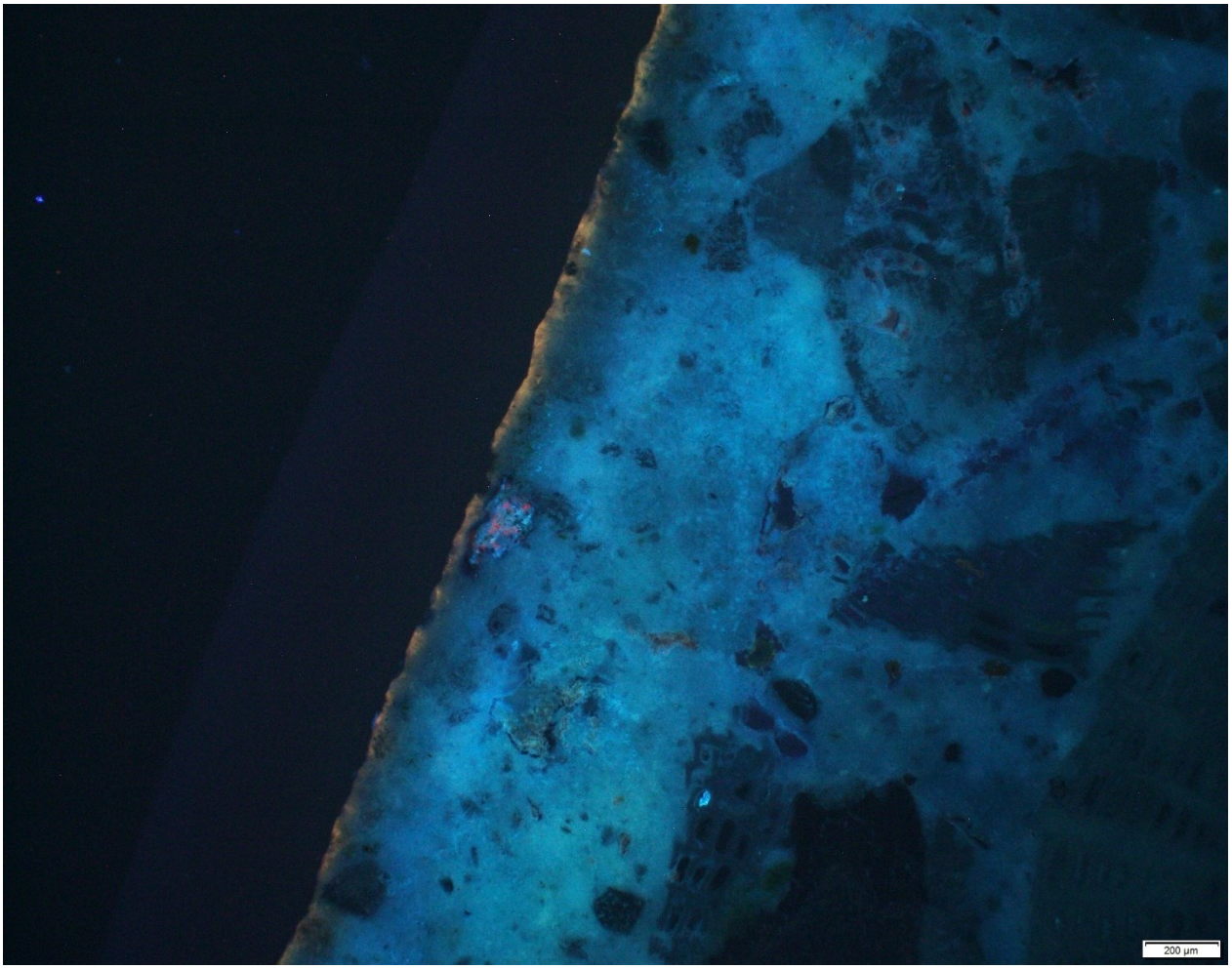

Figure 40*) Photomicrograph of the surface of sample NPT 6d (scale bar= 200 µm) taken under UV light. Fluorescence in UV light can suggest the presence of organic materials. In this specific case, organic traces have been detected with the organic residue analysis on the surface of the sample, suggesting that probably an organic binder was used to apply the pigment on the plaster surface.*

Chapter 3.6: Geological samples – results

XRD analysis aided the identification of stones, confirming the major mineralogical phases were either calcium carbonate or calcium sulfate. The other minerals detected are compatible with what observed in the thin sections: mainly aragonite, quartz or chert, muscovite (an aluminum and potassium phyllosilicate), ankerite (a carbonate mineral with formula $Ca(Fe,Mg,Mn)(CO_3)_2$), lizardite (a sub-group of serpentine) and palygorskite (a magnesium and aluminum phyllosilicate). The TA results display a typically pure limestone with occasional traces of exothermic reaction due to the presence of organics (samples LCY 012, 015 and 016). Patterns of low-intensity peaks in the region of 400–450°C can be associated either with the decomposition of bitumen or other organics present in the matrix.

Burning and slaking reveal that all the tested samples were suitable for the production of lime. Three out of the five slaked limes set underwater (**fig. 41**), displaying a degree of hydraulicity. The remaining two, on the other hand, are pure aerial lime.

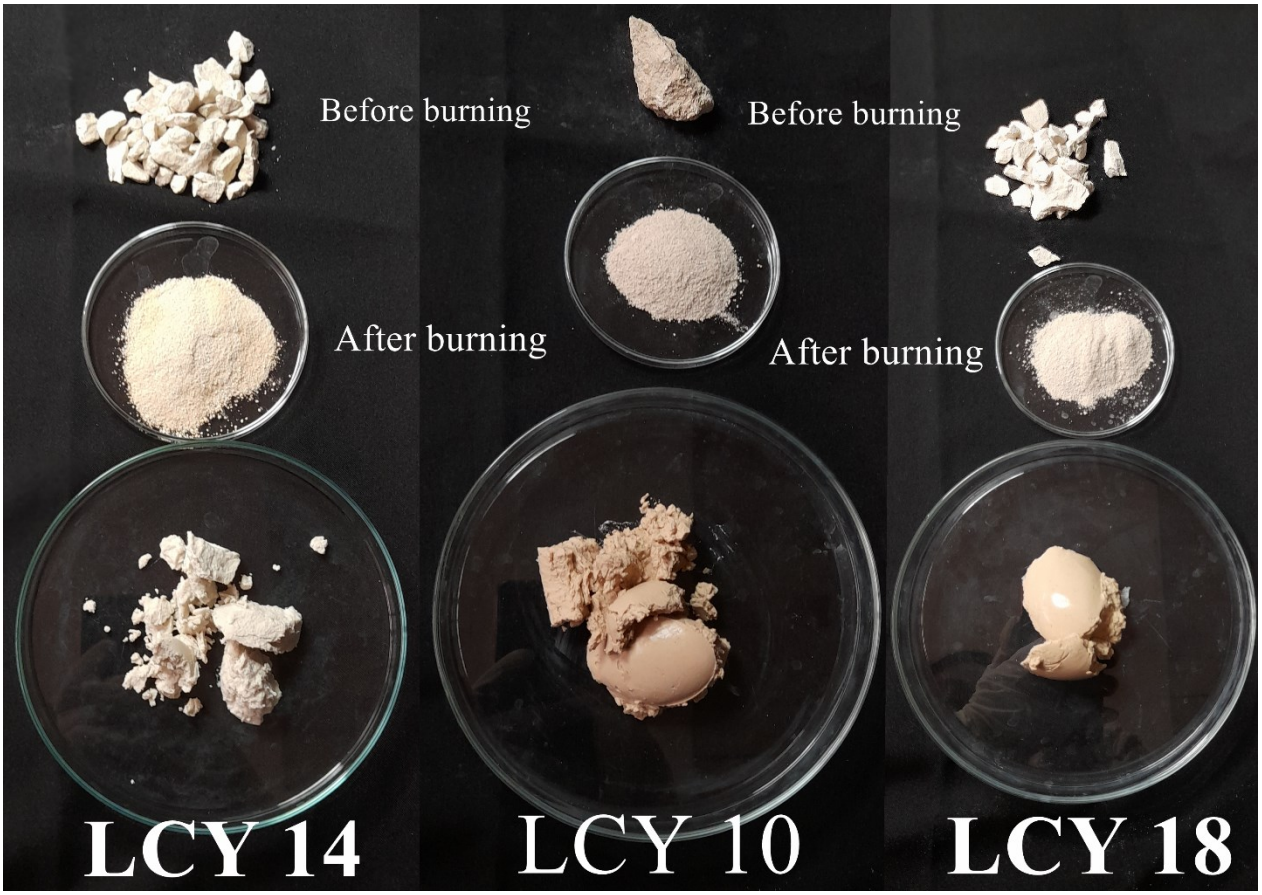

Figure 41) *Photograph of samples LCY 014, LCY 010 and LCY 018 displaying the stone before burning, the quicklime obtained after burning, and the slaked putty. In the case of sample LCY 014, the quicklime set underwater conditions, producing a hard putty which cannot be easily worked. Sample LCY 010 produced a semi-hard putty, still partially workable, although a fraction of it hardened underwater. LCY 018, on the other hand, did not harden underwater, and the slaked putty was soft and malleable.*

REFERENCES

AHMED, I.

2024. Restoration of Doleshwar Mosque: Reviving Craft and Engaging Craftsmen of Lime-surkhi. *Studies in Conservation*, pp. 1–16. https://doi.org/10.1080/00393630.2024.2355783

ALVAREZ, J.I., R. VEIGA, S. MARTÍNEZ-RAMÍREZ, M. SECCO, P. FARIA, P.N. MARAVELAKI, M. RAMESH, I. PAPAYIANNI, J. VÁLEK

2021. RILEM TC 277-LHS report: a review on the mechanisms of setting and hardening of lime-based binding systems. *Materials and Structures* 54, 63. https://doi.org/10.1617/s11527-021-01648-3

BANFILL, P.F.G.

2018. Hygrothermal properties of NHL mortars, in T. Brostrom, L. Neilsen, S. Carlsten (eds.)*, Conference Report: The 3rd International Conference on Energy Efficiency in Historic Buildings,* Uppsala University, pp. 71–79.

BELL, I. M., R.J.H. CLARK, P.J. GIBBS

1997. Raman spectroscopic library of natural and synthetic pigments (Pre~ 1850 AD). *Spectrochimica Acta Part A: Molecular and Biomolecular Spectroscopy* 53(12), pp. 2159–2179. https://doi.org/10.1016/S1386-1425(97)00140-6

BURGIO L., R.J.H CLARK

2001. Library of FT-Raman spectra of pigments, minerals, pigment media and varnishes, and supplement to existing library of Raman spectra of pigments with visible excitation. *Spectrochimica Acta Part A: Molecular and Biomolecular Spectroscopy* 57(7), pp.1491–1521. https://doi.org/10.1016/S1386-1425(00)00495-9

CARNEY, M.

2016. *Paleoethnobotanical and Geoarchaeological Analyses at the Flying Goose Site (45PO435)*, master thesis, Washington State University. http://dx.doi.org/10.13140/RG.2.1.2278.3609

CASTELLANO, L.

2021. A new anthracological sequence from Niğde-Kınık Höyük (Turkey): woodland vegetation and arboriculture in southern Cappadocia from the Late Bronze Age to the Ottoman Period. *Archaeological and Anthropological Sciences* 13, 49. https://link.springer.com/article/10.1007/s12520-021-01284-6

CALZOLARI, L., L. MEDEGHINI, I. BAIOCCHI, G.L. ZANZI, S. MIGNARDI
2023. Aqua Alexandrina and Fragole cistern: characterization of mortars from Roman constructions, Rome (Italy). *Archaeological and Anthropological Sciences* 15, 183. https://doi.org/10.1007/s12520-023-01885-3

CHEVER, L., S. PAVÍA, R. HOWARD
2010. Physical properties of magnesian lime mortars. *Material Structure* 43, pp. 283–296. https://doi.org/10.1617/s11527-009-9488-9

DURAN, A., M.C. JIMENEZ DE HARO, J.L. PEREZ-RODRIGUEZ, M.L. FRANQUELO, L.K. HERRERA, A. JUSTO
2010. Determination of pigments and binders in Pompeian wall paintings using synchroton radiation – high-resolution x-ray powder diffraction and conventional spectroscopy – chromatography. *Archaeometry* 52, pp. 286–307. https://doi.org/10.1111/j.1475-4754.2009.00478.x

EASTAUGH, N., V. WALSH, T. CHAPLIN, R. SIDDALL
2008. *Pigment Compendium. A Dictionary and Optical Microscopy of Historical Pigments*. Oxford: Butterworth-Heinemann.

FAHMY, A., A. GOŁĄBIEWSKA, W. WOJNICZ, A. STANISŁAWSKA, J. KOWALSKI, J. ŁUCZAK, A. ZALESKA-MEDYNSKA, S. DOMÍNGUEZ-BELLA, J. MARTÍNEZ-LÓPEZ, E. MOLINA-PIERNAS
2023. Multi-functional monodispersed SiO2–TiO2 core-shell nanostructure and TEOS in the consolidation of archaeological lime mortars surfaces. *Journal of Building Engineering* 79, 107809. https://doi.org/10.1016/j.jobe.2023.107809

FAUST, G.T.
1950. Thermal Analysis Studies on Carbonates I. Aragonite and Calcite. *American Mineralogist* 35(3-4), pp. 207–224.

MARUCCI, G., A. BEEBY, A.W PARKER, C.E. NICHOLSON
2018. Raman spectroscopic library of medieval pigments collected with five different wavelengths for investigation of illuminated manuscripts. *Analytical Methods* 10, pp. 1219–1236. https://doi.org/10.1039/C8AY00016F

MILANO, S., G. NEHRKE
2018. Microstructures in relation to temperature-induced aragonite-to-calcite transformation in the marine gastropod Phorcus turbinatus. *Plos One*. https://doi.org/10.1371/journal.pone.0204577

MOROPOULOU, A., A. BAKOLAS, E. AGGELAKOPOULOU
2004. Evaluation of pozzolanic activity of natural and artificial pozzolans by thermal analysis. *Termochimica Acta* 420, pp. 135–140. https://doi.org/10.1016/j.tca.2003.11.059

MOROPOULOU, A., A. BAKOLAS, S. ANAGNOSTOPOULOU
2005. Composite materials in ancient structures. *Cement and Concrete Composites* 27, pp. 295–300. https://doi.org/10.1016/j.cemconcomp.2004.02.018

MOROPOULOU, A., A. BAKOLAS, K. BISBIKOU
2000. Investigation of the technology of historic mortars. *Journal of Cultural Heritage* 1, pp. 45–58. https://doi.org/10.1016/S1296-2074(99)00118-1

VÁLEK, J., E. VAN HALEM, A. VIANI, M. PÉREZ-ESTÉBANEZ, R. ŠEVČÍK, P. ŠAŠEK
2014. Determination of optimal burning temperature ranges for production of natural hydraulic limes. *Construction and Building Materials* 66, pp. 771–780. https://doi.org/10.1016/j.conbuildmat.2014.06.015

VÁLEK, J, O. SKRUŽNÁ
2019. Performance assessment of custom-made replications of an original historic render – A study of application influences. *Construction and Building Materials* 229, 116822. https://doi.org/10.1016/j.conbuildmat.2019.116822

UHL, D., A. JASPER
2018. Charred conifer remains from the Late Oligocene-Early Miocene of Northern Hesse (Germany). *Acta Palaeobotanica* 58(2), pp. 175–184. http://dx.doi.org/10.2478/acpa-2018-0012

PART 4. DISCUSSION

Introduction

As anticipated in the first chapter of the present thesis, plasters can be categorised in a number of different ways. The approach adopted here systematises the samples in categories defined as "systems", where both the chemical, mineralogical and functional contexts are taken into account simultaneously. It must be highlighted that the term "system" implies a specific logic systematization of the samples with rigid chemical properties, mineralogical compositions and functional categories. Due to the limited size of the samples' pool, a proper systematization is not fully possible in this study; furthermore, the boundaries between the systems presented here are more fluid, especially for what concerns the functionality of the mortars grouped. Thus, it must be pointed out that the term "system" is used in a preliminary – and perhaps debatable – manner. However, the term has been adopted in light of the high potential it presents to ease cross-context comparisons and research on plasters and mortars worldwide.

Chapter 4.1: Systematization of the samples

For this research, six systems in total have been constructed. **Tab. 12** summarizes these groups, highlighting the major attributes. The samples were grouped into the systems according to a combination of elements, including the functional group, chemical composition and microstructural features.

System no.	Brief description	Functional group	Chemical composition (XRD-SEM)	Microstructural features
1	Double-layered, lime-based plasters often topped by pigment layer(s).	Wall plasters/ seat sealing	Lime-based binders with presence of mg-calcite, aragonite and silica. Low content of amorphous phases.	Presence of two distinguishable layers with different aggregate types and/or sizes.
2	Waterproofing mortars laid on top of structures apt to the retaining or disposal of liquids. Single-layered with distinctive pink colour. Lime-based.	Lining mortars/rendering	Lime-based binders with high contents of amorphous phases, and presence of clay minerals (such as illite and muscovite).	Presence of numerous ceramic fragments in the matrix.
3	Multi-layered, lime-based plasters with a series of successive preparation layers usually including a waterproofing and/or natural hydraulic strata.	Floors	Varies for each of the layers, but usually includes at least one layer of waterproofing or hydraulic binder with high content of amorphous phases.	Presence of several layers with different aggregates, A:B ratios, and porosity. Often display presence of tramping cracks.

4	Lime-based plasters considered as outliers since they do not show more than one of the systems' main characteristics.	Various	Lime-based binders.	Various.
5	Hydraulic mortars, typically single-layered; macroscopically displaying pink or white, colouration.	Wall plasters, floors	Hydraulic binders with high amorphous phases.	These mortars are characterised by their hardness and compactness.
6	Gypsum-based plasters and mortars characterised by a single-layered structure and the lack of aggregates.	Mortars, wall plaster	Gypsum binders with low or absent amorphous phases; presence of CASH phases (<0.5%).	Lack of aggregates in the binder mixture; presence of Si-based impurities (from the rock processing); coarse matrix; high porosity.

Table 12*) The table summarises the six systems providing for each a brief description, the functional categories to which the samples belong, the chemical composition and the microstructural characteristic features.*

Chapter 4.1.1: System 1 – double-layered lime plasters

System 1 is the largest group in the present research, including 35 samples (see **tab. 13** for the full list). Nearly the totality of the samples retain the function of wall plasters, and often present painting layer and/or incised decorations on the surface. This typology of plasters has been found consistently in all the archaeological contexts dating from the Hellenistic period onwards. Macroscopically, they consist of a maximum of 2 cm thick white plasters, hard and compact with well-sorted aggregates. Two distinct mortar layers are clearly visible on the sections of the samples, even at the naked eye (**fig. 44**): usually, the upper layer appears whiter and slightly softer to the touch. From a microscopic perspective, the analysis of the thin sections reveals a remarkable similarity across all 35 samples.

The first layer – or ground layer – consists of a coarser and partially porous mixture of fine lime binder with miscellaneous, generally well-sorted, fine to medium-sized (on average below 1-1.5 mm) aggregates. For the majority, aggregates are composed of bioclasts, quartz, well-rounded micritic limestones naturally rich in bioclasts, and of a variety of igneous rocks – commonly including diorite, basalt, and serpentine; rarely olivine. This layer can be minimally or considerably porous, depending on each sample; however, it is usually more porous than the superimposing layer. The higher porosity of this layer is definitely not a result of degradation processes – which would deteriorate the external layers more than the inner ones – but rather the result of a specific composition and, possibly, application technologies. From the perspective of composition, coarse aggregates are known to increase structural properties, such as the overall strength and durability, while simultaneously enhancing the porosity of mortars. Furthermore, this first layer was applied

directly to the associated wall/masonry structure with the knowledge that a second, or more, layer would be applied. This resulted in a generally lower necessity for evening and smoothing of the layer – techniques which effectively decrease the porosity by mechanical action, pressing the particles of the mixture and forcibly closing the pores. As this more porous layer is present in practically all the samples of this system, it is safe to consider this production and application process a well-known and established techniques which survived, nearly unchanged, since the Hellenistic to the Late Roman period.

Observing the thin sections in PLM it is possible to notice how the bond between the ground layer and the finishing one is sharp and clear (**fig. 42**), suggesting that the first layer's mixture was fully – or at least partially – dried before the application of the second layer. Moreover, it is possible to observe how the lime binder is denser in proximity to this interface, which could have happened during the drying of the layer when water evaporated from the surface. In addition, this denser layer could also be the proofing element for the possible use of smoothing tools on the surface. In fact, flat and especially metallic tools can pull fine binder particles to the surface.

The second layer consists of a thin (always below 1 cm) lime plaster with a fine and compact binder mixed with well-sorted crushed shells and – occasionally – limestone fragments (average aggregate dimension is between 0.5–0.9 mm). The binder appears denser, with fewer and smaller pores or cracks. Aggregates for this layer are carefully selected; in fact, it is even possible to recognize how only specific types of shells are employed for this mixture (bryozoans and benthic foraminifera mostly), while a larger variety is observable in the ground layer. The selection of bryozoan bioclasts and benthic foraminifera as main aggregates for the finishing layer does not seem to be a casual one, seen the consistency of its occurrence. Both these species occur frequently in the Mediterranean and were not hard to source in Cyprus in any of the analysed periods. However, to current knowledge, there is no evidence for the use of these bioclasts specifically for the production of wall plasters. Typically, the most superficial layers of wall renderings or stuccoes were enriched with marble powder to give the surface a bright and shining finishing; however, Cyprus lacks deposits of marble. In this light, it is possible that this specific categories of bioclasts were selected to obtain an effect similar to the one caused by the addition of marble powder.

In terms of the binder's mineralogical composition, the main mineral phase is calcium carbonate ($CaCO_3$), whose values differ slightly between the finishing and the ground layers. According to XRD and TA, the binder-rich fraction (<63 μm) from the samples' finishing layer generally display a $CaCO_3$ percentage of over 70%, while the one from the ground layers vary between 60–70%. Other mineral phases in the finishing layer are mainly Si-based minerals (chert, quartz), feldspars and aragonite (all together less than 5%) or amorphous (between 5–25%); in the ground mortar it is possible to observe a higher content of Si-minerals and aragonite (up to 10%), and an increased presence of amorphous phases (above 20%). The finishing layer contains a relatively higher proportion of binder to aggregate compared to the ground layer.

A 30% of the samples in System 1 present an additional paint layer, while the remaining have well-polished, and smooth surfaces (**tab. 14**). In rare circumstances it is possible to observe tool marks

on the surface of the samples, even below the pigment, suggesting that they could be the traces of the tools employed for the application of the mortar (**fig. 43**). An additional commentary on the pigments, the colour palettes and the application techniques is included in the following chapter (**ch. 4.2**).

LBA	IA	H	LH-ER	ER	LR	U
--	--	YSC 10	NPA 26	NPA 25	NPT 4	YM1
		YSC 12	NPA 28	NPA 27	NPT 6 (a,b,d)	YM 2
		YSC 13	NPA 29	NPA 30*	NPT 7 (a,b)	NPA 14
		YSC 17		NPER 2	NPT 10	NPA 16
		YSW 1			NPT 11 (a,b,c)	NPA 17
		YM 1				NPA 18
		YM 2				NPA 23
		NPA 21				
		NPA 22				
		NPA 24*				
		YSC 11**				
		11	**3**	**4**	**10**	**7**

Table 13*) List of all the samples grouped in System 1 category divided by chronological period. Legend: LBA=Late Bronze Age, IA=Iron Age, H=Hellenism, LH=Late Hellenism, ER=Early Roman, LR=Late Roman, U=uncertain. * indicates samples containing one NHL layer (described in chapter 4.1.5); ** indicates samples which belong to this category but have not been fully analysed due to insufficient material.*

Sample ID	Type of finishing	Finishing description
YSC 10	Pigment	Red pigment laid on flat surface. Traces of brush or tool marks, either from the polishing or the pigment application.
YSC 11	Limewash?	Fine, bright white layer applied by brush as evidenced by the brushstrokes' marks.
YSC 12	Smooth (limewash?)	Bright white, even and smooth surface with traces of brushstrokes.
YSC 13	Smooth	Flat, even, smooth surface – no tool marks.
YSC 17	Smooth	Flat, even, smooth surface with sporadic traces of tool marks.
YSW 1	Smooth	Flat, even, smooth surface – no tool marks.
YM 1	Smooth	Flat, even, smooth surface – no tool marks.
YM 2	Smooth	Flat, even, smooth surface – no tool marks.
NPA 14	Polishing + pigment	The surface was smoothed and evened with the use of some sort of tool which left marks on the surface. Red pigment stripes were then applied on this surface, possibly by brush.
NPA 16	Smooth	Even and flat surface with traces of polishing. Bad preservation status.
NPA 17	Smooth	Flat, even surface, no tool marks.
NPA 18	Smooth	Flat, even, smooth surface with traces of tool or brush marks.

NPA 21	Pigment	Black paint layer applied with calcite/lime as a binder on a dry layer of plaster.
NPA 22	Pigment	Red paint layer applied with calcite/lime as a binder on a dry layer of plaster.
NPA 23	Smooth	Flat, even, smooth surface with traces of tool or brush marks.
NPA 24	Pigment	Light-blue, crumbling pigment applied on a pink plaster layer with the use of a now lost binder (possibly organic).
NPA 25	Pigment + incision	Smooth white surface with vertical incision painted in red with the use of a brush (visible brushstrokes).
NPA 26	Pigment + incision	Smooth white surface with vertical incision painted in red with the use of a brush (visible brushstrokes).
NPA 27	Pigment	Flat and evened surface smoothed with some tool, as visible from the marks left underneath the pigment. The decoration presents three vertical bands in black, red and white.
NPA 28	Pigment	Flat and evened surface smoothed with some tool, as visible from the marks left underneath the pigment. The decoration presents three vertical bands in black, red and white.
NPA 29	Pigment	Flat and evened surface smoothed with some tool, as visible from the marks left underneath the pigment. The decoration presents three vertical bands in black, red and white.
NPA 30	Smooth	Flat and evened surface of pink plaster without traces of smoothing tools.
NPER 2	Smooth	Flat, even, smooth surface with traces of tool marks.
NPT 4	Smooth	Flat, even, smooth surface – tool marks.
NPT 6 (a,b,d)	Smooth	Flat, even, smooth surface – tool marks.
NPT 7 (a,b)	Smooth	Flat, even, smooth surface – tool marks.
NPT 10	Pigment	The specific sample does not present traces of pigment, however, the original wall to which it belonged was decorated with frescoes.
NPT11(a,b,c)	Limewash?	Flat surface with clear brushstrokes suggesting the possible application of a white limewash over the surface.

Table 14*) List of the samples of system 1 with corresponding surface treatment. As evidenced in the paragraph, the majority of the wall plasters and seat sealings present evened and smoothed surface, with only a minor percentage displaying traces of pigmentation. Where available, data concerning the finishing technique(s) are provided.*

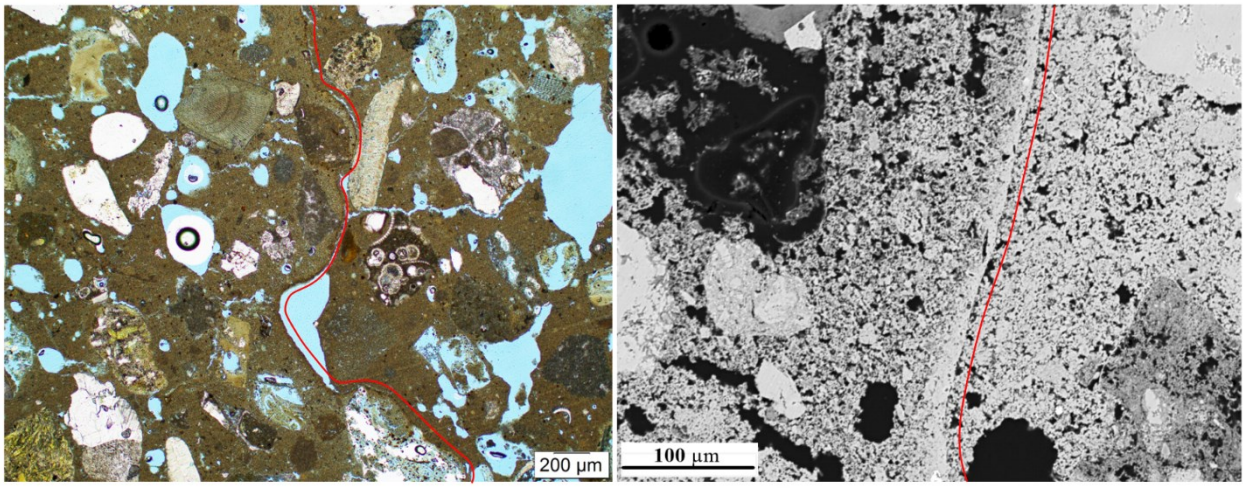

Figure 42*) Photomicrograph of sample NPA 27 in PPL (left) and in BSE (right). The red line highlights the layer bond between the coarse substratum (on the left in both pictures) and the finer finishing layer (on the right in both pictures).*

Figure 43*) Microphotograph of sample NPT 11 with evidence of brush or tool marks on the finishing surface. The finishing layer is completely white, with no traces of pigments. The slight yellow to pink spots are caused by the depositional context of the sample, which is characterized by a soil rich in iron content, similar to terra rossa. Furthermore, certain types of microorganisms' decomposition can cause this type of red stains on the surface.*

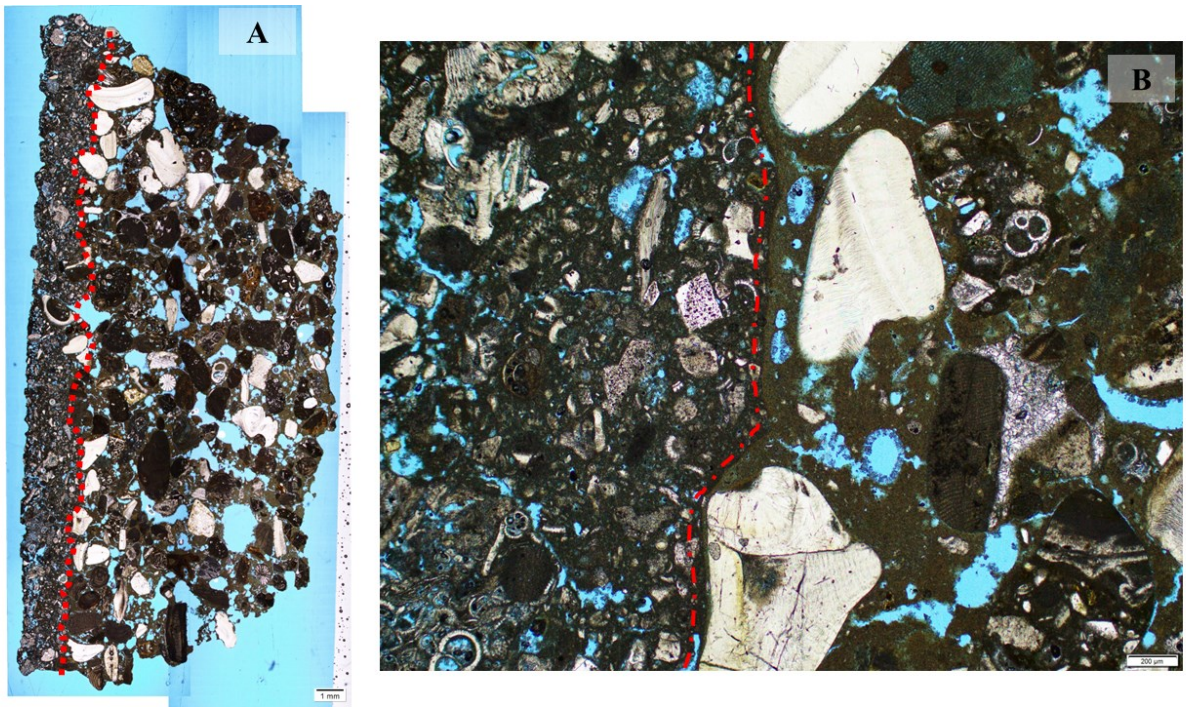

Figure 44A) *Photomicrograph scan of sample YM 2 (scale 1 mm) with the layer border outraced in red. The ground layer (on the right) is more porous and has larger sized aggregates, while the finishing layer is thin, compact and with fine grained aggregates.* ***B)*** *Zoom in on the layer bond in sample YM 2 (scale 200 µm).*

Chapter 4.1.2: System 2 – waterproofing mortars

This category includes samples from structures associated with the storage or disposal of water (or other liquids), thus expected to be watertight and waterproof, at least to some extent (**tab. 15**). It is important to distinguish waterproofness from hydraulicity, keeping into consideration that the first is a physical property that can be also partially achieved by manipulating the morphological structure of the mortar, while the second is a chemical property strictly depending on the presence of specific mineral phases – namely unstable silica phases (Weiner 2010; see also chapter 1.1 on the distinction between hydraulicity and watertightness).

The samples included in System 2 are constituted by mixtures of air lime binders with pozzolanic aggregates. They are macroscopically characterized by a distinctive pink colour, a result of the addition of fine ceramic particles in the binder: the larger fragments of ceramic usually do not exceed 1 mm in size, while sometimes can be as fine as powder, with particles in the order of a few tens of microns. The air lime binder is typically fine and compact, moderately porous, and usually mixed with the aggregate in a 1:2.5 ratio. Aside from the ceramic particles, the most common additions to this mixture are local micritic and bioclastic limestone fragments, bioclastic conglomerates, chert, feldspars, and, occasionally, serpentine (**fig. 45**).

The mineralogical composition of the binder-rich fraction of the System 2 samples, analysed by means of XRD, shows a lime binder ($CaCO_3$ equal or above 60%), with varying content of

amorphous phases (between 6.4% up to 49.9%) and less impactful presence of other minerals such as aragonite (not higher than 1.5%), silica (below 6%), and feldspars (around 1%).
The TA curves display weight loss in the region between 250°-600°C, suggesting the presence of chemically bound water to hydraulic components (on the use of TA for the determination of hydraulicity see Elsen *et al.* 2012; Moropoulou 1995).
SEM-EDS mapping was employed to carefully evaluate the presence of reaction rims, and it was possible to distinguish two different types of mortars based on the lack (type A) or presence (type B) of reaction rims. Type A and B mortars featured the presence of visible rims around the ceramic particles in PLM, leading to suspect the presence of a chemical reaction rim. However, as shown in **figure 46A,** in the type A mortars there is no reaction rim between the ceramic aggregates and the binder; nonetheless, the latter is visibly denser in the interface area with ceramic fragments, suggesting that the ceramic porosity enhanced the suction of the binder, creating a physical – but not pozzolanic – reaction rim. On the other hand, type B mortars revealed the presence of a chemical reaction between the binder and the aggregates in SEM-EDS analyses (**fig. 46B**).
Despite not being chemically hydraulic, these samples present a relatively low porosity (on average 26 vol.%). Furthermore, during open porosity and water absorption testing, the weight loss due to the exposition to water was minimal – about 0.1 %, highlighting a certain resistance to the natural dissolution of calcium carbonate.

LBA	IA	H	LH-ER	ER	LR	U
--	--	YHC 1	--	NPT 12	NPVT 1	--
		YSC 4**		NPA 7*		
		YSC 5**		NPA 8*		
				NPA 10		
		3		**4**	**1**	

Table 15*) List of all the samples grouped in System 2 category divided by chronological period. Legend: LBA=Late Bronze Age, IA=Iron Age, H=Hellenism, LH=Late Hellenism, ER=Early Roman, LR=Late Roman, U=uncertain. * indicates samples which present characteristics anomalous for this system and are – therefore – further discussed in chapter 4.1.4; ** indicates samples belonging to this category but not fully analysed due to insufficient material available*

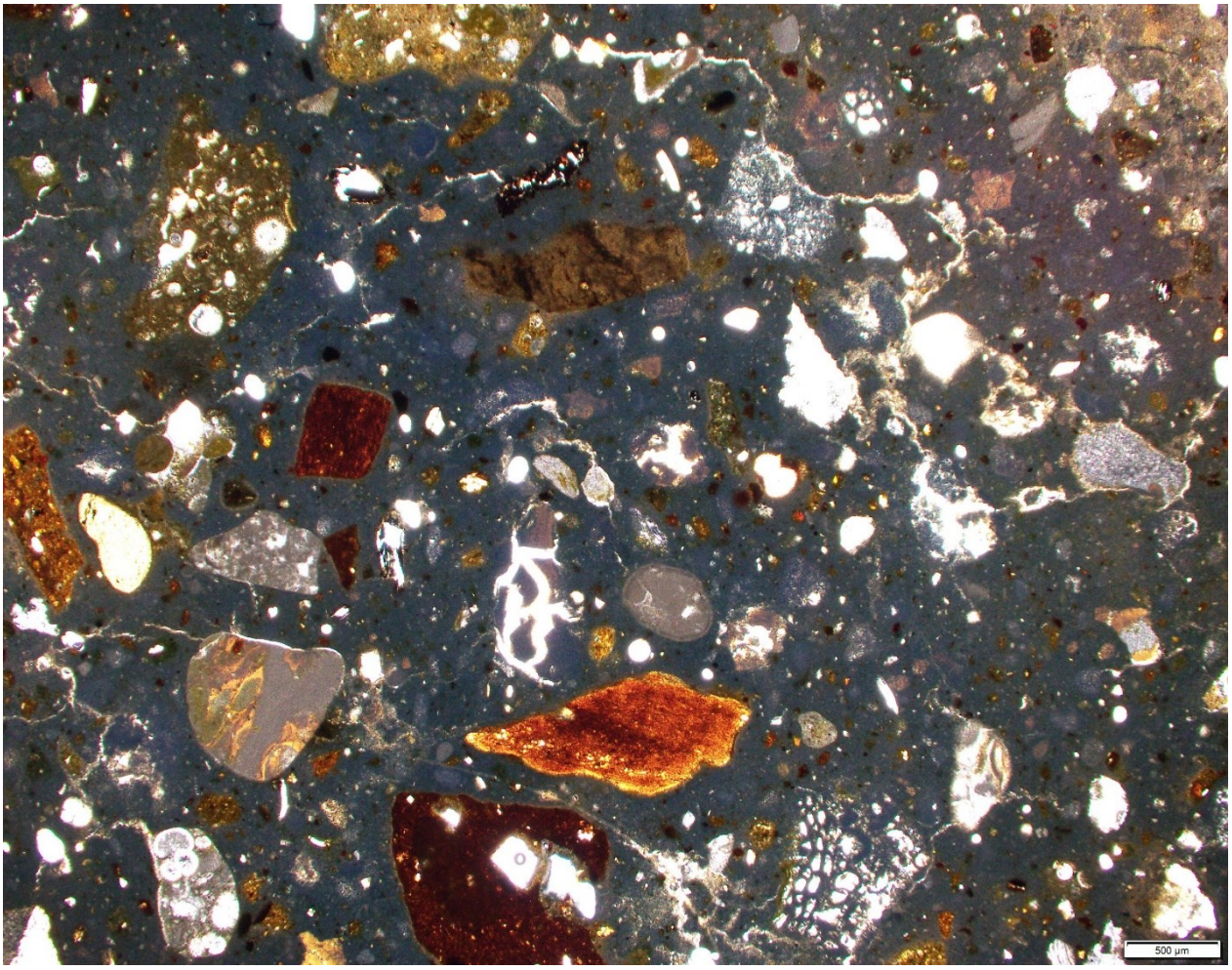

Figure 45) *Photomicrograph of sample NPT 12 displaying the characteristic matrix of a system 2 sample: dark-grey, compact binder with diverse typologies of ceramics embedded in the matrix (scale 500 µm).*

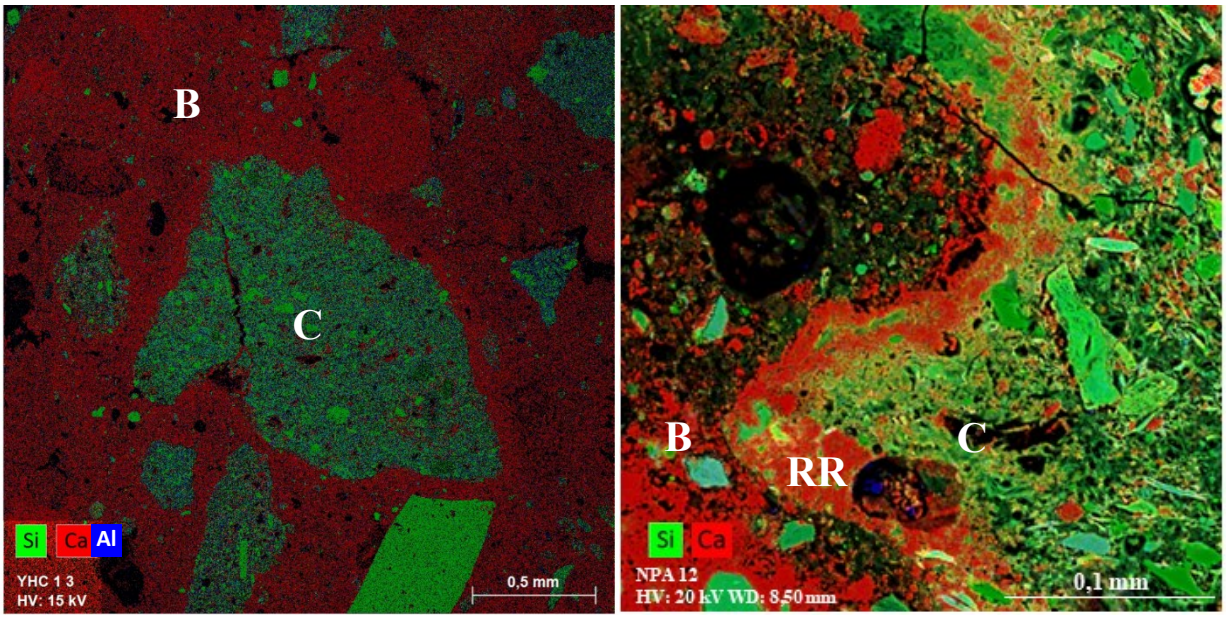

Figure 46A) *SEM-EDS elemental distribution map of Si, Ca, and Al in sample YHC 1 displaying a ceramic aggregate (C) surrounded by the binder matrix (B); no traces of reaction rims are visible, although the binder appears denser around the ceramic particle (SEM TESCAN MIRA, EDS software Brucker Esprit 2.5).* ***4B)*** *SEM-EDS image of sample NPA 12 with elemental distribution of Si and Ca, displaying a ceramic aggregate (C) with clear traces of reaction rims (RR) (SEM Zeiss EVO 25, EDS software Aztec 5.1).*

Chapter 4.1.3: System 3 – multi-layered floor plasters

This group encompasses samples from floor structures displaying a sequence of multiple preparatory layers for the final surface (**tab. 16**). With the exception of samples NPA 19 and 20, the rest of the floors vaguely resemble the structured preparation illustrated by Vitruvius in the *De Architectura* (Caldeira *et al.* 2019, 4). The floor sequence (reconstructed by author in **fig. 47**) consists of a series of preparation layers on top of which a mosaic decoration could be laid out; however, in none of the Paphian samples traces of mosaic have been detected. The construction starts with a masonry layer, called *statumen*, with relatively regularly sized stones laid vertically on the ground. On top of the *statumen*, a layer called *rudus* is applied; a *rudus* is generally constituted by a mixture of sand or gravel and lime, and – according to Vitruvius – it should be at least 22 cm thick. Over the *rudus* the so-called *nucleus*, a "ceramic mortar" (Caldeira *et al.* 2019, 4) is applied, and finally the bedding for the mosaic is laid out. The Paphian samples present variations of this formula, with the notable wide-spread presence of a *nucleus* constituted of a lime mortar mixed with ceramic aggregates. However, as previously mentioned, none of the surface were designed to support mosaics, and the finishing is usually constituted by a thinner layer of pozzoloanic mortar (as in the case of NPT 3a, NPA 9, NPA 11-13, NPER 1 and NPHH 1). The finishing deviating from the Vitruvian standard could be associated with the function of the rooms where these floors were applied; in fact, in at least one of the samples (NPHH 1), the context and usage of the room is clearly associated with a *latrina*, a space that would benefit from water-retaining properties and increased durability. To further prove this point, it must be noticed how

the cluster of samples NPA 11-13 is a floor structure pertaining to a well, while NPA 9 is located in proximity of a large water/sewage channel (although it is not directly connected to it), and NPT 3a is a floor renowned to have functioned as a watertight pavement for *naumachiae*. It is indeed possible that for this specific reason the *nucleus* layer was not further covered by the substratum for mosaics' application.

A completely different structure and situation occurs for samples NPA 19 and NPA 20, non-coincidentally dated to pre-Roman times. In these instances, the floor seems to be constituted by a single, thick layer of lime mixed with large-sized aggregates (possibly gravels) and thoroughly compacted on the surface. Due to the limited number of pre-Roman samples, hypothesizing that this technique was a standard before the introduction of the Roman floor system would be hazardous; nonetheless, it remains an interesting point to be further explored.

LBA	**IA**	**H**	**LH-ER**	**ER**	**LR**	**U**
--	--	NPA 20	NPA 19	NPA 11-13*	NPT 3 (a*,b)	NPA 9**
			NPH 1*	NPER 1*		
		1	**2**	1	**1**	**1**

Table 16*) List of all the samples grouped in System 2 category divided by chronological period. Legend: LBA=Late Bronze Age, IA=Iron Age, H=Hellenism, LH=Late Hellenism, ER=Early Roman, LR=Late Roman, U=uncertain. * indicates samples which present characteristics typical of other Systems and are – therefore – further discussed in chapter 4.1.5; ** indicates samples belonging to this category but not fully analysed due to insufficient material available*

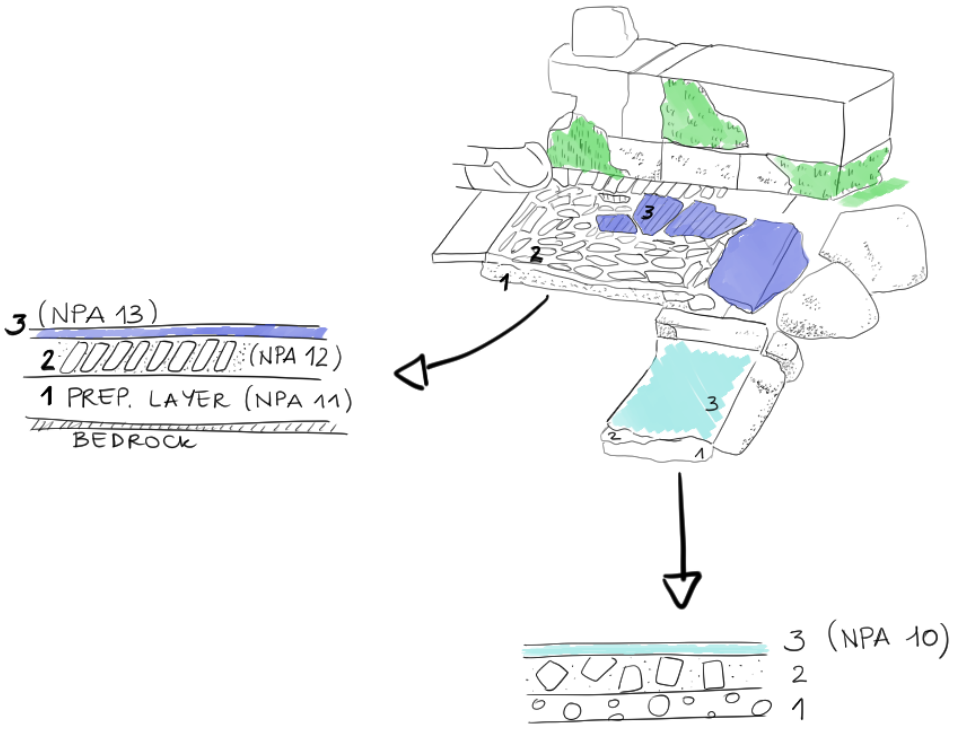

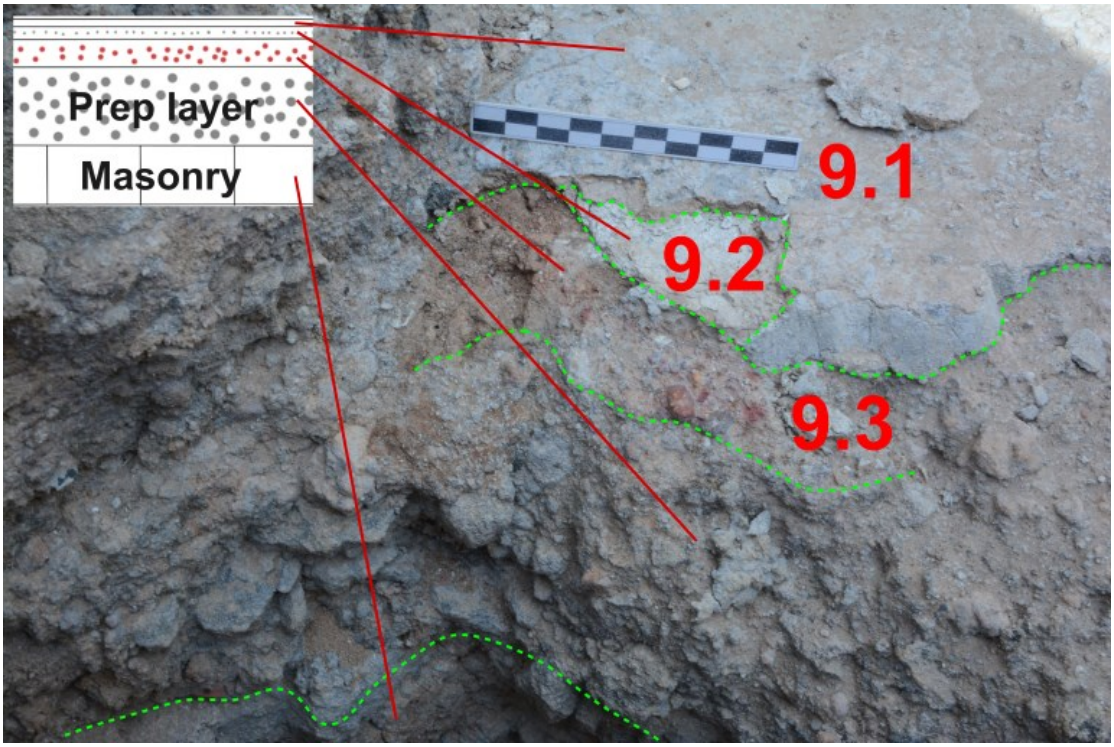

***Figure 47) Top**: reconstruction of the floor sequence S.233 in the Agora in Nea Paphos. Several samples (NPA 10 to 13) were collected in order to properly study and analyse the floor sequence. Legend: purple plaster – 1 = preparation layer (similar to the* rudus*), 2 = layer with large bricks (similar to Vitruvius'* nucleus*), 3 = surface; blue plaster – 1 = preparation layer composed of lime and gravel (*rudus*), 2 = preparation layer composed of lime mixed with squared stone blocks, 3 = finishing surface; in green traces of a masonry mortar similar to sample NPA 15. The drawing (by author) is not in scale. **Bottom:** photograph of structure n. 145 with the several layers retraced and schematically reconstructed on the right, top corner. According to Vetruvius' structure: masonry =* stratumen*; prep. layer =* rudus*; 9.3 =* nucleus*; 9.2 = bedding mortar. 9.1 could possibly be a refurbishment phase of 9.2.*

Chapter 4.1.4: System 4 – Lime-based plasters outliers

This system only includes samples that do not fit the previous categories, even though they are all lime-based. The reason they are not included in any category can be various: either they present a unique layering structure, aggregates not observed anywhere else or a functional category that does not belong to any of the major groups. The following table (**tab. 17**) briefly characterizes these outliers, and the discordant elements embedded in them.

Sample ID	Functional category	Discordant characteristics
NPT 1	Wall plaster	This plaster is topped with a red pigment, similarly to many of the already mentioned samples of System 1. However, there are two major difference between NPT 1 and the other specimens of that group: - Lack of a double-layered structure; the sample is single-layered; - Application of the pigment directly on the plaster's surface (fresco or semi-fresco technique) (**fig. 48b**).
NPT 6C	Seat sealing	This seat sealings differs from the others (included in System 1) from the point of view of the aggregates composition. This is the only sample out of the collected ones whose main aggregates is identifiable with an organic material (most likely grass) fully decomposed, which has created an irregular and striking pore structure (**fig. 48c**).
NPT 9	Wall plaster	This sample shares the same characteristics of the System 1 wall plasters; however, an additional layer of modern mortar for repair and conservation was applied, disrupting the observations and analyses.
NPA 6	Floor	This sample is constituted by a mixture of crushed limestone (or partially burnt lime) and sand compacted to form a brittle layer of flooring surface.
NPA 7 *NPA 8*	Waterproofing m.	Samples NPA 7 and 8 were collected from a water channel and expected to be either waterproofing mortars or NHL plasters. However, they lack the characteristics of both. No pozzolanic additives have been recognized in the matrix, and XRD, TA and SEM analyses all concord in categorizing these samples as air lime-based mortars.
KISS 4	Plaster lining	This sample belongs to the category of NHL (System 5) – at least by its chemical composition. Nonetheless, its function does not mirror the tendential use of NHL plasters in connection with water or liquid storage and disposals. KISS 4 was in fact laid as a plaster lining for an oven.
KISS 2	Wall plaster	This single layered wall plaster is composed of NHL binder, as all the other samples collected in Kissonerga. It is included in the outliers as the function is different from the usual one for NHL-based mortars.

YE 1	Wall plaster	This lime-based wall plaster sample differs from the ones included in System 1 because of the presence of a single, extremely thick (around 15 cm) layer, evened, flattened and smoothed. Furthermore, this sample is dated to approximately the 6th century BCE, falling outside the chronological frame of this project.
YSC 16	Masonry mortar	YSC 16 is the only example of masonry mortar realized with a lime binder rather than a gypsum one.
YSC 18	Wall/floor plaster	This single-layered lime-based plaster is directly attached to a stone (**fig. 48a**); it is characterised by a remarkably flat surface. However, it was collected out of its original location, making the identification of the functional category nearly impossible. It has been included in the outliers to avoid erroneously including it in a different group.

Table 17*) List of the outliers included in System 4. All the samples are lime-based plasters or mortars with element(s) that distinguish them from the regular categories.*

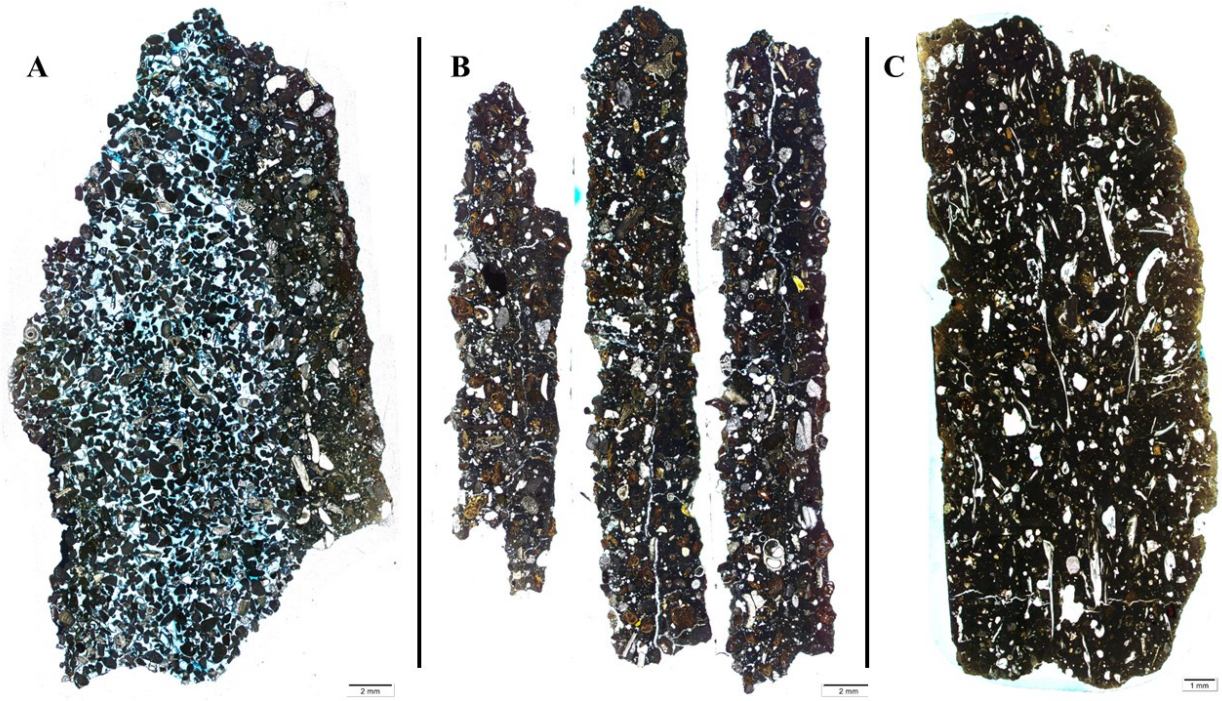

Figure 48 A*) Photomicrograph scan of sample YSC 18 with the stone layer on the left and the mortar on the right; scale bar = 2 mm;* ***B****) Scan of the thin section of sample NPT 1, the single-layered wall plaster; scale bar = 2 mm;* ***C****) Scan of the single layered seat sealing of Nea Paphos Theatre – sample NPT 6c. This sample is characterised by the presence of peculiarly shaped voids; scale bar = 1 mm.*

It is particularly complicated to draw any coherent conclusion from this set of outliers, as they do not share common characteristics that allow for a deeper interpretation. In several circumstances the lack of well-preserved contexts further complicate the formulation of any valuable hypothesis.

It is noteworthy that the lowest amount of outliers, statistically, has been recorded in Nea Paphos Agora, where the context is well known and interpreted.

Chapter 4.1.5: System 5 – Natural Hydraulic, and hydraulic Lime-based binders

NHL-based mortars often contain ceramic aggregates, just like the air lime-based waterproofing mortars of System 2. In addition, the microscopic structure of these two systems appears quite similar: a fine lime binder, usually mixed with relatively well-sorted aggregates, the majority of which consists of crushed ceramics, accompanied by crushed shells, limestone fragments, and chert. The most striking difference on a macroscopic level is the colour of the binder, which usually varies between dark grey and dark brown for System 2, and light grey for System 5 (**fig. 49**).

Given the remarkable closeness, all the samples now grouped in System 5 were initially considered part of System 2, at least until XRD, TA and SEM-EDS were performed. It is important to underline that it is not possible to say with a hundred percent certainty whether the historic binders under study are natural hydraulic or not. However, comparing the results of different analytical methods, reasonably points out to the hydraulic character of these specimens. Estimations of cementation index (CI) or H_2O/CO_2 ratios (Moropolou *et al.* 2000) are – precisely – appraisals, thus subject to adjustments and revaluations according to future available data.

In XRD-QPA an indication of possible hydraulicity comes from the detection of high percentages of amorphous phases (for further information see Arizzi, Cultrone 2021). The average percentage of amorphous content in these samples is around 40%, while air lime binders usually display around 20-30% of amorphous phases in their XRD spectra. TA measurements provide an estimate of possible hydraulicity via the calculation of the ratio between the loss of H_2O in the 200°-600° region and that of CO_2 in the 600°-900° one. This ratio (after Moropoulou *et al.* 2000) allows to categorize lime binders in pozzolanic (ratio < 3), hydraulic (ratio 3-9), and aerial (ratio > 9). The majority of the Paphian samples is included in the slightly to moderately hydraulic region (on average, the ratio is around 6).

The CI can be calculated after the SEM-EDS analysis of the samples by taking into consideration the following oxides: SiO_2, Al_2O_3, Fe_2O_3, CaO and MgO. Following the Holmes and Windgate (2002) classification, the majority of the analysed samples follow into the category of slightly to eminently hydraulic, with only few being considerable as natural cements according to this classification. However, according to the more calibrated classification proposed by Válek *et al.* (2014, 772) none of the samples can be considered a natural cement. In fact, there cannot be natural cements in Roman times, as the slaking would require powdering the burnt product with a modern mill to make it reactive. The fact that the CI of the samples are this close to the definition of a natural cement can be the result of either analytical faults – such as the method employed not being the most appropriate for it – or of the presence of SiO_2 and Al_2O_3 molecules in the binder which do not take part in the hydraulic reaction, but still increase the CI.

In addition to the calculation of Cis, SEM-EDS mapping was employed as a visual aid to identifying possibly NHL binders: as a matter of fact, in the majority of the analysed samples of

System 5 it is possible to observe very fine (< 10 µm) silica particles dispersed in the binder, which are reactive and could potentially cause hydraulic reactions (**fig. 50**).
Overall, it appears clear that none of the analyses, if taken individually in consideration, can be a definitive proof of the natural hydraulic character of these samples. However, a careful and balanced consideration of the optical characteristics in PLM and the mineralogical and chemical data allows to legitimately suggest the presence of NHL binder in these pool of samples (**tab. 18**). This hypothesis is further strengthened by the experimental burning and slaking of the geological stones: in fact, some of the slaked limes produced set and hardened underwater, as a properly hydraulic lime.

LBA	IA	H	LH-ER	ER	LR	U
KISS 3			NPHH 1	NPER 1		NPA 12*
KISS 4	--	--	NPT 3 (a)		--	NPA 13*
2			**2**	**1**	**1**	**2**

Table 18) *List of all the samples grouped in System 5 divided by chronological period. Legend: LBA=Late Bronze Age, IA=Iron Age, H=Hellenism, LH=Late Hellenism, ER=Early Roman, LR=Late Roman, U=uncertain. * indicates the samples for which the hydraulic character is not fully confirmed.*

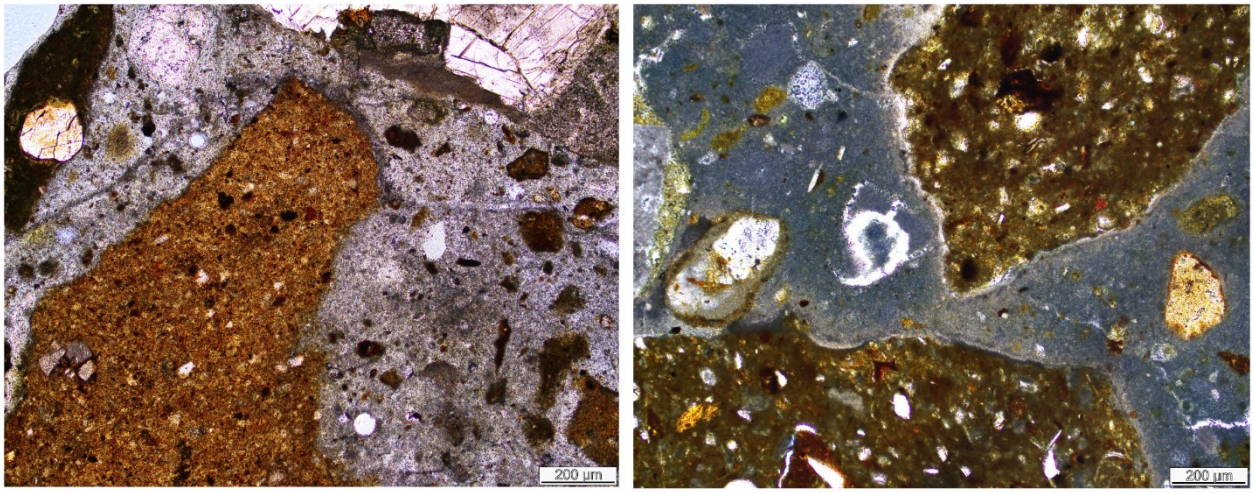

Figure 49*) Photomicrographs of samples NPT 3A (left) and NPT 12 (right) compared to illustrate the differences between the fabrics of System 2 and System 5; scale bar = 200 µm. NPT 3A is one of the samples of the so-called System 5 (NHL binders): the fabric has a glassy texture and a characteristic light-grey colour. The fabric of sample NPT 12, belonging to System 2 (waterproofing plasters), is much darker and displays the presence of possible reaction rims around the ceramic particles.*

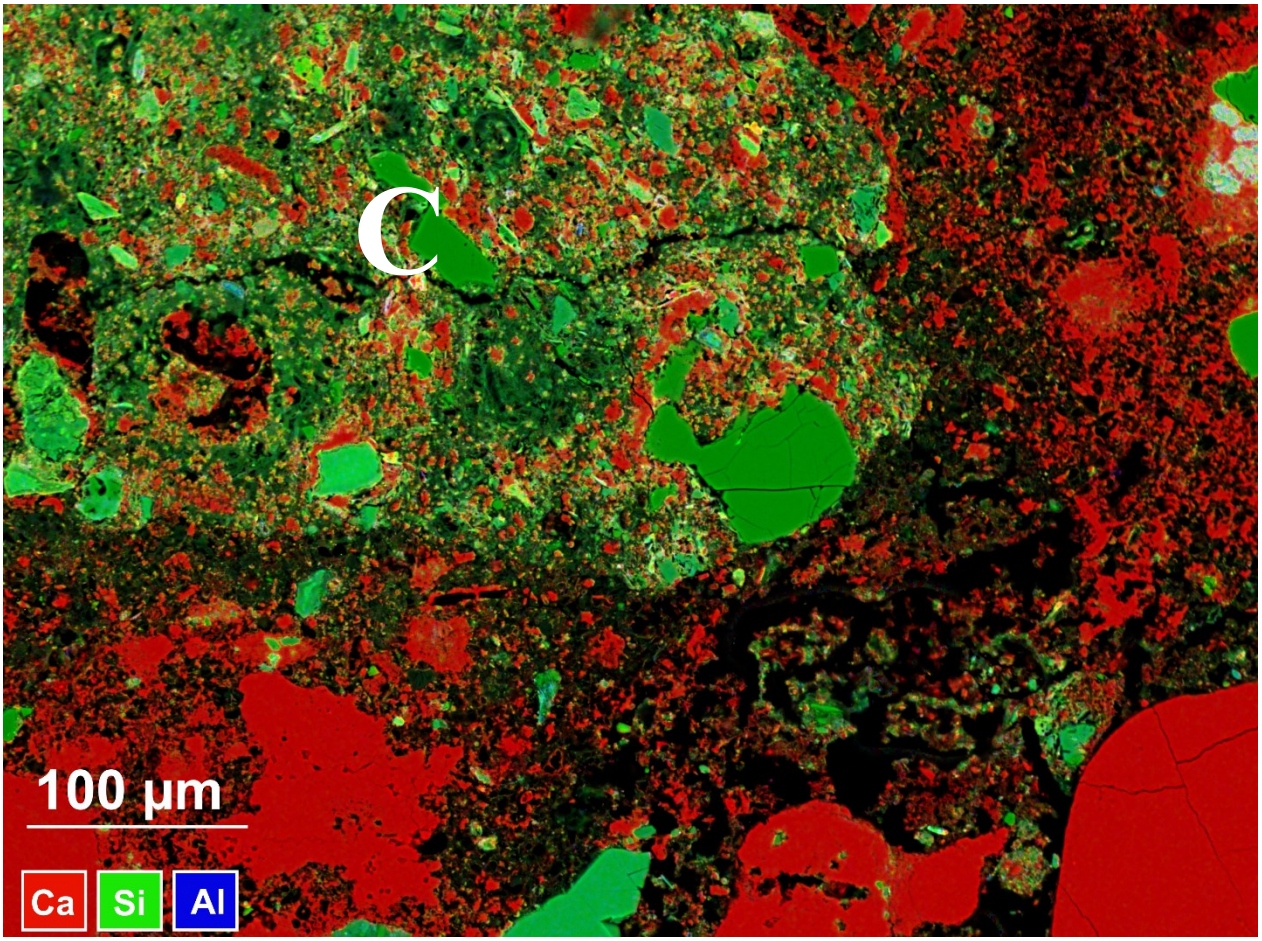

Figure 50*) SEM-EDS elemental distribution map of Ca, Si and Al in sample NPA 12. C = ceramic particles*

Chapter 4.1.6: System 6 – gypsum-based plasters and mortars

Except for the samples collected in Kouklia-*Palaepaphos* (KPH), gypsum-based samples have been consistently identified in the archaeological sites with the primary function of masonry mortars. At a macroscopic level, System 6 samples consist of thick, single layer mortars with a white to grey colour, a soft and dusty consistency, and the lack of visually distinguishable aggregates. The few samples with different functional purposes than masonry mortars appear to be thinner and display characteristic large and transparent crystals on the surface. Analysis in PLM was complicated by the sensitivity of gypsum to water during the preparation of the thin sections: unfortunately, part of the crystals were fully lost or abraded, causing an issue in the proper estimation of the samples' porosity. Eye-catching under the microscope is the presence of inchoate yellow particles without reflective properties in XPL (**fig. 51)**. These "glassy" particles have been identified in nearly all the samples, across different chronological phases and archaeological sites; however, they have not been detected in any of the collected typologies of gypsiferous stones. It is possible that they are the results of the burning process of the raw materials, however, a more

definitive answer to their origin has not been found yet. The yellow particles' chemical composition displays a high content of Si – as detected with SEM-EDS measurements.
From a mineralogical perspective, these samples contain high percentages of gypsum (above 79%) and low amounts of calcite. A distinguishing and unexpected feature is the detection of C-(A)-S-H phases (although lower than 0.5%) in the gypsum-based samples from Yeronisos and Nea Paphos. This element is completely missing from the samples collected in Palaepaphos. The presence of C-(A)-S-H phases is completely unexpected, as they are associated with hydraulic materials. While an analytical error might have occurred, it is significant to notice how these phases were detected in similar quantities an almost all the samples. C-(A)-S-H phases are produced at high temperatures, while gypsiferous stones are usually burnt at temperatures around 250°C; burning of gypsum at higher temperatures is absolutely possible, but it would produce considerable amounts of anhydrite, which were not detected in XRD. Ultimately, the discussion around the C-(A)-S-H phases is still open and only additional analyses – including experimental burning of Cypriot gypsum stones – can completely answer to their presence.
Other detected mineralogical phases in XRD correspond to quartz (lower than 1%) and amorphous material, whose percentage remains well below 20%. TA curves of the binder-rich fractions of these specimens confirm the quantification obtained via XRD-QPA, with only minor differences attributable to the well-known issue of calcite hidden in the XRD amorphous values. Additionally, TA was performed on the mixed and total fraction of these mortars, revealing that the quantity of gypsum is much higher in the coarse fraction that includes the aggregates (**tab. 20**). This interesting feature highlights the fact that gypsiferous stone was either additionally added to the mixture, or part of the original rock were not fully burnt and carbonated, remaining in the binder in the form of coarse crystals.

LBA	IA	H	LH-ER	ER	LR	U
--	KPH 1	YW 1	NPT 2	NPA 15	--	--
	KHP 2	YW 2	NPT 8			
	KPH 3	YSC 1				
		YSC 2				
		YSC 7				
		YSC 8				
		YSC 9				
	3	**7**	**2**	**1**		

Table 19) *List of all the samples grouped in System 6 divided by chronological period. Legend: LBA=Late Bronze Age, IA=Iron Age, H=Hellenism, LH=Late Hellenism, ER=Early Roman, LR=Late Roman, U=uncertain.*

sample	wt. loss (%)		content (%)	
	50-250°C	**600-800°C**	**$CaSO_4*2H_2O$**	**$CaCO_3$**
NPT 8/a	19.2	2.4	91.9	5.5
NPT 8/b	18.3	3.5	87.4	7.9
NPT 8/m	18.6	3.0	88.8	6.9

Table 20*) Results of TA performed in all three fraction of the System 6 sample NPT 8. NPT 8/a corresponds to the bulk sample, which was powdered, but not sieved; NPT 8/m corresponds to a sieved portion of NPT 8/a to an analytical fineness of more than 63*

microns; NPT 8/b corresponds to the finest fraction of the sieved sample, which is considered as binder-rich. As evident from the calculation of the content of gypsum, the bulk sample presents a higher percentage of gypsum, suggesting the use of gypsiferous stones as aggregates, or the presence of larger crystals as remnants of the burning process.

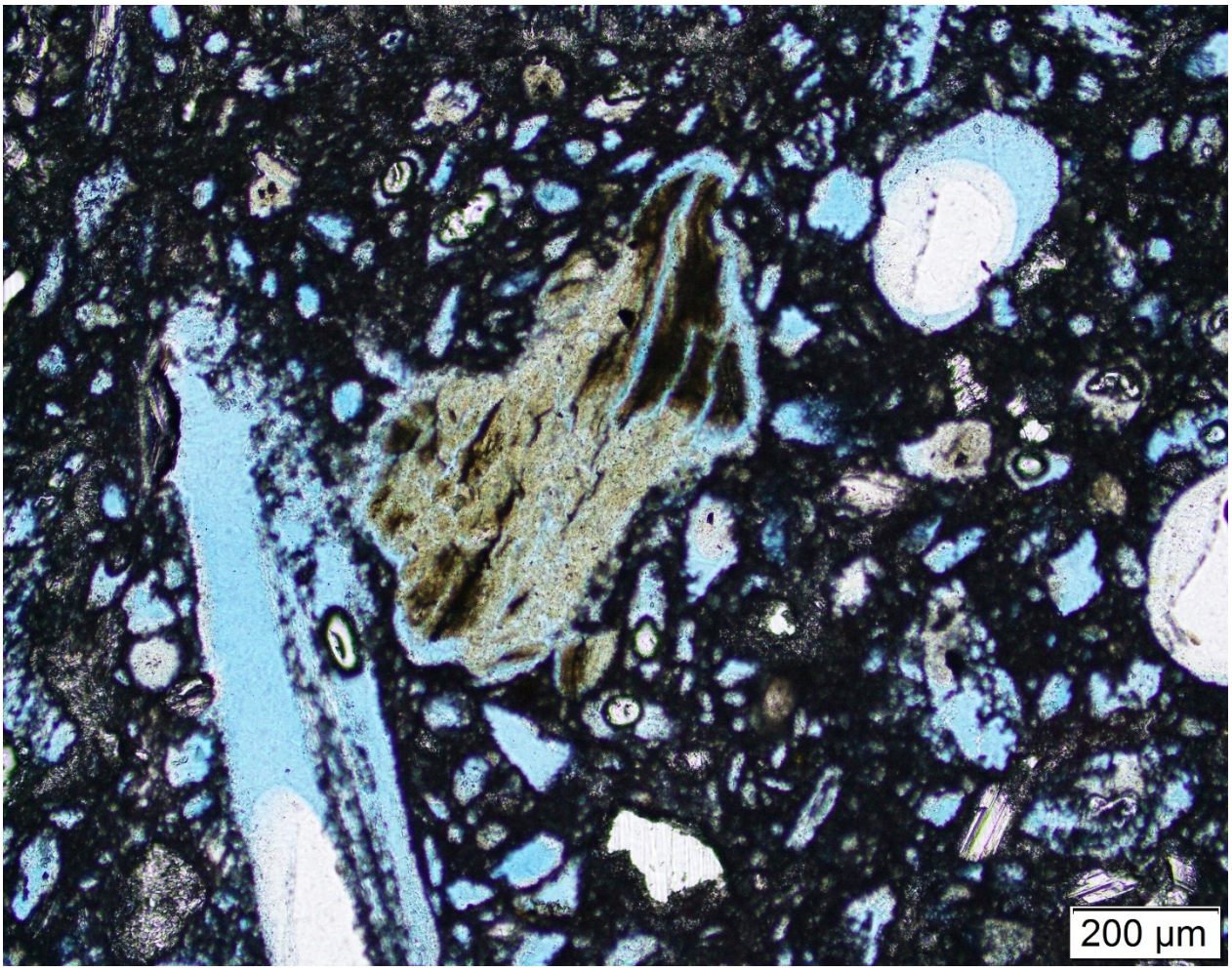

Figure 51) *Microphotograph of sample KPH 3 with focus on a larger inchoate yellow particle rich in Si content; PPL.*

Chapter 4.2: The colour palette of the Paphian region

Although initially not included in the main aims and objectives, the presence of several painted plaster fragments allowed for a partial overview of the pigment palette in use in Paphos between the Late Hellenistic and the Roman times. It is important to preface this section of the present study by underlining that the pool of samples is still relatively small; however, there are plenty of published data on Cypriot pigments (Radpour *et al.* 2019; Balandier *et al.* 2017; Kakoulli *et al.* 2010; Siddall 2006), allowing for a confirmation of our data. Furthermore, the dimensions of the collected samples does not allow for an aesthetical or stylistic appraisal, as the pigments are preserved in scanty traces. The most common pigment among the Paphian samples is red, with black and white coming in close second. Occasionally, yellow, green and light blue have been observed in trace amounts.

In terms of painting techniques, the Paphian wall plasters under study are realized with a *secco* technique, meaning that the paint was applied when the underlying plaster was dried using an organic or inorganic medium. The fresco-secco technique was well known during both Roman and Hellenistic times (Jiménez-Desmond *et al.* 2024; Peréz-Diez *et al.* 2023; Kakoulli 2002, 56), although it was considerably less spread than the fresco one. According to the standard in the Roman age, in order to produce a frescoed wall, three – or more – preparation layers were laid on the masonry: a background layer, a middle layer to even the wall surface, and a finishing smooth layer to spread the pigment on (Lanzón *et al*. 2023). The samples under study, mostly dating to the Roman age, present this sequence of layers, although not always this exact. However, in the Paphian case, the pigments are not applied directly to the surface, as this technique would leave unmistakable traces at the microscopic level that are not visible in the samples under study (**fig. 52**). Rather, the pigment was applied to the dried-up finishing layer with the aid of an additional medium. The most common mediums in the past were Arabic gum, animal glues, wax, and eggs (Casoli 2021); in the Paphian samples no organics were detected. This means that either the organic was not preserved to an extent sufficient to be detected with standard analytical techniques, or that the medium employed for the application of the pigments was not of organic nature. It seems most plausible that the pigment layers in the samples under study were realized mixing the pigments with lime water, according to the so-called *mezzo fresco* technique (Jiménez-Desmond *et al.* 2024, 167).

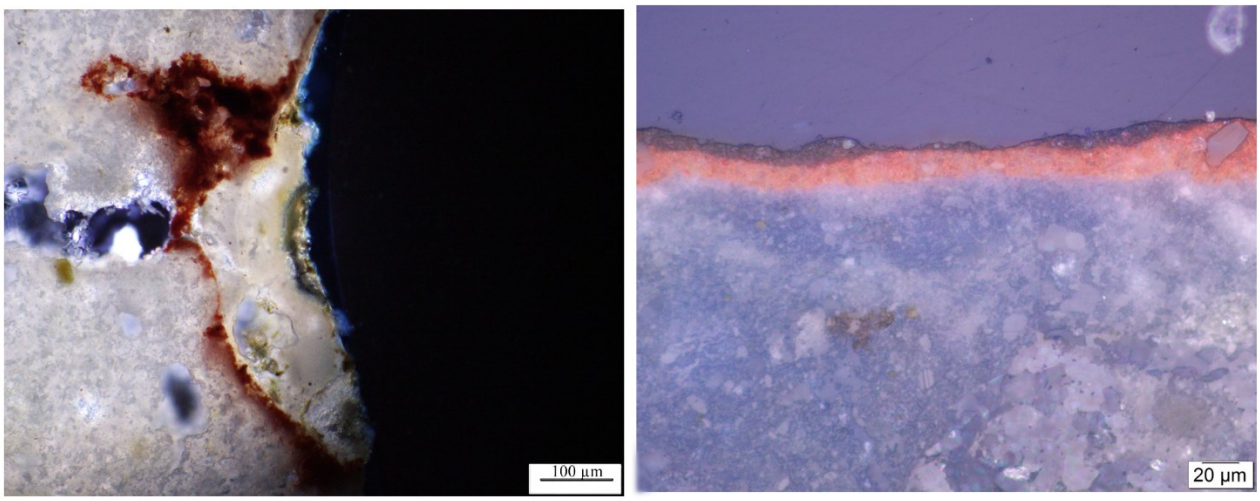

Figure 52*) Photomicrograph of sample NPT 1 (left) with traces of a potentially fresco application of red pigment, as detectable by the pigment seeping through the mortar mixture; photomicrograph of sample NPA 28 with traces of the double layer of pigment applied on a dried finishing mortar.*

Reds

Red washes present different hues and tones, from bright intense crimson to brownish brick red (see chapter 3.5.2, **fig. 34**). The particles of the pigments are very fine, although still clearly distinguishable in both PLM and SEM (see **fig. 53**); in nearly all instances, the pigment layer is

topped by transparent crystals, most likely a result of post-depositional accumulation of salts and other pollutants, or of recrystallization of the binder.

According to historical sources, Romans produced red pigments mostly from minerals such as cinnabar, realgar or iron oxides (Pliny, *Nat. Hist.* 13–14) – particularly hematite (Siddall 2006); likewise, Hellenistic wall plasters from across the Mediterranean seem to favour cinnabar and hematite as sources of red (Kakoulli 2002, 64). Cyprus is rich in hematite, especially in the region of the Troodos Mountains (Kassianidou 2013), and previous studies (such as Radpour *et al.* 2019) mention the predominance of hematite-based reds in Cypriot wall paintings dating to Roman times. In the case of the samples from both Nea Paphos and Yeronisos island, red colour has been constantly identified as hematite (Fe_2O_3), with presence of other iron oxides ascribable to red ochres, and occasional contaminations of anatase. The presence of this latter compound has posed a series of interesting questions. Anatase is a commonly occurring titanium oxide's polymorph (TiO_2) which is suitable for the production of white, red, brown and black pigments. Typically associated with modern synthetic white pigment, it has often been used as a discrimen to identify copies or imitations, and to date historic paintings (Edwards *et al.* 2006, 1356–1357). However, recent studies by Edwards *et al.* (2006) have determined the use of anatase in combination with hematite for the production of red pigments in a Roman villa in Cambridgeshire. This significant discovery opens the floor to the discussion of the use of anatase in ancient pigments, and particularly in Roman times. Nonetheless, in the present study, differently from Edwards', the presence of TiO_2 was minimal and not proportional to the amount of hematite. This leaves two open issues: was the anatase a natural contamination or an intentional addition to the red hematite? And if an addition, which was the purpose of it? Answering these questions will only be possible with a more in-depth and extensive study on red pigments in the region.

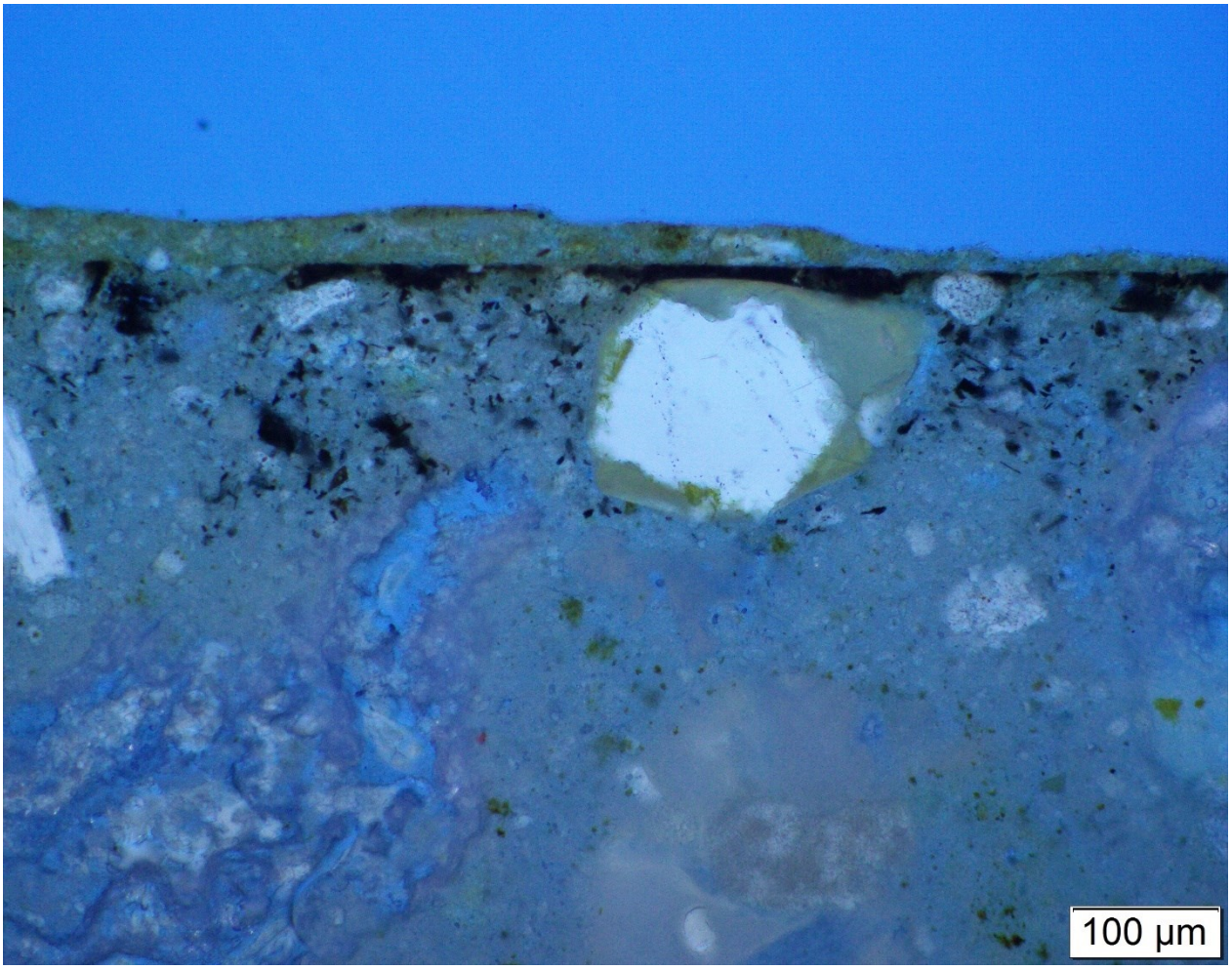

Figure 53*) Photomicrograph of Sample NPA 21 in PPL with focus on the double pigment layer.*

Blacks

Black has been detected in several of the samples from Nea Paphos, both as a monochromatic paint layer, and as a decorative element overlaying red and white pigments. Ancient sources as Pliny (*Nat. Hist.* 35.25) list soot as the most ideal black pigment, although mineral variations such as umber and pyrolusite are often documented as well (Radpour *et al*. 2019, 17; Siddall 2006; Kakoulli 1997). The analysed samples consistently display carbon-based pigments with occasional presence of goethite, a mineral component of ochres.

Whites

The vast majority of the wall plaster samples collected from Yeronisos and Nea Paphos presented a flat, even, smooth, bright white finishing, which suggested the use of either a limewash or a specific strongly covering pigment.

Historical sources such as Pliny and Vitruvius list a variety of different supplies for the production of white pigments, including clays from Greece (Pliny, *Nat. Hist.* 35.19), possibly rich in kaolinite and montmorillonite content (Siddall 2006). Another interesting pigment is the so-called

"*anularian* (ring) white", which, according to Pliny (*Nat. Hist*. 35.30) was a mixture of chalk and glass. To conclude the palette of Hellenistic and Roman whites, lead-based white pigments were also known and widespread (Kakoulli 2002, 64).
The initial hypothesis of the use of a specific white pigment has been contradicted by the analytical results, according to which white is mostly composed of calcium carbonate, with occasional impurities – this finding is in accordance with the published analyses of Radpour *et al.* 2019 (16) on wall paintings from Nea Paphos. Scanty traces of cerussite ($PbCO_3$) on one plaster sample possibly indicate the use of a lead-based white pigment.
In addition to the white surfaces, traces of calcite have been detected in all the painted surfaces. While, on one hand, this could be a symptom of the pigment layer's decomposition – resulting in the resurfacing of the white calcite from the substratum – it is not possible to exclude that calcium carbonate was mixed to the pigments either as a binder (*mezzo fresco* technique) or as a mean to create lighter shades of colour – a technique widely documented in the whole Mediterranean region.

Yellow and green
Despite Cyprus being listed as one of the main sources of both malachite ($Cu_2CO_3(OH)_2$) and earth green (a derivation of celadonite and glauconite) (Radpour *et al.* 2019, 13; Apostolaki *et al.* 2006; Kakoulli 1995), no consistent traces of green decorations have been documented in the samples under study. Only one green pigment particle has been identified in sample NPT 1 (**fig. 54**) amidst the yellow layer, suggesting it could possibly be just an impurity.
Yellow also occurs in one specimen solely (NPT 1), where it underlays a red, hematite-based layer. The yellow paint is highly degraded; however, it can be identified with goethite or another form of ochre. This pigment has been detected in the wall paintings of Nea Paphos by Radpour *et al*. (2019, 15-16) and is listed among the most common source of yellow for Roman artists.

Blue
Blue is historically one of the rarest and most precious pigments, along with purple. In Antiquity, natural blue dies were produced from the processing of the *Indigofera tinctoria* plants (Roshan *et al.* 2021; Pliny *Nat. Hist.* 35.27), while minerals suitable for the production of blue were azurite and lapis lazuli. Given the rarity of this pigment, blue was the first colour synthetically produced in history (Eastaugh *et al.* 2004) in the form of calcium copper silicate ($CaCuSi_4O_{10}$), more commonly known as Egyptian Blue. This pigment was among the most widespread blues in the mediterranean during the Hellenistic and Roman times (Radpour *et al*. 2019, 12; Kakoulli 2002, 64).
Occurring in one specimen only (NPA 24), the light blue pigment from Nea Paphos appears significantly diverse from the other analysed pigments. While black, red, and even yellow paints are solidly attached to the substrata, this light-blue layer is flaky, leading the research team to hypothesise the presence of a now degraded organic binder. The pigment has been securely

identified with Egyptian blue, although not pure. It was probably mixed with a Si-based material, either for the production of a hue, or possibly as a binder. Concerning the binder, none of the analytical methods applied (organic residue analysis, Raman spectroscopy, FTIR) allowed for the detection of any organic material, meaning that the binder was either inorganic, or – if it was organic – it did not survive in sufficient quantities to be detected.

Figure 54) *Photograph of the surface of sample NPT 1 under the stereomicroscope (scale = 200 µm). Small green spots (circled) are visible in a limited part of the sample's surface, above the yellow paint and underneath the red one.*

REFERENCES

APOSTOLAKI, CH., V. PERDIKATSIS, E. REPUSKOU, H. BRECOULAKI, S. LEPINSKI

2006. Analysis of Roman wall paintings from ancient Corinth/Greece. *2nd International Conference on Advances in Mineral Resources Management and Environmental Geotechnology*, Hania, Greece, September 25–27; pp. 729–34.

ARIZZI, A., G. CULTRONE

2021. Mortars and plasters—how to characterise hydraulic mortars, *Archaeological and Anthropological Sciences* 13, 144. https://doi.org/10.1007/s12520-021-01404-2

BALANDIER, C., C. JOLIOT, M. MÉNAGER, F. VOUVE, C. VIEILLESCAZES

2017. Chemical analyses of Roman wall paintings recently found in Paphos, Cyprus: The complementarity of archaeological and chemical studies. *Journal of Archaeological Science: Reports* 14, pp. 332–339. http://dx.doi.org/10.1016/j.jasrep.2017.06.016

CASOLI, A.

2021. Research on the Organic Binders in Archaeological Wall Paintings. *Applied Sciences* 11(19), 9179. https://doi.org/10.3390/app11199179

CALDEIRA, B., R.J. OLIVEIRA, T. TEIXIDÒ, J.F. BORGES, R. HENRIQUES, A. CARNEIRO, J.A. PEÑA

2019. Studying the Construction of Floor Mosaics in the Roman Villa of Pisões (Portugal) Using Noninvasive Methods: High-Resolution 3D GPR and Photogrammetry. *Remote Sensing* 11(16), 1882. https://doi.org/10.3390/rs11161882

EASTAUGH, N., V. WALSH, T. CHAPLIN, R. SIDDALL

2004. "Egyptian blue". *The pigment compendium: Optical microscopy of historical pigments,* Oxford: Elsevier Butterworth Heinemann, pp. 147–148.

EDWARDS, H.G.M., N.F. NIK HASSAN, P.S. MIDDLETON

2006. Anatase – a pigment in ancient artwork or a modern usurper? *Analytical and Bioanalytical Chemistry* 384, pp. 1356–1365. https://doi.org/10.1007/s00216-005-0284-2

ELSEN, J., K. VAN BALEN, G. MERTENS

2012. Hydraulicity in Historic Lime Mortars: A Review, in J. Válek, J.J. Hughes, C.J.W.P Groot (eds.), *Historic Mortars. Characterisation, Assessment and Repair, RILEM Bookseries* 7, pp. 125–140, Springer.

HOLMES, S., M. WINGATE

2002. *Building with Lime: A Practical Introduction*. Practical Action Publishing.

JIMÉNEZ-DESMOND D., J.S. POZO-ANTONIO, A. ARIZZI

2024. The fresco wall painting techniques in the Mediterranean area from Antiquity to the present: A review. *Journal of Cultural Heritage* 66, pp. 166–186. https://doi.org/10.1016/j.culher.2023.11.018

KAKOULLI, I., C. FISCHER, D. MICHAELIDES

1995. Hellenistic and Roman Wall Paintings in Cyprus: A Scientific Examination of Their Technology. Master's thesis, London: Courtauld Institute of Art, University of London.

1997. Roman wall paintings in Cyprus: a scientific investigation of their technology, in H. Bearat, M. Fuchs, M. Maggetti, D. Paunier (eds.), *Roman Wall Painting: Materials, Techniques, Analyses and Conservation, Proceedings of the International Workshop, Fribourg 7-9 March 1996*, pp. 131–142, Fribourg: Institute of Mineralogy and Petrology.

2002. Late Classical and Hellenistic painting techniques and materials: a review of the technical literature. *Reviews in Conservation* 3, pp. 56-67.

2010. Painted Rock-cut tombs in Cyprus from the Hellenistic and Roman periods to Byzantium: material properties, degradation processes and sustainable preservation strategies. *Studies in Conservation* 55, pp. 96–102. https://doi.org/10.1179/sic.2010.55.Supplement-2.96

KASSIANIDOU, V.

2013. Mining landscapes of prehistoric Cyprus. *Metalla* 20, pp. 5–57.

LANZÓN M., M. JOSÉ MADRID-BALANZA, I. MARTÍNEZ-PERIS, V.E. GARCÍA-VERA, D. NAVARRO-MORENO

2023. Roman wall paintings from the Roman Forum district of Carthago Nova: Characterisation of mortars and pigments. *Construction and Building Materials* 408, 133543. https://doi.org/10.1016/j.conbuildmat.2023.133543

MOROPOULOU, A., A. BAKOLAS, K. BISBIKOU

1995. Characterization of ancient, byzantine and later historic mortars by thermal and X-ray diffraction techniques. *Thermochimica Acta* 269/270, pp. 779–795. https://doi.org/10.1016/0040-6031(95)02571-5

2000. Investigation of the technology of historic mortars. *Journal of Cultural Heritage* 1, pp. 45-58. https://doi.org/10.1016/S1296-2074(99)00118-1

PÉREZ-DIEZ, S., F. CARUSO, E. FRINE NARDINI, M. STOLLENWERK, M. MAGUREGUI

2023. Secco painting technique revealed in non-restored Pompeian murals by analytical and imaging techniques. *Microchemical Journal* 194, 109365. https://doi.org/10.1016/j.microc.2023.109365

PLINY THE ELDER, *Naturalis Historia,* J. Bostock, H.T. Riley, K.F.T. Mayhoff, Perseus Digital Library 2006.

RADPOUR, R., C. FISCHER, I. KAKOULLI

2019. New Insight into Hellenistic and Roman Cypriot Wall Paintings: An Exploration of Artists' Materials, Production Technology, and Technical Style. *Arts* 8(2), 74. https://doi.org/10.3390/arts8020074

ROSHAN, P., R.S. BLACKBURN, T. BECHTOLD

2021. Indigo and Indigo Colorants. *Ullman's Encyclopedia of Industrial Chemistry*, pp. 1–16. https://doi.org/10.1002/14356007.a14_149.pub3

SIDDALL, R.

2006. Not a day without a line drawn: Pigments and painting techniques of Roman Artists. *Infocus*. http://dx.doi.org/10.22443/rms.inf.1.4

VÁLEK, J., E. VAN HALEM, A. VIANI, M. PÉREZ-ESTÉBANEZ, R. ŠEVČÍK, P. ŠAŠEK

2014. Determination of optimal burning temperature ranges for production of natural hydraulic limes. *Construction and Building Materials* 66, pp. 771–780. https://doi.org/10.1016/j.conbuildmat.2014.06.015

WEINER, S.

2010. *Microarchaeology. Beyond the Visible Archaeological Record*. Cambridge: Cambridge University Press.

PART 5. CONCLUSIONS AND FURTHER DIRECTIONS

As discussed in the previous chapters of this thesis, there has been a lack of published material available for the appraisal of the Cypriot plaster industry's state-of-the-art. Undoubtedly, the major accomplishment of the present research project lays in its role of paving stone to fill the gaps in this specific research field. Although the results provided focus on a limited geographical and chronological context, the author firmly believes that they will open the way for a new wave of academic interest on plasters and mortars in Cyprus.
To briefly re-summarise the aims and objectives presented in the introductive chapter (**pp. 10-12**), this project was developed on three major axis: the first set of questions concerned the general topic of the characterisation and classification of the analysed samples; the second axis revolved around the raw material provisioning process, and the recognition of specific technological features, in addition to questions concerning the uses and functions of these materials; lastly the project focused on synchronic and diachronic developments in the plaster industry. While convincing conclusions can be formulated for the first two topics, the last field leaves a number of unanswered questions and an open discussion.

The systematic study of plasters samples of different chronological and contextual backgrounds allowed to appraise the sources of raw materials. While it is still not possible to pinpoint or distinguish a specific mining site for the limestones and gypsiferous stones, this study proves how all the sampled local geological formations are relatively equally suitable for producing highly performant plasters. The selective use of hydraulic and NHL binders for the production of mortars and plasters associated with water-retaining functions demonstrates a strong knowledge of the material properties, and the capability of the work forces to distinguish the most suitable raw materials for the manufacturing of this specific product.
The analysis of the aggregates reveals how their sources were also located in proximity of the sites. In the majority of cases, lime binders are mixed with either sea (rich in bioclastic content) or river (richer in metamorphic rocks) sand, crushed shells, and/or ceramic fragments. Sea sand, as well as river sand, is easily collectible within short distance to the settlements under study; likewise, the pottery employed as aggregate is also of local production, and probably recycled from waste. In sites such as Nea Paphos and Kissonerga there is rather abundance of river sand as aggregate in the mortars, especially compared to Yeronisos; this phenomenon can be easily explained by the hydrogeological context, where Nea Paphos and Kissonerga are located near river basin, while Yeronisos lacks sweet water sources, and thus readily available river sand. At any rate, the presence of river sand has been detected in Yeronisos, suggesting that the aggregates for the production of plasters were imported from the mainland.

From what concerns the technological aspect, it was possible to observe consistent production techniques for both gypsum and lime-based plasters. In particular, the gypsum-based samples presented relevant similarities on an inter-site level: the possible absence of aggregates, the

presence of glassy silica-based particles, alongside with the similar macroscopic characteristics (colour, density, porosity, softness) reveal a consistency in the production of these materials. In fact, there is no relevant change between the samples dating to the Iron Age and the ones belonging to the Roman period. However, it must be noted that the majority of the gypsum samples consistently date to the Hellenistic or Hellenistic-Roman period, with a statistically significant lower number for the Iron Age and the Middle to Late-Roman.

A pressing question relating to technology was that of the burning process of limestone. In order to produce a suitable lime binder, limestones have to be burnt at temperatures exceeding 1000°C for long periods of time (Válek 2015); while certainly 1000°C can be reached in open fires, or partially closed ones, maintenance of the optimal burning atmosphere to guarantee the complete burning would require a built structure, like a kiln. There is no evidence of kilns for lime production in Cyprus until the Late Roman times (Nocoń *et al.* 2023, 134; Demesticha, Michaelides 2001, 290); however, all the lime-based plasters in the present study display characteristically well-burnt binders, without traces of unburnt or partially burnt particles, implying that whether specific structures for lime burning existed or not, the local craftsmanship had mastered the production process. It is possible that kilns for ceramic production were employed for lime burning as well, although this theory cannot be proven at the moment. There is evidence of pottery kilns dating as early as the MBA (Pizzo 2020; Davit *et al.* 2014; Webb, Frenkel 2013, 69; Smith 2008, 45; Al-Radi 1983, 9).

Another interesting category of samples from the productive point of view is the so-called System 1, the double-layered wall plasters discussed in chapter 4.1.1. These samples, widely documented in Hellenistic and Roman contexts, present a nearly unvaried structure and coherent productive processes. The selection of specific aggregates for the finishing layer, its application on top of a dried and evened substrate, the use of the same – or very similar – binders in both layers, are all elements typical of most of the samples from this category. While it is possible to affirm with a reasonable degree of certainty that the technologies behind the production of double-layered wall plasters remained substantially unchanged from the Late Hellenistic to the Late Roman times, there is no sufficient data to appraise the state of production of wall plasters before the 1st century BCE. The only samples belonging to this functional category and dated prior to the 1st century BCE come from the workshop area of Palaepaphos-*Hadjiabdoulla*and are limited in number (only two); these samples are significantly different from the rest of System 1. On one hand, it would be possible to hypothesise that the wall plaster fashion changed during the Hellenistic times; however, on the other, there are no sufficient data backing up this theory, as there is a lack of sufficient material to appraise the state of the art before Hellenism, at least in this region. Furthermore, while the double-layered wall plasters of Hellenistic to Roman times come from public or elitist private spaces, the Iron Age samples of Palaepaphos were collected in an area clearly designed for working activities. This element further enhances the issue of incomparability of these types of samples.

The diachronic changes and developments in the plaster industry are the main unanswered question of the present project. As evidenced in the illustration plates of the Methodology section (part 2),

there is a significant difference in terms of sheer numbers between the samples collected for the Late Bronze and Iron Age, and the ones dated to the Hellenistic and Roman periods. This discrepancy is caused by a series of factors, including the state of preservation of single sites, the lack of documentation for certain others, and the general larger availability of preserved architectural structures dated to the later chronological periods. Specifically for this reason, it is possible to trace an outline of changes – or lack of – for the Hellenistic and Roman times, while a general appraisal of the industry in the previous chronological phases is not possible at all. Nonetheless, the samples analysed shed light on productive techniques and raw materials selection processes at site-specific levels.

The present study initiated a research on the plaster industry of Cyprus, highlighting how well-developed this was during the Hellenistic and Roman periods. Although no production centres have been identified up to date, it appears clear that this industry was highly specialized and made use of high-end materials and tools. Local limestones were carefully selected for their properties, rather than being collected from the nearest source(s). Aggregates were equally attentively culled and processed in order to obtain additives enhancing the strength and durability of the mixture (*i.e.* grinding of the aggregates' particles to a well-sorted, uniform size). Recurring construction techniques and recipes have been identified, especially for the production and application of wall and floor plaster. A higher degree of inter- and infra-site variability can be observed in the other functional categories, with the waterproofing samples constituting a pivotal open discussion point.

Chapter 5.1: Site-specific conclusions

While it is undoubtedly important to analyse plasters and mortars from a material science perspective, analysing their functions and productive processes, as archaeologists we are somewhat obliged to answer to more archaeological and sociological questions, which relate strictly to the sampling contexts. Short conclusions concerning each documented site are provided in the following paragraph, highlighting how the analysis of the archaeological context and the interpretation of the data in light of it allow for an appraisal of plaster production on a broader scale.

Chapter 5.1.1: Kissonerga-Skalia

This settlement is chronologically the oldest considered in the present study. The limited amount of samples collected in the site are all NHL-based plasters or mortars with different functionalities. The fact that NHL was not used here only for the restricted purpose of coating or building water-related structures allows to hypothesise the presence of outcrops of limestones suitable for NHL production. While these outcrops have not been located yet, it is worth to mention that several limestones collected in the surrounding area of modern-day Kissonerga produced mildly to moderately hydraulic limes during the burning experiments. It is not possible to conclude whether the selection of this raw material was dictated by its proximity or by the knowledge of its superior

properties. A wider study in the region, including the surrounding Chalcolithic and Bronze Age sites could find the answer to this question.

Chapter 5.1.2: Palaepaphos

Only a minimal part of the settlement was sampled, meaning that the characterisation of the plasters is solely circumstantial to the specific structure of sampling.

The workshop area of *Hadjiabdoulla*is the only archaeological context in which gypsum-based plasters have been detected with a different functionality than masonry mortars. Whether the choice of plastering the walls with a gypsum-based material was related to the types of work performed inside the complex is still unclear. Geologically speaking, there is no particular predominance of gypsiferous deposits in the surrounding of Palaepaphos, where on the contrary limestones are abundantly present. Thus, this choice can be related to different – or combined – factors: a specific functionality related to the works performed in the rooms; a fashion preference for gypsum over lime during the Iron Age; or rather a conscious choice made by the local elites responsible of building the structure. At any rate there is no evidence allowing to lean towards one hypothesis over the others, and it is even possible that the explanation is entirely different. An extended study on the *ashlar* buildings of the Iron Age city-kingdoms would help shedding light on this question.

Chapter 5.1.3: Yeronisos Island

The most interesting feature concerning Yeronisos is the limited availability of raw materials and resources for the production of plasters and mortars on the island. Archaeological excavations have revealed a consistent habit of re-use on the site, highlighting the general difficulty of construction material provisioning. It has already been discussed whether limestones were burnt on the mainland and transported in the form of quicklime to Yeronisos, or if the limitedly present limestones were burnt on the site (Connelly *et al.* 2002); less focus has been put on the gypsum-based mortars, for which raw materials are completely absent *in situ*. While gypsum requires low burning temperatures, easily achievable in provisional fire pits, lime burning necessitates of specific structures, high burning temperatures, and a long time for the complete calcination. Any of these elements would have left some form of archaeological evidence in a highly undisturbed stratigraphy as the one of Yeronisos. Thus, it is possible to assume that lime was transported to the island as quicklime, while gypsum could have theoretically either been transported as burnt powder or as stone to produce gypsum plasters on the spot – avoiding the risks of exothermic reactions due to likely contact with water during the transportation via sea. Nonetheless, it must be noted that mineralogical analyses of the gypsum binders did not reveal presence of minerals such as thermal anhydrite, suggesting that also the gypsum binders were produced by burning gypsiferous stones at high temperatures.

Chapter 5.1.4: Nea Paphos

Nea Paphos is not only exceptionally well preserved and documented; the extensive dimensions of the archaeological site allowed for both a synchronic and diachronic appraisal of the plaster production *in loco*. Unfortunately, as in the previous cases, no lime-kiln has been identified for the archaeological period under study; however, a much later structure located in close proximity to the Agora complex has been unearthed in recent archaeological excavations (Nocoń *et al.* 2023).

On a diachronic level, Nea Paphos displays a high degree of consistency in the plaster production between the foundation period (Early Hellenistic) and the Late Roman Age. If compared to the other sites, the employment of a higher quality of raw materials is detectable in the Roman samples. The lime and gypsum binders are extremely fine, hard, and compact and remained exceptionally preserved until the present day; the aggregates selected are always well-sorted, indicating a higher attention to the size and shapes for the production of the mixtures. Furthermore, in terms of pigments, there is a stark difference with the previously-mentioned sites, where the only colour for wall plasters was either white or – rarely – red; in the site of Nea Paphos a wider variety of colours appears, including the prestigious Egyptian Blue pigment, prerogative of the richer social classes.

On a synchronic level, it is possible to observe how both the fully public areas (Agora, Theatre) and the semi-private ones (Villas and elitist houses) share similar raw materials and production techniques. Unfortunately, the lack of private mid or low-class domestic buildings does not allow for a proper evaluation of differences in the industry of construction materials directed to public buildings and fully private ones.

Chapter 5.2: Limitations of the study

As anticipated in the previous section of the present chapter, the major limitations of the study concern the interpretation of developments and changes in the Paphian plaster industry from a diachronic perspective. Furthermore, it was not possible to assess the existence of differences between plasters produced for public spaces as opposed to the ones produced for private structures. Although one can argue that the Domestic Quarter of Nea Paphos is representative of private architecture, it must be taken into account that Roman houses and villas often retained a public or semi-public character. Moreover, all the domestic units in consideration in the present thesis belonged to elitist individuals/families and, thus, represent an architecture destined to high social classes.

Other than the lack of data to answer some of the initial research questions, the sticking point of the present study is in the definition of Systems and the identification of NHL and hydraulic binders.

The word “system” automatically implies a logic systematization of the samples according to a specific and non-varying set of characteristics, be them functional, chemical, structural, or all of the above combined. While systems in the present research are intended to be used in this meaning, it is undoubtedly true that there are no strict sets of rules, and that sometimes the categories

according to which they are organized are not as definite as they should be. Therefore, it is safer to consider the systems as a preliminary, pre-screening category, which – with additional studies – can generate an organic structure similar to the one employed for ceramic studies based on fabric types.

Concerning the individuation of possible hydraulic and NHL binders, there are several points to keep in consideration. Currently, there is not an analytical technique fully reliable to identify NHL in historic mortars, as the degradation processes also play a role in the estimation. The presence of NHL can be assumed in certain circumstances by combining the results of TA, XRD and SEM-EDS, along with referring to the surrounding geological context. According to the results obtained in the present study, there are several samples which could be categorized as NHL, while a minor percentage should be classified as pozzolanic mortars. However, the hydraulic properties of these samples are purely estimations, and a more comprehensive study on the water-related plasters in Cyprus should be carried out to prove – or disprove – this data.

Chapter 5.3: Further directions

This project is but a paving stone to a much-needed broader research on the plaster production in Cyprus. While limited studies have been carried out in circumscribed areas of the island for isolated periods of time, there is a complete lack of an island-wide database, which would allow a direct and efficient appraisal of the newly excavated materials. Furthermore, considering how limited are the evaluations possible for the chronological phases preceding the Hellenistic period, a thorough study of the Bronze Age and Iron Age plaster industries should be carried out, in the region of Paphos *in primis*, and in the rest of the island.

Ideally, a wider geological sampling could be performed especially targeting the sources of possible NHL, in order to pinpoint the locations of the closest outcrops to the archaeological sites and to evaluate their accessibility in the past. On this topic, valuable information could be acquired from a study on the systems of transport of raw materials.

REFERENCES

AL-RADI, S.M.S.

1983, *Phlamoudhi Vounari: A Sanctuary Site in Cyprus*, Göteborg: Paul Åströms Förlag.

CONNELLY, J.B., A.I. WILSON, C. DOHERTY

2002. Hellenistic and Byzantine Cisterns on Geronisos Island. *RDAC* 2002, pp. 269–292.

DAVIT, P., F. TURCO, S. COLUCCIA, L. OPERTI, F. CHELAZZI, L. BOMBARDIERI

2014. Technological and compositional characterization of Red Polished Ware from the Bronze Age Kouris Valley (Cyprus). *Mediterranean Archaeology and Archaeometry* 14, pp. 1–18.

DEMESTICHA, S., D. MICHAELIDES

2001. The Excavation of a Late Roman 1 Amphora Kiln in Paphos, Cyprus, in E. Villeneuve, P.M. Watson (EDS) *La céramique byzantine et proto-islamique en Syrie-Jordanie: IVe-VIIIe siècles apr. J.-C.: Actes du colloque tenu à Amman les 3, 4 et 5 décembre 1994*, pp. 289–296, Beyruth: Institut français d'archéologie du Proche-Orient.

NOCOŃ, K., M. MICHALIK, S. JELLONEK

2023. Cooking pottery assemblage found in a late Roman lime kiln in the Nea Paphos. *Herom* 11, pp. 133–160. http://dx.doi.org/10.1400/293344

PIZZO, P.

2020. *Pyrotechnology in Middle Bronze Age Cyprus Pottery production at Erimi*-Laonin tou Porakou, Unpublished MA thesis, University of Turin.

SMITH, J.S.

2008. Settlement to Sanctuary at Phlamoudhi – Melissa, in J.S. Smith (ed.), *View from Phlamoudhi, Cyprus (The Annual of The American School of Oriental Research, vol. 63)*, pp. 45–68, Boston: American Schools of Oriental Research.

VÁLEK, J.

2015. *Lime Technologies of Historic Buildings*. Prague: Ústav teoretické a aplikované mechaniky, Akademie věd České republiky, v.v.i.

WEBB, J. M., D. FRANKEL

2013. Area 2, in J.M. Webb and D. Frenkel (eds.), *Ambelikou Aletri. Metallurgy and Pottery Production in Middle Bronze Age Cyprus*, pp. 201–226. Uppsala: Paul Åströms Förlag.